Physics Lib.

VOLUME 34 SECOND SERIES NUMBER 12

JAN 4 1930

# THE PHYSICAL REVIEW

## A JOURNAL OF EXPERIMENTAL AND THEORETICAL PHYSICS

CONDUCTED BY

THE AMERICAN PHYSICAL SOCIETY

BOARD OF EDITORS

*Managing Editor* JOHN T. TATE, University of Minnesota, Minneapolis

G. BREIT, P. W. BRIDGMAN, L. W. MCKEEHAN; I. S. BOWEN, R. S. MULLIKEN, H. D. SMYTH; E. U. CONDON, C. J. DAVISSON, F. K. RICHTMYER

## DECEMBER 15, 1929

Separations in Hyperfine Structure – – – – – –S. GOUDSMIT AND R. F. BACHER 1501
On the Zeeman Effect in Doublet Band Spectra – – – – – – – – E. L. HILL 1507
Zeeman Effect in the MgH Bands – – – – – – G. M. ALMY AND F. H. CRAWFORD 1517
Fine Structure and Zeeman Effects in Helium Band Lines – – – – – – – – – – – – – – – –ROBERT S. MULLIKEN AND GEORGE S. MONK 1530
Continuous Spectra of Flames Containing the Halogens –H. C. UREY AND JOHN R. BATES 1541
Infra-Red Absorption Spectra of Benzene and Its Halogen Derivatives – – – – – – – – – – – – – – – – – – – –J. FENTON DAUGHERTY 1549
Status of the γ-Ray Change – – – – – – – – – – – – – N. FEATHER 1558
Effect of Light on the Electron Emission from Cerium Dioxide – – – –C. E. BERGER 1566
Some Thermal and Electrical Properties of Beryllium – – – – – EVAN JARRETT LEWIS 1575
Electrical Resistivities and Temperature Coefficients of Lead, Tin, Zinc and Bismuth in the Solid and Liquid States – – – – – – –W. B. PIETENPOL AND H. A. MILEY 1588
Errors in the Use of Gratings with X-Rays Due to the Divergence of the Radiation – – – – – – – – – – – – – – – – – – – – – – – – – – – –H. E. STAUBS 1601
Empirical Calculation of the Fugacities in Gaseous Mixtures. II. Its Relation to the Tangents on Certain Thermodynamic Diagrams. Approximate Equations for Some Important Thermodynamic Properties of Gas Mixtures – – – – – – LOUIS J. GILLESPIE 1605
Heat Capacities of Real Gases and Mixtures of Real Gases – – – –JAMES A. BEATTIE 1615
A Theory of the Permanent Magnetic Fields of the Sun and Earth. A Correction – – – – – – – – – – – – – – – – – – –

# THE AMERICAN PHYSICAL SOCIETY


OFFICERS OF THE SOCIETY

| | | |
|---|---|---|
| President: | HENRY G. GALE | University of Chicago, Chicago, Ill. |
| Vice-President: | W. F. G. SWANN | Bartol Research Foundation, Philadelphia, Pa. |
| Secretary: | W. L. SEVERINGHAUS | Columbia University, New York City |
| Treasurer: | G. B. PEGRAM | Columbia University, New York City |
| Editor: | JOHN T. TATE | University of Minnesota, Minneapolis, Minn. |
| Local Secretary for the Pacific Coast: | L. B. LOEB | University of California, Berkeley, Calif. |


# THE PHYSICAL REVIEW


Published by the American Physical Society at 450 Ahnaip St., Menasha, Wis. Executive office: University of Minnesota, Minneapolis, Minn. Two volumes annually, twelve issues per volume.


First series. From July 1, 1893, to January 1, 1913, the REVIEW was conducted by Edward L. Nichols, Ernest Merritt and Frederick Bedell, with the financial support of Cornell University. The first four volumes were issued annually; subsequent volumes, semi-annually; thirty-five volumes in all.

Second series. On January 1, 1913, the REVIEW was transferred to the American Physical Society as announced on the first page of the new series which was then begun. Since then it has been conducted by a Board of Editors elected by the Society. Semi-annual volumes begin in January and July. Since July 1, 1929, the REVIEW has been issued twelve times a month.

Communications are referred to page 2 of the advertisements for further information.

Annual Subscription, throughout the Postal Union, $10.00 in advance.

Single copies of current volume, $.60.

General Index, 1893-1920, $4.00, in advance.

Bound Volumes, $6.00 per volume; Back Numbers, $1.00 per copy for issues prior to July 1, 1929 (Vols. 1-33), $.60 per copy for issues subsequent thereto. Postage is free when remittance accompanies order; otherwise postage is extra. No bound volumes can be supplied. The REVIEW offers to purchase a limited number of First Series, Vol. 1, No. 1 ($2.00 each); Second Series, Vol. 7, No. 1, January 1916; Vol. 7, No. 2, February 1916; Vol. 7, No. 4, April 1916; and Vol. 7, No. 5, May 1916 (at $2.00 each).

Advertisements. Rates will be supplied by the Editor on request. Copy for each number must be received at Minneapolis two weeks prior to the dates of issue; old copy is repeated until new copy is received. Send electrotypes direct to the printers, George Banta Publishing Co., Menasha, Wis.

Discount of ten percent is allowed subscription agencies and members of the American Physical Society.

Changes of address and Complaints of failure to receive the REVIEW, in the case of members of the Physical Society, should be addressed to the Treasurer; in the case of other subscribers to 450 Ahnaip St., Menasha, Wis.; or to the Editor. New copies can be sent free in response to complaint of non-delivery only if notice of non-delivery is received within three months of date of issue.

Editorial Correspondence should be addressed to the PHYSICAL REVIEW, University of Minnesota, Minneapolis, Minn.


Entered at the postoffice at Menasha, Wis., as second class matter.
Acceptance for mailing at special rate of postage provided for in section 1103, Act of October 3, 1917, authorized September 6, 1926.

*Second Series* *December 15, 1929* *Vol. 34, No. 12*

THE

# PHYSICAL REVIEW

## SEPARATIONS IN HYPERFINE STRUCTURE

By S. Goudsmit and R. F. Bacher
University of Michigan

(Received November 12, 1929)

Abstract

The quantum mechanics conception of a spinning electron in an $s$ state makes it probable that its interaction energy with a nuclear moment $i$ is simply proportional to the average of $is\cos(is)$. Expressions for this average cosine have been obtained and applied to different examples. In more complicated cases it can only be said that the interaction energy is proportional to $ij\cos(ij)$, which makes the interval rule hold for hyperfine structure.

THE existence of hyperfine structure has been accounted for by the introduction of a new quantum number[1] $i$, together with the quantum numbers $s$, $l$, and $j$ associated with resultant spin moment, resultant orbital moment, and total moment respectively. The new quantum number is associated with the nucleus intrinsically in the same way that $s$ is associated with the electron, and because of its similar properties might be interpreted as a nuclear spin moment. The $i$ causes a single state of the multiplet to be split up into several states ($2i+1$ or $2j+1$ depending on which is smaller) each of which is denoted by a particular value of the new total quantum number $f$. In the hyperfine structure those transitions occur for which $f$ changes by $\pm 1$ or 0, except that the transition $0 \rightarrow 0$ is forbidden, similar to the selection rules for $j$. The separations in hyperfine structure are then due to the interaction energy between the nuclear moment and the total extranuclear moment. Similar to ordinary multiplets, the hyperfine structure separations usually follow the interval rule, i. e. the separation of two adjacent states is proportional to the largest $j$ of the two states. A discussion of hyperfine structure separations involves knowing whether the coupling which exists between the extranuclear moments is the Russell-Saunders type which gives rise to multiplets, or whether it is the $(j, j)$ coupling which is found most frequently in the heavy elements.[2]

[1] E. Back and S. Goudsmit, Zeits. f. Physik **43**, 321 (1927); **47**, 174 (1928).

[2] For a discussion of ordinary multiplet separations and the different vector couplings see S. Goudsmit, Phys. Rev. **31**, 946 (1928); S. Goudsmit and C. J. Humphreys, Phys. Rev. **31**, 960 (1928).

The interaction energy between the nuclear magnetic moment and the extranuclear electrons has not yet been treated in a satisfactory way. A treatment based on the classical vector model has been given by Pauling and Goudsmit.[3] Hargreaves[4] gave a quantum mechanical treatment in which however he neglected the interaction between the nucleus and the electron spin, which for small $l$ is of the same order as the interaction with the orbital moment. Finally the calculations of Casimir,[5] which take into account both interactions, can be applied only in the simple case of a single outer electron. The common result of all the calculations is that the interaction energy will be of the form

$$A\,ij\cos(ij) \tag{1}$$

which might be stated as the interval rule. Using the quantum mechanics expressions for the cosines (1) becomes

$$Aij\left[\frac{f(f+1)-i(i+1)-j(j+1)}{2ij}\right].$$

The separation between states $f+1$ and $f$ is therefore

$$A\left[\frac{(f+1)(f+2)-f(f+1)}{2}\right]=A(f+1). \tag{1'}$$

The separation is proportional to the largest $f$ of the two states. As an example, let us consider the unassigned bismuth term 49461 with $j=1\frac{1}{2}$, $i=4\frac{1}{2}$ and $f$ consequently 6, 5, 4, 3, with separations respectively 0.563, 0.473, 0.379 $cm^{-1}$. That these separations are proportional to the larger $f$ may be seen by dividing respectively by it to obtain the interval unit A = 0.094, 0.095, 0.095. As another example consider the bismuth term $6p^3\,{}^2P_{1/2}$ with $j=1/2$, and $i=4\frac{1}{2}$ giving two states with $f=5$, 4. The measured separation is 1.875 $cm^{-1}$ giving an interval unit of 0.375 $cm^{-1}$.

As the results of Casimir show, the interaction energy between the electron spin and the nucleus for the case of an electron in an $s$ state, where $l$ is 0, is proportional to the cosine between $i$ and $s$, i.e.

$$ais\cos(is). \tag{2}$$

This expression does not hold for other states. In quantum mechanics an $s$ state differs considerably from the orbital picture of the atom. One must consider for an $s$ state that the charge distribution representing the electron, surrounds the nucleus completely whereas in the classical picture the nucleus and the electron are separated. This explains the fact that for an $s$ state, the results obtained by Casimir on the basis of the quantum mechanics show that the most stable state for the nucleus is with its magnetic moment in the same

[3] L. Pauling and S. Goudsmit, "The Structure of Line Spectra," McGraw-Hill, now being published.

[4] J. Hargreaves, Proc. Roy. Soc. **A124**, 568 (1929).

[5] We are greatly indebted to H. B. G. Casimir in Leiden for the use of his unpublished work on the study of the nuclear spin problem.

direction as the magnetic moment of the electron, meaning that if $i=\frac{1}{2}$, of the two states $f=0$ and 1, the former will be the lower, which is the opposite to what is expected on the classical theory. This result means that the constant $a$ is positive.

This factor $a$ comes out to be proportional to the ratio of the magnetic and mechanical moment of the nucleus and to $Z^3/n^3$ for the state under consideration. For deeply penetrating orbits

$$a \sim Z_i z^2/n^3_{eff} \tag{3}$$

where $Z_i$ is the nuclear charge effective for the inner part of the orbit, $z$ is the effective nuclear charge outside the electron core, and $n_{eff}$ is the Rydberg denominator. The actual numerical factor occurring in $a$ is however not known with certainty.

The interaction energy between $i$ and $ap$, $d$ or $f$ electron is of a more complicated nature as it involves an interaction with both the orbit and the spin. It is very probable that in this case the correct quantum mechanics treatment will differ considerably from the treatment with the help of the classical atomic model. It is therefore possible to consider here the hyperfine structure separations of only those configurations which involve a deeply penetrating $s$ electron* which is supposed to contribute the main part of the hyperfine structure and we shall therefore be interested in the evaluation of $\overline{\cos(is)}$.

For two $s$ electrons, the interaction energy may be calculated completely in terms of each of the electrons. If the subscripts denote the two electrons, the interaction energy is given by

$$a_1 i s_1 \overline{\cos(is_1)} + a_2 i s_2 \overline{\cos(is_2)}$$

remembering that $s_1$ and $s_2$ form the resultant moment $j$ the average cosines can be worked out and one obtains

$$ij \cos(ij)\left[\frac{a_1 s_1}{j}\cos(s_1 j)+\frac{a_2 s_2}{j}\cos(s_2 j)\right]. \tag{5}$$

The expression between the brackets is thus the constant of expression (1). Substituting the quantum mechanics expressions for the cosines one obtains

$$A = a_1 \frac{j(j+1)+s_1(s_1+1)-s_2(s_2+1)}{2j(j+1)} + a_2 \frac{j(j+1)+s_2(s_2+1)-s_1(s_1+1)}{2j(j+1)} \tag{6}$$

In the case of two $s$ electrons this reduces to

$$A = \tfrac{1}{2}a_1 + \tfrac{1}{2}a_2. \tag{7}$$

It is quite probable that this expression (6) can be applied to more complicated cases where an $s$ electron is added to a general multiplet $S$-state of the preceding ion.

* Added to Proof: In a recent letter to the Editor in Phys. Rev. H. E. White also considers the hyperfine structure in the case of a deeply penetrating $s$ electron arriving at qualitatively the same results as obtained in this paper.

In the case of an $s$ electron and an arbitrary other electron the evaluation of $a\ is\ \overline{\cos\ (is)}$ depends upon the type of coupling of the quantum vectors of the extranuclear electrons. For Russell-Saunders coupling

$$a_1 i s_1\ \overline{\cos\ (i s_1)} = a_1 i s_1 \cos\ (ij) \cos\ (js) \cos\ (s s_1). \tag{8}$$

It must be remembered that in this expression the interaction with the $s$ electron alone is taken into account and the interaction with the other electrons is regarded as negligible.

$$a_1 i s_1\ \overline{\cos\ (i s_1)} = ij\ \cos\ (ij) \left[ a_1 \frac{s_1}{j} \cos\ (s_1 s)\ \cos\ (sj) \right]. \tag{9}$$

The expression in brackets is again the constant $A$ of (1). Substituting the quantum mechanics cosines we get

$$A = a_1 \frac{s(s+1)+s_1(s_1+1)-s_2(s_2+1)}{2s(s+1)} \cdot \frac{j(j+1)+s(s+1)-l_2(l_2+1)}{2j(j+1)}. \tag{10}$$

In case of two electrons where $s_1 = s_2 = \frac{1}{2}$

$$A = a_1 \frac{j(j+1)+s(s+1)-l_2(l_2+1)}{4j(j+1)}. \tag{11}$$

Equation (10) will also be applicable in the case where one has the $s$ electron added to a more general configuration than a single electron, meaning that $s$ can have values other than $\frac{1}{2}$.

In $(j, j)$ coupling a similar treatment gives

$$a_1 i s_1\ \overline{\cos\ (i s_1)} = a_1 i s_1 \cos\ (ij) \cos\ (j s_1)$$

$$= ij\ \cos\ (ij) \left[ \frac{a_1 s_1}{j} \cos (j s_1) \right]$$

$$A = a_1 \frac{j(j+1)+s_1(s_1+1)-j_2(j_2+1)}{2j(j+1)}. \tag{12}$$

There exist relations between the values of $A$ in the case of Russell-Saunders coupling and in the case of the $(j, j)$ coupling which are similar to the well-known sum rule of the Landé $g$ values. For instance, if for a given configuration a certain $j$ value occurs for only one level the value of $A$ for this level will be the same for all couplings. Expression (11) can easily be connected with the Landé $g$ value. Comparison with the well-known $g$ formula gives at once

$$A = \tfrac{1}{2} a_1 (g-1). \tag{13}$$

A similar but more complicated expression can be found in the case of the $(j, j)$ coupling.

## Applications

*Cadmium I.* Table I gives the $5s\ ns$ and $5s\ 5p$ configurations of Cd I[6] for

[6] H. Shüler and H. Brück, Zeits. f. Physik **56**, 291 (1929). S. Goudsmit, Naturwiss. **17**, 805 (1929).

which the Russell-Saunders coupling holds and for which (7) or (11) can be applied.

TABLE I. *Cadmium I. Hyperfine structure.*

| Configuration | $\Delta\nu$ | Form. (1′) | $A$ | $a_1$ |
|---|---|---|---|---|
| $5s6s\ ^3S_1$ | 0.396 cm$^{-1}$ | $3A/2$ | $a_1/2+a_2/2$ | |
| $5s7s\ ^3S_1$ | 0.369 | $3A/2$ | $a_1/2+a_2'/2$ | |
| $5s8s\ ^3S_1$ | 0.354 | $3A/2$ | $a_1/2+a_2''/2$ | |
| Limit | 0.35 | $3A/2$ | $a_1/2$ | 0.47 cm$^{-1}$ |
| $5s5p\ ^3P_2$ | 0.28 | $5A/2$ | $a_1/4$ | 0.44 |
| $^3P_1$ | 0.21 | $3A/2$ | $a_1/4$ | 0.55 |

The nuclear moment of cadmium is $\frac{1}{2}$ giving rise in every case to a doublet fine structure. In the tables the first column gives the configuration and term, the second column the separation, the third the separation from (1′) or the interval rule, the fourth gives $A$ in terms of the constant $a_1$ of the $s$ electron, and the fifth gives the value of $a_1$ determined from the separation. As the constants $a$ contain the factor $(1/n_{eff}^3)$ they will decrease rapidly with increasing quantum number $n$. This means that $a_1$ is expected to be much larger than $a_2$ and that furthermore $a_2$ will decrease going from $6s$ to $8s$. The values of $a_1$ obtained from the separations agree sufficiently well since the expressions are only approximate. This $a_1$ on the average is about 0.47 cm$^{-1}$ and this value leads to the prediction of the magnitude of the fine structure of the $5s\ ^2S_{\frac{1}{2}}$ of Cd II. This term will be split up into two levels, $f=1$ and $f=0$ with separation $a_1$ or 0.47 cm$^{-1}$.

*Thallium I.*[7] In this case the expressions can be applied to only the low state $7s\ ^2S_{\frac{1}{2}}$.

TABLE II. *Thallium I. Hyperfine structure.*

| Configuration | $\Delta\nu$ | Form. (1′) | $A$ | $a_1$ |
|---|---|---|---|---|
| $6s^27s\ ^2S_{1/2}$ | 0.40 cm$^{-1}$ | $A$ | $a_1$ | 0.40 cm$^{-1}$ |

*Thallium II.* For the $6s\ 7s\ ^3S_1$ we can use (II). From thallium I the $a$ for the $7s$ electron was found to be 0.40 cm$^{-1}$; according to (3) the $a$ for the same electron in thallium II will be about 4 times as large, or 1.60 cm$^{-1}$. This value has been used for the calculation of $a_1$ for the $6s$ electron in Table III.

TABLE III. *Thallium II. Hyperfine structure.*

| Configuration | $\Delta\nu$ | Form. (1′) | $A$ | $a_1$ |
|---|---|---|---|---|
| $6s7s\ ^3S_1$ | 5.1 cm$^{-1}$ | $3A/2$ | $a_1/2+a_2/2$ | 5.2 cm$^{-1}$ |
| $6s6p\ ^3P_2$ | 3.5 | $5A/2$ | $a_1/4$ | 5.6 |
| $^1P_1$ | 0 | $3A/2$ | 0 | — |
| $6s7p\ ^3P_2$ | 3.4 | $5A/2$ | $a_1/4$ | 5.4 |
| $^3P_1$ | 3.9 | $3A/2$ | $a_1/2$ | 5.2 |
| $[^1P_1]$ | −0.6 | $3A/2$ | $-a_1/4$ | — |
| $6s6d\ ^3D_2$ | 1.6 | $5A/2$ | $a_1/12$ | 7.7 |
| $^3D_1$ | −2.0 | $3A/2$ | $a_1/4$ | 5.3 |
| $^1D_2$ | 2.4 | $5A/2$ | 0 | — |
| $6s7d\ ^3D_3$ | 3.6 | $7A/2$ | $a_1/6$ | 6.2 |
| $^3D_2$ | 0.6 | $5A/2$ | $a_1/12$ | 2.9 |
| $^3D_1$ | −2.3 | $3A/2$ | $-a_1/4$ | 6.1 |
| $^1D_2$ | 0.3 | $5A/2$ | 0 | — |

[7] E. Back, Ann. d. Physik **70**, 333 (1923). H. Schüler and H. Brück, reference 6.

The $6s\ 7p$ configuration of thallium II is certainly much nearer to the $(j, j)$ coupling than to Russell-Saunders coupling as can be seen from an examination of the position of the singlet and triplet terms and in this case we must use (12). The $6s\ 6d$ follows the Russell-Saunders coupling again. The values of $a$ given in the last column agree satisfactorily particularly for those terms for which the separations are known with some certainty. The values of $\Delta\nu$ given in Table III have been recalculated with the use of proper intensity relations from the observed lines of McLennan, McLay and Crawford[8] and according to them have an error of about 0.5 $cm^{-1}$. For $6s\ 7p\ {}^1P_1$ a separation of $-3.4$ would be expected but of the two possibilities for that term both show a separation of about 0.5. The $6s\ 6d\ {}^1D_2$ separation observed is much too large. Especially interesting is the inversion of the ${}^3D_1$ terms.

The values of $a$ are somewhat irregular to show with certainty the effect of different screening with different outer electrons. The value of $a$ for the $6s$ electron in case the second electron is removed completely will probably be about 7 or 8 $cm^{-1}$. This will be the doublet separation of the hyperfine structure of the $6s\ {}^2S_{\frac{1}{2}}$ state of thallium III.

*Lanthanum I and II.* In lanthanum only a preliminary paper by Meggers and Burns[9] has been published, the few results which are certain, are in agreement with the theory developed here. The fine structure seems to occur only in those terms involving a single $6s$ electron. Table IV gives the results of the $5d\ 6s$ configuration of lanthanum II which is an interesting intermediate case between Russell-Saunders and $(j, j)$ coupling, and the equations derived here are valid only for the ${}^3D_1$ and ${}^3D_3$ state for which all couplings give the same. The hyperfine structure of ${}^3D_3$ makes it probable that $i=2$, however the splitting up of the $5d\ 6s\ {}^1D_2$ does not agree with expectations. The agreement of the $a_1$ of La I with the $a_1$ of La II seems to be entirely accidental.

TABLE IV. *Lanthanum. Hyperfine Structure.*

| La II Configuration | $\Delta\nu$ (total) | Form. (1) | $A$ | $a_1$ |
|---|---|---|---|---|
| $5d6s\ {}^3D_3$ | 0.71 $cm^{-1}$ | $14A$ | $a_1/6$ | 0.30 $cm^{-1}$ |
| ${}^3D_1$ | $-0.375$ | $5A$ | $-a_1/4$ | 0.30 |
| La I Configuration | $\Delta\nu$ | Form (1) | $A$ | $a_1$ |
| $5d^26s\ {}^4F_{1\frac{1}{2}}$ | $-0.46$ | $5A/2$ | $-a_1/5$ | 0.30 |
| ${}^4F_{2\frac{1}{2}}$ | [+0.04]* | $12A$ | $a_1/105$ | |
| ${}^4F_{3\frac{1}{2}}$ | [+0.38]* | $16A$ | $5a_1/63$ | |
| ${}^4F_{4\frac{1}{2}}$ | [+0.67]* | $20A$ | $a_1/9$ | |

* Predicted values.

[8] J. C. McLennan, A. B. McLay, and M. F. Crawford, Proc. Roy. Soc. **A125**, 570 (1929).

[9] W. F. Meggers and K. Burns, J.O.S.A. **14**, 449 (1927). The uncertainty in $i$ has little effect on the results derived here.

*DECEMBER 15, 1929* *PHYSICAL REVIEW* *VOLUME 34*

# ON THE ZEEMAN EFFECT IN DOUBLET BAND SPECTRA

By E. L. Hill*
Jefferson Physical Laboratory, Harvard University

(Received November 4, 1929)

Abstract

A theoretical investigation is given of the Zeeman effect for doublet bands of diatomic molecules which are included in the type forms of Hund's cases (a) and (b). With case (b) as a starting point, using the perturbation theory of the new quantum mechanics, the magnetic terms are first treated as a small correction to the coupling energy between the electron spin and orbital magnetic moments.

In the next approximation the terms which lead to a Paschen-Back effect are included. The physical interpretation according to which the term system degenerates into that due to a free spin electron plus that due to a symmetrical top, is discussed briefly in its relation to the experimentally observable patterns. The formal mathematical solution is then given and briefly discussed.

## Introduction

IN VIEW of some experimental work which has been carried out in this laboratory[1] on the Zeeman effect in the 5211A band of MgH, it has become of interest to extend previous theoretical work on the effect of a magnetic field on the spectra of diatomic molecules. We shall consider only molecules which can be included in the type form of Hund's case (a) or (b), or which are intermediate between these limiting cases. Hund has considered the general arrangement of the magnetic terms for the limiting cases.[2] Van Vleck has also considered the question[3] from a qualitative point of view, and on the basis of Hund's analysis and an assumed behavior for the spin electron in strong magnetic fields, has proposed a scheme which might be expected to account for some abnormally large Zeeman patterns which had previously been observed experimentally. The basic idea of the theory is that of a gradual uncoupling (Paschen-Back) effect of the electron spin from the rest of the molecule by the magnetic field, and a consequent degeneration of the term system into that

* National Research Fellow.

[1] F. H. Crawford and G. M. Almy, Phys. Rev. **33,** 1084 (1929). See also the following paper in this issue.

[2] F. Hund, Zeits. f. Physik **36,** 657 (1926). For various other papers dealing with different phases of the Zeeman effect in band spectra see:

E. C. Kemble, Chapter VII, Sec. 6 of Bulletin 57 of the National Research Council, "Molecular Spectra in Gases."

E. C. Kemble, R. S. Mulliken, and F. H. Crawford, Phys. Rev. **30,** 438 (1927).

E. U. Condon, Phys. Rev. **30,** 781 (1927).

R. de L. Kronig, Phys. Rev. **31,** 195 (1928); Zeits. f. Physik **46,** 814 (1928); Ibid., **50,** 347 (1928).

W. Watson and B. Perkins, Jr., Phys. Rev. **30,** 592 (1927).

F. H. Crawford, Phys. Rev. **33,** 341 (1929).

[3] J. H. Van Vleck, Phys. Rev. **28,** 980 (1926).

due to a free spin on which is superposed the pattern due to a symmetrical top. At that time the theory was mainly suggestive, although its general correctness was undoubted, but it is the purpose of the present paper to put it on a more definite footing by applying to it the methods of the new quantum mechanics. We are thus enabled to follow quantitatively the progression from zero to strong fields. The reader is referred to the following paper in this issue for a discussion of the relation of the theoretical predictions to the experimental data in the above-mentioned band of MgH.

*Notation.* At present the symbolic designations for the various quantum numbers in diatomic molecules are by no means standard. In this paper we shall conform to some suggestions for a standard notation which have been recently communicated to us by Professor R. S. Mulliken. For the convenience of the reader a conversion table from the symbols used in reference 4 to those used in the present paper is appended. The reader is referred to reference 4 for a complete discussion of the meanings of these symbols.

| | |
|---|---|
| Reference 4. | $k, s, \sigma_k, \sigma_s, \sigma, j_k, j, m, m_k, m_s, S, P, D, \cdots$ |
| Present | $L, S, \Lambda, X, \Omega, K, J, M, M_k, M_s, \Sigma, \Pi, \Delta, \cdots$ |

## Hamiltonian Function

Let $(xyz)$ be a fixed set of Cartesian axes in space such that the external magnetic field is symmetrical about the $z$-axis, the field strength being $H$ (gauss). We shall start with Hund's case (b) as an appropriate unperturbed system. Equivalent results could undoubtedly be obtained by starting at case (a), and have been partially so obtained by the author (through stage I) but the complete analysis involving the Paschen-Back effect of the spin is analytically more complicated by such a procedure.

The perturbative terms in which we are interested are of two types; 1) the coupling energy, $H_1$, between $S$ and $L$, and 2) the added terms due to the presence of the magnetic field, with the Hamiltonian $H_2$. As usual we shall assume that the energy differences associated with different values of $\Lambda$ are large compared to the energy differences of adjacent rotational states, so that we may average $H_1$ over the precession of $L$ about the nuclear axis. Assuming the applicability of the "cosine" law of interaction between $S$ and $L$ we get[5]

$$H_1 = A(\Lambda \cdot S) = A(\Lambda_x S_x + \Lambda_y S_y + \Lambda_z S_z), \tag{1}$$

where $A$ is a constant.

In $H_2$ we retain only terms linear in $H$, and neglect the small magnetic moment due to the nuclear rotation, so that[6]

$$H_2 = (He/4\pi mc^2)(\Lambda_z + 2S_z). \tag{2}$$

[4] Cf. E. L. Hill and J. H. Van Vleck, Phys. Rev. **32**, 250 (1928) for a calculation very similar to that of the present paper.

[5] All energies are expressed in $cm^{-1}$.

[6] In this paper we shall neglect the small "rho-type" doubling which is present in $^2\Sigma$ states. On this account we cannot get complete agreement between theory and experiment for high rotational levels as the formula will not predict the proper doublet separations even in the absence of a field for transitions beginning or ending on a $^2\Sigma$ level.

The matrix elements of $H_1$ have already been derived (reference 4, Eqs. (16) and (17)). To find the matrix elements of $\Lambda_z$ we have only to use the unnumbered equation in the middle of p. 258 of reference 4 in conjunction with the case (b) amplitude matrices (reference 4, Eq. (9)).[7] To derive the matrix elements of $S_z$ we use an argument based on the discussion of the case (b) amplitude elements given on p. 254 of reference 4. We first note that as $S$ is involved only in the precessions about $J$ and about the axis of the external field, $S_z$ will be diagonal in all quantum numbers except $J$. Furthermore, as the vectors $S$ and $K$ play quite analogous roles in the precession about $J$, we need only take those amplitude elements from Eq. (9) which are diagonal in $K$, inter-change the quantum numbers $K$ and $S$ in them, and then normalize the $B$-factors so that $\sum_{J'\,M'}(S_x^2+S_y^2+S_z^2)\,(J,\,M;\,J',\,M')=S(S+1)$. Lastly we must multiply each of the elements of $S_x$, $S_y$, and $S_z$ for which $J'=J\pm1$ by a factor $(-1)$ in order to take account of the fact that $S$ and $K$ are coupled vectorially, and so have slightly different phases.

As the final result of this analysis we find for the elements of the complete perturbing function $H_p=H_1+H_2$:

$$
\begin{aligned}
H_p(K,J;\,K+1,J+1)&=\Lambda(\Delta\nu_n)\left\{\frac{Q(K+1;\Lambda)E(J+1;K;S)E(J+2;K;S)Q(J+1;M)}{4U(K+1)U(J+1)}\right\}^{1/2}\\
H_p(K,J;\,K+1,J)&=\Lambda\left(A+\frac{(\Delta\nu_n)M}{J(J+1)}\right)\left\{\frac{Q(K+1;\Lambda)E(J+1;K;S)F(J-1;K;S)}{4U(K+1)}\right\}^{1/2}\\
H_p(K,J;\,K+1,J-1)&=-\Lambda(\Delta\nu_n)\left\{\frac{Q(K+1;\Lambda)F(J-1;K;S)F(J-2;K,S)Q(J;M)}{4U(K+1)U(J)}\right\}^{1/2}\\
H_p(K,J;\,K,J+1)&=(\Delta\nu_n)\left[\frac{Q(J+1;M)}{U(J+1)}\right]^{1/2}\left\{[E(J+1;S;K)F(J;S;K)]^{1/2}\right.\\
&\qquad\left.-\left(\frac{\Lambda^2}{2K(K+1)}\right)[E(J+1;K;S)F(J;K;S)]^{1/2}\right\}\\
H_p(K,J;\,K,J)&=\left(\frac{(\Delta\nu_n)M}{J(J+1)}\right)\left\{G(J;S;K)+\left(\frac{\Lambda^2}{2K(K+1)}\right)G(J;K;S)\right\}-\left(\frac{A\Lambda^2}{2K(K+1)}\right)G(K;S;J),
\end{aligned}
\tag{3}
$$

where

$$
\left.\begin{aligned}
&E(a\,;b\,;c)=(a+b)(a+b+1)-c(c+1)\,;\,F(a\,;b\,;c)=c(c+1)-(a-b)(a-b+1);\\
&G(a\,;b\,;c)=a(a+1)+b(b+1)-c(c+1)\,;\,Q(a\,;b)=a^2-b^2;
\end{aligned}\right\}\tag{4}
$$

$$
\left.\begin{aligned}
U(a)&=a^2(2a-1)(2a+1)\\
\Delta\nu_n&=He/4\pi mc^2.
\end{aligned}\right\}\tag{5}
$$

The remaining elements can be obtained by using the Hermitian character of $H_p$; i.e., as all elements of $H_p$ are real, $H_p\,(K,\,J;\,K',\,J')=H_p\,(K',\,J';\,K,\,J)$. All elements are, of course, diagonal in $\Lambda$ and $M$.

[7] The following corrections are to be made in Eq. (9) of reference 4. In line 2 put $U(j+1)$ instead of $U(j)$; in lines 7 and 8 put $F(j,j_k)$ instead of $F(j+1,j_k)$.

The energy function of the unperturbed system can be written as the sum of two parts; i.e., $W_0+H_r$, where $W_0$ does not involve the quantum numbers[8] $K, J, M$, while $H_r$ is the diagonal matrix whose elements are

$$H_r(\Lambda, K, J, M\ ;\ \Lambda, K, J, M) = B[K(K+1)-\Lambda^2] \tag{6}$$

where

$$B = h/8\pi^2 cI. \tag{7}$$

As $W_0$ does not contain any of the quantum numbers in which $H_p$ has off-diagonal elements, it does not enter into any of the calculations, and will not be mentioned specifically again.

*Interaction with Λ-type doubling.* In the perturbing Hamiltonian as given above we have listed only terms within a given electronic multiplet $(n, v, \Lambda)$, and have thus tacitly left out of account the terms which are chiefly responsible for the phenomenon of Λ-type doubling. From the theoretical work of Kronig,[9] Wigner and Witmer,[10] and of Van Vleck,[11] on the symmetry properties of the wave equation, even inclusive of spins, it follows that the approximate wave functions associated with the two Λ-levels (levels with a given $|\Lambda|$) are respectively even and odd with respect to a "reflection in the origin." As our perturbing function, inclusive of magnetic terms, is even with respect to this transformation, it contains no terms connecting these so-called + and − levels, which may thus still be treated separately. These we treat in the usual manner, assuming that the electronic states are really widely separated as compared to adjacent rotational levels, and so consider first the perturbations of the terms within each electronic state separately. Inclusion of the terms non-diagonal in Λ would give the Λ-doubling corrections.

## Calculation of Term Values

Because of the fact that our perturbing function $H_p$ has elements off-diagonal in two quantum numbers, $K$ and $J$, the term values can be found only by approximation methods. As a preliminary step let us separate $H_p$ into two parts which we shall call $H_p'$ and $H_p''$ respectively. $H_p'$ shall consist of all elements of $H_p$ which are diagonal in $J$, thus having elements which are off-diagonal as well as diagonal in $K$. $H_p''$ shall consist of all remaining elements of $H_p$, and thus in particular has no elements diagonal in $J$. This division of the calculation into two parts simplifies the analysis, as $H_p'$ includes all of the terms of $H_p$ which are responsible for rotational distortion in addition to some of the small magnetic terms, and represents the Hamiltonian to be associated with a molecule in a state intermediate between (b) and (a) in which the magnetic field produces only a small perturbation, while $H_p''$ contains the terms which lead to the Paschen-Back effect. In stage I of the calculation we use $H_p'$ alone, neglecting $H_p''$, while stage II contains the considerations relative to $H_p''$.

*Stage I.* The elements of the matrix $H_p'$ associated with a given state $(\Lambda, J, M)$ are found from (3) to be, on substituting $S=\frac{1}{2}$, $K=J\pm\frac{1}{2}$,

[8] We neglect explicitly the dependence of the vibrational energy on the quantum numbers $K, S, J$, as well as the variation of $B$ with the rotational state.

[9] R. de L. Kronig, Zeits. f. Physik **46**, 814 (1928); **50**, 347 (1928).

[10] E. Wigner and E. Witmer, Zeits, f. Physik **51**, 859 (1928).

[11] J. H. Van Vleck, Phys. Rev. **33**, 467 (1929).

$$
\begin{aligned}
H_p'(J_1;J_1) &= B\{-\beta J[1-\Lambda^2/(J+\tfrac{1}{2})]-\lambda\Lambda^2/(2J+1)\}\\
H_p'(J_1;J_2) &= H_p'(J_2;J_1) = B\{(\lambda+\beta)\Lambda/(2J+1)\}\{(J+\tfrac{1}{2})^2-\Lambda^2\}^{1/2}\\
H_p'(J_2;J_2) &= B\{\beta(J+1)[1+\Lambda^2/(J+\tfrac{1}{2})]+\lambda\Lambda^2/(2J+1)\},
\end{aligned}
\tag{8}
$$

where

$$
\begin{aligned}
\beta &= (\Delta\nu_n/B)(M/J(J+1))\\
\lambda &= A/B.
\end{aligned}
\tag{9}
$$

The unperturbed energy has the elements

$$
\begin{aligned}
H_r(J_1;J_1) &= B[(J+\tfrac{1}{2})(J+\tfrac{3}{2})-\Lambda^2]\\
H_r(J_2;J_2) &= B[(J^2-\tfrac{1}{4})-\Lambda^2].
\end{aligned}
\tag{10}
$$

The notation $J_1$ refers to the spin component for which $K=J+\frac{1}{2}$, and similarly $J_2$ refers to the component for which $K=J-\frac{1}{2}$. The energies can now be found by solving the usual determinantal equation:

$$
0=\begin{vmatrix} (H_r+H_p')(J_1;J_1)-W & H_p'(J_1;J_2) \\ H_p'(J_2;J_1) & (H_r+H_p')(J_2;J_2)-W \end{vmatrix}
\tag{11}
$$

the roots of which are readily found to be

$$
\begin{aligned}
W(\Lambda,K,J,M) = B\{&(J+\tfrac{1}{2})^2-\Lambda^2+\beta(\Lambda^2+\tfrac{1}{2})\\
&\pm\tfrac{1}{2}[(2J+1)^2(1-\beta)^2+\Lambda^2(\lambda+\beta)(\lambda-4+5\beta)]^{1/2}\},
\end{aligned}
\tag{12}
$$

where the upper sign is to be associated with the $J_1$ state; i.e. with $K=J+\frac{1}{2}$. It may be remarked that if we set $\beta=0$; i.e., $H=0$, (12) reduces to the rotational distortion formula (reference 4, Eq. (27)).

If one is interested only in the dependence of (12) on the magnetic field, it is probably a sufficiently accurate procedure to expand as a power series in $(\beta)$ and retain terms of first order only, thus

$$
W(\Lambda,K,J,M)\cong B\{(J+\tfrac{1}{2})^2-\Lambda^2\pm\tfrac{1}{2}\gamma+\beta(\Lambda^2+\tfrac{1}{2})\pm(\beta/2\gamma)[-(2J+1)^2+\Lambda^2(3\lambda-2)]\},
\tag{12'}
$$

where

$$
\gamma=[(2J+1)^2+\lambda(\lambda-4)\Lambda^2]^{1/2}.
$$

The next term of second degree in the small quantity $(\Delta\nu_n/B)$ with a coefficient of the order of $(1/J)$, is ordinarily quite negligible. The dependence of (12′) on $\beta$ could also have been determined directly from the perturbation theory for non-degenerate systems by employing the case (b) transformation function $S$ (reference 4, Eq. (33)) and the formula

$$
\Delta W(K,J,M)=\sum_{K'\,K''} S(K,J;K',J)H_2(K',J,M;K'',J,M)S(K,J,M;K'',J,M).
$$

This procedure would amount to first removing the degeneracy associated with $H_1$ by means of the transformation $S$, and then considering $H_2$ as a small correction term.

*Stage II.* The perturbative Hamiltonian $H_p''$ which we have so far neglected, contains interaction terms between levels with values of $J$ differing by one unit and values of $K$ which may or may not differ. Up to the present we have assumed that such terms do not lie close enough together to influence one another appreciably. This, however, is by no means a sufficient approximation,

for if we consider the arrangement of terms as a function of the parameter $\lambda$ in the absence of an external field ($\beta=0$), we find that for $\lambda \leqq 0$ and $\lambda \leqq 4$, levels differing by an unit in $J$, but having the same value of $K$ lie very close together. The same is true for high rotational states even in molecules where $\lambda$ differs appreciably from these critical values (e.g., in the upper level for the 5211A band of MgH where $\lambda \sim 6$). This behavior of the terms is predicted by (12) and is also found experimentally.[12] We must accordingly make a second transformation in order to eliminate these terms from $H_p''$. That it is not a valid procedure to use the perturbation theory of non-degenerate systems follows from the fact that such a calculation would be made by a series expansion in terms of the parameter $(\Delta\nu_n/\nu(K, J; K, J'))$ where $h\nu\ (K, J, M; K, J', M) = W(K, J, M) - W(K, J', M)$. We have just seen that this quantity may become very large.

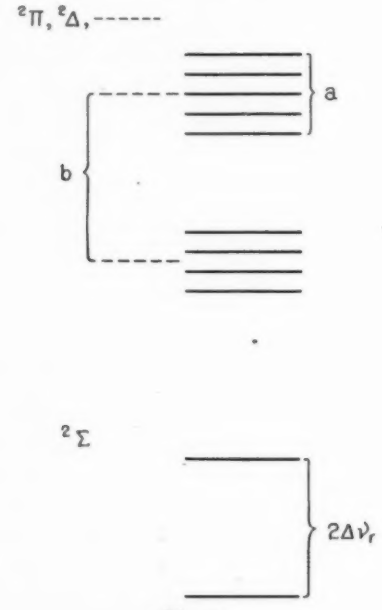


Fig. 1.

The physical interpretation of this phenomenon has already been discussed by Van Vleck,[3] but we shall repeat and amplify the argument here in order to elucidate the mathematical formalism. Levels of the type just mentioned, having the same value of $K$ but different values of $J$, compose the so-called "spin-doublets" ($S=\frac{1}{2}$), and their separations are measured by the magnitude of the coupling between $S$ and $\Lambda$. If the separations of these levels are small, so that the effective forces between $S$ and the rest of the molecule are weak, the magnetic field may be strong enough to over-power these forces and to partially or wholly uncouple $S$ from the rest of the molecule. In the limit in which the Zeeman separations are great compared to the spin doublet separations, $S$ becomes completely free from the rest of the molecule, and is

[12] Cf. especially R. S. Mulliken, Phys. Rev. **32**, 388 (1928).

quantized parallel or anti-parallel to the axis of the external field. In this limit the term system should consist of the terms due to a symmetrical top superposed on the two states for the free spin in the magnetic field. In a $^2\Sigma$ state, neglecting the presence of the small "rho-type" doubling, the part due to the top should be absent, so that each rotational level splits into a doublet with separation $(2\Delta\nu_n)$ in the field. The more general condition as existing in $^2\Pi$, $^2\Delta$, $\cdots$ states is roughly as shown in Fig. 1. From the Zeeman formulae for the symmetrical top,[13] it can be seen that "a," which is approximately the pattern width due to a symmetrical top, vanishes $\sim 1/K$, the number of levels in the group increasing as $K$, and the separations between the individual components decreasing as $1/K(K+1)$. The deviation of "b" from $(2\Delta\nu_n)$ is a rough measure of the interaction energy between $S$ and $\Lambda$.

In the limit of a field sufficiently strong to practically break down the coupling between $S$ and $\Lambda$, one can introduce the value of the component of $S$ along the axis of the external field as a quantum number; i.e., $M_s=\pm\frac{1}{2}$. The transitions which give rise to the spectral lines can be divided into four types: 1) $M_s'=\frac{1}{2}\rightarrow M_s''=\frac{1}{2}$; 2) $M_s'=-\frac{1}{2}\rightarrow M_s''=-\frac{1}{2}$; 3) $M_s'=\frac{1}{2}\rightarrow M_s''=-\frac{1}{2}$; 4) $M_s'=-\frac{1}{2}\rightarrow M_s''=\frac{1}{2}$. Transitions of types 1) and 2) give rise to two superposed (unresolved) patterns clustering about the average position of the no-field doublets on the photographic plate. Transitions of types 3) and 4) give rise to two "wings" spaced approximately symmetrically with respect to the central pattern, and with a separation that approaches $(4\Delta\nu_n)$ as the magnetic field is increased, or as one proceeds out in the band to successively higher rotational states. It may be remarked that the decrease in intensity of the outer "wings" with increasing magnetic field (or molecular rotation) is directly attributable to the selection rule $\Delta M_s=0$ which may be expected to obtain accurately in the limit. The reader is referred to the following paper in this issue for a discussion of these relations in the band MgH $\lambda$5211.

In putting these considerations into mathematical dress, we must first find the transformation function $T$ appropriate to the determinantal Eq. (11). According to standard perturbation theory we have only to solve the set of linear equations obtained from the single matrix equation

$$T(H_r+H_p')=WT, \tag{13}$$

the elements of $T$ to be normalized to satisfy the condition

$$TT^{-1}=1. \tag{14}$$

The following solution may readily be shown to satisfy (13) and (14)

$$\begin{aligned} T(J_1, M\,;J_1, M)&=T(J_2, M\,;J_2, M)=\left\{\left[\tau(J, M)+\omega(J, M)\right]/2\tau(J, M)\right\}^{1/2}\\ T(J_1, M\,;J_2, M)&=-T(J_2, M\,;J_1, M)=\left\{\left[\tau(J, M)-\omega(J, M)\right]/2\tau(J, M)\right\}^{1/2}, \end{aligned} \tag{15}$$

where

$$\begin{aligned} \tau(J, M)&=\left\{(2J+1)^2(1-\beta)^2+\Lambda^2(\lambda+\beta)(\lambda-4+5\beta)\right\}^{1/2}\\ \omega(J, M)&=\left\{(2J+1)(1-\beta)-\Lambda^2(\lambda+\beta)/(J+\tfrac{1}{2})\right\}. \end{aligned} \tag{16}$$

[13] Cf. e. g., D. M. Dennison, Phys. Rev. **28**, 318 (1926); E. U. Condon, Phys. Rev. **30**, 781 (1927).

The perturbing function in the new system of quantization is given by the matrix

$$TH_p''T^{-1} \tag{17}$$

for which the element $(K, J, M; K', J', M)$ is given by

$$\sum_{K'',K'''} T(K,J,M;\,K'',J,M)H_p''(K'',J,M\,;K''',J',M)T(K',J',M;\,K''',J',M) \tag{18}$$

as

$$T^{-1}(K''',J',M\,;\,K',J',M)=T(K',J',M\,;\,K''',J',M).$$

In the application of (18) it is sufficient to neglect the dependence of the elements of $T$ on the magnetic quantum number $M$ to the same degree of accuracy that one has in using (12′) in preference to (12). With this simplification $T$ becomes identical with the transformation function $S$ derived in the rotational distortion problem (reference 4, Eq. (33)).

An examination of (18) shows that the new perturbing function contains only terms connecting states for which $J'=J\pm 1$, as $H_p''$ has no terms diagonal in $J$, by definition. The elements connecting states for which $K'\neq K$ we discard as such levels do not ordinarily lie close to each other. The remaining elements, connecting states for which $J=K\pm\frac{1}{2}$, are readily found from (18) using the matrix elements of $H_p''$ from (3), the result being

$$\begin{aligned}\delta B/2=(\Delta\nu_n)&\left\{\frac{(K+\frac{1}{2})^2-M^2}{(K+\frac{1}{2})^2}\right\}^{1/2}\\ \times\Bigg[&\left\{\frac{\tau(K+\frac{1}{2})+\omega(K+\frac{1}{2})}{2\tau(K+\frac{1}{2})}\right\}^{1/2}\left\{\frac{\tau(K-\frac{1}{2})+\omega(K-\frac{1}{2})}{2\tau(K-\frac{1}{2})}\right\}^{1/2}\left\{1-\frac{\Lambda^2}{2K(K+1)}\right\}\\ &+\left\{\frac{\tau(K+\frac{1}{2})+\omega(K+\frac{1}{2})}{2\tau(K+\frac{1}{2})}\right\}^{1/2}\left\{\frac{\tau(K-\frac{1}{2})-\omega(K-\frac{1}{2})}{2\tau(K-\frac{1}{2})}\right\}^{1/2}\left\{\frac{(K^2-\Lambda^2)\Lambda^2}{4K^2}\right\}^{1/2}\\ &-\left\{\frac{\tau(K+\frac{1}{2})-\omega(K+\frac{1}{2})}{2\tau(K+\frac{1}{2})}\right\}^{1/2}\left\{\frac{\tau(K-\frac{1}{2})+\omega(K-\frac{1}{2})}{2\tau(K-\frac{1}{2})}\right\}^{1/2}\left\{\frac{[(K+1)^2-\Lambda^2]\Lambda^2}{4(K+1)^2}\right\}^{1/2}\Bigg].\end{aligned} \tag{19}$$

The energies of the two states in question before the introduction of the perturbation (19) are found from (12) to be:

$$\left.\begin{aligned}W(K_1,M\,;K_1,M)&=f(K+\tfrac{1}{2},M)-\tfrac{1}{2}\tau(K+\tfrac{1}{2},M)=B\epsilon_1\\ W(K_2,M\,;K_2,M)&=f(K-\tfrac{1}{2},M)+\tfrac{1}{2}\tau(K-\tfrac{1}{2},M)=B\epsilon_2\end{aligned}\right\} \tag{20}$$

where

$$f(K-\tfrac{1}{2},M)=B\left\{K^2-\Lambda^2+(\Delta\nu_n/B)\left[M(\Lambda^2+\tfrac{1}{2})/(K^2-\tfrac{1}{4})\right]\right\}, \tag{21}$$

and where $K_1$ and $K_2$ refer to the components for which $J=K\pm\frac{1}{2}$ respectively. If $|M|\leqq K-\frac{1}{2}$ the energy values can be found from a second determinantal equation of exactly the same form as (11) using (19) and (20) instead of (8) and (10), the roots being

$$(B/2)\left[(\epsilon_1+\epsilon_2)\pm\left\{(\epsilon_1-\epsilon_2)^2+\delta^2\right\}^{1/2}\right]. \tag{22}$$

The allocation of the two roots (22) to the two levels concerned is at first sight ambiguous, inasmuch as the first term in the square root can also be written as $(\epsilon_2-\epsilon_1)^2$. This means that it is not sufficient to establish the correlation in the usual manner by the asymptotic relation of (22) with (20) when $\delta$ is formally set equal to zero. As a second condition we shall use a rule derived from perturbation theory[14] which states roughly that the first effect of a perturbation between two energy levels is to push them apart. Applying this to (22) we conclude that if $\epsilon_1>\epsilon_2$ the upper sign is to be assigned to the state $(K_1,M)$ and the lower sign to the state $(K_2,M)$; while if $\epsilon_2>\epsilon_1$ the reverse correlation should be used. To make the equation formally correct in the latter case for the asymptotic point $\delta=0$, one should write $(\epsilon_2-\epsilon_1)^2$ instead of $(\epsilon_1-\epsilon_2)^2$. This consideration is, in a sense, equivalent to determining the energy and its derivative (with respect to $\delta$) for each of the two states.

Formula (22) can be thrown into a form resembling the more usual expression used in atomic spectra[15] if we use (12′) instead of (12) to determine $\epsilon_1$ and $\epsilon_2$, and collect powers of $(\Delta\nu_n)$; i.e.,

$$\epsilon_1+\epsilon_2=\xi+\kappa(\Delta\nu_n)\ ;\qquad \epsilon_1-\epsilon_2=\nu_0+\alpha(\Delta\nu_n)\ ;\qquad \delta=\eta(\Delta\nu_n)$$

where $B\nu_0$ is the (algebraic) frequency separation[16] of the no-field doublet levels in $cm^{-1}$ while $\xi$, $\kappa$, and $\eta$, are complicated functions of the quantum numbers, which can be determined from (12′), (19), (20), and (21). Substituting these values in (22) we get

$$(B/2)\left[\xi+\kappa(\Delta\nu_n)\pm\left\{\nu_0^2+2\nu_0\alpha(\Delta\nu_n)+(\alpha^2+\eta^2)(\Delta\nu_n)^2\right\}^{1/2}\right]. \tag{22′}$$

## Special Cases

There are some particular cases included under the general formula (22) to which it seems well to give special consideration, partly because of their simplicity, and partly also because of certain ambiguities which might be encountered in the preceding formal treatment.

$^2\Sigma$ *States* $(\Lambda=0)$. From (12) we readily find that

$$\epsilon_1=K(K+1)+(\Delta\nu_n/B)(M/K+\tfrac{1}{2})\ ;\qquad \epsilon_2=K(K+1)-(\Delta\nu_n/B)(M/K+\tfrac{1}{2})\ ;$$

while

$$\delta=2(\Delta\nu_n/B)\left\{\frac{(K+\tfrac{1}{2})^2-M^2}{(K+\tfrac{1}{2})^2}\right\}^{1/2}$$

as from (16), $\tau(J,M)=\omega(J,M)$. With these values of its arguments (22) reduces to the very simple form

$$BK(K+1)\pm\Delta\nu_n \tag{23}$$

[14] F. Hund, Zeits. f. Physik **40**, 742 (1927); also for example the last section of E. C Kemble and C. Zener, Phys. Rev. **33**, 512 (1929).

[15] E. g., W. Heisenberg and P. Jordan, Zeits. f. Physik **37**, 263 (1926).

[16] See the preceding paragraph for consideration of the difficulties connected with the sign of $\nu_0$.

quite in agreement with our previous conclusion that if we neglect rho-type doubling, a magnetic field of any strength should be large enough to uncouple completely the spin from the rest of the molecule and quantize it with respect to the external field. The two signs in (23) are of course to be associated with $M_s = \pm\frac{1}{2}$ respectively.

$K=\Lambda$, $J=\Lambda-\frac{1}{2}$. This is the lowest level in ${}^2\pi$, ${}^2\Delta$, $\cdots$, electronic states, and is of considerable interest as it presents an anomalous behaviour in the correlation of levels between (a) and (b)[4,13]. Here the off-diagonal elements, (as well as the term in the lower right-hand corner) of (11) vanish, leaving as the only solution

$$B[\Lambda(1-\lambda/2)]+(\Delta\nu_n)M(\Lambda-1)/(\Lambda+\tfrac{1}{2}). \tag{24}$$

To this degree of approximation, this level for a ${}^2\Pi$ state ($\Lambda=1$) is magnetically dead as the term in $(\Delta\nu_n)$ vanishes. In carrying through the analysis of the perturbations between the levels $K=\Lambda$, $J=\Lambda-\frac{1}{2}$, $|M|\leqq\Lambda-\frac{1}{2}$, and the levels $K=\Lambda$, $J=\Lambda+\frac{1}{2}$, $|M|\leqq\Lambda+\frac{1}{2}$, everything goes through just as before except that now $\epsilon_2$ is given by (24), and $\delta$ may be simplified by using the condition $\tau(\Lambda-\frac{1}{2}, M)=\omega(\Lambda-\frac{1}{2}, M)$. (22) now predicts a small magnetic effect for the level $K=1$, $J=\frac{1}{2}$, in a ${}^2\Pi$ electronic state, but it is of practical importance only in case the separation of the doublet levels in the absence of a magnetic field is very small even at the origin.

*Levels for which* $M=\pm(K+\frac{1}{2})$. These two levels (for a given value of $K$) exist only in the magnetic components associated with the $K_1$ state. As by (19) the perturbing terms vanish, a situation exactly similar to that discussed in the preceding "special case" obtains, the energy being given directly by (20); i.e.,

$$W(K_1,\overline{M})=f(K+\tfrac{1}{2},\overline{M})-\tfrac{1}{2}\tau(K+\tfrac{1}{2},\overline{M})$$
$$\overline{M}=\pm(K+\tfrac{1}{2}).$$

The writer is very much indebted to Professor J. H. Van Vleck for his initial suggestion of this problem and for his criticisms of the first draft of this paper; he is also indebted to Mr. G. M. Almy for many discussions of the experimental data.

# THE ZEEMAN EFFECT IN THE MgH BANDS

By G. M. Almy and F. H. Crawford
Jefferson Physical Laboratory, Harvard University

(Received November 4, 1929)

Abstract

**Experimental.**—The investigation of the Zeeman effect in the MgH $^2\Pi \rightarrow {}^2\Sigma$ bands at 7 field strengths between 5,000 and 28,000 gauss is described. The bands were produced by a Mg arc, operating in hydrogen. A powerful magnet, equipped with a Back-box, was used in conjunction with a 21-foot concave grating.

**Calculation of Zeeman patterns.**—With the use of the results obtained by Hill in the preceding article, theoretical patterns for representative lines in the band are plotted. Thus in the $P_1$ and $Q_1$ branches the first line should become in the field a sharp doublet of separation $2\Delta\nu_n$; the second a pair of quartets, one on either side of the no-field position of the line; the third a pair of sextets similarly situated. For the higher lines considered only the extreme energy levels ($M = \pm J$) and "zero lines" ($M = 0$) are obtained from which the appearance of the unresolved patterns may be predicted. In general for these lines a no-field doublet consists in the field of a central band filling the no-field interval and two outer components or wings, one on either side.

**Comparison of observed patterns with theory.**—A detailed description of the observable patterns in the band $\lambda 5211$ and a quantitative comparison with the theory are put in tabular form. The first lines show a fine structure in good numerical agreement with the calculations, while for the higher doublets the unresolved patterns correspond closely to those predicted. In the latter case, a central band practically fills the no-field interval, its intensity increasing with the field. The wings become more widely separated and less intense, approaching the separation $4\Delta\nu_n$ as the Paschen-Back effect begins.

Numerical intensity calculations have not been made but certain observations on intensities are correlated (1) with the distribution of components in the theortical patterns, (2) with the relative orientations of spin and magnetic field in the two states of the molecule. The most clean-cut observation on intensities fitting in with the theory is the decrease in the intensity of the wings relative to that of the central band as the Paschen-Back effect begins. Then only transitions for which $\Delta M_s = 0$ have an appreciable probability. These give the central band, whereas $|\Delta M_s| = 1$ corresponds to the wings, whose intensity is correspondingly small.

## Introduction

THE effect of a magnetic field upon molecular spectra arising from transitions between doublet states (i.e. $^2\Sigma, ^2\Pi, ^2\Delta, \cdots$)[1a] has been the subject of several experimental investigations. Many qualitative observations have been made, and some quantitative measurements, but the lack of an adequate theory as a guide in the interpretation of results has apparently discouraged the gathering of much data. When the present work on the MgH bands ($^2\Pi \rightarrow {}^2\Sigma$) was begun, the task of ordering the large and often overlapping Zeeman patterns was not attacked with much success until Hill provided the theory which he develops in the preceding article.

[1a] For the details of the new notation see the preceding article.

The Zeeman effect in the MgH bands was first studied qualitatively by Watson and Perkins[1] whose observations agreed in many of the essential features with those made in an earlier report of the present work.[2,3]

The object of this paper is to give an account of the experimental part of the work, a more complete description of the Zeeman patterns in the MgH band λ5211, and to make a detailed application of Hill's results to this band, including a quantitative comparison of the predicted and observed patterns. Due to their complexity theoretical intensity calculations as well as a consideration of the polarization of the patterns are left for later treatment.

## Apparatus and Experimental Procedure

The source was a 110-volt direct current arc between Mg electrodes, operating in an atmosphere of hydrogen. The gas, from a commercial cylinder, was slowly pumped through a Back-box enclosing the magnet poles, a pressure of 5 to 10 cm of Hg being maintained. For low fields a pressure of 5 cm was ample but at fields around 30000 gauss a pressure of 10 cm was required to bring out the bands with satisfactory intensity. The Mg electrodes, about 2 by 5 mm in section, were mounted in the usual manner with their ends between the pole tips, one stationary, one made to vibrate mechanically parallel to the field so as to strike the other several times a second. The bands were considerably enhanced by placing a large inductance in series with the arc. The field was produced by a water-cooled magnet of Weiss type,[4] the magnet current being held constant by means of adjustable rheostats.

Photographs were taken in the first and second orders of a 21-foot concave grating, the dispersion in the second order being about 0.93A per mm. Since the intensity was much greater in the first order, and the "ghosts" of a very strong Mg atomic triplet falling near the origin of the band λ5211 were much weaker, the first order plates were used for the measurement of the fine structure of the lines near the origin. The second order plates were used for the more intense lines situated at a distance from the origin. The temperature of the grating room was held practically constant by a device described elsewhere.[4]

Usable photographs of the band λ5211 were obtained at fields of 4770, 8350, 16000, 21500, and 28400 (2 sets of plates) gauss without a polarizing prism, and, using a Nicol prism, at 14350 gauss with polarization perpendicular to the field, and at 13500 gauss with polarization parallel to the field. Plates were also inserted to photograph the bands λλ4845, 5622, but these were not obtained with sufficient intensity to be of great use. Eastman Speed-

[1] Watson and Perkins, Phys. Rev. **30**, 592 (1927).

[2] Crawford and Almy, Phys. Rev. **33**, 1084 (1929).

[3] After the experimental work on MgH was well along it was learned that Mulliken and Delaup, at the University of Chicago, had also begun a study of the same problem. In order to prevent duplication of effort they very kindly agreed to turn to the study of the Zeeman effect in other molecules.

[4] Kemble, Mulliken, and Crawford, Phys. Rev. **30**, 448 (1927). The magnet and other equipment are described in detail in this reference.

way plates were used for wave-lengths less than 5000A, Eastman Astronomical Green Sensitive for greater wave-lengths. The length of exposure varied from about 5 hours at the lowest field to over 16 hours at the highest field, the electrodes being replaced frequently during an exposure. A no-field com-

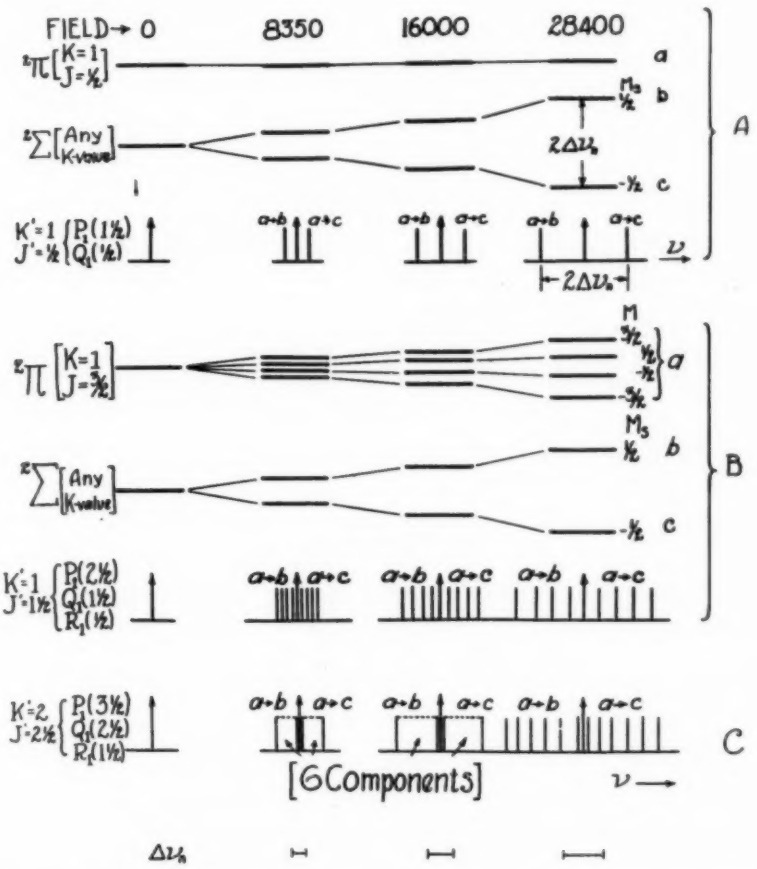


Fig. 1. Theoretical Zeeman energy-level and Zeeman pattern diagrams for $^2\Pi \rightarrow {}^2\Sigma$ transitions with small $K$ values. $A$ refers to lines with $K'=1$ and $J'=1$, $B$ to those with $K'=1$ and $J'=1\frac{1}{2}$, and $C$ to those with $K'=2$ and $J'=2\frac{1}{2}$ (magnetic energy-levels omitted in this case). All separations and patterns are to scale except the $^2\Pi \rightarrow {}^2\Sigma$ interval. In all cases the $^2\Sigma$ level is broken up in the field into two substates symmetrically placed with respect to the no-field position and $2\Delta\nu_n$ cm$^{-1}$ apart. In the $^2\Pi$ level the number of substates is $2J+1$, there being however, only a single level for $J=\frac{1}{2}$ since this state is magnetically insensitive. The position of the no-field line is represented in each Zeeman pattern by a vertical arrow. Each pattern is drawn under its corresponding field, given in gauss at the top of the figure.

parison band and two iron arc spectra were photographed on each plate, the exposures usually being made in the order; iron arc, MgH with field, MgH without field, iron arc. The field strength was determined from photographs of the Zeeman patterns of the Zn triplet λλ4660, 4722, 4811, obtained by replacing the Mg electrodes with brass.

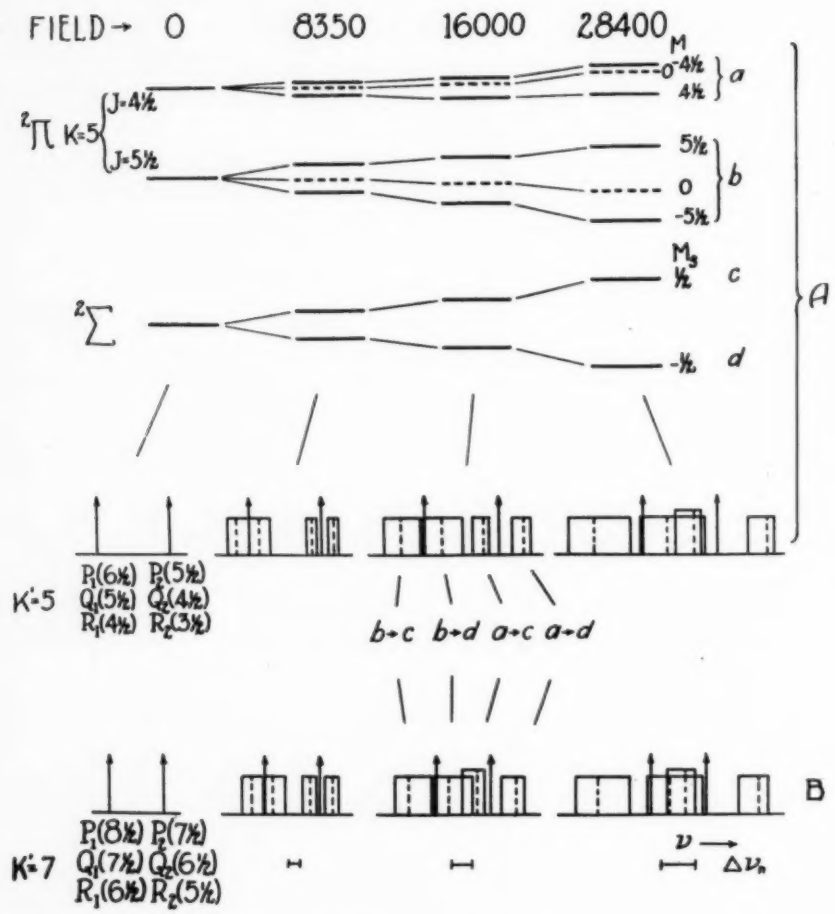


Fig. 2. Zeeman energy levels and Zeeman patterns for representative intermediate $K$ values. $A$ gives magnetic energy levels and Zeeman patterns for all lines having $K'=5$. Due to the large number of sub-levels $(2J+1)$ in each case only the levels with $M=\pm J$ and $M=0$ are plotted. The latter (dotted), though it represents no actual energy level, is drawn in to emphasize any asymmetrical distribution of the sub-levels which may exist,—there being of course as many sublevels above this line as below it. In the Zeeman patterns again only the extreme components in a subgroup are definitely placed, the subgroup being represented by a block. A dotted vertical line represents the hypothetical transition from $M=0$ to $M_s=\pm\frac{1}{2}$ and thus divides the number of components in a block in half. The components in a block originate in transitions such as $a$ to $c$ or $d$ (10 each) and $b$ to $c$ or $d$ (12 each). Overlapping blocks are drawn to different heights merely to distinguish them. As in Fig. 1 the vertical arrows give no-field positions. $B$ gives similarly the Zeeman patterns for lines with $K'=7$. The magnetic energy levels are so similar in general character to those under $A$ that they are omitted. Attention is called to the fact that for this range of $K$ values at low fields the low-frequency member of a doublet gives a broad, nearly symmetrical band while the high-frequency member becomes a doublet. Cf. Fig. 4, $P$ branches, $K'=3$, 4, and 5, at $H=8350$. Since the no-field doublet intervals are computed from Hill's equation (22), setting $H=0$, they do not include sigma-type doubling and the consequent difference between the $Q$ and the $P$ and $R$ doublets. The same source of error is present, of course, in the Zeeman patterns.

The plates were measured with a Wolz comparator, on which the smallest division was 1/300 mm. In the band λ5211, first order, this corresponds to about 0.023 $cm^{-1}$. Hence settings were read to 0.002 $cm^{-1}$, but could be repeated, in the fine-structure measurements, only to within about 0.04 $cm^{-1}$. In these patterns an average of from 10 to 20 readings of each position was taken. In unresolved patterns the exact location of the edges was, of course, less accurately determinable than the position of a sharp line. Two to four independent settings were made in each of these measurements.

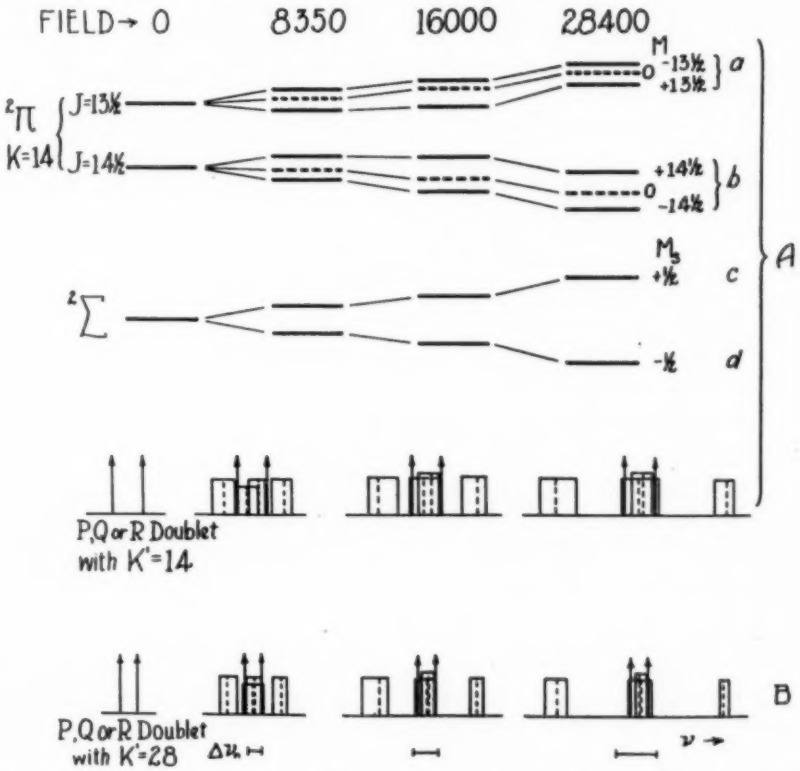


Fig. 3. Zeeman energy levels and Zeeman patterns for lines of large $K$ values. The same conventions are employed as in Fig. 2. In these cases most significant changes in intensity are observed to occur as the field increases. At 8350 gauss the two central overlapping blocks are very faint and shade off at the edges, while most of the intensity of the original doublet is concentrated in the two outer blocks or wings. As the field increases the intensity of the central part increases at the expense of the outer wings until at 28400 gauss the latter are just discernible after long exposure and separated by about $4\Delta\nu_n$ while the central band is quite intense and practically fills the no-field interval. See text in this connection and also Fig. 4.

## Calculation of Zeeman Patterns

In the preceding article Hill has considered from the point of view of the quantum mechanics the Zeeman effect for doublet bands of molecules of the type of MgH. According to Mulliken,[5] the transition giving rise to the band

[5] Mulliken, Phys. Rev. **32**, 388 (1928).

system of which λ5211 is a member is $^2\Pi \rightarrow {}^2\Sigma$, and the molecular constants λ (Mulliken's $\Delta E/B$) and $B$ have the values 5.7 and 6.1 respectively.

The magnetic energy pattern is calculated, in the general case, by means of Hill's Eq. (22). In the $^2\Sigma$ state ($S=\frac{1}{2}, \Lambda=0$) this reduces to the much simpler form (23). The physical basis for the simplicity of the $^2\Sigma$ state in the field lies in the very small coupling between $S$ and $K$, which is shown by the lack of an appreciable doubling in this state at no field. A small magnetic field overpowers this coupling, so that $S$ and $K$ are quantized separately. Since $K$ measures only molecular rotation in this state, its mutual energy with the field is presumably negligible. Hence we may expect the $^2\Sigma$ state to form a sharp doublet in the field, the two components corresponding to the two values of $M_s$, $\frac{1}{2}$ and $-\frac{1}{2}$. These two magnetic levels are separated by $2\Delta\nu_n$ since unit magnetic moment is to be associated with $S=\frac{1}{2}$.

For the $^2\Pi$ state ($S=\frac{1}{2}, \Lambda=1$) Hill's Eq. (22) is used. From the numerical results, which are not given here, the more picturesque energy-level and spectral diagrams may be sketched, as is done in Figs. 1–3 for representative values of $K$. For the terms for which $K$ is 1 or 2 the energies for all permitted values of $M$ ($J$ to $-J$) have been calculated, enabling one to diagram the fine structure of the spectrum patterns (Fig. 1). For larger $K$ only the energies corresponding to $M=J$, $-J$, and 0 have been calculated. The first two give the extreme components. The last, since $J$ is half-integral, does not correspond to an actual energy level but divides the *number* of levels $(2J+1)$ in half (Figs. 2 and 3).

Since no intensity calculations have been made, all of the components of a Zeeman pattern are represented as of equal intensity. Where the structure is so fine as to exclude hope of resolution the patterns are represented by blocks instead of series of fine lines.

## Results

In presenting the results a few general features of the Zeeman effect in these bands will first be given. This will be followed by a detailed description of the observable patterns and a quantitative comparison with the theory, put in tabular form. Finally certain observed intensity relations will be correlated in a general way with the theory.

*General Features.* Aside from a few lines near the origin for which patterns are resolved (see Table II), the Zeeman effect may be broadly described as follows. For intermediate values of $K$, say 4 to 10, a low field splits the high-frequency member of each doublet (i.e., each member of the $P_2$, $Q_2$, $R_2$ branches) into a diffuse doublet of width approximately equal to $2\Delta\nu_n$ while the low-frequency members (i.e., $P_1$, $Q_1$, $R_1$ branches) become diffuse bands of about the same total width ($2\Delta\nu_n$). But as the field increases it becomes more natural to consider the pattern associated with the doublet as a whole, rather than the patterns of the individual lines. Thus the pattern associated with a no-field doublet consists of a broad central band, most intense at the edges, somewhat narrower than the no-field doublet interval. There is evidence also of outer components or wings on each side of the central band which grow fainter and farther apart as the field increases.

For higher values of $K$, the first apparent effect of the field is to widen the no-field doublets, with, however, a faint band extending from one member to the other, most intense at the center. In other words, the wings are at low fields the most intense part of the pattern. As the field increases the

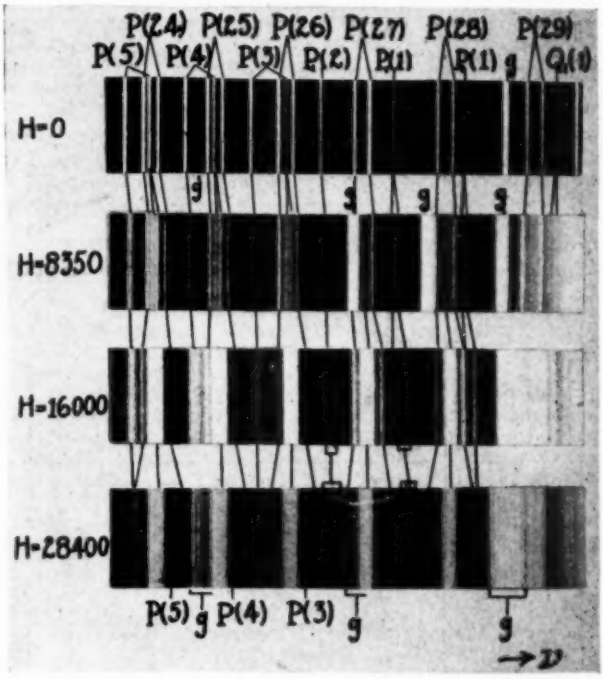


Fig. 4. Reproductions of enlargements of the region near the origin. The head of the band is to the left. A second order plate was used at 8350 gauss (enlargement about 12 times), first order for the others (enlargement about 24 times); the scale differs slightly in the two cases. Lines are designated according to the value of $K$ in the initial $^2\Pi$ state; the usual line notation can be quickly ascertained by reference to Table I. Thus $P$ (29) consists of the lines $P_1$ ($30\frac{1}{2}$) and $P_2(29\frac{1}{2})$, the subscript 1 denoting in all branches the low-frequency member of the doublet. $g$ indicates a "ghost" of the Mg atomic line λ5183; the ghosts naturally vary in position and prominence with the order and the exposure length. The connecting lines follow the progress of patterns with change in field. Of the two lines designated by $P_1$ (1) the low-frequency one has $J'=1\frac{1}{2}$ and is a diffuse doublet at low fields. At higher fields each member of the doublet becomes broader and at 28400 gauss each is resolved into 4 components (cf. Fig. 1$B$) though the left set is faint and obscured partially by other lines. The high-frequency one ($J'=\frac{1}{2}$) remains a sharp doublet of width $2\Delta\nu_n$ for all fields (cf. Fig. 1$A$). $P_1$ (2) gives a broad band (cf. Fig. 1$C$), the left half of which decreases in intensity as the field increases. The right half is resolved into 6 components at 28400 gauss (hardly visible in reproduction) of separation given by the theory. $P(26)$, $P(27)$ and $P(28)$ illustrate the behavior of the wings with increasing field which was described under Fig. 3, and in the text.

central band increases greatly in intensity at the expense of the wings which continue to move out. The latter remain distinct up to 20000 gauss and are discernible at 28000 gauss, their separation approaching $4\Delta\nu_n$ as the field increases.

*Comparison of theoretical and observed patterns.* A detailed description of the observable lines of the band λ5211 and, where possible, a quantitative

TABLE I.

| Branch: | $P_1$ | $Q_1$ | $R_1$ | $P_2$ | $Q_2$ | $R_2$ |
|---|---|---|---|---|---|---|
| $K'$: | $J''-3/2$ | $J''-1/2$ | $J''+1/2$ | $J''-1/2$ | $J''+1/2$ | $J''+3/2$ |

TABLE II. *The theoretical patterns of the lines in this table appear in Fig. 1; reproductions of the photographs of the P line patterns in Fig. 4. + or − in front of a number indicates a line to the high or low frequency side, respectively, of the no-field position.*

| Line | Field and $\Delta\nu_n$ | Appearance of Zeeman pattern | Comparison with theory ($cm^{-1}$) | | | | | Remarks on intensity |
|---|---|---|---|---|---|---|---|---|
| | | | Doublet width | | | | | |
| | | | Calc. | Obs. $P$ | Obs. $Q$ | | | |
| $P_1(1\frac{1}{2})$ | 8350 | Doublet | 0.78 | 0.73 | 0.76 | | | Approximately same intensity. |
| $Q_1(\frac{1}{2})$ | 0.39 | | | | | | | |
| | 16000 | Doublet | 1.50 | 1.34$s$ | 1.55 | | | |
| $K'=1$ | 0.75 | | | | | | | |
| | 21500 | Doublet | 2.02 | 2.04 | | | | |
| | 1.01 | | | | | | | |
| | 28400 | Doublet; in $P$ one member $s$, in $Q$ both $s$. | 2.66 | 1.32 = half-width | | | | |
| | 1.33 | | | | | | | |
| $P_1(2\frac{1}{2})$ | 8350 | Diffuse doublet | 0.78 | 0.85 | | | | |
| $Q_1(1\frac{1}{2})$ | 0.39 | | | | | | | |
| | 16000 | Very diffuse doublet | Width of $P$ doublet components | | | | | $P$ pattern most intense at outside edges of doublet members; $Q$ at inside edges. |
| | | | | Calc. | Obs. | | | |
| $K'=1$ | 0.75 | | Pos. | 1.18 | 1.2 | | | |
| | | | Neg. | 1.18 | 1.2 | | | |
| | 28400 | Each member of above doublet resolved into 4 components; distinct only in pos. $P$ group. | Position with respect to no-field | | | Difference | | Intensities in pos. $P$ group about as 4:3:2:1 (high to low frequency); approximately equal in pos. $Q$ group; other groups faint and confused. |
| | 1.33 | | Calc. | Obs. $P$ | Obs. $Q$ | Calc. | Obs. (ave.) | |
| | | | +2.15 | +2.22 | | | | |
| | | | +1.65 | +1.71 | +1.74 | 0.50 | 0.51 | |
| | | | +1.11 | +1.12 | +1.13 | 0.54 | 0.60 | |
| | | | +0.41 | +0.51 | +0.52 | 0.70 | 0.61 | |
| | | | −0.51 | −0.34$s$ | −0.49 | 0.92 | 1.01 | |
| | | | −1.01 | −0.93$s$ | | 0.50 | 0.59 | |
| | | | −1.55 | −1.56$s$ | | 0.54 | 0.63 | |
| | | | −2.25 | −2.19$s$ | | 0.70 | 0.63 | |
| | | | Width of $P$ pattern | | | | | |
| | | | Calc. | Obs. | | | | |
| $P_1(3\frac{1}{2})$ | 8350 | Unresolved band | 1.47 | 1.5 | | | | In $P$ neg. half slightly stronger |
| $Q_1(2\frac{1}{2})$ | 0.39 | | | | | | | |
| | 16000 | Unresolved broad band | 2.81 | 3.0 | | | | Intense streak in center, esp. in $Q$. |
| $K'=2$ | 0.75 | | | | | | | |
| | 28400 | Pos. half of $P$ pattern resolved into 6 components (not resolved in reproduction); neg. half faint and confused. | Position with respect to no-field | | | Difference | | |
| | | | Calc. | Obs. | | Calc. | Obs. | |
| | | | +2.47 | +2.12 | | | | |
| | | | +1.93 | +1.63 | | 0.54 | 0.49 | Intensities of 6 components approximately the same. |
| | | | +1.42 | +1.17 | | 0.51 | 0.46 | |
| | | | +0.95 | +0.71 | | 0.47 | 0.46 | |
| | | | +0.52 | +0.34 | | 0.43 | 0.37 | |
| | | | +0.15 | +0.06 | | 0.37 | 0.28 | |

comparison of theory and observation are given in Tables II-V. For the most part only the appearance of the patterns for the three fields for which

calculations were made is described. The plates at 4770 gauss give little additional information, showing in all cases what one would expect in the transition from zero field to 8000 gauss. Similarly the patterns at 21500

TABLE III. *Theoretical patterns in Fig. 2; reproduction of P lines in Fig. 4.*

| Lines Obs. | Field and $\Delta\nu_n$ | Description of Zeeman patterns and comparison with theory |
|---|---|---|
| $P_1(4\frac{1}{2})$ to $P_1(8\frac{1}{2})$ $R_1(5\frac{1}{2})$ $R_1(6\frac{1}{2})$ | 8350 0.39 | Unresolved broad bands; edges fairly definite in $P$ and $R$ branches, but very uncertain in $Q$ branch. |

Width of band

| $K'$ | Calc. | Obs. $P$ | Obs. $R$ |
|---|---|---|---|
| 4 | | 1.5 | |
| 6 | 1.57 | 1.5 | |
| 7 | 1.57 | 1.5 | 1.4 |
| 8 | 1.57 | 1.5 | 1.4 |

| | 16000 0.75 | Unresolved broad bands. As $K'$ increases pos. half becomes relatively stronger and extends, with decreasing intensity, to the other member of the doublet; i.e., to the corresponding $P_2$, $Q_2$, $R_2$ line. Qualitatively consistent with theory. |
|---|---|---|
| | 28400 1.33 | Unresolved bands. Neg. part very faint. Pos. part intense, shading off but extending to the other member of the doublet. Consistent with theoretical pattern. |
| $P_2(3\frac{1}{2})$ to $P_2(9\frac{1}{2})$ $Q_2(4\frac{1}{2})$ $Q_2(6\frac{1}{2})$ $Q_2(7\frac{1}{2})$ $R_2(5\frac{1}{2})$ | 8350 0.39 | Diffuse doublets; diffuseness increasing with $K'$. Intensities of two components approximately the same. Theory demands that the width of each component increase from 0.36 $cm^{-1}$ at $K'=5$ to 0.60 $cm^{-1}$ at $K'=9$; this agrees with the observed increasing diffuseness. |

Doublet width

| $K'$ | Calc. | Obs. $P$ | Obs. $Q$ | Obs. $R$ |
|---|---|---|---|---|
| 3 | 0.78 | 0.68 | | |
| 4 | .78 | .67 | | |
| 5 | .78 | .66 | 0.65 | |
| 6 | .78 | .61 | | |
| 7 | .78 | .63 | .57 | 0.64 |
| 8 | .78 | .63 | .58 | |
| 9 | .78 | .60 | | |

| | 16000 0.75 | $P_2$ lines obscured by higher $P$ doublets. Observable $R_2$ and $Q_2$ lines correspond closely to the predicted patterns, consisting at $K'=7$ of two bands whose inside edges are separated by about 0 6 $cm^{-1}$, as the theory predicts. Neg. band shades into pattern of the other member of the doublet; i.e., the corresponding $R_1$ or $Q_1$ line. Pos. band weaker than neg. |
|---|---|---|
| | 28400 1.33 | Pos. component of $P_2$ doublet observed; remainder obscured. $R_2(5\frac{1}{2})$ much like predicted pattern; intensity of wing much less than that of neg. part. |

Position of wing with respect to no-field line

| $K'$ | Calc. | Obs. $P$ | Obs. $R$ |
|---|---|---|---|
| 3 | 1.82 | 1.73 | |
| 4 | 1.91 | 1.80 | |
| 5 | 1.98 | 2.10 | |
| 6 | 2.02 | 1.96 | |
| 7 | 2.05 | 1.93*s* | 1.9 |

gauss interpolate between those at 16000 and 28400 gauss. Reproductions of the Zeeman patterns of some lines most favorably situated for observation appear in Fig. 4.

Since no calculations of the intensity distribution within the patterns have been made, calculated separations are always figured from the theoretical

TABLE IV. *Representative theoretical pattern ($K'=14$) in Fig. 3.*

| Lines | Field and $\Delta\nu_n$ | Description of Zeeman patterns and comparison with theory. |
|---|---|---|
| $Q$, $R$ doublets for which $10<K'<20$ | 8350<br>0.39 | No-field doublet forms a single broad pattern with intense diffuse line showing through in neg. edge and doublet in pos. edge, as in lines of lower $K'$. Assuming the intense line near neg. edge is $b\rightarrow c$ in Fig. 3, its separation from the outside component of the doublet at the positive edge is as follows: |

| $K'$ | Calc. | Obs. $Q$ | Obs. $R$ |
|---|---|---|---|
| 11 | | | 2.26 |
| 12 | | 2.02 | |
| 13 | | 2.05 | |
| 14 | 2.06 | 1.91 | |
| 15 | 2.03 | | 1.95 |
| 16 | 2.00 | 1.95 | |
| 17 | | 2.00 | |
| 18 | | 2.06 | |

| | | |
|---|---|---|
| | 16000<br>0.75 | Intense outer components of pattern at 8350 gauss have moved out, becoming distinct wings, separated from, though less intense than the broad central band of approximately uniform intensity which fills the no-field interval. The wings are narrower than the theory indicates as well as the central band. For discussion of the discrepancy in the absolute width of the central band see text following tables. |

| $K'$ | Separation of wings Calc. | Separation of wings Obs. $Q$ | Separation of wings Obs. $R$ | Width of central band Calc. | Width of central band Obs. $Q$ | Width of central band Obs. $R$ | Width of central band / No-field doublet width Calc. | Width of central band / No-field doublet width Obs. $Q$ | Width of central band / No-field doublet width Obs. $R$ |
|---|---|---|---|---|---|---|---|---|---|
| 11 | | | | | | 1.74 | | | 0.89 |
| 12 | | | | | 1.58 | | | 0.99 | |
| 13 | 3.33 | | | 1.06 | 1.51 | | 1.03 | .98 | |
| 14 | 3.27 | 3.34 | | .96 | 1.41 | | 1.04 | .94 | |
| 15 | 3.21 | | | .88 | | | 1.04 | | |
| 16 | | 3.27 | 3.45 | | | 1.96 | | | 1.07 |

| | | |
|---|---|---|
| | 28400<br>1.33 | Central bands very intense. Wings observed in $Q$ branch, but very weak. Central bands most intense at edges in $Q$ branch; fairly uniform in $R$ branch. |

| $K'$ | Width of central band Calc. | Width of central band Obs. $Q$ | Width of central band Obs. $R$ | Width of central band / No-field doublet width Calc. | Width of central band / No-field doublet width Obs. $Q$ | Width of central band / No-field doublet width Obs. $R$ |
|---|---|---|---|---|---|---|
| 11 | | | 1.68 | | | 0.86 |
| 13 | 1.24 | | 1.50*s* | 1.20 | | .80 |
| 14 | 1.19 | 1.36 | 1.66*s* | 1.28 | 0.90 | .90 |
| 15 | 1.16 | 1.45*s* | 1.42*s* | 1.37 | .99 | .78 |
| 16 | | 1.33*s* | | | .93 | |
| 17 | | 1.46 | 1.64 | | .97 | .90 |
| 18 | | 1.39 | 1.74*s* | | .98 | .94 |

"zero line" ($M=0$) of the unresolved patterns. Where the calculated width of an unresolved pattern is given, it is the interval between the extreme com-

TABLE V. *Theoretical patterns in Fig. 3 (for $K'=28$); reproductions of some P doublets in this group appear in Fig. 4.*

| Lines | Field and $\Delta\nu_n$ | Description of Zeeman patterns and comparison with theory |
|---|---|---|
| *P*, *Q*, *R*, doublets for which $K'>20$ | 8350<br>0.39 | A no-field doublet still appears as a doublet, widened, with a fainter band extending between, most intense at the center. That is, nearly all of the intensity is in the wings. |

Doublet or wing separation

| $K'$ | Calc. | Obs. *P* | Obs. *Q* | Obs. *R* |
|---|---|---|---|---|
| 21 | | 2.38 | 2.01 | 2.31 |
| 22 | | 2.36 | 1.95 | 2.28 |
| 23 | | 2.38 | 1.96 | 2.26 |
| 24 | | 2.38 | 1.97 | |
| 25 | | 2.38 | 1.96 | |
| 26 | | 2.37 | 1.95 | |
| 27 | 1.69 | 2.37 | 1.95 | |
| 28 | 1.69 | 2.36 | 1.95 | |
| 29 | | 2.37 | 1.92 | |

The poor agreement between calc. and obs. is not surprising since the predicted no-field doublet separation is less than one third of the observed value. See text.

16000
0.75

Members of doublet observed at 8350 gauss have moved out, their separation approaching $4\Delta\nu_n$. The central band is now more intense than the wings, its intensity being slightly greater at the edges. Its width is somewhat less than the no-field interval. The wings are narrower than the theory indicates; but the pos. wing is sharper and more intense than the neg. which agrees with the theoretical pattern.

| $K'$ | Separation of wings Calc. | Separation of wings Obs. | | Width of central band Calc. | Width of central band Obs. | | Width of central band: No-field doublet width Calc. | Width of central band: No-field doublet width Obs. | |
|---|---|---|---|---|---|---|---|---|---|
| | | *P* | *Q* | | *P* | *Q* | | *P* | *Q* |
| 21 | | 3.64 | 3.18 | | | 1.34 | | | .95 |
| 22 | | 3.47 | | | 1.75 | 1.25 | | .94 | .91 |
| 23 | | 3.38 | | | | 1.27 | | | .95 |
| 24 | | 3.47 | | | 1.71 | | | .91 | |
| 25 | | 3.37 | | | 1.68 | 1.30 | | .89 | .96 |
| 26 | | 3.44 | 3.08 | | 1.75 | 1.24 | | .93 | .91 |
| 27 | 3.08 | 3.50 | | .60 | 1.60 | | 1.15 | .86 | |
| 28 | 3.02 | 3.36 | | .57 | 1.61 | 1.30 | 1.16 | .86 | .94 |
| 29 | | 3.57 | | | 1.78 | 1.20 | | .94 | .91 |

28400
1.33

Strong central band practically filling no-field doublet interval. Wings very faint and separated by about $4\Delta\nu_n$. Pos. wing slightly more intense than neg.

| $K'$ | Separation of wings Calc. | Separation of wings Obs. | Width of central band Calc. | Width of central band Obs. | | Width of central band: No-field doublet interval Calc. | Width of central band: No-field doublet interval Obs. | |
|---|---|---|---|---|---|---|---|---|
| | | *P* | | *P* | *Q* | | *P* | *Q* |
| 25 | | | | 1.86 | 1.32 | | .99 | .98 |
| 26 | | 5.63 | | 1.93 | 1.29 | | 1.03 | .95 |
| 27 | 5.27 | 5.45*s* | .70 | 1.69*s* | 1.30 | 1.35 | .91 | .96 |
| 28 | 5.25 | 5.63 | .67 | 1.82 | | 1.37 | 1.09 | |

ponents. In measuring such a pattern, one cannot tell where the exact positions of the extreme components are and measures to the edge of the blackened portion of the plate. Hence measured widths should be slightly higher, perhaps 0.1 $cm^{-1}$, than calculated widths.

In these tables "pos." means "high-frequency," "neg." means "low-frequency." "*s*" indicates that the line in question is superimposed on another or confused with others so that measurements are at best questionable. The connection between $K'$ and $J''$ is given in Table I.

The most serious descrepancy between theory and observation appears in the width of the central band in the patterns for the higher rotational doublets (Tables IV and V). The theory gives approximately the actual separation of the wings, but the predicted width of the central band is less than the observed. Qualitatively theory and observation agree, for each indicates that the central band practically fills the no-field interval at high fields. (Cf. Fig. 3 and Fig. 4.) It is the size of this interval, obtained by setting the field equal to zero in Hill's Eq. (22), which the theory underestimates. The cause of the discrepancy is ostensibly the same as that which is responsible for the fact that in the absence of a magnetic field the doublet separation does not decrease to zero for large values of $K$, but rather approaches an asymptotic value (about 1.85 $cm^{-1}$ in the $P$ branch). This phenomenon has been termed "rho-type doubling" by Kemble and by Mulliken and is attributed to a sort of "magnetization by rotation" of the molecule which is of importance only in $\Sigma$ states. It has been investigated theoretically by Van Vleck,[6] but as yet it has not been shown that this theory will give quantitatively the results found in MgH.

*Intensity relations in Zeeman patterns.* Certain rough correlations may be made between observed intensities and (1) the calculated distribution of components in the unresolved patterns, and (2) relative orientations of $S$ and $K$, and $S$ and field in the two molecular states involved in the transition.

In the first place it may be noted that the blocks in the theoretical patterns of $P_2$, $Q_2$, $R_2$, lines are in general considerably narrower than in the $P_1$, $Q_1$, $R_1$ patterns. This greater concentration of the components should result in greater intensity in the observed patterns. As experimental confirmation the following observations may be mentioned:

(1). For intermediate values of $K'$ (3 to 10) at 8350 gauss the $P_2$, $Q_2$, $R_2$ doublets are sharp and more intense than the corresponding $P_1$, $Q_1$, $R_1$ patterns, indicating that they do actually represent more concentrated groups of components (cf. Fig. 2 and Fig. 4).

(2). As $K'$ increases the wings become sharper. Where both are observable the high-frequency one is perceptibly sharper than the low-frequency (cf. Fig. 3B and Fig. 4, $H=16000$).

(3). The wings are usually much narrower than their predicted widths, which may be partially due to non-uniform distribution within the patterns; the less concentrated part may be simply under-exposed on the plates (cf. Fig. 3, $K'=14$).

[6] Van Vleck, Phys. Rev. **33**, 467 (1929).

Finally we shall consider the relations between intensities and relative orientations of $S$ and $K$, and $S$ and $H$ (field) in the two states. For the present these relations must be regarded as purely empirical. Starting from zero field the first apparent effect of the field is merely to widen the doublets; in other words, practically all of the energy is in the wings. This means that at low fields the anti-parallel orientation of $S$ and $K$ in the initial $^2\Pi$ state combines almost entirely with the final $^2\Sigma$ substate in which $S$ is anti-parallel to $H$, while parallel $S$ and $K$ combines almost entirely with parallel $S$ and $H$. This effect is most pronounced in doublets of large $K'$.

As the field is increased this rule breaks down, for the wings decrease in intensity, while the central band increases. That is, anti-parallel $S$ and $K$ combine more and more readily with parallel $S$ and $H$, while parallel $S$ and $K$ combine with anti-parallel $S$ and $H$. This is to be regarded as the beginning of the Paschen-Back effect; for as the field is increased without limit the state in which $S$ and $K$ are anti-parallel is replaced by the state in which $S$, torn loose from $\Lambda$, lies parallel to $H$, while the state in which $S$ and $K$ are parallel goes into the state in which $S$ lies anti-parallel to $H$. Observing the rule $\Delta M_s = 0$ which holds at very high fields, one sees that the wings, corresponding in this case to $|\Delta M_s| = 1$, are produced by very improbable transitions and should be very weak. Such is the observed behavior, the wings being very much fainter than the central band at 28400 gauss. See the preceding paper for a discussion of the Paschen-Back effect to be expected.

It is also observed that in the pattern of a given line the parts nearest the no-field position of that line are most intense. Thus the low $P_1$, $Q_1$, $R_1$ patterns are strongest at their centers; the low $P_2$, $Q_2$, $R_2$ doublets shade away from the no-field line (this may account for the rather too small observed separation in the $P_2$ doublets at 8350 gauss, Table IV; it is very pronounced in the observable $Q_2$ doublets). In general, throughout the band, patterns shade away from the no-field position. We can state this behavior in terms of the orientation of $S$ and $H$ as follows. The $^2\Pi$ magnetic substates in which $S$ has a component parallel to $H$ combine more readily with the $^2\Sigma$ substate in which $S$ is parallel to $H$ ($M_s = +\frac{1}{2}$) than the substate in which $S$ is anti-parallel to the field ($M_s = -\frac{1}{2}$), while the $^2\Pi$ substates in which $S$ has a component anti-parallel to $H$ combine more readily with the substate in which $M_s = -\frac{1}{2}$.

We wish to express our appreciation to Dr. E. L. Hill for many discussions of the application of the theoretical results. We are also greatly indebted to the Milton Fund of Harvard University for financial aid which has enabled us to carry on this work.

# FINE STRUCTURE AND ZEEMAN EFFECTS IN HELIUM BAND LINES

By Robert S. Mulliken and George S. Monk
Ryerson Physical Laboratory, University of Chicago

(Received October 31, 1929)

Abstract

Second and third order grating photographs of helium (λλ6400, 5733, 4546 and others) having the $2^3\Pi$ state as their final electron level show fine structures in the band lines. The $3^3\Pi \rightarrow 2^3\Sigma$ bands (λλ4650, 4670) show no evidence of fine structures in their lines. The observed results can be completely explained by assuming that each rotational level of the $2^3\Pi$ electron state has a characteristic partially resolved fine structure, as shown in Fig. 3, but that the fine structures which presumably exist for the other electron states involved ($2^3\Sigma$, $3^3\Sigma$, $4^3\Sigma$, $3^3\Pi$, etc.) are much narrower and completely unresolved in our work. There are two types of fine structures in the $2^3\Pi$ levels, one for the odd $K$ values ($A$ levels), another for the even $K$ values ($B$ levels). The theoretical interpretation of the observed fine structures as partially resolved triplets is discussed.

The Zeeman effect of the λ6400 band ($3^3\Sigma \rightarrow 2^3\Pi$) was investigated at three field strengths. In the field, the original fine structures disappear, and the Zeeman patterns which replace them are found to be in excellent agreement with those predicted for a $^1\Sigma \rightarrow {}^1\Pi$ transition. Thus it is evident that the effect of the spin ($S=1$) which gives rise to the original fine structure is completely overpowered by the external field (Paschen-Back effect).

## Introduction. Theoretical Expectations

As IS now well known, the electron levels of $He_2$ fall into two systems, par-$He_2$ and ortho-$He_2$, paralleling the par-He and ortho-He terms. The ortho-$He_2$ and par-$He_2$ levels probably, on theoretical grounds, respectively correspond to $S=1$ and $S=0$ like the analogous atomic levels.[1,2] $S$ is the quantum number of the resultant spin.

In the ordinary states of the He atom, we have one $1s$ electron and one "series" electron. Each has a spin quantum number 1/2, thus giving the two possible $S$ values 0 and 1. In the observed states of the $He_2$ molecule, two electrons are undoubtedly in $1s\sigma$ orbits forming a closed shell.[1] This leaves two outer electrons, namely the series electron, and one other which according to Weizel[1] is in a $2p\sigma$ orbit. These two should give $S=0$ and 1 as in the atom.

According to theory one would expect a triplet fine structure, but a very narrow one because of the smallness of the nuclear charge, in the ortho-He levels ($S=1$) with $L>0$,[2] while the par-He levels ($S=0$) should be single. These predictions are in agreement with experiment. Also, one would expect the triplet separations in the ortho-He levels to diminish rapidly with increase

[1] Cf. especially W. Weizel, Zeits, f. Physik **51**, 328; **52**, 175; **54**, 321 (1928–9).

[2] Cf. W. Heisenberg, Zeits. f. Physik **39**, 499 (1926) and F. Hund, Linienspektren und Periodisches System der Elemente, p. 136–7, J. Springer, Berlin (1927).

in $n$ or $l$ of the series electron. The $1s2p$, $^3P$ helium term should, and does, show the largest separations. ($^3P_0-{}^3P_1$, $\Delta\nu=0.991$, $^3P_1-{}^3P_2$, $\Delta\nu=0.077$; $^3P_2$ lies below $^3P_1$ and $^3P_1$ below $^3P_0$ in the energy level diagram). As compared with $msnp$ triplets of heavier two-valence-electron atoms, the separations here are very small, and the order of the levels is inverted and distorted. The latter peculiarities are explained as follows.[2] (1) The interaction energy which differentiates the members of a triplet consists of three terms, ($a$) the energy of interaction of $s_1$ with $l_2$, ($b$) interaction energy of $s_2$ with $l_2$, ($c$) interaction energy of $s_1$ and $s_2$ ($s_1$ is the spin of the $1s$ electron, $s_2$ and $l_2$ are the spin and $l$ of the series electron). (2) For the lightest atoms, the three energies are of the same order of magnitude, while for heavier atoms ($s_1l$) and ($s_1s_2$) are negligible compared with ($s_2l$). (3) The energy ($s_1l$) is negative while ($s_2l$) is positive; for helium, the former is numerically larger than the latter so that $^3P_2$ lies below $^3P_0$, instead of above it as in the alkaline earth metals. (4) The ($s_1s_2$) energy is different for $^3P_1$ than for $^3P_0$ and $^3P_2$, and causes $^3P_1$ to be displaced downward relatively to $^3P_2$; in $2^3P$ of helium, this displacement is such as to cause $^3P_1$ to come close to $^3P_2$.

Just as in the corresponding atomic levels, one would theoretically expect the par-$He_2$ levels to be single and the ortho-$He_2$ levels to have a triplet fine structure. The expected relations are, however, made somewhat more complicated here by the molecular rotation. For (the hypothetical case of) a *rotationless* molecule one would expect fine structures only if $\Lambda>0$, as is the case for $\Pi$, $\Delta$, $\cdots$ states ($\Lambda=1, 2, \cdots$), corresponding to $\pi$, $\delta$, $\cdots$ orbits of the series electron. The separations should be of about the same order of magnitude as in the ortho-He levels, and should diminish in a similar way with increasing $n$ and $l$ of the series electron. One would probably expect to find the largest separations in the $1s\sigma^2 2p\sigma 2p\pi$, $^3\Pi$ state. The separations should depend, as in the He atom, on three interaction energies ($s_1l_2$), ($s_2l_2$), and ($s_1s_2$), where $s_1$ refers here to the spin of the $2p\sigma$ electron and $s_2$ and $l_2$ to the $s$ and $l$ of the $2p\pi$ electron ($l=1$). The magnitudes of these three energies cannot very readily be estimated, but it is evident from the different character of the electron orbits that they might, relatively and absolutely, be considerably different than for the $1s2p$, $^3P$ state of He.[3]

For a *rotating* molecule, triplet fine structures are to be expected even if $\Lambda=0$, while for $\Lambda>0$ the fine structures should be greatly modified by the rotation. The fine structures for the case $\Lambda=0$, $S=1$ ($^3\Sigma$ states) have been discussed theoretically by Kramers.[4] For each value of the rotational quantum number $K$, except $K=0$, there should be a narrow group of three levels ($J=K, K\pm1$). The energy differences here depend entirely on differences in

[3] Other things being equal, however, the separation $^3\Pi_2-{}^3\Pi_0$ would tend to be smaller by a ratio 2/3 than a corresponding separation $^3P_2-{}^3P_0$, since the separate axis-quantization of $l$ and $s$ multiplies the coupling energies ($s_1l$) and ($s_2l$) by a factor 2/3 as compared with their values for direct coupling of $l$ and $s$ as in atoms: cf. R. S. Mulliken, Phys. Rev. **33**, 742 (1929). The axis-quantization of $s$ must also alter the form of the energy ($s_1s_2$), as compared with the coupling which exists in atoms.

[4] H. A. Kramers, Zeits. f. Physik **53**, 422 (1929).

the $(s_1s_2)$ energy: this is practically the same for $J=K+1$ and $J=K-1$, except for very small $K$, but differs for $J=K$ from its values for $J=K\pm1$ by an amount nearly independent of $K$.[5] Relations in agreement with this are found in the rotational levels of the $^3\Sigma$ normal state of $O_2$. Since the interaction energy $(s_1s_2)$ varies, other things being equal, inversely as the cube of the distance between the two electrons concerned, one expects the largest separations for the smallest $n$ values of the series electron. By analogy with $O_2$, where the distances between the electrons are comparable with those in the lowest $^3\Sigma$ levels of $He_2$, one might reasonably expect measurable separations in the $1s\sigma^2 2p\sigma 2s\sigma$, $^3\Sigma$ and the $1s\sigma^2 2p\sigma 3p\sigma$, $^3\Sigma$ ($^3u$) states of $He_2$, but very probably not in any of the more excited states. No definite *prediction* of measurable separations can be made, however, even for the two $^3\Sigma$ states mentioned, without detailed calculations which are hardly possible at present. As a matter of fact, the data given below indicate no measurable separations in the $2s\sigma$, $^3\Sigma$ state.

For a rotating $He_2$ molecule with $\Lambda>0$, we have Hund's case *b*, since the coupling energy of $L$ and $S$ is too small to resist the tendency of the rotation to cause $S$ to become uncoupled from the electric axis and coupled to the rotation axis. Thus we have, as for $\Lambda=0$, a rotational quantum number $K$, and $J=K, K\pm1$. For the lowest $K$ values, the interaction of $L$ and $S$ should give a small interaction energy,—smaller, however, than for a rotationless molecule, and rapidly diminishing with increasing $K$. For larger $K$ values the $(s_1s_2)$ energy should alone be of importance. If, however, there is an appreciable tendency toward Hund's case *d* (uncoupling of $l$ from the electric axis), small $(ls)$ energy terms should appear even for large $K$ values, but since case *d* occurs only for large $n$ or $l$ values, no *measurable* fine structures are to be expected in practise from this cause.

The foregoing considerations need to be supplemented by admitting the possibility of abnormally large fine structures in isolated cases of particular rotational levels. This phenomenon may be expected in so-called perturbed levels, where there is an interaction between rotational levels belonging to different electronic states of the molecule.[6, 7]

[5] Besides the $(s_1s_2)$ energy, there is *another* interaction energy which tends to produce a differentiation of the three levels $J=K, K\pm1$. This is the energy of orientation of the spin in the small magnetic field parallel to $K$ produced by the rotation of the nuclei. But this energy is negligible, since it is of the order of $mK/2M$ ($m$=electron mass, $M$=nuclear mass) times as large as the very small energy of interaction of the spin of one electron with the orbital motion of another for an orbit having dimensions similar to those of the distance between the nuclei.

[6] For an example of this phenomenon in the upper $^2\Sigma$ levels of the CN molecule, cf. F. A. Jenkins, Phys. Rev. **31**, 554–5 (1928). Here, for certain $K$ values, the ordinarily very narrow spin doublets ($J=K\pm1/2$) show large separations.

[7] Cf. G. H. Dieke in regard to perturbations in $He_2$ (Nature, March 23, 1929). Dieke discusses the splitting of the $4\pi$, $^3\Pi$ term and suggests that it corresponds to the expected spin fine structure.

## Comparison with Experiment, Explanation of Results

Previously to the present work, no evidence of triplet structure in the ortho-$He_2$ levels had been reported, except in the case of certain perturbed rotational levels of the $4p\pi$, $^3\Pi$ and $5p\pi$, $^3\Pi$ electron states. Dieke first pointed out[7] that there is evidence in the $4p\pi$, $^3\Pi$ levels of the predicted triplet structure. According to Curtis and Long, and Curtis and Jevons,[8] the line $Q(9)$ in the $4p\pi$, $^3\Pi \rightarrow 2s\sigma$, $^3\Sigma$ band is a doublet with the low-frequency component stronger. The doublet separation is relatively large: the measured $\Delta\nu$ is 6.5 $cm^{-1}$ in the 0,0 band, 6.8 $cm^{-1}$ in the 0,1 band, and 6.6 $cm^{-1}$ in the 1,1 band.

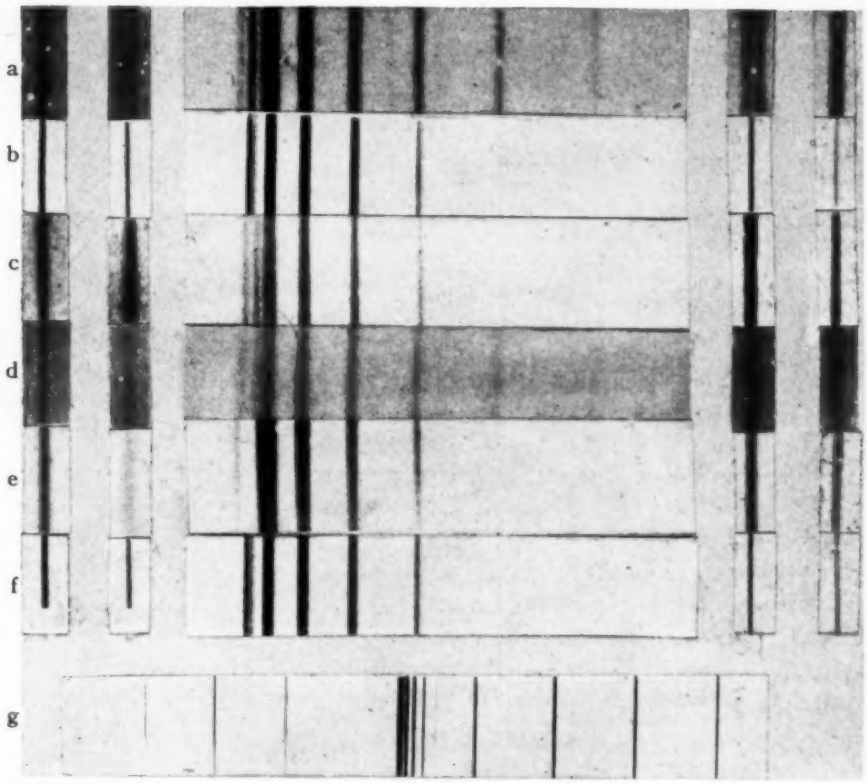


Fig. 1. Enlargements of λ6400 band from second order grating photographs. Strip *g* shows the band as a whole; strips *a*, *b*, *c*, *d*, *e*, *f*, show the *Q* branch as a whole, on a larger scale, together with the first two lines of the *P* and *R* branches. The various strips correspond to different fields and states of polarization as follows: *b*, *f*, *g*: no field; *c*, *d*, *e*, parallel polarization, increasing field strength, with $H=30{,}500$ gauss in *e*; *a*, perpendicular polarization, $H=30{,}500$. The enlargements for *a* to *f* were made on nearly, but not quite, the same scale, and are fitted together so that the center of gravity of the $Q(1)$ line is matched up as well as possible on the different strips; similarly with the *P* and *R* lines, which were each cut out separately from the original photographs, in order to save space.

[8] W. E. Curtis and R. G. Long, Proc. Roy. Soc. **108A**, 531–2 (1925); W. E. Curtis and W. Jevons, Proc. Roy. Soc. **120A**, 117, 124 (1928)

Since it is known, from its absence in other bands ending on the $2^3\Sigma$ levels, that the perturbation is not in the latter, it is evident that it is characteristic of the $A$ level with $K=9$ of the $4p\pi$, $^3\Pi$ state. (The $A$ levels are involved for the $Q$ branch, the $B$ levels for the $P$ and $R$ branches). Strange as it seems at first sight, the perturbation is apparently approximately the same in the vibrational levels $v=0$ and $v=1$ of $4p\pi$, $^3\Pi$. In addition to the facts already mentioned, Curtis and Jevons state (reference 11, p. 124) that the stronger (low-frequency) component of the $Q(9)$ doublet in the (1,1) band appears to be itself double. If this is correct, the $Q(9)$ line consists of a triplet whose com-

TABLE I. *Fine structures in helium band lines.*
*A. Doublet separations $\Delta\nu$ for lines ending on A levels of $2p\pi$, $^3\Pi$ state.*

| $K$ | λ6400 $Q$ | λ4546 $Q$ | $R_A$ | λ5733 $Q_A$ | $P_A$ | Average |
|---|---|---|---|---|---|---|
| 1 | 0.34 | 0.40 | (masked by $Q(11)$) | — | — | 0.36 |
| 3 | 0.28 | 0.31 | 0.26 | 0.32 | (faint) | 0.29 |
| 5 | 0.26 | 0.30 | 0.25 | 0.25 | 0.29 | 0.27 |
| 7 | 0.29 | 0.20 | 0.25 | 0.20 | 0.29 | 0.25 |
| 9 | 0.24 | 0.20 | | | | 0.22 |
| 11 | 0.22 | | | | | |
| 13 | 0.26 | | | | | |

*B. Fine structures for lines ending on B levels of $2p\pi$, $^3\Pi$ state.*

| | λ6400 | | λ4546 | | | λ5733 | | |
|---|---|---|---|---|---|---|---|---|
| | $P$ | $R$ | $P$ | $R$ | $R_B$ | $Q_B$ | $P_B$ | Average |
| 2 | $\Delta\nu=0.28$ | 0.24 | (double, faint) | (faint) | 0.34 | 0.37 | — | $\Delta\nu=0.31$ |
| 4 | All lines symmetrically broadened | | | | | | | (broad) |
| 6 | " " | | " | " | | | | " |
| 8 | " " | | " | " | | | | " |

*Notes.* (1) The $K$ values are those of the rotational levels of the $2p\pi$, $^3\Pi$ state, which are common to all the bands λλ6400, 4546, 5733. (2) All $\Delta\nu$ values given are weighted means of careful measurements on from two to four different plates, all the measurements having been made by one person. The measurements have also been checked by another observer. They should not, however, be considered at all accurate, since the doublets measured are in most cases barely resolved. The average doublet separation given in the last column is a weighted mean which we take to be characteristic of the $2p\pi$, $^3\Pi$ rotational level. (3) Lines marked "faint" were too weak for a reliable determination of structure. (4) For all doublets ending on $A$ levels, the intensity ratio was about the same (about 2:1 to 3:1, as estimated visually, in favor of the higher frequency component). For the doublets ending on the $B$ level with $K=2$, the visually estimated ratios were about 3:1 to 6:1, with the high-frequency component stronger.

ponents are approximately equal in intensity, and the $A$ level $K=9$ of $4p\pi$, $^3\Pi$ consists of a similar triplet. Such an abnormally spaced triplet is reminiscent of the $2^3P$ triplet of the He atom, although the triplet is much wider here. The nearly equal intensity of the triplet components in $Q(9)$ is as expected, since they correspond to the $J$ values 10, 9, 8, whose statistical weights $(2J+1)$ are nearly equal.—In the $5p\pi$, $^3\Pi\rightarrow 2s\sigma$, $^3\Sigma$ band, according to Curtis and Long, the line $Q(5)$ of the 0, 0 band is a doublet with the *high-frequency* component stronger. The explanation is presumably similar to that just given.

The present work arose from theoretical considerations above indicated, and from the observation that the lines of the λ 6400 band ($3s\sigma$,$^3\Sigma\rightarrow 2p\pi$,$^3\Pi$),

in preliminary photographs taken by Mr. L. E. Pinney with the 21 foot Rowland grating (14,438 lines per inch) in connection with a projected investigation of the Zeeman effect in $He_2$, appeared unusually broad as compared with the lines of other $He_2$ bands. Second and third order photographs taken by the present writers showed that the lines of this band, and of other bands ending on the $2p\pi,{}^3\Pi$ level, do indeed have a fine structure.

In the $Q$ branch of λ6400 (second order photographs), the fine structure consists of narrow doublets, whose width decreases slowly with increasing $K$ (cf. Table I and Fig. 1*b*). In each doublet, the high-frequency component is the stronger, the intensity ratio being the same, so far as could be estimated, for all values of $K$(cf. Fig. 1*b*). Visual estimates indicate about 2:1 or 3:1 for the value of this intensity ratio.

In the $P$ and $R$ branches, the first line consists of a strong component with a weak satellite very close to it on the low-frequency side (cf. Table I), the intensity ratio being much greater than for the $Q$ lines. The remaining lines of the $P$ and $R$ branches are all abnormally broad, as compared with, for example, the individual components of the $Q$ lines, or with lines of some of the other $He_2$ bands. The broadening is, so far as can be seen, completely symmetrical, with a practically uniform intensity over an appreciable width near the center of the line (this was confirmed by photometer traces). This symmetrical broadening might be ascribed to an unresolved doublet or triplet structure.

The λ4546 band ($4s\sigma,{}^3\Sigma \rightarrow 2p\pi,{}^3\Pi$), as studied in third order photographs, shows fine structures which are, within the error of their experimental determination, identical with those in λ6400 (cf. Table I). This identity indicates that the ${}^3\Sigma$ levels ($3s\sigma,{}^3\Sigma$ and $4s\sigma,{}^3\Sigma$) do not influence the observed fine structures. Hence it seems probable that, within the error of the present measurements, the $2p\pi,{}^3\Pi$ levels alone have fine structures of appreciable magnitude, —a conclusion which is in harmony with the theoretical considerations presented in the preceding section. A careful examination of the $3p\pi,{}^3\Pi^0 \rightarrow 2s\sigma,{}^3\Sigma^0$ and $3p\pi,{}^3\Pi^1 \rightarrow 2s\sigma,{}^3\Sigma^1$ bands λλ 4650 and 4670 (the superscript on the right is the vibrational quantum number) gave no evidence of fine structures. This indicates, although it does not prove conclusively, that neither the $2s\sigma,{}^3\Sigma$ nor the $3p\pi,{}^3\Pi$ levels have fine structures of appreciable size, for either of the vibrational quantum numbers 0 or 1. This is in harmony with the theoretical considerations, although the absence of fine structures in the $2s\sigma,{}^3\Sigma$ state is somewhat more surprising than their presence would have been.

Having found, in the λ6400 and λ4546 bands, fine structures apparently characteristic of the $2p\pi,{}^3\Pi$ state, it seemed desirable to confirm these by measurements on other bands ending with this state. For this purpose the λ5733 band ($3d\delta,{}^3\Delta \rightarrow 2p\pi,{}^3\Pi$) was the most suitable, and measurements were made on second order plates. In this band (six branches) a $P$, a $Q$ and an $R$ transition occur to (nearly) every rotational level, of both the $A$ and $B$ types, of the ${}^3\Pi$ state; whereas in the λ6400 and λ4546 bands (three branches) the ${}^3\Pi$ $A$ levels are represented only in $Q$ branch transitions, and the ${}^3\Pi$ $B$ levels only in $P$ and $R$ branch transitions. The relations between band lines and rotational levels for all three bands are shown in Fig. 2.

If the fine structure patterns are determined exclusively by fine structures in the $2^3\Pi$ rotational levels, every line ending on a given $2^3\Pi$ level should show identically the same pattern (including intensity relations) in all branches of all bands involving this level. For example, the lines $Q(3)$ of λ6400, $Q(3)$ of λ4546, and $R(3)$, $Q(3)$ and $P(3)$ of λ5733, which all end on the $A$ level $K=3$ of $2^3\Pi$, should all look alike. Experimentally it is found that all these lines,—except $P(3)$, which is too faint for study,—consist of a doublet with $\Delta\nu = 0.29 \pm 0.03$ and with the high-frequency component about twice as strong as the other component.[9] The lines ending on other $A$ levels show simi-

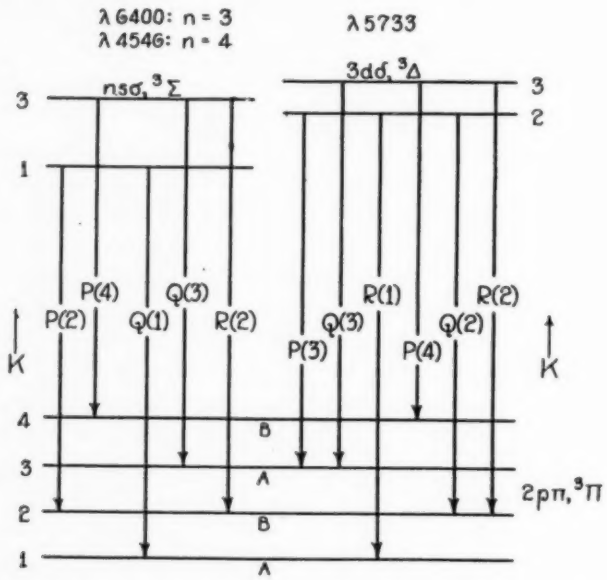


Fig. 2. The figure shows, for the lowest four levels of the $2p\pi$, $^3\Pi$ state, how the lines of the various branches in the λλ6400, 4546, and 5733 bands are related to the rotational levels (cf. ref. 10). The spacings of the levels are not to scale (for the true spacings in the $^3\Pi$ state, cf. Fig. 3).

lar agreements (cf. Table I).[9] Similarly all the lines ending on the $B$ level $K=2$ consist of a doublet of width $0.31 \pm 0.05$ whose high-frequency component is much stronger than the other (cf. Table I).[9] Again, all lines ending on other $B$ levels show unusual breadth, but no resolvable fine structure.

In the last column of Table I, the results obtained for each $K$ level of the $2^3\Pi$ state have been averaged, since we believe that these results are characteristic of the latter. In the energy level diagram Fig. 3, the $2^3\Pi$ rotational levels are shown, together with their fine structures on an exaggerated scale. The diagram is drawn in such a way as to show the statistical weights of

[9] In our preliminary account in Nature (**124**, 91, (1929)), we stated that the separations appeared to be smaller in some of the λ5733 lines, thus indicating a fine structure in the $3d\delta$, $^3\Delta$ levels. Careful remeasurement shows, however, that this is not the case within the error of measurement, which is, however, (relatively) large because of the small separations.

the various fine-structure levels, as indicated by the intensities in the fine structure patterns of the band lines. We shall return shortly to the interpretation of these statistical weights in terms of $J$ values.

In addition to the bands λλ6400, 5733 and 4546, the bands λ5880 ($3d\pi$, $^3\Pi \rightarrow 2p\pi, ^3\Pi$) and λ4440 ($4d\pi, ^3\Pi \rightarrow 2p\pi, ^3\Pi$) were found to contain evidences of fine structure, although these bands were too faint for good measurement on the plates available. In λ5880, all the observable lines of the $P$ and $R$ branches showed evidence of doublet structure with the high-frequency component stronger; the $Q$ lines were too faint for observations on their structure. In λ4440, the $P$ and $Q$ lines were too faint, but the $R$ lines showed doublet structure as in λ5880; a measurement on $R(1)$ gave $\Delta\nu = 0.24$ cm$^{-1}$. These observations on λ4440 and λ5880 are, qualitatively at least, in harmony with the idea

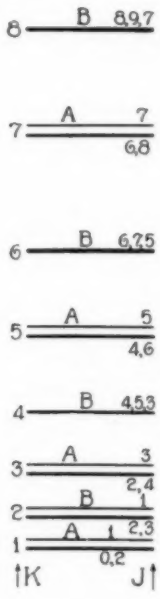


Fig. 3. Empirical fine structures of rotational levels of $2p\pi, ^3\Pi$ state of $He_2$, together with their interpretation in terms of $J$ values.

that the fine structures are due to the $2^3\Pi$ levels alone. Other bands ending on the $2^3\Pi$ levels were too weak for observation on our plates.

Returning to Fig. 3, the $2^3\Pi$ fine structures may be interpreted as follows. According to theory (cf. first section), one expects for each value of $K$ a fine structure with three levels ($J=K$, $K\pm1$), each having a statistical weight $2J+1$ (equal to the number of possible orientations in an external magnetic field). Suppose, for a given $K$, the levels with $J=K\pm1$ approximately fall together, while $J=K$ is distinct; the composite $J=K\pm1$ then has a statistical weight $4K+2$, which is just twice the weight $2K+1$ of the level $J=K$. This supposition accounts well for the observed relations in the $A$ class of rotational levels. To explain the $B$ level fine structures we may assume that $J=K$ and $J=K+1$ approximately fall together for $K=2$, while $J=K-1$ lies

higher; but that for $K=4, 6, \cdots$ the three levels $J=K, K\pm1$ are approximately equally spaced, with a spacing which is large enough to give an observable broadening, but not large enough to give a resolvable fine structure. The assumption made for $K=2$ would give a 12:3 ratio of statistical weights for the two components, in harmony with the estimated experimental ratics for the lines ending on this level.

Just why the $A$ and $B$ levels should show such different fine structures is not evident, but from the introductory discussion it can be seen that the fine structure of any level should be determined by the algebraic sum of different interaction energies not all of the same sign, so that the final result might well be greatly influenced by small changes in the individual interaction energies. The fine structures observed for the $A$ levels are apparently

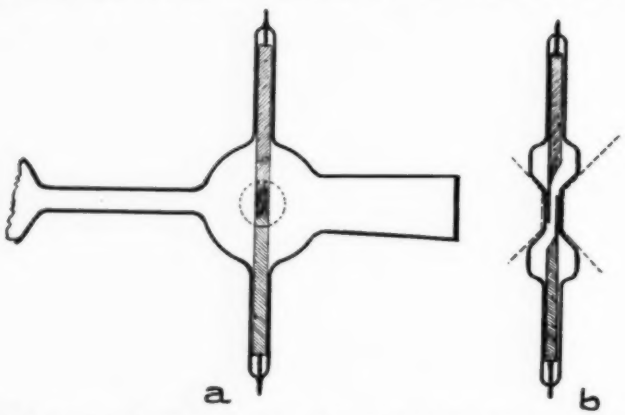


Fig. 4. (*a*) Side view about one-half real size, of discharge tube for Zeeman effect of $He_2$ bands. The dotted circle shows the position of the ends of pole pieces. The shaded portions indicate aluminum electrodes, tapered at the ends (see *b*). The dark shaded region at the center indicates the extent of the area where the discharge takes place in the field. At the left (not shown) is an enlarged portion of the tube to act as a reservoir of He (pressure 1.2 cm Hg). At the right is a flat glass window fused to the tube.

(*b*) Cross section of tube at axis of pole pieces, showing depressions in sides of tube to admit poles. The dotted lines indicate the magnet poles. Pole gaps of 5 mm to 7 mm have been used with these tubes.

similar to those for $^3\Sigma$ states (cf. p. 1531 above), where only an $(s_1s_2)$ interaction energy is involved. But the fine structure observed in the $B$ level $K=2$, as interpreted in the preceding paragraph (cf. Fig. 3), is closely analogous to that observed in the $2\,^3P$ state of the helium atom, where an $(s_1l)$ and an $(s_2l)$ interaction are of importance as well as an $(s_1s_2)$ interaction.

## Zeeman Effects

A study of the Zeeman effect for some of the bands discussed above seemed of interest. At low fields one would expect each fine structure component to show characteristic Zeeman patterns, while at high fields one would expect a Paschen-Back effect, giving rise to Zeeman patterns identical with those of par-$He_2$ bands. The results of a study of the $\lambda$6400 band ($3s\sigma,^3\Sigma\rightarrow 2p\pi,^3\Pi$) in magnetic fields of various strengths are reported below.

The preliminary experiments on the Zeeman effect of the helium bands were made by Mr. L. E. Pinney, who designed and constructed the discharge tube shown in Fig. 4. Although this source is faint, it has the advantage that almost the entire discharge between the electrodes is in the pole gap, parallel to the field. Under the proper conditions, the light which reaches the slit is from the center of the space between the pole pieces. Current of a few milliamperes from the secondary of a 1/2 K. V. A. transformer was used, with the usual spark gap in series, to excite the $He_2$ bands.

The λ6400 band was photographed in the second order (1) without field (2) at two (undetermined) moderate field strengths (3) with a field of 30,550 gauss (determined by comparison with atomic helium lines). The two photographs at moderate field strength were taken in the parallel polarization, while the strong field patterns were photographed both in parallel and in perpendicular polarization. The appearance of the most important lines of the band under these various conditions is shown in Fig. 1, while measurements on the strong-field plates are given in Table II.

TABLE II. *Zeeman effects in $He_2$ λ6400 ($H=30{,}550$ Gauss).*

| Line | Polarization | | Line | Polarization | | Line | Polarization | |
|---|---|---|---|---|---|---|---|---|
| | Par. | Perp. | | Par. | Perp. | | Par. | Perp. |
| $R(10)$ | | *s* | $Q(13)$ | | *s* | $P(10)$ | *d* | *slb* |
| 8 | *slb* | *s* | 11 | *b* | *s* | 8 | *d* | *b* |
| 6 | *b* | *b* | 9 | *b* | *s* | 6 | *d* | *b* |
| 4 | *b* | *b* | 7 | *vb* | *s* | 4 | *b* | double (0.34) |
| 2 | *vb* (0.64) | *vvb*# (0.86) | 5 | double (0.29) | *b* | 2 | *b* | double (0.76) |
| | | | 3 | double* (0.71) | *vb*** (0.51) | | | |
| | | | 1 | double* (1.44) | triple** (1.51) | | | |

*General notes*: In all branches, the lines get narrower with increasing $K$. The numbers given under the description of a line give its over-all width, or in the case of doublets, the apparent doublet separation. *b*, *s*, *v*, *d*, and *sl* respectively stand for broad, sharp, very, diffuse, and slightly. For intensities, cf. text.

*Special notes*: #This line is faintly double. *The high-frequency component of the $Q(3)$ doublet and the low-frequency component of the $Q(1)$ doublet fall together. **The low-frequency component of the $Q(1)$ triplet falls on the edge of the broadened $Q(3)$ line, and is not clearly distinguishable from the latter.

For high field strengths, the observed structures are in excellent agreement with those predicted for a $^1\Sigma \rightarrow {}^1\Pi$ transition.[11] In particular, the line $Q(1)$ appears to be a symmetrical triplet of width $\Delta\nu = 1.46$, in agreement with the theoretical value[11] $\Delta\nu = \Delta\nu_{norm} = 1.43$ for $H = 30{,}550$ ($\Delta\nu_{norm}$ = half-width of normal atomic triplet). In perpendicular polarization, the middle component and the high-frequency component appear as sharp lines with a separation $(1/2)\,\Delta\nu_{norm}$ (cf. Fig. 1*a*), the former being about twice as strong as the latter, in agreement with the theory; the low-frequency component falls at the high-frequency edge of the broad unresolved pattern of $Q(3)$, and so cannot be

[10] Cf. R. S. Mulliken, Phys. Rev. **28**, 1209 (1926).

[11] Cf. W. E. Curtis and W. Jevons, Proc. Roy. Soc. **120A**, 110 (1928).

separately identified. In parallel polarization (Fig. 1*e*), the middle component is absent, in agreement with the theory, while the high-frequency component appears at the same position as in perpendicular polarization; the low-frequency component approximately coincides with and intensifies the high-frequency component of $Q(3)$, which here in parallel polarization is essentially a doublet (see below). At lower field strengths, where the $Q(3)$ pattern no longer overlaps it, the $Q(1)$ line in parallel polarization appears distinctly as a doublet (cf. Fig. 1 *c*, *d*).

The $Q(3)$ line should according to theory[11] appear in parallel polarization on the strong field plate as a doublet of width $\Delta\nu = (1/2)\Delta\nu_{norm} = 0.71$. (Really there should be seven components, but only the outermost should be strong.) The observed interval between the high and low frequency components of this line [as already mentioned, the high-frequency component coincides with the low-frequency component of $Q(1)$]—is $\Delta\nu = 0.71$. In perpendicular polarization, the $Q(3)$ line is merely broadened (width 0.50 $cm^{-1}$); this is in agreement with the theoretical prediction of a pattern of seven components with the middle ones strongest. The $Q(5)$ line in parallel polarization appears as a narrow doublet, while all the other $Q$ lines appear merely broadened, less and less so as $K$ increases. This is all in harmony with the theory. —Without going into details, it may be said that the behavior of the $P$ and $R$ lines at high fields is also in excellent agreement with the theory for a $^1\Sigma \rightarrow {}^1\Pi$ transition (cf. Table II and Fig. 1*a*, *e*; and ref. 11 for theory).

On the two plates taken in parallel polarization at lower field strength [probably about 10,000–15,000 gauss, judging from the $\Delta\nu$ values in $Q(1)$], all the lines appear single and fairly sharp, except $Q(1)$, which is a doublet, and $R(2)$, which is perceptibly broader than the other $R$ lines (cf. Fig. 1*c*, *d*). Even $Q(3)$ shows little if any broadening. The doublet separations in $Q(1)$ are 0.71 and 0.88 on the two plates. The high frequency component of the doublet appears to be stronger and perhaps broader than the low-frequency component. Except for this, there is no indication of the zero-field fine structures.

Evidently the Paschen-Back effect becomes practically complete at moderate values of the magnetic field, as might indeed be expected in view of the narrowness of the original fine structures ($\Delta\nu \sim 0.3$ $cm^{-1}$). Comparative measurements were made of the positions of the centers of the various band-lines (or their Zeeman patterns) in magnetic fields and with zero field. In all cases, the position of the center of the line in the field agrees, within the errors of measurement, with the center, or center of gravity in the case of the $Q$ lines and $P(2)$ and $R(2)$, of the corresponding line with zero field. This is in agreement with what would be expected for a Paschen-Back effect. The results are, however, hardly more than qualitative, on account of the narrowness of the original fine structures and because we are dealing with differential measurements.

Further work on the Zeeman effect in $He_2$ is being carried on by Mr. J. S. Millis.

# THE CONTINUOUS SPECTRA OF FLAMES CONTAINING THE HALOGENS

By H. C. Urey and John R. Bates*
Columbia University and Princeton University

(Received October 7, 1929)

Abstract

According to the Franck-Condon theory for the dissociation of molecules by light, we should also expect that two colliding atoms may recombine with the emission of light. This should occur if conditions are arranged so that there are appreciable quantities of the free atoms present. Experiments were carried out with flames of chlorine and hydrogen and hydrogen-oxygen flames containing the halogens. Spectra of these flames are found to be continuous extending into the ultra-violet. It is shown that the violet limits of these spectra are in agreement with the hypothesis that they are due to the recombination of the normal and excited halogen atoms. Calculations show that there are enough collisions of this type in our flames to account for the intensity of the light emitted.

IT IS well known that the absorption spectra of certain molecules, of which the hydrogen halides are examples, are continuous, with no indication of any band structures whatsoever and that the absorption spectra of other molecules of which the halogens are examples are partly continuous and partly typical band spectra. Franck[1] suggested that these continuous spectra were due to the dissociation of the molecule by light so that the higher energy states are continuous and further that the appearance of this continuous spectrum and the dissociation processes depend upon the shape and relative positions of the two potential energy curves as a function of the internuclear distance in the case of the initial and final states. Condon[2] extended this theory to include the distribution of intensities for the different vibrational quantum number changes in band spectra, and recently has discussed these continuous spectra using the Schroedinger wave mechanics. He shows that the new and older theories give qualitatively the same results, but the new theory enables him to predict the distribution of intensities in the continuous part of these spectra.

According to Franck the absorption of light by the halogens results in the dissociation of these molecules into a normal and an excited atom. It is evident that the reverse process must also be possible so that a normal and an excited halogen atom should recombine with the emission of light to form a normal or excited molecule. Kondratjew and Leipunsky[3] have reported that they have observed such a spectrum from the halogens heated in a quartz tube to 1000°C. In this paper we report the results of an investigation on the spectra of flames containing hydrogen and chlorine and of flames containing hydrogen, oxygen, and the halogens. There are two immediate pos-

* National Research Council Fellow.

[1] J. Franck, Trans. Faraday Soc. **21**, 536 (1925).

[2] E. U. Condon, Phys. Rev. **28**, 1182 (1926); **32**, 858 (1928).

[3] Kondratjew and A. Leipunsky, Zeits. f. Physik **50**, 366 (1928).

sibilities, namely, that the continuous spectra are due to the recombination of normal and excited halogen atoms and that they are due to the recombination of hydrogen and halogen atoms to form the hydrogen halides. We cannot exclude the possibility that it is the latter reaction which is responsible for the emission of light, but as we shall show below, the distribution of intensities in these continuous spectra can be roughly accounted for by applying the Franck-Condon theory to the recombination of normal and excited halogen atoms.

## Experimental

We have taken spectrograms of the hydrogen halogen flames in the visible and ultra-violet and determined the short wave limit of these spectra. Photographs were taken of the inner cone of the flame, just as it emerges from the nozzle of a torch. It was necessary in order to burn the bromine and iodine, to have oxygen mixed with them. This was accomplished by bubbling the latter gas over the liquid halogens. While the ordinary type of torch was sufficient to give the desired results, exposures were found to be shortened materially by using a fish tail type of burner made of glass.

*The hydrogen-chlorine flame.* The hydrogen-chlorine flame gives a perfectly continuous spectrum throughout the visible and into the ultra-violet as far as the water band, which accompanied it, due to the burning hydrogen in the external sheath of the flame. We were able to show that the continuous was not connected with the oxygen-hydrogen part of the flame by burning chlorine in an atmosphere of hydrogen and photographing through a quartz window. The continuous appeared, and the water bands were, of course, absent.

*The hydrogen-bromine and hydrogen-iodine flames.* The hydrogen-bromine and iodine flames, which always had oxygen mixed with the halogen, gave a series of diffuse bands in addition to the continuous spectra throughout the visible but these ended on the violet side further to the red than in the case of chlorine. In order to see if chlorine exhibited the same bands, oxygen was mixed with the chlorine and a series of doublets appeared at shorter wave-lengths than those of bromine, which were in turn shorter than those of iodine. Since oxygen made the flame considerably hotter and caused the *D* lines of sodium to appear due to evaporation of sodium atoms from the glass, it was thought that the bands might be due to sodium halide molecules. A torch constructed entirely of fused quartz, however, gave the bands with no sodium lines present. Since the bands do not appear in the hydrogen chlorine flame, without oxygen, we concluded that they must arise from some compound of oxygen and halogen, such as ClO. These bands are so diffuse on our plates that we found it impossible to measure their positions. These bands lie at approximately the following wave-lengths in the case of oxygen flames containing the three halogens: $Cl_2$, 3600–4350A; $Br_2$, 4250–4675A; $I_2$, 4270–4900A. It is impossible to fix the short wave-length limit of these continuous spectra precisely because there is no sharp limit, but only a rather rapid decrease in intensity toward the violet. We estimate that this rapid decrease in intensity occurred at 3200A, 3400A, and 3600A in the cases of chlorine, bromine, and iodine, respectively. These numbers are certainly in the

order in which the rapid decrease in intensity took place in the three cases, but it was more difficult to fix a limit for the bromine and iodine spectra than for the chlorine spectrum due partly to the presence of the diffuse bands already referred to.

## Discussion of Experimental Results

As mentioned in the introduction, it is necessary to consider the two possibilities that these continuous spectra may be due to the recombination of halogen atoms or the recombination of hydrogen and halogen atoms. In Figure 1 we give a resumé of the principal facts in regard to the limits of the

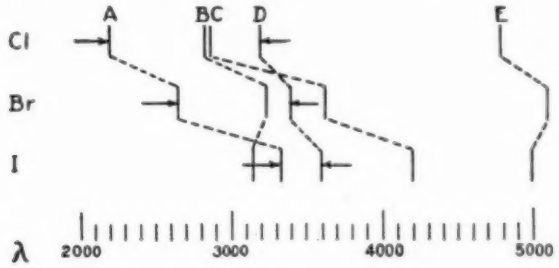


Fig. 1.

A. Long wave-length limit of the continuous absorption of the halogen hydride.
B, Calculated wave-length for $HX \rightarrow H+X$ ($^2P_{1/2}$).
C, Calculated wave-length for $HX \rightarrow H+X$ ($^2P_{3/2}$).
D, Approximate short wave-length limit of the continuous emission of the halogen.
E, Observed wave-length for $X_2 \rightarrow X(^2P_{3/2})+X(^2P_{1/2})$.

continuous absorption of the hydrogen halides and the halogens together with the calculated wave-lengths for dissociation in several different ways. The legend under the figure explains the meaning of the wave-lengths plotted. It appears that there is no satisfactory correlation between the short wave-length limit which we observed for the continuous flame spectra and any of these quantities except the short wave-length limits for the absorption spectra of the halogens. Thus Ribaud[4] found that the absorption spectrum of chlorine reaches a maximum in the neighborhood of 3400A and decreases rapidly in the neighborhood of 3200A, while we observe that the short wave-length limit of the continuous spectrum of the hydrogen chlorine flame is about 3200 A. In the case of bromine the maximum of the absorption spectrum occurs at about 4150A and there is a decided decrease in intensity between 3400 and 3700A, agreeing again fairly well with our observed limit of 3400A for emission in the hydrogen oxygen flame containing bromine. In the case of iodine the maximum intensity of the absorption spectrum is in the discontinuous banded spectrum and decreases slowly with decreasing wave-length. It is difficult to tell whether our observed value of 3600A agrees with the observed falling-off of the continuous absorption spectrum. However, our data are in entire agreement insofar as the relative position of the three limits in the case of the emission spectra and the three limits in the case of the absorption spectra, that is, there is a gradual shift toward longer wave-lengths in both cases as we go from chlorine to bromine to iodine.

[4] G. Ribaud, Ann. de physique **12**, 107 (1919).

In the case of iodine it is possible to construct the two potential energy curves for the normal and excited electronic states respectively from the known band spectrum data. It is necessary to know the equilibrium distance between the nuclei, and the vibrational energy levels. It is then easy to construct the approximate potential energy curves using the empirical formula of Morse.[5] Over the region where the energy levels follow the formula

$$E = h\nu_0(n+1/2) - h\nu_0 x(n+1/2)^2, \tag{1}$$

the potential energy follows the formula,

$$V(r) = D \exp\left[-2a(r-r_0)\right] - 2D \exp\left[-a(r-r_0)\right], \tag{2}$$

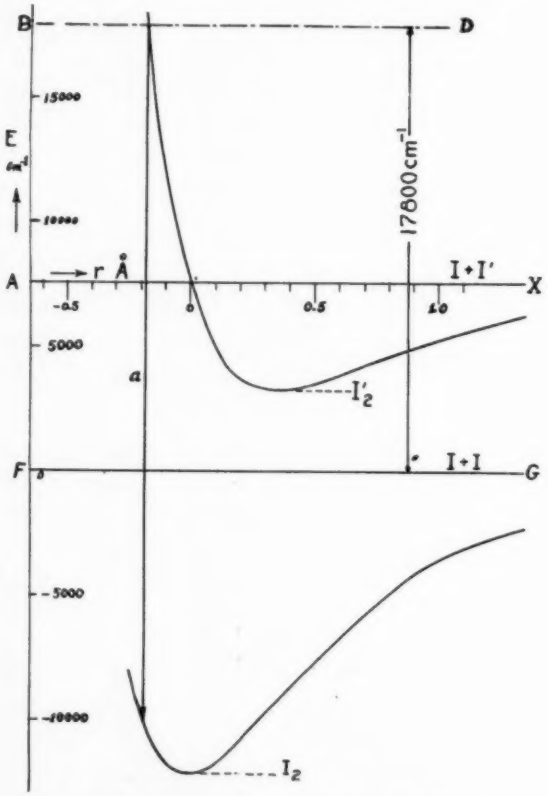


Fig. 2. The $V$ and $V'$ curves of $I_2$.

where $D$ is the energy of dissociation and equals $\nu_0^2/4\nu_0 x$, $a$ is a constant equal to $(8\pi^2 c\mu\nu_0 x)^{1/2}$ ($\mu$ equals the reduced mass), $r$ is the distance between the nuclei and $r_0$ the equilibrium distance. Of course in the region where $V$ is greater than 0, and in which we are most interested, this formula may not hold. Figure 2 shows these potential energy curves for iodine using values for $r_0$, the energy of dissociation and the formula for the vibrational energy levels as given by Birge.[6]

[5] P. M. Morse, Phys. Rev. **34**, 57 (1929).

[6] I. C. T. Vol. 5, p. 409. The curves are similar to those published by Condon (Phys. Rev. **32**, 858 (1928)).

In the case of bromine we do not know the moment of the inertia and thus the potential energy curves can be drawn using the values of $D$ and $a$ from the known vibrational energy levels, but the displacement of the two curves relative to each other along the $r$-axis cannot be determined. In this case we have two rules which might be used. First Mecke[7] has shown that for a great many molecules the product of the vibration frequency for zero amplitude and the square of the equilibrium distance is very nearly a constant, and second, Morse[5] has shown that in the case of some 21 molecular states the product of the frequency of vibration and the cube of the equilibrium

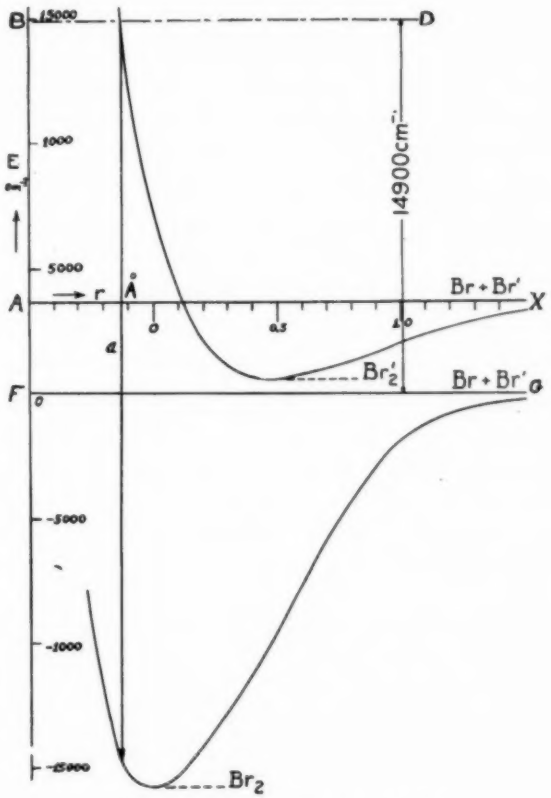


Fig. 3. The $V$ and $V'$ curves of $Br_2$.

distance is very nearly equal to a constant for all these molecules. Unfortunately, neither of these rules holds in the case of iodine, and we are therefore doubtful as to whether we can use it in case of bromine. We have drawn the curves for bromine in Figure 3 by using Morse's expression for the potential energy curves, and have then adjusted the relative position of the two curves so that the maximum intensity in the continuous absorption of bromine is that predicted by the Franck-Condon theory. Thus we draw a straight vertical line from the minimum of the lower potential energy curve and lay off a distance of 27000 $cm^{-1}$ corresponding to 3700A, which is the

[7] R. Mecke, Zeits. f. Physik **32**, 823 (1925).

wave-length of the maximum of the absorption curve of Ribaud and therefore of the most probable transition, and require that the upper potential energy curve shall pass through this point. Condon has used essentially this method to construct the curves to predict the distribution of intensity in the continuous absorption spectra.

Recently Elliott[8] has analyzed three absorption bands of chlorine, and it is possible from his data to secure the equilibrium distance between the nuclei in both the higher and lower electronic states. By using the isotope effect he was able to fix the vibration quantum numbers for the higher energy states, and in this way revised the values for the energy of dissociation and the formula for the vibrational energy levels of this state. He finds in this way that his bands correspond to the transitions in the vibrational quantum numbers, 2→17, 2→18, and 2→19, and he gives the values of the $B$'s for the initial and final states. From the theory of band spectra we know that

$$B_n = \frac{h}{8\pi^2 I_0 c} - \frac{\alpha}{c} n.$$

The values of $B_n$ for the three excited states serve to determine $\alpha/c$ and $I_0$. We find in this way that the equilibrium distances between the nuclei for the initial and final states are $r_0' = 2.19$A and $r_0'' \leqq 1.98$A. Further Elliott secures as the formula for the energy levels of the excited state,

$$E/h = 316(n'+1/2) - 10.9(n'+1/2)^2.$$

Using these values and constructing the curves as in the case of iodine, we find that the Franck-Condon theory would predict the discontinuous absorption spectra from the normal vibrational state. This is contradicted by the experimental data of Kuhn[9] who showed that absorption from the normal vibrational level occurs only in the continuous region. In view of this difficulty we have not attempted to correlate our data with these potential energy curves.[10]

We make the postulate that the temperatures of our flames in the gas of bromine and iodine were approximately the same, and that the violet limit is emitted by the recombination of a normal and an excited atom, such that the sum of the relative translational energy of the two atoms plus the energy required to raise the normal halogen atom in the $^2P_{3/2}$ to the $^2P_{1/2}$ state is the same for bromine and iodine. Referring to Figures 2 and 3, at some point on $r$ the difference in energy between the normal and excited potential energy curves is equal to the observed violet limit of the continuous emission. These transitions are indicated by the arrows. Light of this wave-length is emitted by two colliding atoms having energy represented by the lines $BD$ in each case. The difference in energy between the two states represented by the

[8] A. Elliott, Proc. Roy. Soc. **A123**, 629 (1929).

[9] H. Kuhn, Zeits. f. Physik **39**, 77 (1926).

[10] In an abstract of this paper previously published (Phys. Rev. **33**, 279 (1929)), we stated, that we had drawn such curves for chlorine. The curves used were constructed in a similar way to that used by Condon.[6] However, these curves do not follow the empirical formula of Morse particularly well and it appears in view of Elliott's results, that the constants of the excited chlorine molecule are as yet uncertain or else definitely disagree with the Franck-Condon theory.

lines $FG$ and $BD$ in each figure is the energy of excitation of one atom to the $^2P_{1/2}$ state and the relative translational energy of the two atoms. In the case of iodine and bromine, using the curves as we have drawn them, we find that these energies correspond to 17800 and 14900 $cm^{-1}$ respectively as indicated in the figures. The agreement between these two values is as close as can be expected considering the difficulty of determining the violet limit of the continuous spectrum, and the accuracy with which we can draw the potential energy curves. This comparison serves only to show that it is possible by making these rather simple assumptions, to correlate these continuous spectra with the potential energy curves of iodine and bromine. In view of the fact that the potential energy curves of chlorine do not seem to agree with the observed absorption spectrum, we cannot say whether this rule applies in the case of the flames containing chlorine.

It is necessary to determine whether there are sufficient collisions in which the sum of the relative translational energy and the energy of excitation of the one atom is equal to or greater than 17800 wave-numbers to account for the observed intensity of the radiation. The number of collisions in which this condition is fulfilled, is readily calculated and found to be,

$$n=2N^2\sigma^2(\pi kT/m)^{1/2}[1+(E/kT)]\exp[-(E+E')/kT], \qquad (3)$$

where $N$ is the number of halogen atoms per $cm^3$, $\sigma$ the collision distance of of a normal and excited atom, $m$, the mass of one atom, $T$ the temperature, $E$ the relative kinetic energy and $E'$ the energy of excitation of the halogen atom in the $^2P_{1/2}$ state. Strictly (3) should contain the factor $(1+1/2\exp[-E'/kT])^{-2}$ but this is very nearly unity in the case of bromine and iodine at the temperatures of our flames.[11]

Investigations on the mean life of excited molecules of atoms show that this is always of the order of $10^{-7}$ or $10^{-8}$ seconds in the case of non-metastable states, and that therefore the probability of transition varies from $10^7$ to $10^8$ per second. Assuming that the time of collision is of the order of the time it takes two molecules to move one Angstrom relative to each other, we can calculate the probability that two colliding atoms, one in the normal state and the other in an excited state, will emit light. In the case of iodine atoms at room temperature this equals 1/37400, and does not change rapidly with temperature. Thus only one collision in 37400 will result in the recombination of the atoms with the emission of light. This probability can be estimated in another way. The time during which the transition is possible will be of the order of one half the time of one classical oscillation of the molecule. In the case of iodine this gives a probability for the recombination process with the emission of light of one in about 80000. This latter method of estimation can be justified by the wave mechanical method of calculating

[11] Formula (3) is easily derived from equation (701) of Jeans "Dynamical Theory of Gases" 3rd edition, Cambridge University Press, 1921, by integration between the limits $E(=\frac{1}{4}mv^2)$ and infinity and the fact that the number of atoms in the $^2P_{1/2}$ and $^2P_{3/2}$ states is

$$n(^2P_{1/2})=\frac{N(\frac{1}{2})\exp(-E'/kT)}{1+(\frac{1}{2})\exp(-E'/kT)}$$

$$n(^2P_{3/2})=\frac{N}{1+(\frac{1}{2})\exp(-E'/kT)}.$$

intensities. The Schroedinger wave function for the collision of two atoms in the region of the distance of nearest approach will be very similar to what the wave function would be in this region if the potential energy curve rose to an infinite value as $r$ increases instead of to the finite value of the dissociation energy. It is only this part of the wave function which contributes effectively to matrix amplitude integral, namely,

$$\int \psi_E \psi_n dv,$$

where $\psi_E$ is the wave function for the continuous state of energy $E$ and $\psi_n$ that for the $n$th vibrational state of the molecule. Our assumption of one half the time of classical oscillation is equivalent to assuming that one half the wave function of the oscillator contributes to the calculation of the matrix amplitude for the transition. From these considerations it appears that the probability for recombination with the emission of light in a collision between two atoms will be of the order of $10^{-4}$ or $10^{-5}$. Polanyi and Schay[12] have concluded that the probability of recombination of Na and Cl atoms in the gas phase is of the order of $10^{-4}$ in agreement with our estimated values.

The energy emitted per cc per sec. of shorter wave-length than our violet "limit" is secured by multiplying (3) by $h\nu$ and the probability of light emission in a collision namely, $10^{-5}$. Substituting the numerical values, $N=2.7\times10^{16}$, $\sigma=3\times10^{-8}$, $E+E'$ and $E$ equal to the energy equivalent to 17800 $cm^{-1}$ and 10000 $cm^{-1}$ respectively, and $T=2000°$ K, we find that this energy in the case of iodine is of the order of 0.01 erg per sec. per cc. This can be changed by assuming lower or higher concentrations of iodine atoms. Zahn[13] showed that the energy emitted by a flame containing sodium was about 100 ergs per sec. per cc. Though we do not know the intensity of emission by our flame it was probably no greater than that of a sodium flame for it required from 20 minutes to an hour to secure an exposure with the Hilger E31 quartz spectrograph.

The calculation which we have made is very approximate, but it does indicate that there are enough collisions of the type postulated to account for the comparatively faint emission of our flames. We believe that the coincidence of these violet absorption edges is sufficiently close to those expected from the theory to indicate that the continuous spectra of these flames are in reality due to these recombination processes. In order to complete the discussion we should compare our data with similar curves for the hydrogen halides. This cannot be done because we do not know even approximately the shape of the energy curve in the excited states of these molecules, since no band spectrum has been observed. It may be, in fact, that there is no minimum in the excited states of these molecules. It is therefore impossible to make any similar comparisons with the theory for these molecules.

The experimental part of this paper was carried out while we were at the Johns Hopkins University and we wish to acknowledge our indebtedness to that institution for the facilities furnished us.

[12] M. Polanyi and G. Schay, Z. Physikalische Chem. **1B**, 30 (1928).

[13] H. Zahn, Verh. Physik. Ges. **15**, 1203 (1913); See, Foote and Mohler, Origin of Spectra, p. 166, Chem. Catolog Co., 1922.

# THE INFRA-RED ABSORPTION SPECTRA OF BENZENE AND ITS HALOGEN DERIVATIVES

By J. Fenton Daugherty
University of North Carolina, Chapel Hill

(Received October 3, 1929)

Abstract

The infra-red absorption spectra of liquid benzene and its halogen derivatives have been measured from 1.00$\mu$ to 7.50$\mu$. The near infra-red bands of benzene at 2.17$\mu$, 2.45$\mu$, and 2.71$\mu$ have been found to agree very well with the results of other observers, and several weak bands have been found which have not been previously noted. The region at 3.30$\mu$ has been studied in detail and different maxima have been found at 3.29$\mu$, 3.32$\mu$, and 3.44$\mu$. The region from 5.00$\mu$ to 7.50$\mu$ shows five bands for benzene at 5.06$\mu$, 5.56$\mu$, 6.20$\mu$, 6.74$\mu$, and 7.16$\mu$. The general absorption of the halogen derivatives is very much similar to that for benzene, however, the bands differ somewhat in position of the maxima, and in the weaker bands. The more intense bands in the near infra-red have been classified as overtones or combination bands, and the agreement between calculated and observed bands is satisfactory.

## Introduction

THERE has been a large amount of work done in the study of the infra-red absorption of organic compounds, and some of the more important work has been done by Weniger,[1] who worked with forty-one alcohols, acids, and esters, also Johnson and Spence[2] studied twenty-four aniline dyes as far as 12$\mu$, and Stang[3] made a study of napthalene and several of its monoderivatives in solution. More recent work by Bell[4] has shown that in practically every case of eleven organic compounds studied a very strong band appears at 3.25$\mu$. Ellis[5] has investigated quite a number of organic compounds, and his results show great similarities among these spectra. From these investigations he was able to arrange the absorption bands in a series, and it was suggested that the origin of the different absorption bands may be traced to definite atoms, or pairs of atoms, as absorbing centers.

The present work was undertaken to obtain the complete absorption spectra from 1.00$\mu$ to 7.50$\mu$, and to ascertain whether relationships could be found between the absorption bands. For this work benzene and the monohalogen derivatives, with the exception of mono-fluor-benzene, were studied. The object was twofold. First, to see if there existed any series relations between the bands of benzene, and second, to determine if there was any shifting of the maxima when a halogen was substituted for a hydrogen in the benzene ring.

[1] W. Weniger, Phys. Rev. **31**, 388 (1910).
[2] Johnson and Spence, Phys. Rev. **5**, 349 (1915).
[3] A. H. Stang, Phys. Rev. **9**, 542 (1917).
[4] F. K. Bell, Jour. Amer. Chem. Soc. **47**, 2192 (1925).
[5] J. W. Ellis, Phys. Rev. **23**, 48 (1924); Phys. Rev. **27**, 298 (1926).

## Experimental Procedure

In the present work two different instruments were employed. For the investigation of the spectrum from 1.00$\mu$ to 3.50$\mu$ a Hilger D42 infra-red spectrometer of large aperture with quartz prism was used, and for the region from 3.50$\mu$ to 7.50$\mu$ a Hilger D35 instrument with rock-salt prism was employed. The thermopile, which was interchangeable with either instrument, was of the linear Rubens type. This was quite an advantage since once the galvanometer circuit was critically damped, it was just a matter of changing the thermopile when shifting from one instrument to the other. A Leeds and Northrup galvanometer of 10 ohms resistance and a sensitivity of 10 mm per microvolt was used.

Both spectrometers were first calibrated by setting the wave-length drum for the *D*-lines. A further check was used as a means of calibration. The positions of the water bands as determined by Collins[6] were used to determine the accuracy of the calibration in the regions to be studied, and a very good agreement was found to exist. It was found that a small correction of the order of 0.01$\mu$ must be added to the observed readings in the region from 1.00$\mu$ to 3.50$\mu$, when the D42 spectrometer was used. The D35 instrument was employed when investigating the region from 5.00$\mu$ to 7.50$\mu$, and it was found on checking the calibration for the water vapor band at 6.26$\mu$ a correction of 0.04$\mu$ was necessary.

All the materials studied were first run with slit-widths of 0.25 mm, except in the case of the D35 spectrometer where the collimator slit was 0.39 mm. This gave the general outline of the absorption curves. Having thus located the approximate positions of the absorption maxima, the thermopile slit of the D35 spectrometer was reduced to 0.203 mm, and the collimator slit to 0.303 mm. For the D35 instrument the spectrum embraced by the thermopile in the region of 6.26$\mu$, when the thermopile slit is at 0.25 mm, was 0.155$\mu$, and with the thermopile slit at 0.203 mm, the region exposed to the thermopile would be 0.124$\mu$. When the D42 spectrometer was used with slit-widths of 0.25 mm, the portion of the spectrum embraced by the thermopile in the region of 2.70$\mu$, was 0.015$\mu$, and when the thermopile slit was reduced to 0.125 mm, the portion of the spectrum exposed to the thermopile would be 0.0075$\mu$.

The cells employed in this work were made by gluing, with Le Page's liquid glue, the windows of glass, polished fused quartz, fluorite, or rock-salt as the case might be, to pieces of lead foil or lead sheet depending upon the thickness of cell desired. One window was glued to the lead, glue put on the outer edge of the other window, the hollow part of the lead was then filled with the liquid to be studied, by means of a pipette, and the second window slipped into place. The cell was then clamped in its mount which consisted of two brass disks held together by four bolts. This mount was then placed on a board which was free to move in guides, between fixed limits, and was so arranged that a mirror focused an image of the source on the cell, and a

[6] J. R. Collins, Phys. Rev. **26**, 771 (1925).

second mirror focused this image on the collimator slit of the spectrometer. A diaphragm, with aperture slightly smaller than the diameter of the cell, was placed immediately in front of the cell. The whole assembly was so arranged that the observer could move the cell in and out of the beam of radiation, read the galvanometer deflections, and set the spectrometer wavelength drum without leaving his position.

In Table I will be found cell thicknesses, material of cell windows, and the intervals at which readings were taken for different parts of the spectrum studied.

TABLE I. *Shows cell thicknesses for different parts of the spectrum studied; materials of which cell windows were made; and intervals at which readings were taken for the different parts of the spectrum.*

| Portion of spectrum | Thickness of cell | Material of cell windows | Intervals at which readings were taken |
|---|---|---|---|
| From 1.00$\mu$ to 1.25$\mu$ | 5.25 cm | Ordinary glass | |
| 1.25$\mu$ to 2.00$\mu$ | 3.35 cm | Polished fused quartz | Every 0.01$\mu$ over the whole range and every 0.005$\mu$ at the center of the bands. |
| 2.00$\mu$ to 2.80$\mu$ | 0.074 cm | Polished fused quartz | |
| 2.80$\mu$ to 3.50$\mu$ | 0.012 cm | Microscope cover glasses | |
| 5.00$\mu$ to 7.50$\mu$ | 0.024 cm | Fluorite and rock-salt | Every 0.02$\mu$ and at the center of bands every 0.01$\mu$. |

The source of radiation was a Globar element (55 volts) about three inches long. The center of the element was ground away to about one half the diameter of the original piece. This prevented the ends from becoming overheated and reduced sparking at the end contacts to a minimum. In order to have the source as steady as possible it was operated from a bank of storage batteries. By means of a variable resistance, in series with the Globar element, the desired intensity could be obtained. In the present work currents from 2.4 to 3.0 amperes were employed. In a single run, however, the current was kept very nearly constant.

The benzene was obtained from the Chemistry Department of the University of North Carolina, and was known to contain 0.003 percent of carbon disulphide. This small trace should cause no serious difficulty, as carbon disulphide is very transparent for the region of the spectrum studied, except for one large maximum at about 4.60$\mu$. The other substances were obtained from the Eastman Kodak Laboratories. A boiling point test was made for all the substances and the results checked well with the true boiling points.

## Results and Discussion

The infra-red absorption spectra of benzene, and its mono-halogen derivatives were studied from 1.00$\mu$ to 7.50$\mu$. Table II gives a list of all the maxima observed for the four materials, some of which appear only as slight inflections of the curves being marked by an (*), some other regions which appear only as slight inflections, and may be considered as bands, are not given in the list. Twenty-eight absorption maxima are listed for benzene, and about the same number for each of the halogen derivatives. The more in-

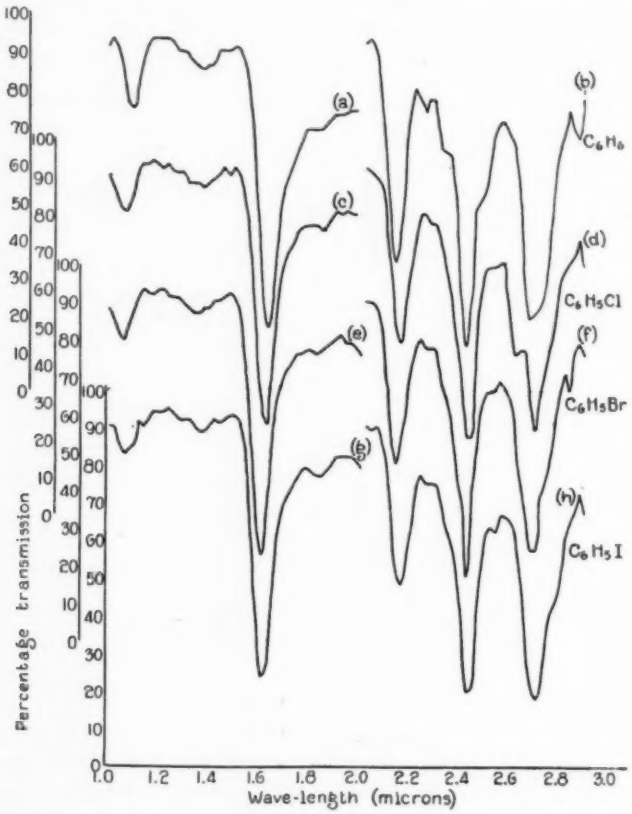


Fig. 1. Curves (a) and (b), benzene; curves (c) and (d), mono-chloro-benzene; curves (e) and (f), mono-bromo-benzene; curves (g) and (h), mono-iodo-benzene.

tense maxima, which are set forth in curves (a) and (b), Fig. 1, are in good accord with those found by other workers in this region.[7] The values of the maxima observed by the writer in every case are slightly less than those given by other observers. This may be due to a difference in calibration or a temperature effect.

A very thorough study was made of the bands for benzene in the region from 1.00$\mu$ to 1.90$\mu$, the results of which are shown in curves (a) and (b), Fig. 2. It appears that the maximum at 1.12$\mu$ has associated with it a smaller

[7] Th. Dreisch, Zeits. f. Physik **30**, 200 (1924).

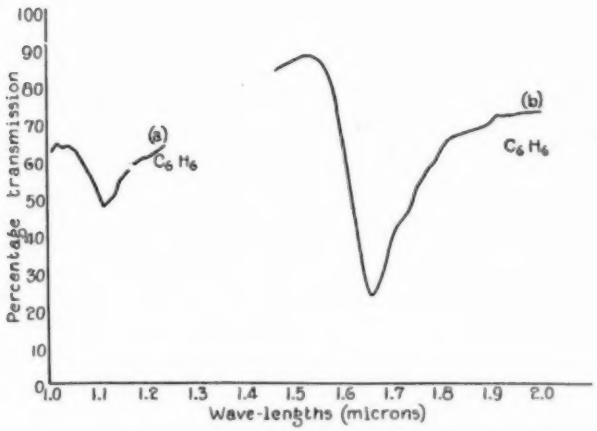


Fig. 2. Curves (a) and (b), benzene.

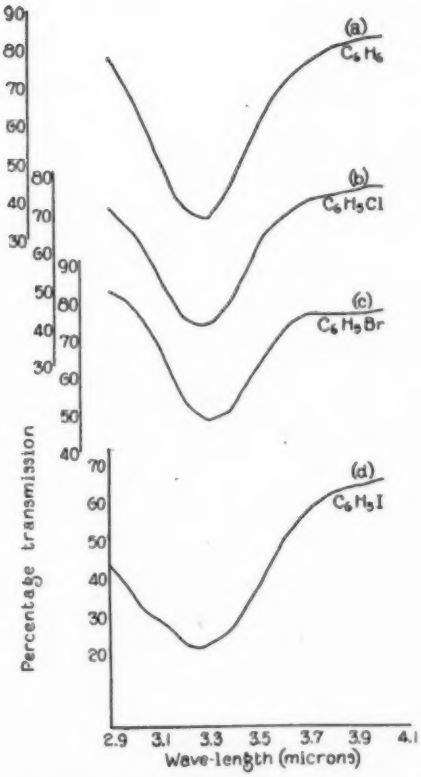


Fig. 3. Curve (a), benzene; curve (b), mono-chloro-benzene; curve (c), mono-bromo-benzene; curve (d), mono-iodo-benzene.

maximum at 1.14$\mu$. Barnes and Fulweiler[8] have made a study of this region with a grating and have found maxima at 1.1372$\mu$ and 1.1445$\mu$ for this band.

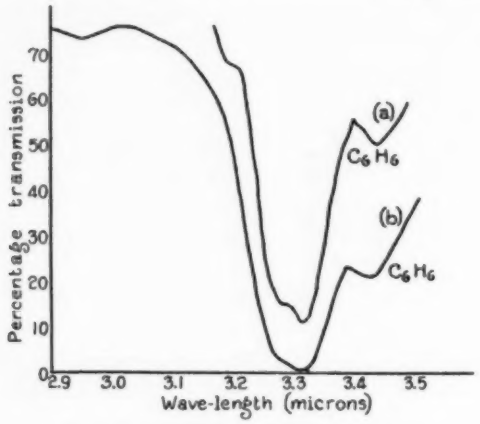


Fig. 4. Curves (a) and (b), benzene.

In addition to the more intense maximum at 1.66$\mu$ there appear three smaller maxima, one at 1.72$\mu$, one at 1.78$\mu$ and another at 1.88$\mu$.

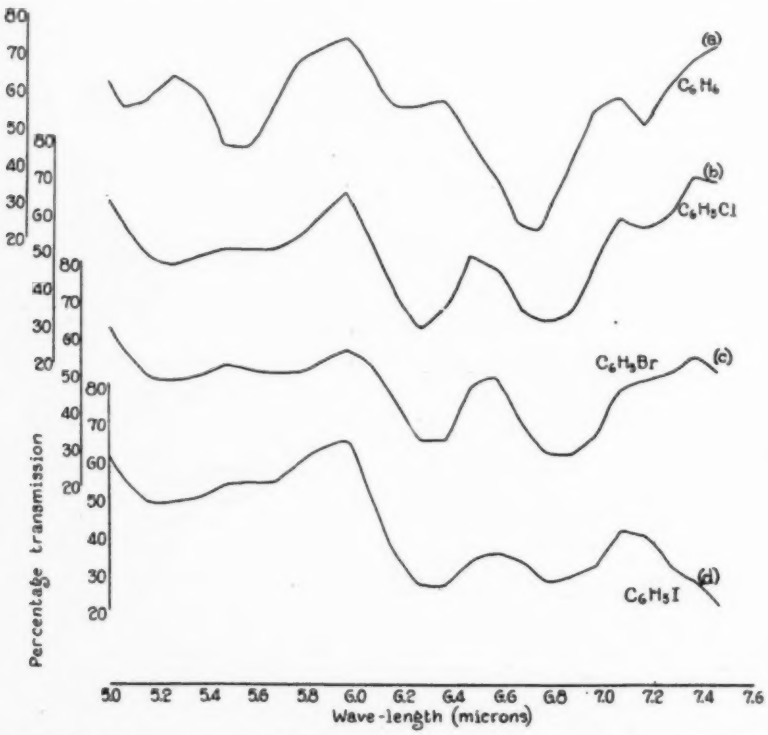


Fig. 5. Curve (a), benzene; curve (b), mono-chloro-benzene; curve (c), mono-bromo-benzene; curve (d), mono-iodo-benzene.

[8] Barnes and Fulweiler, Phys. Rev. **32**, 618 (1928).

It will be noted from the curves of Figs. 1, 3, and 5, that the infra-red absorption spectra for the four materials studied show great similarity throughout the whole region. There are some instances where a shifting of the bands occurs, but it does not appear, from the observed results, that this shifting follows any definite rule. For instance, consider the maximum which occurs at 1.66$\mu$ for benzene. If by substituting in the benzene ring a heavier atom for a lighter hydrogen atom causes any shifting of the bands, one would expect mono-iodo-benzene to show the greatest shift as this is the heaviest molecule studied. For mono-chloro-benzene the band occurs at 1.65$\mu$ which indicates a slight shift toward the shorter wave-length region. For mono-bromo-benzene which is heavier than mono-chloro-benzene, there appears to be a slight shift again as the band is found at 1.63$\mu$. But in the case of mono-iodo-benzene the maximum occurs at the same position, 1.63$\mu$, as the maximum for mono-bromo-benzene. By comparison of the absorption spectra of the different materials studied, it is seen that the intensity of the observed maxima does not seem to be greatly affected when a halogen is substituted in the molecule.

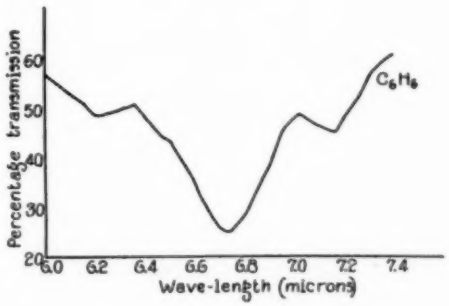


Fig. 6. Curve for benzene.

On the basis of theory benzene is symmetrically constituted and is composed of six carbon atoms and six hydrogen atoms. The most probable arrangement, according to Beckenkamp[9] is that the centers of gravity of the carbon atoms form a spacial six membered ring, while the hydrogen atoms which lie with their axis perpendicular to the main axis of the molecule form a plane ring. This arrangement permits of a possibility of thirty modes of vibration since there are twelve particles. It is likely, however, that some of the vibrations have the same frequency or are inactive.

While the number of actual modes of vibration is not known, due to their intensity and location the following maxima were assumed to be fundamentals, 3.30$\mu$, 6.74$\mu$, 9.80$\mu$; the last value is taken from the work of Coblentz.[10] Also a band at 15.5$\mu$ which was calculated from observed maxima, is considered to be a fundamental band. These fundamentals were given the following frequency notation $\nu_1$, $\nu_2$, $\nu_3$, and $\nu_4$ respectively.

By means of the formula $\nu_n = n\nu_0\,(1-nx)$, where $\nu_n$ and $\nu_0$ are expressed in wave numbers and $(x)$ is a constant, a check for the position of the funda-

[9] J. Bechenkamp, Zeits. f. Anorg. Chem. 139, 220 (1924).

[10] W. W. Coblentz, Investigations of Infra-red Spectra, Carnegie Bull. 35, (1905).

mental at 3.30$\mu$ was obtained. Assuming that the 1.66$\mu$ maximum is the first overtone of the above fundamental, and 1.12$\mu$ is the second overtone, a calculated value of $\nu_1$ in good agreement with the observed value was found.

Since the maximum at 2.71$\mu$ is not identified as a fundamental or overtone, it is assumed to be due to a combination of two fundamental frequencies. This combination, on account of its intensity, probably includes ($\nu_1$) as one of

TABLE II. *Observed bands for benzene and its halogen derivatives.*

| Benzene | Monochlorobenzene | Monobromobenzene | Monoiodobenzene | Benzene | Monochlorobenzene | Monobromobenzene | Monoiodobenzene |
|---|---|---|---|---|---|---|---|
| 1.06$\mu$* | | | | 2.45 | 2.46 | 2.45 | 2.45 |
| 1.12 | 1.09$\mu$ | 1.08$\mu$ | 1.08$\mu$ | 2.51* | 2.65* | 2.55* | 2.57 |
| 1.14* | 1.17* | 1.19* | 1.16* | 2.71 | 2.73 | 2.72 | 2.73 |
| 1.31* | 1.24* | 1.28* | 1.22* | 2.91* | 2.87* | 2.87* | |
| 1.40 | 1.30* | | 1.32* | 2.95* | | | |
| 1.43 | 1.40 | 1.37 | 1.39 | 3.29* | | | |
| 1.48* | 1.50* | 1.45* | 1.46* | 3.32 | 3.28 | 3.30 | 3.26 |
| 1.66 | 1.65 | 1.63 | 1.63 | 3.44 | | | |
| 1.72* | | | | 4.43* | 4.43* | 4.43* | 4.43* |
| 1.78* | | 1.78* | | 5.06 | 5.26 | 5.26 | 5.20 |
| 1.88* | 1.87* | 1.85* | 1.86* | 5.56 | 5.56 | 5.70 | 5.60 |
| 2.17 | 2.19 | 2.17 | 2.19 | 6.20 | 6.26 | 6.30 | 6.30 |
| 2.29* | 2.31* | 2.31* | 2.31* | 6.74 | 6.76 | 6.86 | 6.76 |
| 2.37* | | | | 7.16 | 7.16 | 7.16 | 7.28* |

the component bands. By subtracting the frequency of ($\nu_1$), a value is obtained which corresponds to a band at 15.5$\mu$, this being assumed as a fundamental band. In the work of Coblentz[10] it is noticed that for benzene a very broad region of absorption begins at about 14.4$\mu$ and continues to 15.0$\mu$, where his observations end. It is difficult to say where the center of the absorption band is located. If a thinner cell were used, it is very likely from the appearance of the other fundamentals observed, that the center of the band would be located in the region from 15.0$\mu$ to 16.0$\mu$. This gives considerable evidence that there exists an intense fundamental for benzene in this region. A list of all the fundamentals, overtones, and combinations which the other bands are attributed to are given in Table III.

In the work of Ellis[5] there was a classification of the bands of benzene and it is interesting to make a comparison with the classification in the present work. Ellis considered the spectrum of benzene to consist of two fundamentals, one at 28$\mu$ and another at 6.44$\mu$, and that all near infra-red bands were overtones or combinations of these two frequencies. Thus a band at 1.03$\mu$ was attributed to the twenty-eighth overtone of the band at 28.0$\mu$. Several observed bands in the region from 1.00$\mu$ to 5.00$\mu$ are attributed to combinations. The intense band, for example, at 2.18$\mu$ is identified as the combination of one fundamental and the eighth overtone of the other. In the present work the bands in the near infra-red are assumed to arise from four fundamentals instead of two and the combinations do not include any overtones above the third. The present classification appears to be more in accord with the ob-

[11] J. E. Purvis, Proc. Cam. Phil. Soc. **21**, 556 (1922–23).

served intensities, but a careful study has not been made of the intensities of the bands.

In conclusion from the present work the experimental data seems to indicate for benzene in the liquid state, that there exists only minor differences in the general absorption from its halogen derivatives. However, when the individual bands are considered in detail, they are found to occur at slightly different wave-lengths, and the weak bands occur in some of the liquids that are not observed in the others. It is probable that if these materials were studied in the gaseous state under high resolution, so that the individual lines

TABLE III. *Calculated and observed wave-lengths for benzene and its mono-halogen derivatives.*

| Combination | Observed wave No. | Calculated λ | Observed λ | Observed wave No. | Calculated λ | Observed λ |
|---|---|---|---|---|---|---|
| | For benzene | | | For mono-chloro-benzene | | |
| $\nu_1$ | 3052.6 | 3.28μ | 3.30μ | 3016.7 | 3.32μ | 3.28μ |
| $\nu_2$ | 1483.7 | | 6.74 | 1479.3 | | 6.76 |
| $\nu_3$ | 1020.4 | | 9.80* | 1077.6 | | 9.28* |
| $\nu_4$ | 644.2 | 15.50 | | 653.0 | 15.30 | |
| $2\nu_1$ | 6042.3 | | 1.66 | 6060.6 | | 1.65 |
| $3\nu_1$ | 8968.8 | | 1.12 | 9174.3 | | 1.09 |
| $\nu_1+\nu_2$ | 4536.3 | 2.20 | 2.17 | 4496.0 | 2.22 | 2.19 |
| $\nu_1+\nu_3$ | 4073.0 | 2.46 | 2.45 | 4094.3 | 2.44 | 2.46 |
| $\nu_1+\nu_4$ | 3696.8 | | 2.71 | 3669.7 | | 2.73 |
| $2\nu_1+\nu_2$ | 7526.0 | 1.33 | 1.31 | 7539.9 | 1.32 | 1.30 |
| $2\nu_1+\nu_3$ | 7062.7 | 1.42 | 1.43 | 7138.2 | 1.40 | 1.40 |
| $2\nu_1+\nu_4$ | 6686.5 | 1.50 | 1.48 | 6713.6 | 1.49 | 1.50 |
| $3\nu_1+\nu_4$ | 9613.0 | 1.04 | 1.06 | | | |

| | For mono-bromo-benzene | | | For mono-iodo-benzene | | |
|---|---|---|---|---|---|---|
| $\nu_1$ | 3053.0 | 3.26μ | 3.30μ | 3053.0 | 3.26μ | 3.26μ |
| $\nu_2$ | 1457.7 | | 6.86 | 1479.3 | | 6.76 |
| $\nu_3$ | 1061.6 | | 9.42* | 1052.6 | | 9.50** |
| $\nu_4$ | 630.2 | 15.80 | | 616.7 | 16.20 | |
| $2\nu_1$ | 6153.9 | | 1.63 | 6153.9 | | 1.63 |
| $3\nu_1$ | 9302.5 | | 1.08 | 9302.5 | | 1.08 |
| $\nu_1+\nu_2$ | 4510.7 | 2.22 | 2.18 | 4532.3 | 2.21 | 2.19 |
| $\nu_1+\nu_3$ | 4114.6 | 2.43 | 2.45 | 4105.6 | 2.44 | 2.45 |
| $\nu_1+\nu_4$ | 3683.2 | | 2.72 | 3669.7 | | 2.73 |
| $2\nu_1+\nu_2$ | 7611.6 | 1.32 | 1.28 | 7633.2 | 1.31 | 1.32 |
| $2\nu_1+\nu_3$ | 7215.5 | 1.39 | 1.37 | 7206.5 | 1.39 | 1.39 |
| $2\nu_1+\nu_4$ | 6784.1 | 1.47 | 1.45 | 6770.6 | 1.48 | 1.46 |

* Indicate values taken from work of Coblentz.[10]
** Indicates value taken from work of Purvis.[11]

in the vibration rotational bands would appear, that considerable differences would be noticed.

It has been possible to classify all the more intense bands in the near infra-red region as observed by the writer and other workers. No doubt all the bands could have been classified if the wave-lengths of all the fundamentals were known.

The writer wishes to express his appreciation and thanks to Dr. E. K. Plyler, of the University of North Carolina, for suggesting the original problem, and for his encouragement throughout the duration of the work.

# THE STATUS OF THE $\gamma$-RAY CHANGE

By N. Feather*
Physical Laboratory, Johns Hopkins University, Baltimore

(Received November 12, 1929)

Abstract

It has been general to assume that the emission of $\gamma$-rays in radioactive disintegration is an effect subsidiary to the ejection of the $\alpha$ or $\beta$ particle from the nucleus. Recently, however, the general experimental proof that the time interval concerned in this nuclear process is considerably greater than the time of relaxation of the inner extra-nuclear electrons—and, more particularly, an experiment by Jacobsen and its interpretation in terms of $\gamma$-ray disintegration constants as small as $10^5$ sec$^{-1}$—have together resulted in a revision of opinion. In the present paper Jacobsen's interpretation is examined in more detail and is shown to imply that the emission of a quantum of $\gamma$ radiation between the $\beta$ particle disintegration of radium C and the $\alpha$ particle disintegration of radium C′ is an absolute necessity. This condition is attended with certain difficulties. In the course of the investigation it is shown that where $\alpha$ particles may be emitted either immediately following an earlier disintegration, or with the intermediate emission of any single member of a number of $\gamma$-ray quanta, then, as long as all the $\alpha$ particles possess identical velocities, the $\alpha$ activity of the immediate product of the former disintegration decays strictly according to the exponential law characterized by the disintegration constant of the $\alpha$ particle change.

In a second part of the paper an attempt is made to connect the complexity of the "normal" $\alpha$ radiation of thorium C and the emission of long range $\alpha$ particles from radium C and thorium C with the occurrence of certain lines in the $\gamma$-ray spectra of the elements in question.

## Introduction

WE KNOW of three ways in which energy is spontaneously set free in the nuclear processes of radioactive disintegration. This available energy may appear as kinetic energy—possessed either by an expelled $\alpha$-particle or by a $\beta$-particle—or it may be emitted in the form of radiant energy, as a quantum of $\gamma$ radiation. Yet, from a broad general standpoint, these three modes do not appear to be of equal importance in nature. Considered merely in respect of quantity, $\alpha$-particle kinetic energy represents roughly 85 percent, $\beta$-particle kinetic energy roughly seven percent and $\gamma$-ray energy the remaining eight percent of the total radiation from radioactive materials. But, in spite of this distinction, in the matter of fundamental importance, the $\alpha$-particle change is not in a class by itself, with the $\beta$-and $\gamma$-ray changes subsidiary to it. Rather is it the $\gamma$-ray change which is peculiar, since in each case it is apparently incidental to some instance of particle disintegration, either $\alpha$ or $\beta$. Every atom of uranium, for example, is believed to undergo an

* Fellow of Trinity College, Cambridge. Associate in Physics, Johns Hopkins University.

invariable[1] sequence of $\alpha$ and $\beta$-particle disintegrations before passing over into an atom of uranium-lead, but concerning the various $\gamma$-ray quanta which may be emitted in the process there exists a wide range of possibility. Once $\gamma$-ray changes are included, the concept of the disintegration series loses all its simplicity.

The secondary nature of $\gamma$-ray emission was early recognised; it was only with the proof of the nuclear origin of the rays that the problem of their dependence became acute. More recently, with the spectral analysis of this type of radiation, and the establishment of systems of nuclear energy levels from which it is derived, the difficulties in the way of a satisfactory solution have, if anything, increased. At first the difficulty was concerned chiefly with the principle of conservation. If there was, in fact, a difference in the total energy radiated during the active lives of different atoms passing down the same disintegration series then it became difficult to escape the conclusion that for one and the same atomic species (uranium-lead, for example) different nuclei must possess different amounts of intrinsic energy—and that these different energy states must be permanent. A similar difficulty was encountered when the heterogeneity of $\beta$-particle velocities was finally established. Chalmers[2] has exhibited this difficulty in its most intractable form. For the present it is unlikely that in either case any solution will be found; it is very probable that these relatively small differences in internal energy-content as between otherwise identical nuclei may constitute a feature of common occurrence with the ordinary inactive elements. Some experiments of Rutherford and Chadwick[3] on artificial disintegration seem to admit of no other interpretation.

## The Time Intervals Involved in $\gamma$-ray Emission

Apart from this question of conservation, however, and arising in most instances directly from the experimental work of Jacobsen,[4] there has recently been a growing concern with the more general problem of the status of the $\gamma$-ray change. Yet, even if Jacobsen's work be neglected, the crucial experiment of Ellis and Wooster,[5] proving that the order in time is invariably "$\beta$-particle emission$\rightarrow\gamma$ ray change," of itself is sufficient to lead to an important conclusion.[6] For the reorganization of the nucleus resulting in the emission of the $\gamma$-ray quantum is thereby shown to be slow compared with the time of relaxation of the extra-nuclear electrons of the $K$ level. The work of Black[7] similarly shows that it is slow compared with the time of relaxa-

[1] The sequence is not strictly invariable, both for uranium $X_1$ and for radium C there are alternative modes of particle disintegration. For radium C, as for thorium C, the schematic representation of the "branching" is $B \xrightarrow{\beta} C \begin{cases} \xrightarrow{\beta\ C' \xrightarrow{\alpha}} \\ \xrightarrow{\alpha\ C'' \xrightarrow{\beta}} \end{cases}$ Reference to this diagram will make clearer subsequent discussions.

[2] Chalmers, Proc. Camb. Phil. Soc. **25**, 331 (1929).

[3] Rutherford and Chadwick, Proc. Camb. Phil. Soc. **25**, 186 (1929).

[4] Jacobsen, Nature **120**, 874 (1927).

[5] Ellis and Wooster, Proc. Camb. Phil. Soc. **22**, 844 (1925).

[6] Cf. Chalfin, Zeits. f. Physik **53**, 130 (1929).

[7] Black, Proc. Camb. Phil. Soc. **22**, 838 (1925).

tion of the $L$, $M$ and $N$ level electrons.[8] The inevitable nature of radioactive change, combined with its slowness, in many cases extreme, has long been recognised as the primary difficulty in the way of an explanation of particle disintegration in general;[9] here the same feature is seen to be characteristic of the $\gamma$-ray change also. Chalfin[6] has insisted that disintegration constants or transition probabilities have as real significance for $\gamma$-ray as for $\alpha$ or for $\beta$-particle processes. Now the range of value of these constants is very different in the two latter cases; the smallest $\alpha$-particle disintegration constant is $10^{-18}$ sec$^{-1}$, the smallest $\beta$-particle disintegration constant $10^{-9}$ sec$^{-1}$.** There is at present no evidence to prove that $\gamma$-ray transition probabilities as small as 1 sec$^{-1}$ do not exist, though in many cases they must be very much larger than this.

Jacobsen's experiments,[4] already referred to, have been interpreted as affording some indirect information concerning such transition probabilities. Making observations of the emission of $\alpha$-particles from different regions in a beam of recoil atoms arising from the radium C $\beta$-particle disintegration, Jacobsen in effect showed that the $\alpha$-particle activity of the subsequent product does not decay exponentially with the time, but instead rises from zero initially to a maximum and then decays, exactly as would be the case if the $\alpha$-particle change were the second of two of nearly equal half period. Since the former process cannot involve the emission of particles, either charged or uncharged, it was suggested that it represents the general $\gamma$-ray emission which is known to take place intermediate in time between the $\beta$ and $\alpha$-particle changes. On this hypothesis the $\alpha$-particle disintegration constant was estimated as $10^5$ sec$^{-1}$, whilst a similar value was assigned for the effective $\gamma$-ray change.

The term "the general $\gamma$-ray emission" has been employed the more to emphasise the complexity of this radiation, "the effective $\gamma$-ray change" to stress the simplification which is made by comprehending these complex processes under a single constant of probability. For a complete explanation of the natural $\beta$-ray spectrum of radium C, $\gamma$-rays of nearly 50 different frequencies would be required. Suppose that partial transition probabilities $\lambda_1, \lambda_2, \cdots, \lambda_r, \cdots, \lambda_n$ be accorded to them, respectively, and let us investigate the problem more fully. At any time $t$ let $N$ be the number of atoms which have undergone the $\beta$-particle change only, $N_1, N_2, \cdots, N_r, \cdots, N_n$ the numbers which have undergone successive changes $\beta\gamma_1, \beta\gamma_2, \cdots, \beta\gamma_r, \cdots, \beta\gamma_n$, respectively, and $N\alpha_1, N\alpha_2, \cdots, N\alpha_r, \cdots, N\alpha_n$ the numbers which have undergone both $\beta$ and $\alpha$-particle changes with intermediate emission of $\gamma_1, \gamma_2, \cdots, \gamma_r, \cdots, \gamma_n$, respectively. For sake of simplicity we are assuming that not more than a single $\gamma$-ray quantum is emitted by each atom disintegrating. Furthermore, concerning the $\alpha$-particle change, it is an experimental fact that the velocity of the particle ejected by any atom

[8] Rough estimates of these times are, for the $K$ electrons, $10^{-15}$ sec, for the $N$ electrons $10^{-10}$ sec.

[9] See, for example, Lindemann, Phil Mag. 30, 560 (1915).

** If we neglect the $\beta$-ray bodies potassium and rubidium.

is independent of the $\gamma$-ray quantum just previously emitted. We must therefore assume that a single $\alpha$-particle disintegration constant, $\lambda\alpha$, applies uniformly throughout. Now suppose that in a small fraction of the cases no $\gamma$ ray is emitted between the two particle disintegrations.[10] Since the $\alpha$-particle emitted in such a case is indistinguishable from any other, $\lambda\alpha$ must apply here also. Writing $N\alpha$ for the number of atoms which at the time $t$ have undergone $\beta$- and $\alpha$-particle changes in this way, in immediate succession, the complete equations of radioactive decay may be written[11]

$$\frac{dN}{dt}=-\left(\lambda\alpha+\sum_1^n\lambda r\right)N, \qquad \frac{dN\alpha}{dt}=\lambda\alpha N,$$

$$\cdots\cdots\cdots\cdots \qquad \cdots\cdots$$

$$\frac{dN_r}{dt}=\lambda r N-\lambda\alpha N r, \qquad \frac{dN\alpha_r}{dt}=\lambda\alpha N r,$$

$$\cdots\cdots\cdots\cdots \qquad \cdots\cdots$$

From these equations we obtain

$$N+N\alpha+\sum_1^n Nr+\sum_1^n N\alpha_r=N_0.$$

Taking as initial conditions $N=N_0$, and writing $\lambda\alpha+\sum_1^n\lambda r=\lambda$, the relevant solutions become

$$N=N_0e^{-\lambda t},$$

$$\cdots\cdots\cdots$$

$$Nr=\frac{\lambda_r N_0}{\lambda-\lambda\alpha}(e^{-\lambda\alpha t}-e^{-\lambda t}),$$

$$\cdots\cdots\cdots$$

If $A$ is the total $\alpha$-particle activity of the preparation at the time $t$, then

$$A=\frac{dN\alpha}{dt}+\sum_1^n\frac{dN\alpha_r}{dt},$$

or

$$A=\lambda\alpha\, N_0e^{-\lambda t}+\frac{\lambda\alpha N_0}{\lambda-\lambda\alpha}(e^{-\lambda\alpha t}-e^{-\lambda t})\sum_1^n\lambda r,$$

$$=\lambda\alpha N_0e^{-\lambda\alpha t}.$$

[10] With some $\gamma$-ray bodies it is almost certainly the case that on the average less than one quantum is emitted per atom disintegrating—but actually this is not so with radium C.

[11] There is implicit here the assumption that the radium C $\beta$-particle disintegration does not result in sets of atoms effectively "earmarked" to emit various $\gamma$-rays, after times statistically determined by the relevant disintegration constants $\lambda r$. In such circumstances, with a source consisting of atoms collected immediately after the $\beta$-particle change, the quality of the $\gamma$-rays would vary with time. We can only assume that this is not the case, since the possibility of a direct experimental investigation seems very remote.

This result[12] indicates that, in spite of the occurrence of $\gamma$-ray emission, the quanta of which may be characterised by any number of different disintegration constants, yet, as long as no atom in the course of disintegration emits more than one quantum of radiation, and always provided that some atoms emit none at all, then the $\alpha$-particle activity of the preparation decays accurately according to the exponential law determined by the disintegration constant of the $\alpha$-particle change.

Such circumstances as we have assumed, therefore, cannot conspire to the result which Jacobsen found experimentally. However, the conditions with radium C are more complex than we have considered. Probably in this case, on the average, between one and two quanta of $\gamma$-radiation are emitted per atom disintegrating. Whilst this does not necessarily invalidate the supposition that in some instances the actual number is zero, it is incompatible with the supposition that this number is never greater than unity. Yet, as long as we retain the former permissible condition, it may be shown that the $\alpha$-particle activity, starting from some value initially different from zero, decreases at first, whilst its rise to a maximum at a later time is entirely dependent upon the relative values of $\lambda\alpha$ and the various constants $\lambda r$. If, therefore, Jacobsen's experiments are reliable in the more minute particulars it must be conceded that his suggested explanation stands or falls with the decision for or against the absolute necessity for $\gamma$-ray emission in all cases following the $\beta$-particle disintegration of radium C. It will be obvious that there is at least ample scope for an alternative hypothesis—as well as an urgent need for the development of other means of experimental attack upon this difficult problem. However, until fresh experiments have been performed it would be rash to make any further speculations.

## Energy Considerations—Abnormal Particle Effects

There is a further aspect of the problem of the status of the $\gamma$-ray change which is best considered in its relation to a distinction which has already been drawn. Particle disintegration in general fits well with the scheme of the disintegration series; the inclusion of $\gamma$-radiation, on the other hand, plays havoc with its basic simplicity. Nevertheless, in certain cases, even as regards particle disintegration, anomalies occur—and the question arises, may not these anomalies be in some way connected with peculiarities of the associated $\gamma$-ray changes? The most pronounced abnormalities characterise the disintegration of the C bodies in all three series—there is the well-known dual disintegration of radium C, thorium C, and actinium C, there is the emission of groups of long range $\alpha$- particles of rare occurrence by radium C and thorium C or their subsequent short-lived products,[13] and, finally, there is the additional complexity recently revealed in the "normal" $\alpha$-particle emission of thorium C by the work of Rosenblum.[14] These two latter features, at least, possess

[12] Soddy, Phil. Mag. **18,** 739 (1909), in connection with the characteristics of hypothetical "rayless" changes, reached a result mathematically merely a special case of the above ($n=1$).

[13] See Nimmo and Feather, Proc. Roy. Soc. **122A,** 668 (1929).

[14] Rosenblum, Comptes rendus **188,** 1401 (1929).

numerical characteristics which might be made the basis of tentative hypotheses.

It is interesting to calculate the energy differences as between the common and the uncommon modes of disintegration in the different cases. For the satellite lines in the $\alpha$-particle spectrum of thorium C this may be done directly. Rosenblum's results indicate groups of particles of energy respectively $0.4\times10^5$ electron volts greater, and 3.0 and $4.7\times10^5$ electron volts less, than the normal. For the groups of long range $\alpha$-particles, where the immediate data consist of ranges, the calculation is very much less certain. To employ the simple Geiger law, as was done by Bates and Rogers,[15] may lead to grave error. In the following table Laurence's[16] correction curve has been used. This curve, showing the departure from the simple law as a function of the range, has been linearly extrapolated. Energy differences are probably correct in all cases, at least to 3 percent.

| Product | $\alpha$ particle range* cm | Energy electron volts$\times10^{-6}$ | Energy difference |
|---|---|---|---|
| Radium C | 6.96 | 7.69 | — |
| | 8.1 | 8.45 | 0.76 |
| | 9.16 | 9.10 | 1.41 |
| | 10.0** | 9.62 | 1.93 |
| | 11.0 | 10.20 | 2.51 |
| Thorium C | 4.78 | 6.02 | −2.75 |
| | 8.62 | 8.77 | — |
| | 9.90 | 9.56 | 0.79 |
| | 11.70 | 10.59 | 1.82 |

* "Extrapolated ionization range" in air at 15°C and 760 mm.
** Rather more doubtful than the rest.

Let us first consider the results of Rosenblum's experiment. There are three possible explanations: the effect may be extra-nuclear, or, if intra-nuclear, then either primary or secondary. The magnitude of the energy differences and the sharpness of the satellite lines [17] almost certainly rules out the first explanation. If the effect were a primary intra-nuclear phenomenon then either we must assume that the disintegration of an atom of thorium C is "governed" by five partial disintegration constants, $\lambda\beta$, $\lambda\alpha_1$, $\cdots$, $\lambda\alpha_4$, corresponding to the $\beta$-particle mode and the four $\alpha$ particle modes, or we must regard thorium C as a mixed element each atom of which has in some way become "earmarked" to undergo one mode of disintegration rather than another. In the first case the Geiger-Nuttall, or some equivalent relation, would indicate that the frequencies of the different $\alpha$-particle modes should be uniquely related to the respective energies, the group of highest energy being the most abundant—and, in the second case, on the basis of a similar argument, we should not expect the four $\alpha$-particle groups to decay with the

[15] Bates and Rogers, Proc. Roy. Soc. **105A,** 97 (1924).
[16] Laurence, Proc. Roy. Soc. **122A,** 543 (1929).
[17] The writer has had the opportunity of examining a reproduction of an original photograph.

same period. Periods roughly in the ratios 2/3: 1:60: 550 might be anticipated. Neither conclusion will bear the test of experiment: the most intense group is not that of highest energy, whilst, if tested over an interval of 30 hours against the $\alpha$-particles of thorium C′, the $\alpha$-particle emission of thorium C exhibits a simple exponential decay.[18]

There remains only the possibility, on the basis of present ideas, that the effect is both nuclear and also secondary in character, that is, that the small energy differences found outside the atom are due, not to the fact that the different groups of $\alpha$-particles haveoriginated in fundamentally distinct quantum levels within the nucleus, but rather to some internal process which has changed the intrinsic energy of the disintegration particle in one nucleus and not in another. We are as yet almost entirely ignorant of the mechanism of $\gamma$-ray emission. There is the suggestion that it is probably concerned with $\alpha$-particle transitions;[19] it may, in fact, be just such a process as that for which we are here in search. The second most prominent line in the $\gamma$-ray spectrum of thorium B corresponds to a quantum of energy $3.02\times10^5$ electron volts. Some of the atoms of thorium C which undergo $\alpha$ transformation must have emitted this $\gamma$-ray.[20] Now Rosenblum has shown that in a number of cases the $\alpha$-particle is ejected with $3.0\times10^5$ electron volts energy less than the normal. In a similar manner we know that the $\beta$-particle disintegration of thorium C″ follows the $\alpha$-particle disintegration in all cases—and in a certain fraction of these the $\gamma$-ray of energy $0.408\times10^5$ electron volts is finally emitted. Now there are cases in which the thorium C $\alpha$-particle has already carried away $0.4\times10^5$ electron volts excess energy. It may be that in each case we are here concerned merely with numerical coincidences, but it is tempting to believe that more than this is involved. Nevertheless, in respect of the third satellite line, corresponding to $4.7\times10^5$ electron volts energy defect, nothing as promising can be found; thorium *B* possesses no $\gamma$-rays of this energy, although there is, in fact, a weak line, (number 28) in the natural $\beta$-ray spectrum of thorium C″[21] which corresponds to a $\gamma$-ray of energy $4.79\times10^5$ electron volts.

In the $\gamma$-ray spectrum of radium C—we are concerned now with the long range $\alpha$-particles—there are prominent lines corresponding to quanta of energy 0.773 and 1.426 million electron volts, respectively, and individual lines in the natural $\beta$-ray spectrum[22] (E49 and E57) suggest weak $\gamma$-rays of energy 1.95 and 2.53 million electron volts, respectively. These four energy values are in good agreement with the first four entries in the last column of our table. If this agreement be significant it relates the most prominent group of

[18] Marsden and Barratt, Proc. Phys. Soc. Lond. **24,** 50 (1911).

[19] Kuhn, Zeits. f. Physik **44,** 32 (1927). Phil. Mag. **8,** 625 (1929). In the second paper additional evidence is advanced for assigning transition probabilities smaller than $10^{10}$ sec$^{-1}$ to certain $\gamma$-ray processes.

[20] It is to be supposed that an equivalent fraction of those undergoing the $\beta$ transformation will likewise have emitted the $\gamma$-ray in question.

[21] Black, Proc. Roy. Soc. **109A,** 166 (1925).

[22] Ellis, Proc. Camb. Phil. Soc. **22,** 369 (1924).

long range $\alpha$-particles with the $\gamma$-ray of $1.426 \times 10^6$ electron volts energy,[23] and this appears f om measurements of internal (extra-nuclear) absorption to be the most intense in the spectrum.[24] Again, however, it may be that we are concerned merely with cases of numerical coincidence. In addition there might seem to be an *a priori* objection to the reality of the supposed connection, for, whilst the emission of a long range $\alpha$-particle is an extremely rare occurrence, the emission of the more abundant $\gamma$-rays is relatively frequent. Yet the objection is not entirely cogent. Ordinarily it must be assumed that the $\gamma$-ray emission and the $\alpha$-transition are consecutive processes, but, in a small fraction of the cases, when the latter event occurs very shortly after the preceding $\beta$-particle change, it may be possible that the total energy of the two processes should appear as kinetic energy associated with the $\alpha$-particle.[25]

In the parallel case of the long range $\alpha$-particles from thorium C difficulties at once appear. In the first place, since energy differences refer to energies in excess of the value characteristic of the $\alpha$-particle disintegration of thorium C′, we ought logically to restrict our investigations to that branch of the series. Now there is no known $\gamma$-ray definitely attributable to thorium C itself, and the $\gamma$-radiation, if any, of thorium C′ must be very small in amount. There is, therefore, no material for comparisions such as we have previously made. Since, however, the chance of a very small time interval between $\beta$ and $\alpha$-particle changes is presumably much greater in the case thorium C→thorium C′ than in the corresponding case in the radium series, it may be that a very weak $\gamma$-radiation from thorium C would be sufficient to explain the effect. Finally, we should notice in passing that a moderately strong $\gamma$-ray, supposedly due to thorium C″, possesses exactly the energy ($0.79 \times 10^6$ electron volts) representing the difference between the energies of the 9.9 cm and the normal 8.6 cm $\alpha$-particle groups. Yet, for the characteristic energy of the most abundant of all the groups of long range $\alpha$-particles—that of 11.7 cm range from thorium C—it is not possible to find any simple numerical relationship of the type that we have been discussing.

[23] Also it arbitrarily attributes the particles to an atom of atomic number 84. There is no definite experimental evidence on this point.

[24] It is now known from measurements of the excited spectra that the true intensity is, in fact, much smaller than this; cf. discussion on the structure of atomic nuclei, Proc. Roy. Soc. **123A,** 385 (1929).

[25] Cf. Nimmo and Feather. reference 13 p. 685.

# THE EFFECT OF LIGHT ON THE ELECTRON EMISSION FROM CERIUM DIOXIDE

By C. E. Berger
Department of Physics, Lehigh University

(Received November 4, 1929)

Abstract

**Materials showing increased electron emission when illuminated.**—Ultra-violet light was found to increase the electron emission from hot filaments coated with cerium dioxide, or thorium oxide, or calcium oxide, or calcium iodide.

**Characteristics of the photo-emission from cerium dioxide.**—In the case of cerium dioxide on platinum at about 1000°C the photo-emission varied linearly with the intensity of the ultra-violet light; wave-lengths above 3000A were not effective. Air, hydrogen, or oxygen, in small amounts caused a decrease in the photo-emission. The saturation photo-currents showed distinct increase with increase in temperature. Sufficient evidence was not obtained to decide whether this constitutes a variation of the true photoelectric effect with temperature or whether some other cause operates such as change of surface by bombardment.

## Introduction

THE fact that the electron emission which occurs when light falls upon oxide-coated conductors is greater when these are hot than when they are cold was first announced by Case.[1] Case reported that light from a tungsten lamp caused a large electron emission from the plate of a Western Electric Audion tube. Merritt[2] proved that the hot oxide-coated filament of the Western Electric tube showed the same effect. Investigations of a similar nature on the Western Electric filament were carried out by Koppius,[3] Gibbs and Meachem,[4] Arnold and Ives,[5] and Majorana.[6] W. H. Crew[7] found the same effect with a hot filament consisting of a platinum strip coated with a mixture of the oxides of barium and thorium. In each of the preceding experiments of the photo-emission from the cold filament was but a small fraction of that from the hot filament.

The present investigation was undertaken with the purpose in view of determining whether any other oxides or compounds exhibited a variation of photo-emission with temperature. It was found that several other oxides and compounds did exhibit a change in photo-emission with temperature but the magnitudes of the changes found were not as great as in the case of the Western Electric filament.

[1] Case, Phys. Rev. **17**, 398 (1921).
[2] Merritt, Phys. Rev. **17**, 525 (1921).
[3] Koppius, Phys. Rev. **18**, 443 (1921).
[4] Gibbs and Meachem, Phys. Rev. **19**, 415 (1922).
[5] Arvald and Ives, Proc. Nat. Acad. Sci. **7**, 323 (1921).
[6] Majorana, Il Nuovo Cimento p. 218, 1926.
[7] Crew, Phys. Rev. **28**, 1269 (1926).

## Apparatus and Procedure

The materials were studied on either platinum, or tungsten, or nichrome filaments. The platinum filaments were thin platinum strips 1 cm long and 3 mm wide. A current of 5 amp. was sufficient to heat them to about 1000°C. The tungsten filaments consisted of 25 cm of 5 mil tungsten wire wound in a coil 1.5 cm long. The nichrome filaments were nichrome ribbon, 1 mm wide, 10 cm long, wound in a coil. In each case the filament was spot-welded to leads of 35 mil tungsten wire which was sealed through the glass walls of the tube (see Fig. 1). The plate was a flattened cylinder made of one turn of nichrome ribbon 4 mm broad. This ribbon was first heated in a good vacuum in a separate tube for two hours at a temperature just slightly below the melting point. Of lengths of about 40 cm thus heated most of it would fuse so that only about 5 or 6 cm were available for use. The treatment left it very clean and bright. The average distance from the plate to the edges of the filament when mounted in the tube was 1 mm.

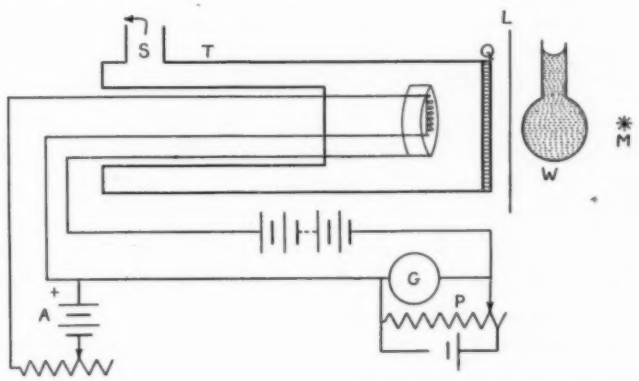


Fig. 1. Diagram of apparatus.

Oxides were coated on the filaments by applying saturated aqueous solution of the corresponding nitrates to the filament, warming it over a bunsen flame to remove the water, and then continuing the heating until the nitrate decomposed leaving the oxide on the filament. The other salts investigated were applied to the filament in the form of an aqueous solution and sufficient heat applied to drive off the water.

Fig. 1 shows the essential portions of the set-up. *T* is a Pyrex, two-electrode tube, 4 cm in diameter and 15 cm long and fitted with a Cooper-Hewitt graded quartz-to-Pyrex seal, 2.5 cm in diameter. *Q* is the quartz window. The tube was evacuated through a side tube, *S*, which led to a two-stage mercury diffusion pump and a McLeod gauge. A battery of large lead cells, *A*, supplied the filament current. A high sensitivity Leeds and Northrup galvanometer (1900 meg), *G*, was in the plate circuit together with a plate battery of Burgess dry cells. Galvanometer deflections due to thermionic currents could be balanced out by means of dry cells and a 10 meter Kohlrausch slide-wire *P*. The light source, *M*, was a Gallois quartz mercury arc

run by storage batteries at 126 v and 3.5 amp. The light was passed through the 3 cm thin quartz bulb, *W*, which contained distilled water. The bulb focused the light on the filament and removed heat radiation from the beam. *L* is a shutter. The distance from the source to the filament was usually 10 cm.

In making a run a heater was first slipped over the tube and the pumps were started. The tube was baked out at 400°C for two hours and then at 300°C for one hour. In every case the pumping was continued until the pressure reading on the McLeod gauge was $10^{-6}$ mm Hg. The pumps were run constantly during readings. The mercury arc was always allowed to run for half an hour before readings were taken in order to insure steady illumination. The shutter was opened and light thrown on the cold filament. No effect was observed. Then the filament was heated by a current, the temperature of the central hottest portion of it was measured with a Leeds and Northrup optical pyrometer, and the galvanometer deflection caused by the thermionic current was balanced out. The shutter was opened again and any current caused by the light could be read from the scale.

## Qualitative Results

An increase in photo-emission with increasing temperature was found in the following materials: calcium iodide on platinum, calcium oxide on platinum, calcium oxide on tungsten, thorium oxide on platinum, cerium oxide on platinum, cerium oxide on nichrome, cerium oxide on tungsten. No effect was found with barium iodide on platinum and zirconium oxide on tungsten although in this latter case it was found on dismantling the tube that a thin coat of some material had distilled on the inner surface of the quartz window and possibly this prevented ultra-violet light from entering the tube.

In the case of calcium iodide the total radiation from the arc gave no measurable current with the filament cold. When current was passed through the filament and it became a dull red there was, in addition to a thermionic current of $40\times10^{-8}$ amp., a photo-current of $1\times10^{-8}$ amp. Thin pieces of mica or of window glass interposed in the path of the light completely annulled the photo-current hence the effect was due to the ultra-violet below about 3000A. Because the thermionic currents are unsteady and capricious this material was not investigated further.

Calcium oxide on platinum and on tungsten yielded no measurable photo-current with the total radiation from the arc when the filament was cold. When the filament was at a dull red there was always a measurable photo-current but reproducible results were not obtained. Calcium oxide was coated on three different platinum strips. Each of these was mounted in turn in the tube under as exactly identical conditions as possible. If the filament current in a given case was held constant and the plate voltage varied from zero to 135 v the form of the photo-current curve was quite dissimilar in the three cases. Preparations are now being made to investigate this matter more thoroughly. It is of interest to note that one of the filaments yielded a plate voltage-photo-current curve of the same form as found by W. H. Crew[7] for

a mixture of barium and thorium oxides i.e. at about 8 v plate voltage the photo-current curve experienced a large relative maximum quite unlike ordinary plate voltage-photo-current curves.

A sample of thorium oxide on platinum yielded no photo-current when the filament was cold. When the filament was at a bright red and emitting a thermionic current of $1.8\times10^{-7}$ amp. the total radiation from the arc caused a photo-current of $1.2\times10^{-8}$ amp. A thin piece of glass inserted in the path of the beam of light caused the photo-current to drop to zero, and therefore the effect is not caused by the visible portion of the spectrum.

Cerium oxide yielded quite steady thermionic and photo-currents and it was decided to study it in some detail. The oxide was obtained by decomposition of a sample of cerium nitrate of the General Chemical Co. There were probably small amounts of the nitrates of praesodymium and neodymium present as impurities. The oxide produced had a yellowish red color.

The most important qualitative observations are: none of the metals used in the tube yielded sufficient photo-current to afford a reading on the galvanometer of the sensitivity used. This was true both for the cold condition and when heated. On the contrary although the cerium dioxide when coated on platinum, or tungsten, or nichrome, yielded no measurable current when cold, it never failed to yield a measurable photo-current when hot and in all cases this photo-current increased with the temperature of the filament. All told, about nine different tubes were made and in every case, no matter what the metal of the filament, the result was qualitatively the same. It is fair to suppose, then, that the variation of photo-emission with temperature is a property of the oxide rather than the underlying metal or else that if the variation is due to some interaction between the oxide and metal this interaction is not confined to a single metal.

With the disposition of the tungsten seals as is shown in Fig. 1 some of the ultra-violet light passes the filament and falls on the place where the tungsten leads pass through the walls. It is conceivable given a small amount of surface contamination on the glass, that the ultra-violet light might change the surface conductivity and thus yield a spurious "photo-current" in the form of a conduction current between the filament and plate. The glassware was very thoroughly cleaned with hot chromic acid, alcohol, and ether, to prevent this. But a more convincing proof is offered in the fact that the variation in photo-current with temperature was observed in a tube in which each lead was sealed through a separate side tube and the light passed back into the vacuum system. Hence the currents observed are hardly false effects due to conductivity changes.

As well as could be determined with the eye there was no lag in the response of the filament to the light; the photo-current rose immediately to its maximum value. The water cell was of sufficient diameter to absorb the heat radiation from the light of the arc; therefore the current is hardly due to heating effects.

The photo-current was found to be due to radiation shorter than about 3100A. A piece of soda glass 1 mm thick interposed between the quartz win-

dow and the arc reduced the photo-current to zero. A piece of colorless mica 0.1 mm thick did the same in the case of most of the samples of mica tried; two samples of mica reduced the current by 95 percent of its original value. A filter of Corex D glass, 2 mm thick and with a lower limit of transmission of 2600A reduced the photo-current to 55 percent of its original value; thicker pieces of Corex D, 3.49 mm and 4.99 mm, yielded reductions in current to 45 percent and 35 percent respectively. No attempt was made to use a quartz monochromator because reduction in the intensity of the ultra-violet light would require working at temperatures so high that the thermionic current becomes too large to handle conveniently on a galvanometer that is sensitive enough to record the photo-current.

## Plate Current-Plate Potential Curves

Figure 2 shows the variation of photo-current with varying plate potential at various temperatures for cerium oxide on platinum. The curves show a distinct variation of the saturation currents with temperature of the filament. The plate potentials were raised to at least 40 v in every case, and in

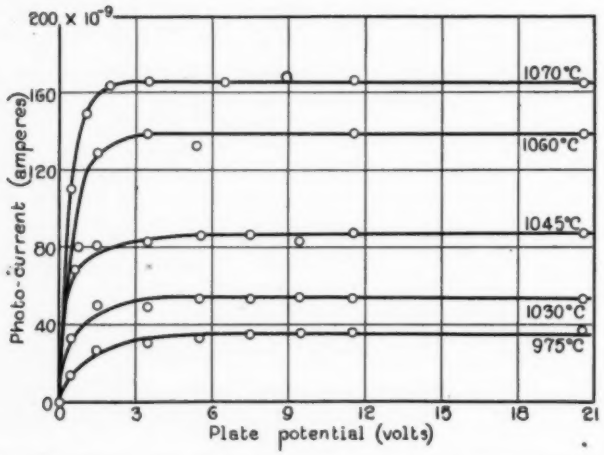


Fig. 2. Photo-current plate potential curves at various temperatures.

two cases to 160 v, to make certain that the current values at 21 v were really saturation values. The currents rise to saturation at remarkable low positive plate potentials. It has been previously stated under the discussion of the qualitative observations that one sample of calcium oxide on platinum showed a high maximum in the photo-current at about 8 v and that this had the same form as the maxima found by W. H. Crew[7] for the photo-currents from mixtures of barium and thorium oxides. In the present case of cerium oxide no such maxima were ever observed although very careful search was made for them. The question of the reproducibility of the curves is, of course, of interest. In order to test this point the filament current was increased by half an ampere after the readings at 1070°C in Fig. 2 were taken and the filament allowed to remain at the higher temperature for half an hour. Then the current was decreased until the temperature was 1030°C and readings taken

there to see if the points coincided with those previously obtained at this (1030) temperature. At two of the plate potentials the readings were exactly the same as before, the others checked to within 3 percent except one which showed 5 percent difference. Attention should be called to the large magnitude of the photo-currents from the relatively small area of oxide.

### Variation of Saturation Current With Temperature

In Fig. 3, Curve I shows the variation of the photo-current with filament temperature, the plate potential being 40 v. Since by "filament" temperature is meant the temperature of the central hottest portion and since the

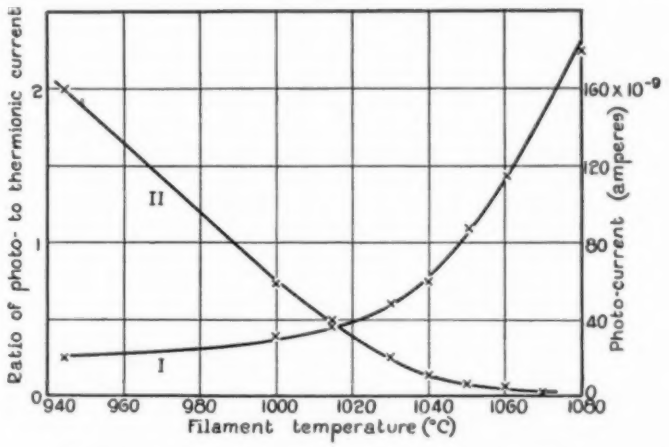


Fig. 3. Curve I—Variation of saturation photo-current with temperature.
Curve II—Variation of the ratio of photo-current to thermionic current with temperature.

end portions of the filament are much cooler than the center the curve can only be considered as giving an approximate representation of the variation of the photo-current with temperature. Curve II in the same figure represents the ratio of the photo-current to the thermionic current with a plate potential of 40 v. It can be seen that although the thermionic current is many times larger than the photo-current at higher temperatures the photo-current is the larger at the lower temperatures. The same effect was noted qualitatively in the case of calcium oxide on platinum. Case[8] reported an instance in which the photo-current was about two hundred times the thermionic current in an experiment with his barium cell.

### Variation with Intensity of Light

The intensity of the light incident on the filament was varied by inserting diaphragms with different size apertures between the arc and the quartz-water bulb. In order to measure the relative intensities the method of W. T. Anderson and F. W. Robinson[9] was used and found to be very convenient. It may be briefly described by stating that the ultra-violet light is allowed to

[8] Case, Phys. Rev. **18,** 413 (1921).
[9] Robinson, Jour. Am. Chem. Soc. **47,** 718 (1925).

fall upon a quartz vessel containing an aqueous solution of oxalic acid and uranyl sulfate. The oxalic acid undergoes decomposition, gas bubbles coming off visibly; the rate of decomposition, of the oxalic acid being proportional to the intensity of the ultra-violet light. A titration with potassium permanganate solution is used to determine the amount of oxalic acid decomposed in a given time. In the present experiment the solution was placed in the quartz vessel against the quartz window of the tube and the relative intensities of the beams with different diaphragms determined by titration. The results are shown in Fig. 4. The photo-current varies with the intensity of light in a manner which seems to be best represented by a linear relation.

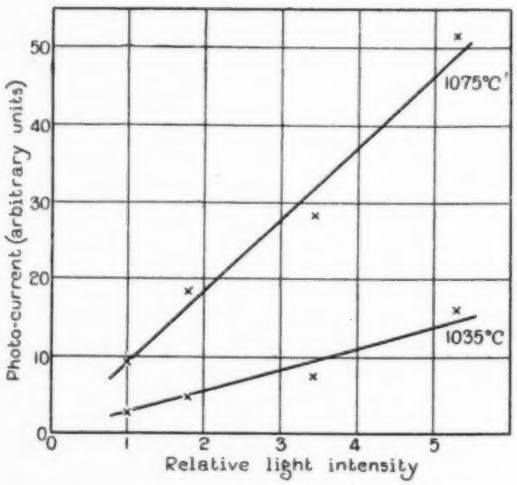


Fig. 4. Variation of the saturation photo-current with light intensity at two different temperatures.

## The Effect of Gases

In view of the fact that the oxides of cerium are rather easily reduced and re-oxidised it was thought to be of interest to investigate the effect of gases upon the photo-current particularly hydrogen and oxygen. Before discussing the method used it can be said at once that the presence of small amounts of air, or hydrogen, or oxygen, caused a reduction in the photo-current. The system was pumped down until the pressure was $10^{-6}$ mm of Hg. The saturation photo-current (plate potential 40 v) was measured at 1000°C. After air was allowed to leak slowly into the system until the pressure fell to $10^{-5}$ mm the photo-current was only 30 percent of its former value. The comparison between air and oxygen and hydrogen was made on a different filament than the one just mentioned. The method of introducing the hydrogen and oxygen was as follows: after the reading had been taken with air at $10^{-5}$ mm hydrogen was let into the tube until the pressure was atmospheric; then the tube was pumped down to about $10^{-5}$ mm Hg, and then hydrogen was again admitted until the pressure was atmospheric. The process was repeated until the tube had been pumped out and washed with hydrogen five

times. Finally hydrogen was allowed to leak in until the pressure was $1.5\times 10^{-4}$ mm Hg. Then the photo-current was measured. The same precess was used for oxygen. The results of the comparison between air and hydrogen and oxygen are shown in Fig. 5. There is no evidence of increased photo-emission due to reaction of oxygen or hydrogen with the cerium oxide; on the contrary the emission is decreased in each case.

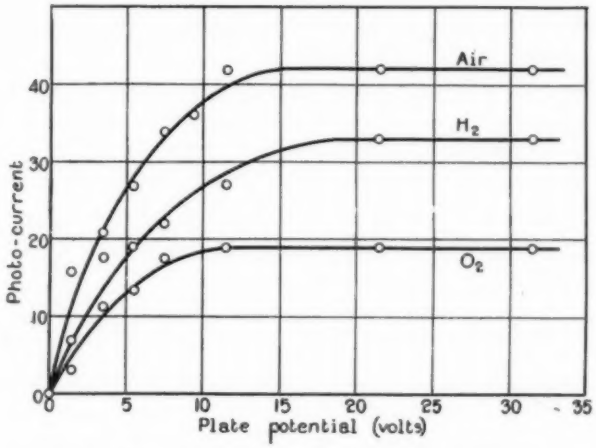


Fig. 5. Effect of gases on saturation photo-current.

## Discussion of Results

It is of considerable interest to inquire as to whether or not the preceding experimental results indicate a variation of the true photoelectric effect with temperature. Discarding such patently invalid explanations as spurious condition effects or thermal effects of illumination we can turn to the question of the possibility of release in some manner of space charge electrons by the illumination. As has been pointed out by Crew[7] the release of space charge electrons around the filament is not a reasonable explanation of the source of the photo-current because the pure metal filaments do not yield these same photo-currents and space charge electrons exist in the case of the pure metal filaments as well as in the case of the oxide-coated ones.

There exists considerable collateral evidence pointing toward a possible explanation of the effects here reported. In the case of thermionic emission from filaments of barium oxides on platinum Barton[10] has shown the electron emission to be accompanied by the emission of singly charged, negative, molecular oxygen ions. When this is considered in conjunction with the work of Harris[11] on the same filament which showed chemical combination between the underlying platinum and metallic barium or strontium it seems reasonable to suppose that some decomposition of the oxides has occurred. The results of Koller[12] on the thermionic emission from this same filament seemed to be

[10] Barton, Phys. Rev. **26**, 360 (1925).
[11] Harris, Phys. Rev. **24**, 679 (1924).
[12] Kaller, Phys. Rev. **25**, 671 (1925).

explained best by the assumption of the formation of a thin surface layer of metallic barium or strontium on the oxide, presumably due to positive ion bombardment of the oxide. The recent experiments of MacNabb[13] show that thermionic emission from commercial oxide-coated filaments depends for its origin upon the bombardment of the oxides by positive ions from carbon dioxide gas released from the filament. Again, the decrease in photoelectric work function of Western Electric oxide-coated filaments as temperature was increased seemed to be explained best by Koppius[3] as due to change in the oxide surface because of bombardment by gases. It may possibly be, then, that in the present experiments the surface of the cerium oxide is changed by impacts of postive ions formed from gas liberated from either the oxide itself or from the underlying platinum.

The viewpoint that the results obtained for cerium oxide indicate a case of variation of the true photoelectric effect with temperature finds support in the linear variation with light intensity, in the form of the plate potential curves, and in the reproducibility of the curves.

In conclusion it can be said that there are not sufficient experimental data available to decide whether the true photo-current from cerium dioxide does undergo variation with temperature or whether the variations are due to variations in the surface of the oxide.

This investigation was carried on at the Physics Laboratory of Cornell University. The writer wishes to thank Professor E. Merritt for suggesting the investigation and for his continued interest and helpful advice. Grateful appreciation for helpful suggestions is also expressed to Professor E. Kennard and to Mr. H. Banta who has given invaluable help in the construction of the apparatus.

[13] MacNabb, J.O.S.A. & R.S.I. **19**, 33 (1929).

# SOME THERMAL AND ELECTRICAL PROPERTIES OF BERYLLIUM

By Evan Jarrett Lewis
Cornell University

(Received August 29, 1929)

Abstract

**Specific heat.**—The specific heat of beryllium was obtained from cooling data by equating the heat loss per cm length per unit time from beryllium to that from zinc. The values obtained increase rapidly with a rise in temperature from 0.0389 at −175.6°C to 0.593 at 190°C.

**Thermal conductivity.**—The modified Forbes method of Bidwell was used to determine the thermal conductivity of this metal. Values of $k$ were calculated with three different sets of distances from the first junction as origin for each run at a given surrounding temperature. $k$ was found to increase with a rise in temperature from 0.232 at −176.2°C to 0.508 at 190.4°C.

**Specific resistance.**—The specific resistance varies according to the heat treatment given the sample. Values recorded in this article are those obtained after a steady condition had been established after repeated treatments from liquid air temperature to 700°C. Measurements made on two samples check each other closely. They are: 1.56 microhms at −191°C; 6.76 microhms at 22°C; 19.05 microhms at 305°C; and 40.00 microhms at 690°C.

**Temperature coefficient of resistance.**—The temperature coefficient of resistance, $\alpha$, is not a constant over the above range. It increases with a rise of temperature but not linearly. The graph of this quantity plotted against temperature shows three distinct sections, $\alpha$ has the following values: 0.000371 at −190°C; 0.00667 at 20°C; 0.00800 at 310°C; 0.00858 at 500°C; and 0.01196 at 685°C.

**Thermoelectric power.**—The thermoelectric power of beryllium against lead seems to vary linearly with temperature. However, at −50°C the graph of the thermoelectric power plotted against temperature shows a break. This, considered in connection with the results obtained for the temperature coefficient of resistance, suggests the probability of a change in allotropic form.

**Wiedemann-Frantz-Lorentz law.**—The Wiedemann-Frantz-Lorentz law, that $k/\sigma T$ is a constant, is not obeyed by this metal.

THREE years ago, soon after beryllium could be obtained in a highly pure state, it was thought desirable to determine certain of the physical properties of the metal.[1] The specific heat was determined in conjunction with the thermal conductivity over the range from liquid air temperature to 200°C, the thermal conductivity being determined by the modified Forbes method of Bidwell.[2] However, the writer introduced one change by bringing the junction

[1] A rod of beryllium, commercially pure, was obtained from the Beryllium Company of America. This showed, when analyzed spectroscopically, traces of aluminum, manganese and chromium, and smaller traces of iron, silicon and magnesium, a total of about 0.5 percent. In addition, x-ray shadow pictures of the sample showed physical imperfections to be so small that they could be neglected without introducing any appreciable error in the calculations.

[2] Bidwell, Phys. Rev. **28,** 584 (1926).

leads out to the edge of the fiber disks and then parallel to the axis of the sample to the top of the containing tube, thus allowing better radiation from the sample to the surrounding constant temperature baths. Investigations of specific resistance and temperature coefficient of resistance were carried out over a much greater range of temperatures, liquid air to 700°C. The thermo-electric power against lead was determined only over the range from liquid air temperature to 200°C. Using the results obtained for the thermal conductivity and the specific resistance the Wiedemann-Frantz-Lorentz relation was calculated.

## Specific Heat

*Procedure.* The determination of the specific heat of beryllium was made from cooling data. A piece of the original beryllium sample 6 cm long and a zinc rod of about the same length but of exactly the same diameter were each mounted with a single junction and three disks in the Pyrex tube used later for gradient data. Cotton plugs were inserted above and below these small rods to prevent heat losses through the ends. Readings of the junction were taken every half minute as each rod cooled through the range of temperatures possessed by various parts of the rod in the thermal conductivity experiment. Several runs were taken on each metal. In order to obtain an average of the runs the readings were plotted against time. One run was plotted and a smooth curve drawn; then the other runs were plotted so as to coincide with the first at the middle of the temperature range needed for determining the thermal conductivity. Then an average curve was drawn through all points plotted. The micro-volt readings used in calculating the specific heat were taken from this average curve.

According to Newton's Law of Cooling, heat loss per cm length is the same for all metals provided the surface is the same and the dimensions of the apparatus are the same. These conditions were met as the cooling data were taken in the tube used for the gradient data and the samples had the same diameter. To make sure that slight variations in the character of the surfaces of the two samples had no effect, runs were made having a coating of soot on each specimen. Within the experimental error this yielded no change in the specific heat. The heat loss curve plotted against temperature is a nearly straight line over a range of 20°C and in the results here reported the range was never more than 6°C. Thus the following equation may be written

$$(1/L \cdot M \cdot S \cdot dT/dt)_{Be} = (1/L \cdot M \cdot S \cdot dT/dt)_{Zn}$$

for any one temperature, where $L$ is the length, $M$ the mass, $S$ the specific heat, and $dT/dt$ the rate of cooling. The specific heat of beryllium was determined from the above equation using the specific heat of zinc determined by drawing a mean graph through all the values given by Landolt and Börnstein.

*Results.* The results of the specific heat measurements are found in Table I and Fig. 1. Over the range from liquid air temperature to 200°C the specific heat, $S$, increases with increase in temperature. At $-175.6$°C the value of

$S$ is 0.0389. Dewar[3] gave 0.0137 as the average specific heat over the range $-253°C$ to $-196°C$. Humpidge[4] gave a value of $S$ equal to 0.445 from 45°C to 50°C, while the value found in this experiment taken from Fig. 1 is $S=$

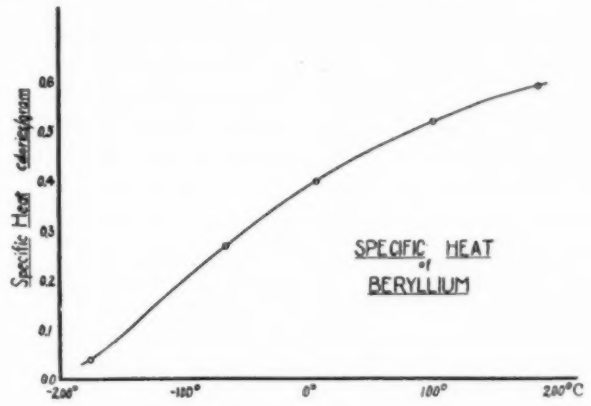


Fig. 1. Specific heat of beryllium.

0.457 at 50°C. The work of Nilson and Pettersson[5] in 1881 gives the average specific heat from 0°C to 300°C as 0.5060 which is lower than found in this experiment, 0.565 at 150°C. Thus the values obtained in the present investigation agree quite well with those reported by early observers.

TABLE I. *Specific heat of beryllium.*

| Various Points | Temp.°C | Specific Heat. |
|---|---|---|
| Liquid Air | −175.6 | 0.0389 |
| $CO_2$ Snow | − 65.0 | 0.270 |
| Ice-Water | 9.5 | 0.399 |
| Hot Water | 104.0 | 0.519 |
| Hot Air | 190.0 | 0.593 |

## THERMAL CONDUCTIVITY

*Apparatus and procedure.* The specimen of beryllium in the form of a rod 21 cm long and 1 cm in diameter was heated at one end by a coil of about 20 turns of asbestos covered nichrome wire. This was insulated from the rod by two layers of mica. Starting 1 cm from the heater coil copper-advance junctions (#29 wire) were placed spirally along the rod at intervals of 2.5 cm and 60°. The junctions were silver soldered and mounted in small holes (No. 60 drill) by wedging in small pieces of copper wire to make a good contact. Great care was taken to have the junctions as near the surface as possible. The specimen was slipped into a Pyrex glass tube 2.5 cm in diamter, 40 cm long, and closed at the lower end. All junction leads and heater coil leads

[3] Dewar, Proc. Roy. Soc. **A89**, 158 (1913).
[4] Humpidge, Proc. Roy. Soc. **35**, 137 and 358 (1883).
[5] L. F. Nilson and O. Pettersson, Berichte **13**, 1451 (1881).

were brought out the top of the tube and cotton was stuffed in the top of the tube to cut down convection currents. The tube containing the specimen was placed in a Dewar cylinder 40 cm long and 6.6 cm in diameter. Constant temperature baths were obtained by filling the Dewar in turn with liquid air, $CO_2$ snow and ether, and water. A higher temperature was obtained by a hot air jacket. As soon as the readings of the junctions reached the temperature of the bath, indicating that a steady state had been reached, the top of the rod was heated by means of the heater coil until the top junction read about 10° higher than that of the surrounding bath. After about an hour readings of each junction were taken and repeated until a steady state had established itself. Usually the rod was later allowed to cool down to the temperature of the surroundings and another set of "zero" readings taken. This permitted discrepancies in junction readings to be taken into account. Cooling data taken as previously described were used again in the calculation of the heat loss per cm length per unit of time.

The $CO_2$ snow and ether were placed in the Dewar cylinder and stirred from time to time, as was the liquid air, to keep the temperature as uniform as possible. For the point near 0°C icewater was pumped out of the bottom of a pail of cracked ice into the bottom of the Dewar and allowed to run out at the top and trickle down through the ice again. In this way a very uniform temperature of about 0.5°C above zero was maintained. A higher temperature of about 98°C was obtained by pumping boiling water through the Dewar. The highest surrounding temperature was obtained by use of a double-walled brass cylinder heavily lagged to prevent radiation, through which heated air was flowing at a constant rate.

The relative temperatures along the rod were obtained by dividing the difference in micro-volts between two junctions by the micro-volts per degree for the particular temperature obtained from the calibration equation of the junction.[6] Relative temperatures along the rod were known to within 0.05°C at the lower temperatures and much better than that for the higher temperatures as the micro-volts per degree increase with a rise in temperature. Actual temperatures may have been uncertain as much as one degree at the most.

The theory of the method has been very clearly given in detail by Bidwell in the article previously mentioned. After obtaining the temperatures at fixed points along the rod, measured from the first junction at the hot end as origin, the method is essentially a graphical one. It depends on the slopes and intercepts of graphs, one of which is $dT/dx$ against $T$ and another the heat loss per unit time plotted against temperature. From these graphs together with three others also mentioned by Bidwell the constants are obtained which, when substituted directly in a relatively simple formula, give the value of $k$ at once.

[6] The junctions used were calibrated against junctions which had previously been calibrated by the United States Bureau of Standards as follows: one pair of copper-advance junctions for the range 0°C to liquid air temperature, accurate to ±0.2°C, and another pair of the same materials for the range from 0°C to 350°C, reliable to ±0.5°C. For the higher temperatures used in the specific resistance experiment chromel-alumel junctions were used which were good to ±3.0°C.

*Discussion of results.* The values of the thermal conductivity of beryllium are given in Table II. It will be seen that $k$ has been calculated for three different sets of distances from the origin and that the value of $k$ decreases as the origin is approached in all cases. The general trend of an increase in the

TABLE II. *Thermal conductivity.*

| Temp. | $k$ 5–10 | $k$ 4–9 | $k$ 3–8 | Av. $k$ 3–10 | Av. Temp. | Grand Av. $k$ | Grand Av. Temp. |
|---|---|---|---|---|---|---|---|
| | | | Liquid Air | | | | |
| −176.04 | | | 0.202 | | | | |
| −176.37 | | 0.220 | | | | | |
| −176.64 | 0.242 | | | 0.221 | −176.37 | | |
| −175.30 | | | 0.204 | | | | |
| −175.61 | | 0.235 | | | | | |
| −175.91 | 0.270 | | | 0.236 | −175.61 | | |
| −176.10 | | | 0.201 | | | | |
| −176.55 | | 0.238 | | | | | |
| −176.81 | 0.277 | | | 0.239 | −176.49 | 0.232 | −176.2 |
| | | | $CO_2$ Snow | | | | |
| −65.91 | | | 0.308 | | | | |
| −66.18 | | 0.342 | | | | | |
| −66.43 | 0.381 | | | 0.344 | −66.17 | | |
| −63.53 | | | 0.277 | | | | |
| −63.85 | | 0.299 | | | | | |
| −64.08 | 0.338 | | | 0.305 | −63.82 | 0.325 | −65.0 |
| | | | Ice-Water | | | | |
| 9.53 | | | 0.358 | | | | |
| 9.31 | | 0.379 | | | | | |
| 9.05 | 0.409 | | | 0.382 | 9.30 | | |
| 9.71 | | | 0.372 | | | | |
| 9.42 | | 0.393 | | | | | |
| 9.18 | 0.423 | | | 0.396 | 9.44 | | |
| 9.63 | | | 0.361 | | | | |
| 9.36 | | 0.399 | | | | | |
| 9.10 | 0.441 | | | 0.400 | 9.36 | 0.393 | 9.4 |
| | | | Hot Water | | | | |
| 105.57 | | | 0.454 | | | | |
| 105.21 | | 0.468 | | | | | |
| 104.88 | 0.492 | | | 0.471 | 105.22 | | |
| 105.63 | | | 0.426 | | | | |
| 105.18 | | 0.440 | | | | | |
| 104.87 | 0.462 | | | 0.442 | 105.23 | 0.457 | 105.2 |
| | | | Hot Air | | | | |
| 190.67 | | | 0.470 | | | | |
| 190.40 | | 0.501 | [illegible] | | | | |
| 190.17 | 0.552 | | | 0.508 | 190.40 | 0.508 | 190.4 |

value of the thermal conductivity with increase in temperature is clearly shown in Fig. 2 where the grand average values are plotted.

The lowest surrounding temperature was obtained through the use of liquid air, as liquid oxygen or hydrogen was not available. This becomes warmer the longer it stands and also during use, as the nitrogen evaporates first.

On this account it is very difficult to have the gradient data taken with the same surrounding temperature as the cooling data. Since this method depends on constants obtained from graphs this introduces an error. The exact temperature may be in error as much as 1°C due to the uncertainty of the junction itself for all temperatures below 0°C. Mounting the junctions also introduces an error as it is impossible to be sure that all the junctions are exactly at the surface of the sample. Thus it can be easily seen how, between extremes, a maximum experimental error of 4.7 percent based on the mean may have crept into the work.

$CO_2$ snow also presented all of the above sources of error, even that due to non-uniform temperature down the cylinder, as there was no free circulation in the ether slush so that some portions of the tube might have been warmer than others thus giving poor gradient data. The average of $k$ for one run at this temperature is probably low. The value of $k=0.344$ for the other run appears, by comparison with values of $k$ at other temperatures, to be the

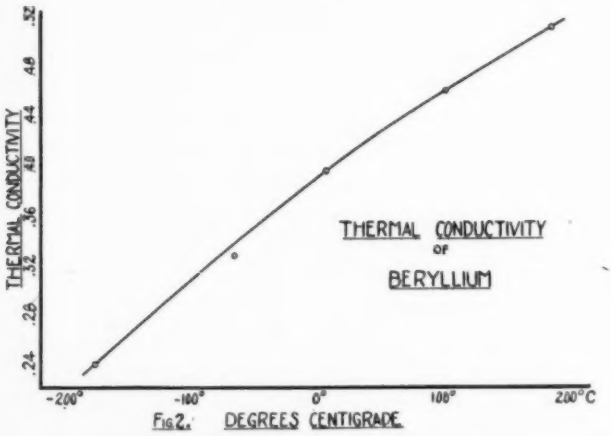


Fig. 2. Thermal conductivity of beryllium.

more nearly correct value. In fact this point would fall almost exactly on the smooth curve, Fig. 2. In all this work the data from which the calculations were made are the averages of twelve different sets of observations. The maximum error here is probably not greater than 5.9 percent.

When ice-water was used as a means of obtaining a surrounding temperature near 0°C, very much better control resulted so that here the maximum error was 2.8 percent. This was obtained because of the good circulation maintained by the pump as previously mentioned. Boiling water was used in a similar manner and the deviation from the mean was 3.1 percent.

A temperature near 200°C was obtained by the use of circulating hot air and did not prove to be as satisfactory as water in maintaining a constant temperature, due to its low specific heat and density. The radiated heat was not carried away fast enough so the surroundings became warmer during the run, thus affecting both the gradient data and the cooling data. The value of

the thermal conductivity at this temperature may be in error as much as 5 percent.

The equation of the graph, Fig. 2, is given by

$$k = 0.3847 + 0.000751t - 0.000000468t^2 - 0.00000000027t^3$$

where $k$ is the thermal conductivity and $t$ the temperature in Centigrade degrees.

In this work it has been assumed that the temperature has been uniform over the cross section of the rod. This is an assumption which is not true because moving any one junction toward or away from the axis of the sample changed the relative temperature between it and the two adjacent junctions which remained fixed, thus showing the cross section was not an equal temperature surface. At the top close to the heater coil the heat flow lines are toward the center so that the equal temperature surface is convex upward, while at the lower end just the reverse is true. For this reason the temperatures recorded are not the exact ones for equal temperature surfaces through the given distances from the origin. This source of error would be very much less if a rod three or four times as long were used. The writer feels that the specimen he used was entirely too short because in working up the graphs more reliance had to be placed on the central junctions than on those at the ends. It would seem that these two sources of error are responsible for the large experimental errors obtained using the various sets of distances in calculating $k$.

## Specific Resistance and Temperature Coefficient of Resistance

*Apparatus and procedure.* The specific resistance of beryllium was found by passing a small current of less than an ampere through a rod of beryllium, 0.792 cm² in area, and a recently calibrated resistance in series. A Wolf potentiometer was used to measure the potential drop across the standard resistance and between two leads inserted 22.5 cm apart in the beryllium rod. Another determination was made with a rod of 0.803 cm² in area and 18 cm between potential leads. In these experiments the distance between the potential leads is known to within 0.05 cm as the holes used were small (No. 60 drill) and No. 22 copper wire was wedged into them with small pieces of the same wire. Slotted copper connectors were slipped over the ends of the sample and fastened by means of steel rings and set screws and the current leads were fasted to these connectors by screws. The contacts thus made were sufficiently good to eliminate local heating. Two pairs of thermo-junctions were placed in the sample, one to read the temperature near one end and the other in the middle. The two pairs of junctions used at any given temperature did not always read alike so that the rod was not at a uniform temperature. Therefore to obtain the correct potential difference over the rod both direct and reverse readings were taken to eliminate any e.m.f. set up by the Be-Cu junction formed by the rod and leads.

For the lower temperatures the rod was immersed in liquid air and $CO_2$ snow and ether. These were stirred constantly during the time the readings

were taken. For the higher temperatures the sample was supported on mica inside of a brass cylinder which was surrounded by a well insulated electric furnace.

Each of the two samples was heated to about 700°C and cooled down to nearly room temperature and readings taken every few degrees. This was repeated until the results were reproduced within the accuracy of the thermo-junctions.

The coefficient of specific resistance was determined by finding for different temperature ranges the third degree equations of the graph obtained by plotting the specific resistance against temperature. These were differentiated with respect to temperature giving equations of the form

$$d\rho/dT = a + bT + cT^2.$$

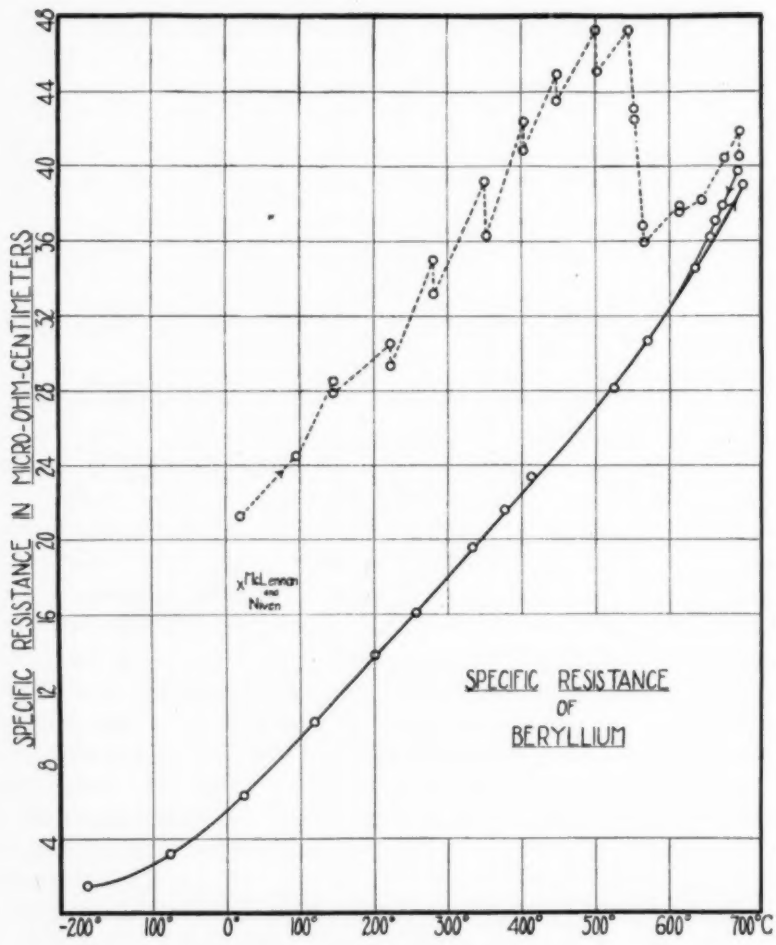


Fig. 3. Specific resistance of beryllium.

The temperature coefficient of resistance, $\alpha$, was found by dividing the computed values of $d\rho/dT$ by $\rho_0$, the resistance at 273°K.

*Results.* The results of the specific resistance measurements on sample 1 are shown graphically in Fig. 3 and are tabulated in Table III. It will be seen that the sample yielded considerably to heat treatment. From this curve it can be easily seen how a great many values of the specific resistance can be

TABLE III. *Specific resistance of beryllium.*

| Sample 1* | | Sample 2 | |
|---|---|---|---|
| Temp. | $\rho \times 10^6$ | Temp. | $\rho \times 10^6$ |
| −189°C | 1.50 | −191°C | 1.56 |
| −77 | 3.22 | −77 | 3.33 |
| +21 | 6.45 | +22 | 6.76 |
| 108.5 | 9.75 | 97 | 9.83 |
| 223 | 14.64 | 212 | 14.85 |
| 315 | 18.60 | 305 | 19.05 |
| 401 | 22.45 | 403 | 23.90 |
| 512 | 27.55 | 504 | 29.00 |
| 607 | 32.45 | 604 | 34.55 |
| 700 | 39.00 | 690 | 40.00 |

* This was the sample analyzed.

obtained for any given temperature, depending upon at what stage of its heat treatment the observation is made. The rather high value of 17.6 microhms at 20°C reported by McLennan and Niven[7] may have been due to not carrying the heat treatment over so wide a range of temperature. Fig. 3 shows that the first measurements taken at room temperature (22.5°C) gave a value of 23.0 microhms. The measurements for the specific resistance on this sample were first continued only to 455°C when the junction oxidized and broke. When the run was continued and another measurement made at room temperature (22.5°C) $\rho$ was found to have a value of 21.5 microhms indicating that some change had taken place. As the temperature was increased in steps of about fifty degrees and held constant for some time, a decrease in the value of $\rho$ resulted. However, between 545°C and 562°C $\rho$ decreased from 47.3 microhms to 36.0 microhms indicating a decided change had taken place at about this temperature. The specific resistance continued to increase with a rise in temperature at about the same rate as it did before the sudden decrease in $\rho$. Another decrease was observed at about 670°C. Most of the change had taken place by this time as measurements made later when the temperature was both increasing and decreasing from room temperature to 700°C checked each other within the limits of accuracy of the junctions used to read the temperature.

A second sample was then measured after it had first been given a heat treatment. The temperature was slowly increased over a period of 24 hours to about 700°C and held there for 12 hours and then cooled slowly to room temperature. This process was repeated to insure a steady condition of the sample as only the specific resistance in such a state was desired. The results for this sample are shown in Table III from which it can be seen that the specific resistance of sample 2 checked well with that of sample 1. The final

[7] McLennan and Niven, Phil. Mag **4** (1927).

value of $\rho$ at 25°C for sample 1 was 6.5 microhms and for sample 2 was 6.7 microhms.

Since the specific resistance of the two samples checked so well, the temperature coefficient of resistance was determined only for sample 2 and the

TABLE IV. *Temperature coefficient of resistance.*
$\rho_0 = 5.88 \times 10^{-6}\Omega$

| Temp. | $\alpha$* | Temp. | $\alpha$ | Temp. | $\alpha$ |
|---|---|---|---|---|---|
| −190°C | 0.000371 | +100°C | 0.00722 | +450°C | 0.00844 |
| −160 | 0.00169 | 140 | 0.00737 | 480 | 0.00864 |
| −130 | 0.00287 | 180 | 0.00752 | 520 | 0.00899 |
| −100 | 0.00391 | 220 | 0.00769 | 550 | 0.00938 |
| −70 | 0.00481 | 250 | 0.00781 | 580 | 0.00983 |
| −40 | 0.00556 | 280 | 0.00791 | 610 | 0.01035 |
| −10 | 0.00619 | 310 | 0.00800 | 640 | 0.01094 |
| +20 | 0.00667 | 360 | 0.00808 | 670 | 0.01160 |
| 50 | 0.00701 | 380 | 0.00817 | 685 | 0.01196 |
| 75 | 0.00712 | 410 | 0.00825 | | |

* These values of $\alpha$ were obtained from six different equations, successive ones of which overlapped each other in temperature range.

values obtained are shown in Table IV and Fig. 4. The graph of the temperature coefficient appears to have three distinct parts, one from −190°C to about −50°C where the temperature coefficient rises rapidly from $4 \times 10^{-4}$ to

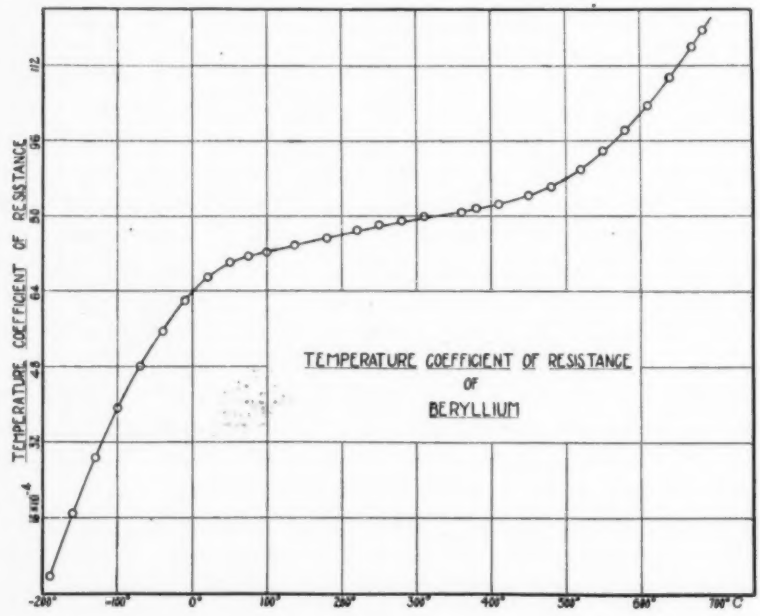


Fig. 4. Temperature coefficient of resistance of beryllium.

$56 \times 10^{-4}$, the second from about 50°C to about 400°C where the increase is nearly linear and with a smaller slope rising from about $72 \times 10^{-4}$ to $82 \times 10^{-4}$, and the third in the range of about 500°C to 700°C where the coefficient rises

more rapidly again from $88\times10^{-4}$ to $120\times10^{-4}$. These results quite strongly indicate that within the temperature range $-190°C$ to $700°C$ the sample passes through two allotropic transformations. Additional evidence of such a transformation at the lower temperature is seen in the thermoelectric power graph,

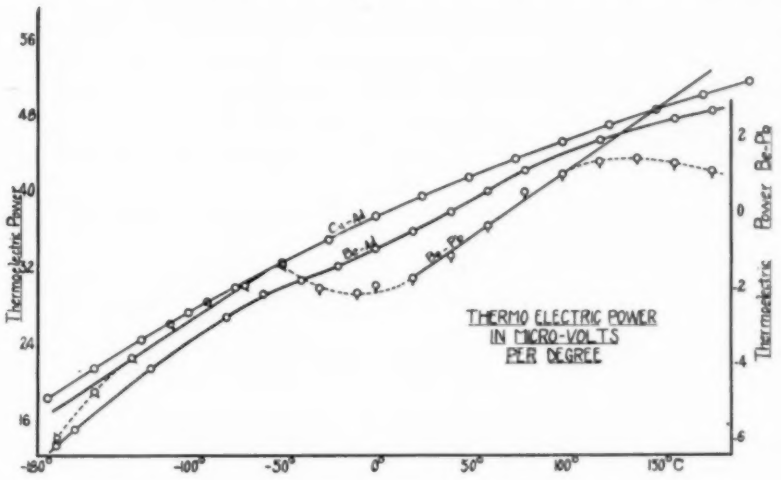


Fig. 5. Thermo-electric power (microvolts per degree) of beryllium.

Fig. 5, which has a break between $-50°C$ and $20°C$. The thermoelectric power was not measured at a sufficiently high temperature to determine whether another break occurs at about $450°C$.

## Thermoelectric Power

*Apparatus and procedure.* The thermoelectric power of beryllium was obtained by first determining the electromotive force given by a beryllium-advance thermo-junction. The equation of the graph obtained by plotting the electromotive force against the temperature was differentiated giving an equation of the form

$$dE/dt = a + bt + ct^2$$

which is by definition the thermoelectric power. Experimentally this was difficult, as the rod of beryllium previously mentioned had to be substituted for a wire. In order to accomplish this two small holes (No. 60 drill) were made in the same transverse plane and close together near each end. A Pyrex cup 4 cm in diameter and 10 cm long, drawn down at one end to fit the rod, was slipped over it a distance of one third its length and a tight joint made with rubber tubing. A copper-advance junction was fastened into one of the holes at either end for reading the temperature, while in the other two were fastened advance wires by wedging in pieces of the same wire. The lower end with its wires was immersed in cracked ice while in the cup were placed, in turn, liquid air, $CO_2$ snow and ether, boiling water, and boiling nitro-benzol. The latter two liquids were heated by an electric heating coil. Also a small

heating coil was wound around the sample itself while using the cold liquids, to prevent the lower end from becoming colder than 0°C. The liquids in the cup and the ice were stirred constantly during the time the readings were taken.

The thermoelectric power of beryllium against advance wire was then plotted. Beryllium is positive to advance. On the same graph the thermoelectric power of copper against advance was plotted. This was taken from the Bureau of Standards' calibration of a Cu-Ad junction. Copper is positive to advance and higher than beryllium. The differences in the thermoelectric power were read from this graph, Fig. 5. Thus the thermoelectric power of Be with respect to Cu was obtained.

From the Smithsonian tables the thermoelectric power of copper with respect to lead is given by

$$dE/dt = 1.34 + 0.094t \ .$$

However, here lead was wanted against copper, so all the signs were reversed. Since the thermoelectric power of lead and beryllium are both against copper, the thermoelectric power of beryllium against lead is obtained by subtraction.

*Results.* The final result of the thermoelectric power of beryllium referred to lead appears to be represented by two straight lines not quite parallel to each other and broken by an offset between −50°C and 20°C, Fig. 5, which indicates a change has taken place in the beryllium in this range, an indication that is in agreement with the results shown in Fig. 4. At the higher temperatures 100°C to 200°C the values do not follow the straight line. Also from −100°C down the experimental values do not follow the straight line. This may possibly be explained if the fact that a rod of beryllium was used instead of a wire is taken into account. It is a very hard matter experimentally to maintain a temperature gradient of nearly 200°C down a rod 0.792 $cm^2$ in area in a length of 17 cm. It may however be definitely stated that Be and Cu have values of thermoelectric power very close to each other.

## Wiedemann-Frantz-Lorentz-Law

Since the specific resistance and thermal conductivity of beryllium have been determined, it seemed advisable to calculate the Wiedemann-Frantz-Lorentz relation which when put in a simplified form is

$$k/\sigma T = K = 24.7 \times 10^7 \ .$$

when $k$ is expressed in ergs and $\sigma$ in e.m.u. This does not hold for beryllium as is seen in Table V. In order for the law to hold for this metal the values of $k$ would have to decrease instead of increase with a rise in temperature. Assuming $\sigma$ to be correct the value of $k$ should be 0.22 at 0°C and at 180°C $k$ should equal 0.20.

Aluminum also shows a rise in thermal conductivity with a rise in temperature. The Wiedemann-Frantz-Lorentz Constant for aluminum is $13.2 \times 10^7$ at −189°C and $19.3 \times 10^7$ at 0°C and only $22.2 \times 10^7$ at 200°C. The value at 200°C is 1.68 times the value at −189°C whereas for beryllium the value

at 180°C is 3.6 times the value at −170°C. Thus according to the data taken on these samples this law does not hold for beryllium.

TABLE V. *Values of thermal and electrical conductivities of beryllium.*

| Temperature | $k$ | $\sigma$ | $k/\sigma T$ |
|---|---|---|---|
| −170°C | 0.251 | $5.88\times10^{-4}$ | $17.4\times10^{7}$ |
| −150 | 0.268 | 5.23 | 17.4 |
| −130 | 0.284 | 4.52 | 18.4 |
| −110 | 0.300 | 3.84 | 20.0 |
| −90 | 0.316 | 3.29 | 22.0 |
| −70 | 0.332 | 2.82 | 24.2 |
| −50 | 0.348 | 2.42 | 27.0− |
| −30 | 0.363 | 2.08 | 30.1− |
| −10 | 0.378 | 1.82 | 33.2 |
| 0 | 0.386 | 1.70 | 35.0 |
| 20 | 0.400 | 1.51− | 38.1 |
| 40 | 0.414 | 1.34− | 41.4 |
| 60 | 0.428 | 1.21− | 44.7 |
| 80 | 0.441 | 1.10− | 47.7 |
| 100 | 0.454 | 1.00 | 51.2 |
| 120 | 0.468 | 0.925 | 54.2 |
| 140 | 0.479 | 0.855 | 56.8 |
| 160 | 0.492 | 0.796 | 59.8 |
| 180 | 0.503 | 0.745 | 62.5 |

The writer wishes to express his thanks to Professor Bidwell for suggesting this problem, to Professors Collins and Gibbs for their helpful suggestions in carrying through the investigation, and to Professor Papish who made a spectrum analysis of the beryllium rod.

# ELECTRICAL RESISTIVITIES AND TEMPERATURE COEFFICIENTS OF LEAD, TIN, ZINC AND BISMUTH IN THE SOLID AND LIQUID STATES

By W. B. Pietenpol and H. A. Miley
Hale Physical Laboratory, University of Colorado

(Received October 25, 1929)

Abstract

A method of measuring the resistance-temperature coefficients of low melting point metals in the solid and liquid states is described. Previous difficulties in the way of making such measurements have been largely eliminated by employing oxide films as containers for the molten metals. The resistivity-temperature curves are shown for the metals (Pb, Sn, Zn, Bi), and the resistance-temperature coefficients are given for 20° intervals throughout the range 20° to 460°C. The temperature coefficients of resistance of zinc above the melting point are found to be positive instead of negative as reported by Northrup and Suydam. Variations in the resistivity values indicate that there are allotropic transformations in zinc slightly above 180°C and at about 340°C. The coefficients of the metals investigated are all positive except those for nonannealed bismuth in the regions 160° to 180°C and 225° to 275°C and those for annealed bismuth in the latter region. The high resistivity values of nonannealed bismuth below 160°C are attributed to three possible factors, (a) lack of random orientation of the crystals, (b) cracks and imperfections in the crystal lattice, and (c) amorphous solid bismuth which may be formed between cleavage faces and in reentrant angles. The origin of these factors is accounted for by a crystalline transformation, in the region 160° to 180°C, which gives rise to them only when the metal is cooled rapidly. When nonannealed bismuth passes through this region from the lower to the higher temperature the negative coefficients are then to be expected. In the range 225° to 275°C the negative coefficients of bismuth are due to a molecular derangement of the metal as it approaches the melting point and passes from the solid to the liquid state.

IN A previous paper "Liquid Wires and their Surface Films"[1] the authors reported a study of the functions of oxide films in supporting molten wires of lead, tin, zinc and bismuth. Reference was made to a method of measuring the resistance-temperature coefficients of low melting point metals in the solid and liquid states. The object of the present article is to describe this method and to give the electrical resistivity and temperature coefficients of lead, tin, zinc and bismuth in the temperature range 20°C to 460°C.

## Experimental Procedure

The lead, tin, zinc and bismuth wires were mounted and heated in a nitrogen container. The container was a brass cylinder, 18 cm in length and 9 cm in diameter, with one end removable. The method of support of the wires in the container is given in Fig. 1. Brass blocks, $B\,B'$, each of 2 cc volume, were mounted firmly, 5.25 cm apart, with their upper faces flush with $P$, the horizontal porcelain plane of support for the wires. Holes, $s\,s'$, 0.9 mm in

[1] Pietenpol and Miley, Phys. Rev. [2] 30, 697–704 (1927).

diameter were drilled in the upper part of the blocks near the inner edge and coated on the inside with Wood's metal so that good contact was made with the clean ends of the wires. (The melting point of the Wood's metal could not be detected in any of the readings.) The holes extended 5 mm into the blocks, and for the lead, tin, and zinc wires they were inclined at a 30° depression angle to the horizontal. They were horizontal for the bismuth wire which would not permit bending. There were four copper wires, No. 8 A.w.g., leading through the center of tubes, in the removable end of the container. The tubes were filled with asbestos cement of high insulating quality. Two of these copper wires were brazed to each of the brass blocks; one pair of them, 1-2 in Fig. 1, was used to conduct a small current through the wire *W*

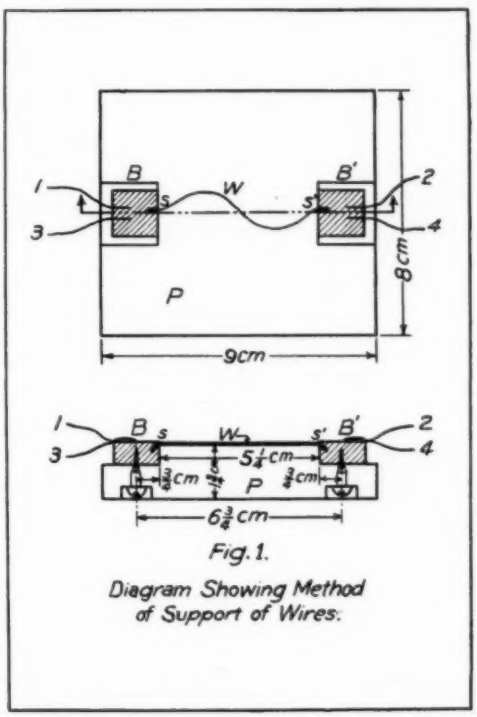


Fig. 1.

Diagram Showing Method of Support of Wires.

Fig. 1. Diagram showing method of support of wires.

under investigation, and the other pair, 3-4, served in the measurement of the potential drop. The entire support for the lead, tin, zinc and bismuth wires could be removed from the container for changing the wires.

After a wire was suspended between the brass blocks, it was heated by sending an electric current through it while in air in order to strengthen the oxide film. The vessel containing the suspended wire was then filled with nitrogen and placed in an electric furnace. The inlet and outlet tubes for nitrogen were closed with porous asbestos plugs which permitted the gas to remain constantly at atmospheric pressure. The temperature of the furnace was measured by a nickel-chromium thermocouple, which was inserted into the container through an asbestos filled tube, so that it registered the temperature in the vicinity of the wire being investigated.

The thermal e.m.f. and the potential drop across the suspended wire were measured by means of potentiometers. A single potentiometer was used to control the current through the heated wire and to measure the potential drop across the wire in order to make the manipulation more convenient. The current was 1/100 of the magnitude of the e.m.f. of the standard cell since the standard resistance used was 100 ohms. The current through the heated wire was 10.19 milliamperes and was kept constant to within 1/100 of a milliampere. The resistance with the current in both directions was determined in order to eliminate thermal e.m.f. which were found to be very small.

## Materials

The lead and tin wires were 14.764 cm in length and 0.75 mm in diameter. The dimensions of the zinc wire were 14.923 cm in length and 0.75 mm in diameter. The nonannealed bismuth wire was 5.239 cm in length and 0.74 mm in diameter, and the annealed bismuth wire was 5.412 cm in length and 0.81 mm in diameter. The wires used were obtained from Baker and Company, Inc., and their chemical analyses were as follows:

C. P. Lead—Gold, arsenic, antimony, copper = minute traces; no bismuth.

| | | | |
|---|---|---|---|
| C. P. Tin — | Lead | = 0.007% | iron = 0.002% |
| | copper | = 0.003 | arsenic and sulphur, |
| | tin | = 99.988 | traces each. |
| C. P. Zinc — | Iron | = 0.005% | cadmium = 0.0018% |
| | lead | = 0.0004 | arsenic and sulphur, |
| | zinc | = 99.993 | traces each. |

C. P. Bismuth—Better than 99.9% bismuth.

## Reliability of the Method

To one unfamiliar with the ability of an oxide coat to retain the shape of a molten metal, the reliability of the method may seem open to question. Careful experiments were made in passing from the liquid to the solid and back to the liquid state, which convinced the authors that the oxide film was dependable as a container. For example, the resistivity of liquid bismuth at the melting point was found to be 124.070 microhm-cm. It was then solidified and brought back to the melting point when its resistivity was 124.192 microhm-cm. In the case of tin, readings were taken on increasing and decreasing temperatures for two samples of different lengths cut from the same wire. Both samples were twice taken from room temperature to the melting point and back. The resistivities of the first sample as measured in the liquid state at the melting point were 47.22 and 47.25 microhm-cm. For the second sample the values were 47.25 and 47.20 microhm-cm. These values check to approximately 0.1 percent which is well within the experimental error.

Fig. 2 shows curves for tin on increasing and decreasing temperatures in the neighborhood of the melting point. The curve $AB$ is for increasing temperature after the wire had been previously liquefied and slowly cooled to room temperature. The rounding of the curve preceding the melting point would indicate a gradual change in structure which has not been emphasized by previous experimenters. That this is not due to possible impurities in the

metal seems evident from the fact that the point $B$ at which the slope of the curve suddenly changes, checks, within the degree of accuracy of the experiments, exactly the melting point of tin, 231.9°C. This was true in the case of tin for all four of the determinations mentioned above, and in the case of all other metals the agreement was very close.

With decreasing temperature, the curve of Fig. 2 falls slightly from $B$ to $C$ indicating a supercooling of the metal. The point $C$ was carefully determined and found in this case to be slightly above 223°C. In several determinations made on tin the average value for the supercooling was 9°C. A similar supercooling was found for bismuth, but no tests were made for lead and zinc. With

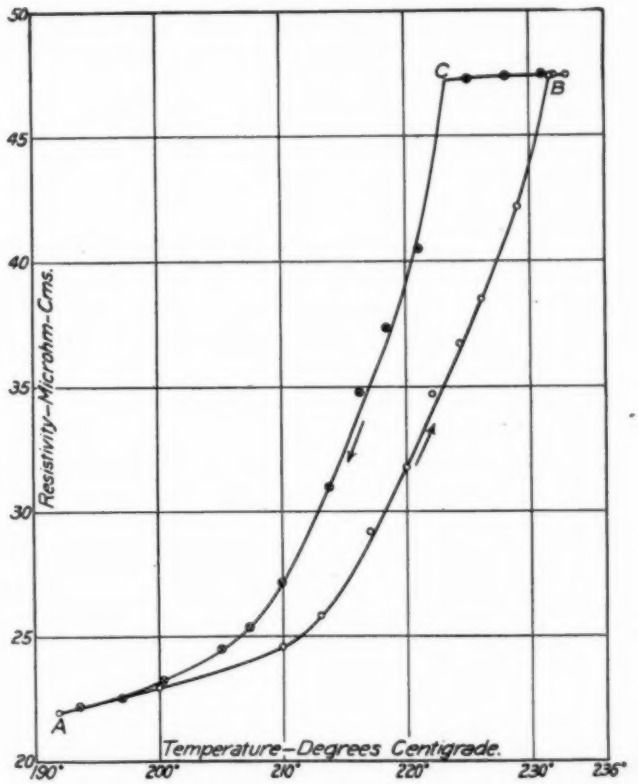


Fig. 2. Resistivity-temperature curves for tin in melting point region.

decrease in temperature below the point $C$, the curve falls rapidly but not suddenly to meet the curve $AB$. This "setting" of a metal is a phenomenon of common observation though its effect upon resistivity has hitherto apparently not been mentioned. As yet no careful observations have been made upon this lag in change of resistivity with different rates of cooling. The readings plotted in Fig. 2 were made with the furnace cooling at the rate of approximately six degrees per hour.

In order to use an oxide film as a container in measuring resistivities of metals through the solid and liquid states, it is necessary that a good film be formed and that the temperature be changed very slowly in passing from one

state to the other. In the liquid state the metal must not be disturbed, and because of the supercooling referred to above the method is better adapted to readings made with increasing than with decreasing temperatures. Further, with decreasing temperatures a non-oxidizing gas must be constantly forced into the furnace with danger of disturbing the temperature equilibrium. The data which follow have in all cases been taken with increasing temperatures.

## Corrections

Corrections were made in the resistivities of the metals for the expansions of the metals as the temperature was increased. Below the melting points the radial and longitudinal expansions of the wires are the same per unit of length. From a consideration of the volume coefficients of expansion of the metals it is found that for each 20°C interval the resistivities obtained below the melting points should be increased by the following amounts: lead, 0.058%; tin, 0.054%; zinc, 0.060%; and bismuth, 0.027%.

The dimensions of the brass blocks and that of the porcelain supporting plane were such, between the points of contact, as to neutralize one another's effects on the length of the bismuth wires as the temperature was increased. This factor was not considered in the case of the other three wires since they were bent in the shape of an *S* and were not affected by such a factor. Because of the close checks on resistivities indicated in the previous section it seems logical to assume that the oxide film acts as an elastic membrane. Thus when the volume changes in passing through the melting point and above the melting point, corrections are made assuming that the films are isotropic and therefore that the radial expansion is twice the longitudinal expansion per unit of length. For an elastic membrane this is apparent from a consideration of Fig. 3. If a membrane in the form of a right circular cylinder of

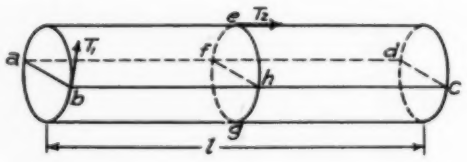


Fig. 3.

radius $r$ and length $L$ is under a tension due to an internal pressure, $p$, in the liquid which it contains, the force on the section *abcd*, when in equilibrium, is $2rLp=2T_1L$ from which the tension, $T_1$, in the film per unit length, tangent to the circumference of the circular cylinder, is $T_1=rp$. Also the force on the circular section, *efgh*, is $\pi r^2p=2\pi rT_2$ from which the tension, $T_2$, in the film per unit length, in the longitudinal direction, is $T_2=rp/2$. Thus since the change in $T_1$ is twice as great as that in $T_2$ for a given increment in $p$ it follows as stated above that the radial and longitudinal strains are in the same ratio.

Considering the expansion of lead[2] 0.0348 cc per cc, the expansion of tin[2] 0.0310 cc per cc, the contraction of bismuth[2] 0.0330 cc per cc, and the ex-

[2] G. Vicentini and D. Omodei, Atti. Acad. Torino **23**, 38 (1888).

pansion of zinc[3] 0.0692 cc per cc, the following corrections were made in the resistivities above the melting points due to the change in volumes in passing through the melting points: lead, an increase of 2.075%; tin, an increase of 1.852%; bismuth, a decrease of 1.925%; and zinc, an increase of 4.129%. Taking for each 20°C interval the expansion of molten lead[2] 0.00232 cc per cc, the expansion of molten tin[4] 0.00197 cc per cc, the expansion of molten bismuth[5] 0.00240 cc per cc, and the expansion of molten zinc[6] 0.00176 cc per cc, the following corrections were made for each 20°C interval above the melting points due to the change in volume in passing through the interval: lead, 0.139% increase; tin, 0.118%; bismuth 0.114%; and zinc, 0.106%.

The electrical resistivity of the oxides of these metals as given by Friedrich[7], Sommerville[8] and Horton[9] is more than $10^{10}$ times the resistivity of the metals. Thus the resistivity correction for the metallic oxide film is negligible in every case. The thickness of the oxide film is such that it falls within the limits of the experimental error in the measurement of the diameter of the wire. These are distinct advantages of the oxide film method of measuring the resistivity of low melting point metals in the liquid state.

## Definition of Resistance-Temperature Coefficient

Various definitions are in use for the resistance-temperature coefficients of metals. The formula which has been much used for expressing the relation between resistance and temperature is:

$$R=R_1(1+a_1(t-t_1)) \tag{1}$$

in which $R_1$ is the resistance at the reference temperature $t_1$, $R$ is the resistance at any temperature $t$, and $a_1$ is the temperature coefficient of resistance for the reference temperature $t_1$. The value of $a_1$ at the temperature $t_1$ depends upon $R_1$, and when the slope of the resistivity-temperature curve is not constant it is also dependent upon the temperature interval $t-t_1$.

The most exact definition of the "temperature coefficient at $t_1$", $a_{t_1}$, is given by the equation:

$$a_{t_1}=(dR/Rdt)_{t_1}. \tag{2}$$

This equation applies to any variation of resistivity with temperature.

The temperature coefficients of resistance given in the present work are defined by the equation:

$$a_{t_1,t_2}=\frac{2(R_2-R_1)}{(R_2+R_1)(t_2-t_1)} \tag{3}$$

[3] M. Toepler, Wied. Ann. **53**, 343 (1894).
[4] A. L. Day, R. B. Sosman, and J. C. Hostetter, Amer. Journ. Sci. [4] **37**, 1 (1914).
[5] E. F. Northrup, Trans. Amer. Electrochem. Soc. **25**, 338 (1914).
[6] P. Pascal and J. Jouniaux, Comptes Rendus **158**, 414 (1914).
[7] E. Friedrich, Zeits. f. Physik **31**, 813 (1925).
[8] A. A. Sommerville, Met. Chem. Eng. **10**, 422 (1912).
[9] F. Horton, Phil. Mag. [6] **11**, 505 (1906).
[10] L. Holborn, Ann. d. Physik **59**, 146 (1919).

in which $R_2$ and $R_1$ are the resistivities respectively at $t_2$ and at $t_1$, and $a_{t_1,t_2}$ is the temperature coefficient of resistance for the temperature interval $t_1$ to $t_2$. This is considered to be a satisfactory approximation of Eq. (2), for 20° intervals in the present work.

## Discussion of the Results

The curves of Fig. 4 are reduced copies of the originals which were drawn on mm cross-section paper, 50×70 cm. This made it possible to read the resistivities to the fourth decimal place and the temperatures to the second decimal place. The resistivity-temperature relations were plotted and from the resulting curves the resistivities were read at the temperatures given in

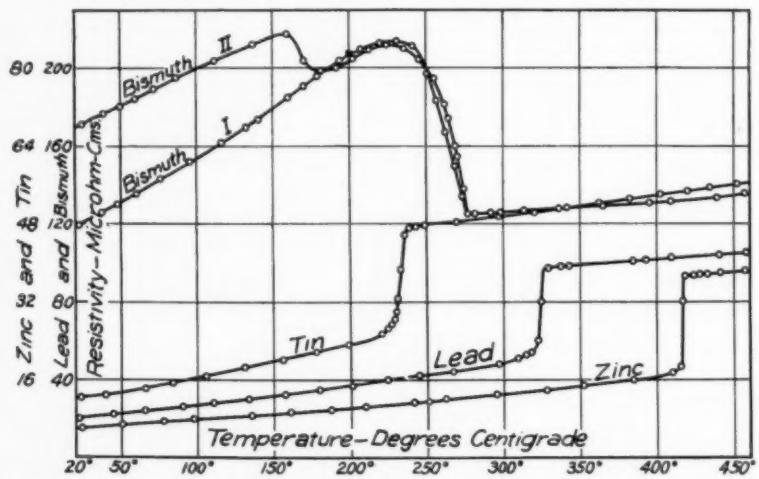


Fig. 4. Resistivity-temperature curves for lead, tin, zinc and bismuth.

the Tables I-IV inclusive. From these resistivity values the temperature coefficients of resistance were calculated for the temperature intervals given in the tables by using Eq. (3). The measurements made on the metals represented in Fig. 4 were extended to above 600°C in most cases, but there was usually a noticeable deviation from a straight line beginning near 500°C. The upper temperature limit was arbitrarily taken as 460°C for each metal in the present work, and this is well within the dependable temperature range for these oxide containers.

The temperature coefficients of resistance possess a higher degree of accuracy than the resistivity values, for they are affected less by any experimental error that might be made in taking the volume measurements of the wires. However, since the wire-lengths were well marked, and the dimensions of the wires were carefully measured, there was little chance for the introduction of an error of appreciable magnitude. The resistance measurements were accurate to within 0.001 percent and the precision of reading the temperature was 0.01°C. The time interval during which the readings for the curves were taken varied from six to nine hours. Several series of readings were made upon different samples of a single metal which showed that the curves were

reproducible to within a fraction of a percent, except for bismuth in the solid state where the variation was somewhat greater. The curves and tables are commented on separately for the different metals.

*Lead.* The curve for lead is slightly convex in the direction of the temperature axis for the solid state, and is a straight line for the liquid state. Table I shows a very good agreement in general with the values of resistivity

TABLE I. *Resistance-temperature coefficients and resistivity of lead.*

| Temp. Range | $a$ | Temp. | Resistivity microhm-cms | Other observers Resistivity | Authority |
|---|---|---|---|---|---|
| 20°– 40°C | 0.00336 | 20°C | 20.648 | 22 | (1) |
| | | | | 20.4 at 0° | (2) |
| 40°– 60° | .00341 | 40° | 22.084 | | |
| 60°– 80° | .00335 | 60° | 23.645 | | |
| 80°–100° | .00332 | 80° | 25.285 | | |
| | | | | 27.97 at 90.35° | (2) |
| 100°–120° | .00311 | 100° | 27.021 | 27.8 | (3) |
| 120°–140° | .00302 | 120° | 28.787 | | |
| 140°–160° | .00299 | 140° | 30.582 | | |
| | | | | 32.79 at 142.7° | (2) |
| 160°–180° | .00293 | 160° | 32.468 | | |
| 180°–200° | .00291 | 180° | 34.413 | | |
| | | | | 36.90 at 196.1° | (2) |
| 200°–220° | .00275 | 200° | 36.478 | 38.0 | (3) |
| 220°–240° | .00273 | 220° | 38.542 | | |
| 240°–260° | .00251 | 240° | 40.697 | | |
| 260°–280° | .00246 | 260° | 42.791 | | |
| 280°–300° | .00322 | 280° | 44.946 | | |
| 300°–320° | .00665 | 300° | 47.938 | | |
| 320°–330° | .0554 | 320° | 54.761 | 50.00 at 319° | (3) |
| 330°–340° | .00116 | 330° | 96.735 | 95.00 at 333° | (3) |
| 340°–360° | .000576 | 340° | 97.867 | | |
| 360°–380° | .000570 | 360° | 99.000 | | |
| 380°–400° | .000577 | 380° | 100.255 | | |
| 400°–420° | .000561 | 400° | 101.418 | 98.30 | (3) |
| 420°–440° | .000559 | 420° | 102.563 | | |
| 440°–460° | .000558 | 440° | 103.716 | 100.55 at 450° | (3) |
| | | 460° | 104.878 | | |

(1) Bureau of Standards, Cir. No. 74, 317 (1918).
(2) J. Dewar and J. A. Fleming, Phil. Mag. **36**, 271 (1893).
(3) E. F. Northrup and V. A. Suydam, Journ. Frank. Inst. **175**, 153 (1913).

as given by other experimenters at certain temperatures. The variation in the resistivity values of lead in the solid state is very regular and there is no indication of an allotropic transformation in the metal.

In order to compare the resistivity-temperature coefficients of lead with those previously given, the value 19.215 microhm-cm was obtained for the resistivity of lead at 0°C by extrapolation. Substituting these values for $R_1$ and $t_1$ and the values 27.021 microhm-cm and 100°C for $R$ and $t$ respectively in Eq. (1), the value $a_{0.100} = 0.00406$ was obtained for lead. The values of $a_{0.100}$ for several observers as given by Holborn,[10] vary from 0.00406 to 0.00422.

*Tin.* The curve for tin is a straight line for the liquid state but deviates from it slightly in the solid state. Table II shows that the value of the resistivity at 20°C is between Dewar and Fleming's value and that given by the Bureau of Standards. Dewar and Fleming's values are higher than the

TABLE II. *Resistance-temperature coefficients and resistivity of tin.*

| Temp. Range | $a$ | Temp. | Resistivity microhm-cms | Other observers Resistivity | Authority |
|---|---|---|---|---|---|
| 20°– 40°C | 0.00365 | 20°C | 12.853 | 11.50 | (1) |
| 40°– 60° | .00355 | 40° | 13.828 | 14.14 at 18.75° | (2) |
| 60°– 80° | .00325 | 60° | 14.845 | | |
| 80°–100° | .00309 | 80° | 15.843 | 18.30 at 91.45° | (2) |
| 100°–120° | .00293 | 100° | 16.842 | | |
| 120°–140° | .00278 | 120° | 17.860 | | |
| 140°–160° | .00273 | 140° | 18.880 | | |
| 160°–180° | .00328 | 160° | 19.940 | 23.63 at 176° | (2) |
| 180°–200° | .00395 | 180° | 21.296 | | |
| 200°–220° | .0178 | 200° | 23.046 | 20.30 | (3) |
| 220°–232° | .0336 | 220° | 31.822 | | |
| 232°–240° | .000787 | 232° | 47.250 | 47.60 at 235° | (3) |
| 240°–260° | .000783 | 240° | 47.580 | | |
| 260°–280° | .000831 | 260° | 48.331 | | |
| 280°–300° | .000827 | 280° | 49.142 | | |
| 300°–320° | .000815 | 300° | 49.961 | 49.44 | (3) |
| 320°–340° | .000804 | 320° | 50.782 | | |
| 340°–360° | .000795 | 340° | 51.506 | 50.76 at 350° | (3) |
| 360°–380° | .000780 | 360° | 52.331 | | |
| 380°–400° | .000771 | 380° | 53.154 | | |
| 400°–420° | .000760 | 400° | 53.980 | 52.00 | (3) |
| 420°–440° | .000748 | 420° | 54.807 | | |
| 440°–460° | .000736 | 440° | 55.633 | 53.30 at 450° | (3) |
| | | 460° | 56.458 | | |

(1) Bureau of Standards, Cir. No. 74, 317 (1918).
(2) J. Dewar and J. A. Fleming, Phil. Mag. **36,** 271 (1893).
(3) E. F. Northrup and V. A. Suydam, J. Franklin Inst. **175,** 153 (1913).

present values and in most cases Northrup and Suydam's are a little less. The variations in the resistivity values of tin are not interpreted as indicating any allotropic transformations in tin between 20° and 220°C. The value $a_{0.100} = 0.00418$ was obtained from Eq. (1) by considering the resistivity of tin at 0°C to be 11.878 microhm-cm. Some values that have been given[10] range from 0.0044 to 0.0047.

*Zinc.* The resistivity-temperature curve for zinc is probably a straight line for the liquid state. The agreement of the resistivities below the melting point with those of other experimenters is good. The value at 415°C is higher than Northrup and Suydam's value at the same temperature, due to the fact that their curve obtained with falling temperature breaks more sharply in this region. At 427°C which is just beyond the melting point their resistivity value, 37.30 microhm-cm agrees well with the value 37.142 microhm-cm, obtained in the present work. Beyond this point their resistivity values decrease for higher temperatures which is just opposite to the results obtained by the writers, as shown in Table III. As Northrup has stated,[11] the negative coefficients of zinc in the molten state have formed a stumbling block in all proposed theories of metallic conduction, and we believe from the present investigation that this difficulty has been removed.

The temperature coefficients of resistance of zinc in the solid state reach a minimum value between 160° and 180°C and between 320° and 340°C. From

[11] E. F. Northrup, Journ. Frank. Inst. **179,** 640 (1915).

TABLE III. *Resistance-temperature coefficients and resistivity of zinc.*

| Temp. Range | $a$ | Temp. | Resistivity microhm-cms | Other observers Resistivity | Authority |
|---|---|---|---|---|---|
| 20°– 40°C | 0.00385 | 20°C | 5.921 | 5.8 | (1) |
| 40°– 60° | .00355 | 40° | 6.395 | 6.2 at 18.8° | (2) |
| 60°– 80° | .00333 | 60° | 6.868 | | |
| 80°–100° | .00312 | 80° | 7.343 | 7.91 at 92.45° | (2) |
| 100°–120° | .00294 | 100° | 7.816 | 7.95 | (3) |
| 120°–140° | .00277 | 120° | 8.289 | | |
| 140°–160° | .00247 | 140° | 8.763 | | |
| 160°–180° | .00221 | 160° | 9.207 | | |
| 180°–200° | .00255 | 180° | 9.622 | 10.37 at 191.5° | (2) |
| 200°–220° | .00270 | 200° | 10.125 | | |
| 220°–240° | .00283 | 220° | 10.687 | | |
| 240°–260° | .00268 | 240° | 11.309 | | |
| 260°–280° | .00242 | 260° | 11.931 | | |
| 280°–300° | .00204 | 280° | 12.523 | | |
| 300°–320° | .00191 | 300° | 13.045 | 13.25 | (3) |
| 320°–340° | .00183 | 320° | 13.559 | | |
| 340°–360° | .00206 | 340° | 14.062 | | |
| 360°–380° | .00253 | 360° | 14.655 | | |
| 380°–400° | .00458 | 380° | 15.417 | | |
| 400°–410° | .00500 | 400° | 16.897 | | |
| 410°–415° | .00533 | 410° | 17.763 | | |
| 415°–423° | .0845 | 415° | 18.243 | 17.00 | (3) |
| 423°–440° | .000625 | 423° | 36.955 | 37.30 at 427° | (3) |
| 440°–460° | .000576 | 440° | 37.349 | 37.20 | (4) |
| | | 460° | 37.783 | 37.08 at 450° | (3) |

(1) Bureau of Standards, Cir. No. 74, 317 (1918).
(2) J. Dewar and J. A. Fleming, Phil. Mag. **36,** 271 (1893).
(3) E. F. Northrup and V. A. Suydam, J. Franklin Inst. **175,** 153 (1913).
(4) L. de la Rive, Comptes Rendus **57,** 698 (1863).

this it may be inferred that there are allotropic transformations in zinc near these regions of minima. By plotting the resistivity values of zinc given in Table III from 20° to 400°C on mm cross-section paper, 60×80 cm, the breaks in the curve become pronounced between 180° and 200°C and between 320° and 360°C. The change is so gradual that no point can be designated with certainty as the point of transition. The data of different resistivity curves show that the greatest changes probably occur at slightly above 180°C and at about 340°C.

The irregularities in the variation of certain properties of zinc with the temperature have led a number of investigators to suspect one or more allotropic transformations of zinc. Le Chatelier[12] found a transition point in zinc between 340° and 350°C from electrical resistance measurements; and Benedicks[13] found two slight breaks in the temperature-resistance curve (a) between 160° and 170°C, and (b) between 320° and 330°C. Monckmeyer[14] and Werner[15] confirmed Le Chatelier's point which has been identified with Benedick's second point. Miss Bingham's work[16] on the electrical resistance of zinc shows a critical point between 200° and 210°C, and between 330° and

[12] H. le Chatelier, Comptes Rend. **3,** 414, 454 (1890).
[13] C. Benedicks, Arkiv. Matem. Astron. Fysik **6,** 24 (1910).
[14] K. Monckmeyer, Zeits. f. anorg. Chem. **43,** 182 (1905).
[15] M. Werner, Zeits. f. anorg. Chem. **83,** 275 (1913).
[16] K. E. Bingham, Journ. Inst. Metals **24,** 333 (1920).

340°C. From her measurements on electrical conductivity, electrolytic potential, density, hardness, and mechanical properties of the metal it is suggested that zinc has three allotropic modifications and that the transition temperatures are about 180°C and 310°C. Pierce, Anderson and Van Dyck[17] conclude, from x-ray diffraction patterns, that within the limits of experimental error, there are no allotropic transformations in zinc in the temperature range 20° to 400°C. The e.m.f. temperature curves of Stockdale,[18] obtained by using electrodes of pure zinc in a special electrolyte, indicate that zinc undergoes a transformation at about 315°C. From a consideration of the existing experimental evidence it seems safe to conclude that there are two allotropic transformations in zinc (a) between 170° and 200°C, and (b) between 310° and 350°C.

The value 5.446 microhm-cm was obtained for the resistivity of zinc at 0°C by extrapolation, and by substituting in Eq. (1) as was done for lead, the value $a_{0.100}=0.00435$ was obtained for the coefficient of zinc. Holborn[10] gives the values of several observers for $a_{0.100}$ for zinc which vary from 0.00402 to 0.00417.

*Bismuth I.* The wire used in obtaining the curve for bismuth I Fig. 4 was well annealed and a microscopic study of the cross-section showed that all crystal orientations* were present. The general outline of this curve agrees well with the one given by Northrup and Suydam with falling temperature and possibly a random crystal orientation. It also agrees well in form with the ones given by Kapitza[19] with falling temperature and with the resistivity measurements made perpendicular or parallel to the cleavage planes. The greatest difference is that their curves break more suddenly at the melting point and have a higher and sharper peak for the solid state near the melting point. Kapitza mentions that some of his curves showed flatter peaks than the ones that he gave. The agreement is very good between the resistivity values given in Table IV and those that have been given by previous experimenters with the exception of the peak values referred to above.

By taking 110.313 microhm-cm for the resistivity of bismuth I at 0°C and substituting in Eq. (1) the value $a_{0.100}=0.00401$ was obtained. The values of some other observers[10] vary from 0.00438 to 0.00458. By taking 112.0 microhm-cm as Northrup and Suydam's value of the resistivity of bismuth at 0°C the value $a_{0.100}=0.00397$ was found. Thus it appears that there is considerable variance in the values of $a_{0.100}$ given by the work of different investigators. The agreement between the value of $a_{0.100}$ given by Northrup and Suydam's work and the one obtained in the present work is well within the limits of the accuracy of the extrapolation.

*Bismuth II.* The curve for bismuth II in Fig. 4 is representative of those that have been obtained in this laboratory with samples of nonannealed bis-

[17] W. M. Pierce, E. A. Anderson and P. Van Dyck, Journ. Frank. Inst. **200**, 349 (1925).

[18] D. Stockdale, Journ. Chem. Soc. **127**, 2951 (1925).

[19] P. Kapitza, Proc. Roy. Soc. **A119**, 358 (1928).

* The angle between the trigonal axis of the crystal and the length of the wire is defined as the orientation.

TABLE IV. *Resistance-temperature coefficients and resistivity of bismuth.*

| Temp. Range | $a$ | Temp. | Resistivity microhm-cms | Other observers Resistivity | Authority |
|---|---|---|---|---|---|
| 20°– 40°C | 0.00311 | 20°C | 119.323 | 120.00 | (1) |
| 40°– 60° | .00320 | 40° | 126.979 | 120.00 at 17.5° | (2) |
| 60°– 80° | .00337 | 60° | 135.382 | 119.00 at 18° | (3) |
| 80°–100° | .00328 | 80° | 144.719 | | |
| 100°–120° | .00293 | 100° | 154.523 | 156.50 | (2) |
| 120°–140° | .00277 | 120° | 163.859 | 160.20 at 100° | (3) |
| 140°–160° | .00321 | 140° | 173.196 | 181.65 at 150° | (2) |
| 160°–180° | .00299 | 160° | 184.866 | | |
| 180°–200° | .00246 | 180° | 196.257 | | |
| 200°–220° | .00164 | 200° | 206.154 | 214.50 | (2) |
| 220°–230° | .000434 | 220° | 212.877 | | |
| 230°–240° | −.000972 | 230° | 213.800 | | |
| 240°–260° | −.01019 | 240° | 211.943 | | |
| 260°–278° | −.01806 | 260° | 172.729 | | |
| 278°–300° | .000322 | 278° | 124.430 | | |
| 300°–320° | .000384 | 300° | 125.316 | 128.90 | (2) |
| 320°–340° | .000405 | 320° | 126.282 | | |
| 340°–360° | .000417 | 340° | 127.310 | 131.55 at 350° | (2) |
| 360°–380° | .000431 | 360° | 128.376 | | |
| 380°–400° | .000467 | 380° | 129.486 | | |
| 400°–420° | .000491 | 400° | 130.711 | 134.20 | (2) |
| 420°–440° | .000570 | 420° | 132.000 | | |
| 440°–460° | .000637 | 440° | 133.513 | 137.00 at 450° | (2) |
| | | 460° | 135.224 | | |

(1) Bureau of Standards, Cir. No. 74, 317 (1918).
(2) E. F. Northrup and V. A. Suydam, J. Franklin Inst. **175**, 153 (1913).
(3) W. Jaeger and H. Diesselhorst, Wiss. Abh. d. Phys. Techn. Reichsanstalt **3**, 269 (1900).

muth. The bismuth II wires were very brittle and would not permit bending while the bismuth I wires were flexible enough to be wound into a spiral. The variation of the resistivity values of the two types of wires was less than one percent in the liquid state. The bismuth referred to by the authors[20] in a previous report was of the type of bismuth II. A study of the discrepancies between the values obtained for the resistivity of bismuth II in the solid state and the values given by other experimenters led to curves of the type of bismuth I which, as already stated, agree well with those given by previous investigators. The wire used for obtaining the curve for bismuth II was drawn by Baker and Company, Inc., and nonannealed wires that were drawn in this laboratory showed similar electrical properties. A microscopic study of the cross-section of bismuth II showed that the crystal orientation was about 0° in the center of the wire and became more and more random towards the circumference of the cross-section. From this one would expect bismuth II to have a higher resistivity than bismuth I in the solid state. It is well known that the resistivity of bismuth is greater along the trigonal axis than across it.

The explanation of the variation of the resistivity of bismuth, when measured in different directions, as due to fissures or cracks between cleavage planes perpendicular to the trigonal axis has come to be pretty generally accepted. Borelius and Lindh[21] seem to believe that most, if not all, of the differences observed between the resistivities of bismuth in different directions

[20] Pietenpol and Miley, Phys. Rev. [2] **33**, 294 (1929).
[21] G. Borelius and A. E. Lindh, Ann. d. Physik **51**, 607 (1916); and **53**, 124 (1917).

are due to fissures and internal stresses. Bridgman[22] attributed the high resistivity observed by different experimenters perpendicular to the cleavage plane to the existence of fissures parallel to the main cleavage plane. Schneider,[23] who finds a high ratio between the resistivities measured perpendicular and parallel to the main cleavage plane, apparently accepts Bridgman's explanation. The high resistivity values recently observed by Bridgman,[24] for specimens in which the bending was known to be severe, are accounted for by means of fissures. Kapitza's reduction of the abnormally high resistivity of some specimens by compression may be referred to as good evidence of the existence of fissures between the cleavage planes. The resistivity values of bismuth measured perpendicular to the main cleavage plane vary from 138 microhm-cm, Bridgman's value when precautions are taken to avoid fissures, to 206 microhm-cm. Kapitza has explained the variation in the resistivity values at a given orientation as due to minute cracks and imperfections in the crystal lattice. The hypothesis suggested to account for the origin of the cracks is a crystalline transformation slightly below the melting point, which gives rise to the cracks during the change of shape that accompanies the transition. Kapitza mentions that the suggestion has been made that the transformation is possibly from the rhombohedral class of the hexagonal system to some class of the cubic system. The present investigation indicates that the region of this allotropic transformation is 160° to 180° C. The experimentally determined point on the curve of bismuth II that is nearest the beginning of this region of negative coefficients is 160.78°C. A transition temperature has been designated as 75°C,[25] 112° and 161°C.[26]

We now believe that there are three factors that contribute to the high resistivity values for bismuth II in the temperature range 20° to 160°C, (a) the crystal orientation referred to above, which approached 0° at the center of the wire, (b) the cracks and imperfections in the crystal lattice which result from rapid cooling of the wire through the region of the allotropic transformation, and (c) the presence of amorphous solid bismuth of abnormal resistivity which may be formed between the contact faces and in the re-entrant angles in addition to the cracks. The fact that the resistivity values of bismuth I and bismuth II are nearly the same for temperatures above 180°C indicates that the factors contributing the high values for bismuth II below 160°C are largely eliminated in passing through the range 160° to 180°C. This is good evidence of an allotropic transformation. Otherwise it would be hard to account for the removal of factor (a) which was observed to be present in bismuth II and not in bismuth I. No break was detected in the curves of bismuth I in passing through the region of the transition. This might be considered as favoring the suggestion that the transformation is from the rhombohedral to some cubical form since such a transition would not be expected to result in a very great change in resistivity.

[22] P. W. Bridgman, Proc. Amer. Acad. Arts and Sci. **60**, 361 (1925).
[23] G. W. Schneider, Phys. Rev. [2] **31**, 251 (1928).
[24] P. W. Bridgman, Proc. Amer. Acad. Arts and Sci. **63**, 351 (1929).
[25] E. Cohen and A. Moesveld, Zeits. f. Phys. Chem. **85**, 419 (1913).
[26] E. Janecke, Zeits. f. Phys. Chem. **90**, 313 (1915).

# ERRORS IN THE USE OF GRATINGS WITH X-RAYS DUE TO THE DIVERGENCE OF THE RADIATION

By H. E. Stauss*
Ryerson Physical Laboratory, University of Chicago

(Received November 14, 1929)

Abstract

The errors in the measurement of x-ray wave-lengths by means of gratings that are to be expected on account of the divergence of the incident beam are considered in more detail than has been done before. In particular, the displacement of the diffracted line, the displacement of the zero order, or reflected, line, the displacement of the center of the incident beam relative to the center of the grating, and the effect of the height of the slits are considered and the expressions for the errors are obtained. These are applied to one of Bearden's spectrograms, and the magnitude of the errors calculated. In this particular case, and apparently in general, the errors are less than other experimental errors.

THE use of plane gratings makes possible the direct determination of x-ray wave-lengths with a high degree of accuracy. Unfortunately, unlike the case in optics, non-parallel radiation must be used with the gratings. It is possible that this condition may introduce errors into the measurements if the ordinary formula for parallel radiation is used in the calculations. One source of error is, as Porter[1] points out, the displacement of the spectrum lines. Bearden,[2] in his measurements of the $K$ lines of copper, finds a discrepancy between his results and Siegbahn's that is greater than the probable error. For the $K_\beta$ line he finds a value of $1.3926 \pm 0.0002$A as compared with 1.3893. Prins[3] thinks that part of the difference may be due to the use of a divergent beam of x-rays. Therefore, it is desirable that a detailed study of the errors that may arise from this cause be made. Two sources of error are to be expected. One is the divergence of radiation in what is assumed to be the plane of incidence, i.e., the plane through the source that is normal to the elements of the grating. The other is the divergence in the plane through the source and the central element of the grating—a plane which is normal to the other one considered.

In connection with the first group of errors, Porter shows that the ordinary grating formula must be replaced by

$$n\lambda = r(\cos\theta_0 - \cos\theta_0')\left(1+\frac{3X^2}{20l_0^2}\right)$$

* National Research Fellow.

[1] A. W. Porter, Phil. Mag. **5**, 1067 (1928).

[2] J. A. Bearden, Proc. Nat. Acad. Sci. **15**, 528 (1929). Similar results have been found by Bäcklin, but the author has not seen a detailed account of his work.

[3] J. A. Prins, Nature **124**, 370 (1929).

where $r$ is the grating space, $\theta_0$ the angle of incidence, $\theta_0'$ that of diffraction, $X$ the length of the grating, and $l_0$ the distance from the source to the grating or from the grating to the point of maximum intensity. This formula is a special case, applicable only when the two lengths mentioned are equal. The general case can be obtained readily, however, by the same methods and with the same assumptions and is

$$n\lambda = r(\cos\theta_0 - \cos\theta_0')\left(1+\frac{3X^2}{20(\theta_0'^2-\theta_0^2)}\left[\frac{\theta_0'^2}{l_2^2}-\frac{\theta_0^2}{l_1^2}\right]\right) \tag{1}$$

where $l_1$ is the distance from the source to the center of the grating and $l_2$ that from the grating to the point of maximum intensity.[4] When $l_2 \neq l_1$, the correction term may be positive or negative, and differs for each line and each order in the spectrum.

The derivation of this formula assumes a point source, which can only be the radiating atom in the target of the x-ray tube. If a slit is considered as a source, the effects due to all parts must be integrated, as in the case of parallel radiation, but the problem is more complex. The errors due to the divergence of the x-rays are so small that there is no reason for developing a new formula.

Eq. (1) shows that the reflected beam, or the line of zero order, will also be displaced if $l_2 \neq l_1$. When the left side is zero, $\cos\theta_0$ cannot equal $\cos\theta_0'$ for then the second factor becomes infinite. Therefore this second term vanishes, or

$$1+\frac{3X^2}{20(\theta_0'^2-\theta_0^2)}\left(\frac{\theta_0'^2}{l_2^2}-\frac{\theta_0^2}{l_1^2}\right)=0$$

This reduces to

$$\theta_0'^2=\theta_0^2\left[1+\frac{3X^2}{20}\left(\frac{1}{l_1^2}-\frac{1}{l_2^2}\right)\right]. \tag{2}$$

When $l_1$ and $l_2$ are greatly different, the displacement of the reflected beam may become important. The displacement may affect the value of $\lambda$ in two ways. The position of the reflected line enters directly into all the angle mea-

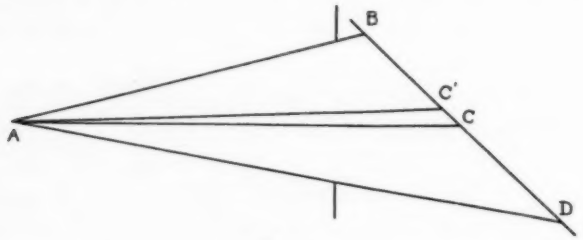


Fig. 1.

surements. It may also enter into the length $l_2$ if this is determined from two exposures at different distances fom the grating. In this case the error in the

[4] This expression is general, but negative values of $n$ must be used for the negative orders.

plate nearer the grating may be considerable, but from the nature of the dependence of $l_2$ upon the measurement of this plate, it is readily seen that a large error in the angle will make only a small error in $l_2$.

The angles used in the previous formulae are measured to the center of the grating. In measuring the photographic plates, the center of the direct beam is used. In cases where slits prevent the beam from covering the grating, the center of the beam and the center of the grating do not coincide. The angle between the two, $CAC'$ in Fig. 1, is readily determined. If $BCA=\theta$, $BC'A=\theta'$, and $BDA=\theta''$

$$BC'=l_1\alpha/\theta' \text{ where } \alpha \text{ is half the slit width}/l_1$$

$$BD=2l_1\alpha/\theta''=2l_1\alpha\left(\frac{1}{\theta'}+\frac{\alpha}{\theta'^2}\right), \text{ since } \theta'=\alpha+\theta''$$

$$BC=BD/2=l_1\alpha\left(\frac{1}{\theta'}+\frac{\alpha}{\theta'^2}\right)$$

$$C'C=BC-BC'=l_1\alpha^2/\theta'^2$$

$$CAC'=CC'\cdot\theta/l_1=\alpha^2\theta/\theta'^2\sim\alpha^2/\theta=s^2/4\theta l_1^2 \qquad (3)$$

where $s$ is the slit-width.

The fact that the source is not a single point, but is extended, will make the diffracted lines asymmetrical because the value of $\theta_0$ will be different for each point in the source. The effect is measured by $d\theta_0'/d\theta_0$ and can be determined accurately enough from the ordinary grating formula, $n\lambda=r(\cos\theta_0-\cos\theta_0')$.

Thus

$$\frac{d\theta_0'}{d\theta_0}=\frac{\sin\theta_0}{\sin\theta_0'}=\frac{\theta_0}{\theta_0'}.$$

For the small values of $d\theta_0$ that are used in practice, the ratio $\theta_0/\theta_0'$ is practically a constant, and hence $d\theta_0'/d\theta_0$ also, and the diffracted beam is symmetrical within the limits of observation.

The second type of divergence, that in a plane through the source and the central element of the grating, involves three-dimensional geometry, and hence the work will only be indicated here. If radiation from a point strikes the grating at a height $h$ above the plane through the point normal to the grating elements, the angle of incidence is $(\theta_0^2+h^2/l^2)^{1/2}$. In the plane of incidence of this beam the grating space is $r/\cos\beta$ where $\beta=h/l_1$. On the photographic plate the angle of diffraction is not measured, but its projection on a plane perpendicular to the lines of the grating. The net result is to produce an error in the wave-length given by

$$n(\lambda'-\lambda)=\frac{r}{2}\left(\frac{\theta_0^2h^2}{2l_1^2}-\frac{\theta_0'^2h'^2}{2l_2^2}\right) \qquad (4)$$

where $h+h'$ is the height of the photographic trace above the source, and $h'$ is $l_2h/l_1$.

The order of these various errors can be determined for Bearden's experiment.[3] In the case of the upper left hand spectrogram in his figure, the spacing of the lines fits approximately the values, $\theta_0 = 0.00247$, $\theta_0' = 0.00459$ for the first order, and $\theta_0' = 0.00988$ for the sixth order. These values seem high, but they will be used. "$l_1$" is about 60 cm and $l_2$ about 215. Then $X$ must be 4 mm. The errors to be expected from Eq. (1) for these figures are $-2.1 \times 10^{-6}$ for the first order and $+1.1 \times 10^{-7}$ for the sixth, or $-0.0002$ % and $+0.00001$ % respectively in the wave-length. The greatest uncertainty in these figures lies in the value of $X$. If this is assumed to be 1 cm instead of 0.4 cm, the errors are increased to $-0.0013$ % and and $+.00007$ %. The error to be expected in $\theta_2$ in Eq. (2) is $3.2 \times 10^{-6} \times \theta$, or 0.0003 % of $\theta$. If $X$ were 1 cm, the error would be 0.0020 %. This latter corresponds to a displacement on the photographic film of 0.0001 mm. The values of $CAC'$ in Eq. (3) is $2.81 \times 10^{-8}$. This represents 0.0006 mm on the photographic film. In order to determine the error due to the divergence in a vertical plane, it will be assumed that the spectrum lines are 1 cm high. The maximum error in $\lambda$ (for the $K_\alpha$ line) is then $-9.66 \times 10^{-14}$ for the first order and $-1.0 \times 10^{-13}$ for the sixth, or errors in $\lambda$ of 0.0006 % and 0.0007 % respectively. The actual errors are less because any point on a spectrum line receives radiation from a large part of the source. It is evident that in this particular experiment all the errors considered above are less than other experimental errors and are negligible in their effect upon the accuracy of the experiment. It would seem, although it cannot be dogmatically stated to be always true, that in most cases the errors due to assuming the formula for parallel radiation are less than the experimental errors of measurement.

# THE EMPIRICAL CALCULATION OF THE FUGACITIES IN GASEOUS MIXTURES. II. ITS RELATION TO THE TANGENTS ON CERTAIN THERMODYNAMIC DIAGRAMS. APPROXIMATE EQUATIONS FOR SOME IMPORTANT THERMODYNAMIC PROPERTIES OF GAS MIXTURES*

By Louis J. Gillespie

(Received November 12, 1929)

Abstract

The thermodynamic account of the behavior of mixtures of real gases at constant temperature may be resolved into two problems: (1) The $p$-$v$-$T$ relationships for pure gases, as embraced in equations of state; and (2) The behavior of gases on mixing at constant temperature and volume, as expressed for example by the excess $\bar{v}_1 - v_1$ of the partial molal volume of a gas in the mixture over its volume when pure at the temperature and pressure of the mixture. In part 1 it was shown that the limiting value of $\bar{v}_1 - v_1$ at zero pressure is finite and positive and can be calculated with considerable success by a linear combination of constants previously tested at higher pressures. We are consequently in a position to calculate the limiting value of the tangents in certain thermodynamic diagrams, and equations are here given for so doing. These include a group of functions of the energy, entropy, heat content, and the $t$–$p$ and $t$–$v$ thermodynamic potentials, as well as a smaller group of functions of the fugacity and equilibrium pressure. The former group takes advantage of the resolution into two problems mentioned above. It is a noteworthy result that their limiting tangents depend only on the cohesive pressure $A$ term of the equation of state. From the limiting values of the tangents there have been derived, by approximate integration, equations explicit in the pressure for the change of energy, entropy, heat content, $t$–$p$ and $t$–$v$ thermodynamic potentials on mixing gases at constant temperature and pressure. From a consideration of the relative accuracy of calculation demanded in the two parts of the resolution it is believed that these approximate equations should furnish, in connection with adequate equations of state, satisfactory thermodynamic calculations for pressures not too high. It is shown that the variation of the mass action function $K_p$ with composition at constant temperature and pressure depends at low pressures chiefly on the cohesive pressure $A$ constants of the gases involved.

## Introduction

THE functions $(f_1/f_p x_1)$ and $(f_1/px_1)$, in which $f_1$ is the fugacity of a gas in a mixture, $p$ the total pressure of the mixture, $x_1$ the mole fraction of gas 1 and $f_p$ is the fugacity of the pure gas 1 at the same temperature and total pressure of the mixture, are of considerable convenience, since each function does not differ greatly from unity at reasonably low pressures (especially the former) and approaches it as a limit as the pressure approaches zero. Plots of the former with the total pressure as the independent variable have been given by Gibson and Sosnick[1] and by Merz and Whittaker[2] and of

* Contribution from the Research Laboratory of Physical Chemistry, Massachusetts Institute of Technology, No. 221.

[1] Gibson and Sosnick, Jour. Amer. Chem. Soc. **49**, 2172 (1927).

[2] Merz and Whittaker, Jour. Amer. Chem. Soc. **50**, 1522 (1928).

the latter by Gibson and Sosnick and by Randall and Sosnick.[3] The tangent of the plot is related to the partial molal volume ($\bar{v}_1$) of the gas 1 in the mixture and to the molal volume ($v_1$) of the pure gas 1 at the temperature and total pressure $p$ of the mixture, in the case of plots of the first function; and to ($v_1$) and ($RT/p$) in the case of plots of the second function.

Evidence was presented in part I[4] that ($\bar{v}_1 - v_1$) does not vanish with the pressure, and that the limiting value at zero pressure is finite and positive under the experimental conditions so far obtaining, and finally that this limiting value can be reasonably well calculated without the aid of any data on mixtures by the use of "linear combination of constants" to form an equation of state for the binary mixture. This evidence is based on data for 12 mixtures, involving 6 gases in 4 binary combinations. The temperature was not the same for all mixtures and the reduced temperatures of the various gases were naturally different even at the same temperature.

Previous study of the pressure data for mixtures of nitrogen and methane of Keyes and Burks[5] by them and by Beattie[6] had already shown linear combination valid for these mixtures at relatively high pressures. These data were for three mixtures, two of which differed considerably in composition, and for a temperature range from 0 to 200°. Lurie and Gillespie[7] had also found linear combination satisfactory for certain mixtures of nitrogen and ammonia at 45°.

It appears safe therefore to use this linear combination to calculate the limiting value at zero pressure of the quantity ($\bar{v}_1 - v_1$) and nearly as safe to calculate its temperature coefficient at constant pressure with due regard to the reduced temperatures of the gases in question. Since the relation between ($v_1$) and ($RT/p$) is given by the equation of state for a pure gas, we can equally well calculate the quantity ($v_1 - RT/p$) and its temperature coefficient if desired.

Rigorous equations will be given, by means of which we can calculate from ($\bar{v}_1 - v_1$) and its derivative the tangents on other diagrams, in which for instance the increase of entropy ($\bar{S}_1 - S_1$), of heat content, or of free energy is plotted as a function of the pressure. Some of these diagrams should prove to be important as the application of thermodynamics to real gases is further extended.

It is a fortunate circumstance for the application of thermodynamics to gaseous equilibria that it is not usually necessary to know the quantity ($\bar{v}_1 - v_1$) to a high degree of precision. Indeed, equating it to zero is equivalent[8] to the fugacity rule of Lewis and Randall,[9] which constitutes a major improvement on the mass action law of ideal gases, when evaluated by means of accurate pressure data for the individual gases.

[3] Randall and Sosnick, Jour. Amer. Chem. Soc. **50**, 967 (1928).
[4] Gillespie, Phys. Rev. **34**, 352 (1929).
[5] Keyes and Burks, Jour. Amer. Chem. Soc. **50**, 1100 (1928).
[6] Beattie, Jour. Amer. Chem. Soc. **51**, 19 (1929).
[7] Lurie and Gillespie, Jour. Amer. Chem. Soc. **49**, 1146 (1927).
[8] Gillespie, Jour. Amer. Chem. Soc. **47**, 305 (1925).
[9] Lewis and Randall, "Thermodynamics," McGraw-Hill Book Co., New York, (1923).

It seems useful to present in section 5 some approximate equations for use at low pressures, based on the evaluation of $(\bar{v}_1-v_1)$ and its temperature coefficient by means of linear combination. In the following section, No. 6, some approximate equations based on $(v_1-RT/p)$ are given because of their particular usefulness, though the approximations made in the integrations have a greater final effect on the accuracy.

## 2. Tangents Which Directly Involve $(\bar{v}_1-v_1)$ With or Without its Temperature Coefficient

For the tangent on the plot of $\ln (f_1/f_p x_1)$ against the pressure we have the exact relation (1), which can be obtained by differentiation of equation 2 of part 1.

$$\left(\frac{\partial \ln (f_1/f_p x_1)}{\partial p}\right)_{Tx} = (\bar{v}_1-v_1)/RT. \tag{1}$$

The subscript $x$ denotes constancy of composition.

Equation (1) leads to equation (2):

$$\left(\frac{\partial (f_1/f_p x_1)}{\partial p}\right)_{Tx} = \frac{\bar{v}_1-v_1}{RT}\,\frac{f_1}{f_p x_1}. \tag{2}$$

The function $(f_1/f_p x_1)$ approaches unity as the pressure approaches zero; $(\bar{v}_1-v_1)$ approaches a finite value not zero; hence

$$\text{Limit}\left(\frac{\partial (f_1/f_p x_1)}{\partial p}\right)_{Tx\,p\doteq 0} = (\bar{v}_1-v_1)/RT \tag{3}$$

Now the plots of this function already published for binary mixtures of argon and ethylene[1] do not clearly show tangents differing from zero at the origin. This is partly due to the scale on which they are drawn and partly to the fact that the plotted values were computed under an assumption equivalent to making $(\bar{v}_1-v_1)$ vanish with the pressure. Similar plots for nitrogen and hydrogen[2] show tangents clearly differing from zero at the origin although the plotted quantities were calculated from a preliminary graph on which the extrapolation to zero pressure was made in a manner equivalent to the assumption that $(\bar{v}_1-v_1)$ vanishes. This inconsistency produces inflections in the published curves at low pressures, which inflections disappear when $(\bar{v}_1-v_1)$ is properly smoothed in the preliminary graph.

In order to pass over to a consideration of the entropy changes on mixing and changes of other thermodynamic functions corresponding to the volume change $(\bar{v}_1-v_1)$ we use the equations of Gibbs

$$\left(\frac{\partial \mu_1}{\partial p}\right)_{Tx} = \bar{v}_1 \quad \text{and} \quad \left(\frac{\partial \mu_1}{\partial T}_{px}\right) = -\bar{S}_1 \tag{4}$$

where the use of the bar and subscript is extended to other quantities, in the manner of Lewis and Randall,[9] indicating the operation $(\partial/\partial n_1)_{tpn_2n_3\cdots}$.

Let the subscript 1 refer to the gas in the mixture whose total pressure is $p$. Let the subscript $1p$ refer to 1 mole of pure gas at the total pressure $p$. Then we shall write $(\bar{v}_1-v_{1p})$ instead of simply $(\bar{v}_1-v_1)$. We shall have

$$\left(\frac{\partial \mu_{1p}}{\partial p}\right)_T = v_{1p} \quad \text{and} \quad \left(\frac{\partial \mu_{1p}}{\partial T}\right)_p = -S_{1p} \tag{5}$$

where $v_{1p}$ and $s_{1p}$ are the volume and entropy of a mole of pure gas at the pressure $p$ and the temperature $T$. From equations (4) and (5) we obtain equations

$$\left(\frac{\partial(\mu_1-\mu_{1p})}{\partial p}\right)_{Tx} = \bar{v}_1-v_{1p} \quad \text{(6a)} \quad \text{and} \quad \left(\frac{\partial(\mu_1-\mu_{1p})}{\partial T}\right)_{px} = -(\bar{S}_1-S_{1p}). \quad \text{(6b)}$$

Since all the symbols represent functions of the state of the system (without reference to the path) we may equate the second partial derivatives of the form $\partial^2/\partial p \partial T$.

Hence

$$(\partial/\partial p)_{Tx}(\bar{S}_1-S_{1p}) = -(\partial/\partial T)_{px}(\bar{v}_1-v_{1p}). \tag{7}$$

This equation gives the tangent on the diagram obtained by plotting against the pressure what we may call the increase of entropy experienced by a gas on being introduced into a mixture.

For the "heat content" $H(=U+pV)$ we use the relation which defines the $t, p$-potential $\phi$, namely $\phi = U+pV-TS = H-TS$.
By differentiation we obtain

$$\phi_1 = \mu_1 = \bar{H}_1 - T\bar{S}_1$$

whereas

$$\phi_{1p} = \mu_{1p} = H_{1p} - TS_{1p}.$$

Hence

$$(\bar{S}_1-S_{1p}) = [\bar{H}_1-H_{1p}-(\mu_1-\mu_{1p})](1/T) \tag{8}$$

Differentiation with respect to pressure gives

$$\begin{aligned}(\partial/\partial p)_{Tx}(\bar{S}_1-S_{1p}) &= [(\partial/\partial p)_{Tx}(\bar{H}_1-H_{1p})-(\partial/\partial p)_{Tx}(\mu_1-\mu_{1p})](1/T)\\ &= [(\partial/\partial p)_{Tx}(\bar{H}_1-H_{1p})-(\bar{v}_1-v_{1p})](1/T).\end{aligned}$$

By comparison with equation (7) we obtain the relation desired

$$(\partial/\partial p)_{Tx}(\bar{H}_1-H_{1p}) = (\bar{v}_1-v_{1p}) - T(\partial/\partial T)_{px}(\bar{v}_1-v_{1p}). \tag{9}$$

For the energy $(U)$ we apply a similar procedure to the defining relation

$$H = U+pV.$$

From this we obtain first

$$\bar{H}_1 = \bar{U}_1 + p\bar{v}_1 \quad \text{and} \quad H_{1p} = U_{1p} + pv_{1p}$$

from which equations we obtain

$$\overline{U}_1 - U_{1p} = \overline{H}_1 - H_{1p} - p(\bar{v}_1 - v_{1p}) \tag{10}$$

and

$$(\partial/\partial p)_{Tx}(\overline{U}_1 - U_{1p}) = (\partial/\partial p)_{Tx}(\overline{H}_1 - H_{1p}) - p(\partial/\partial p)_{Tx}(\bar{v}_1 - v_{1p}) - (\bar{v}_1 - v_{1p}) .$$

Comparison with equation (9) gives

$$(\partial/\partial p)_{Tx}(\overline{U}_1 - U_{1p}) = -p(\partial/\partial p)_{Tx}(\bar{v}_1 - v_{1p}) - T(\partial/\partial T)_{px}(\bar{v}_1 - v_{1p}) . \tag{11}$$

At zero pressure the first term of the right-hand member vanishes, since the data show that the derivative is finite; but not necessarily the second, leaving

$$\text{Limit}_{p=0} (\partial/\partial p)_{Tx}(\overline{U}_1 - U_{1p}) = -T(\partial/\partial T)_{px}(\bar{v}_1 - v_{1p}) . \tag{12}$$

For the Helmholtz free energy ($W$) ($= U - TS$) we obtain

$$\overline{W}_1 = \overline{U}_1 - T\overline{S}_1 \quad \text{and} \quad W_{1p} = U_{1p} - TS_{1p} .$$

From these equations we find

$$\overline{W}_1 - W_{1p} = \overline{U}_1 - U_{1p} - T(\overline{S}_1 - S_{1p}) \tag{13}$$

$$(\partial/\partial p)_{Tx}(\overline{W}_1 - W_{1p}) = (\partial/\partial p)_{Tx}(\overline{U}_1 - U_{1p}) - T(\partial/\partial p)_{Tx}(\overline{S}_1 - S_{1p})$$

and by the use of equations (7) and (11) this is reduced to

$$(\partial/\partial p)_{Tx}(\overline{W}_1 - W_{1p}) = -p(\partial/\partial p)_{Tx}(\bar{v}_1 - v_{1p}) \tag{14}$$

which vanishes at zero pressure. The Helmholtz free energy is the only one of the functions under consideration for which the change approaches asymptotically its value at zero pressure.

## 2. A Equations for the Evaluation of the Tangents at Zero Pressure by Means of Linear Combination

These equations are here set down without proof, as their derivation is tedious and involves only calculus and algebra without addition of physical principles.

For mixtures containing any number of constituents, 1 to $n$, we have

$$\text{Limit}_{p=0} (\bar{v}_1 - v_{1p}) = (A_1^{1/2} - \Sigma x_1 A_1^{1/2})^2 (1/RT) \tag{15}$$

$$\text{Limit}_{p=0} (\partial/\partial T)_{px}(\bar{v}_1 - v_{1p}) = -(A_1^{1/2} - \Sigma x_1 A_1^{1/2})^2 (1/RT^2) . \tag{16}$$

For binary mixtures the relations are:

$$\text{Limit}_{p=0} (\bar{v}_1 - v_{1p}) = x_2^2 (A_1^{1/2} - A_2^{1/2})^2 (1/RT) \tag{17}$$

$$\text{Limit}_{p=0} (\partial/\partial T)_{px}(\bar{v}_1 - v_{1p}) = -x_2^2 (A_1^{1/2} - A_2^{1/2})^2 (1/RT^2) . \tag{18}$$

These values can be substituted into equations (1), (3), (6a), (7), (9) and (12), thus giving limiting values of the tangents for use in the extrapolation

of data to zero pressure. Of the constants in the equations of state (for the pure gases) of Keyes or of Beattie and Bridgeman only the cohesive pressure constant $A$ is necessary. The values of $A$ given in tables are often calculated from critical data, as is the case in the Landolt-Börnstein Tabellen, and should not be used, as such constants from critical data do not correctly represent pressure data when used in van der Waal's equation. The second virial coefficient, commonly denoted by the letter $B$, should not be used, as it is an involved function of the equation of state constants.*

### 3. Transformation of the Results to the Integral Effect on Mixing

Whenever we are interested in the total increase ($I$) of a thermodynamic function ($Z$) which takes place when $x_1$ moles of gas 1, $x_2$ moles of gas 2, $x_3$ moles of gas 3, etc., are mixed at constant pressure and temperature to form 1 mole of mixture we may use the general relation

$$I=\Sigma x_1\overline{Z}_1-\Sigma x_1 Z_{1p}=\Sigma x_1(\overline{Z}_1-Z_{1p}).$$

Then

$$(\partial I/\partial p)_{Tx}=\Sigma\left[x_1(\partial/\partial p)_{Tx}(\overline{Z}_1-Z_{1p})\right].$$

The tangent, $\partial I/\partial p$, can then be found as a sum of terms involving $(\bar{v}_1-v_1)$ plus a sum of terms involving its temperature coefficient. The limiting value of the tangent at zero pressure can also be found by then evaluating the sums by the use of the following relations.

For mixtures containing any number of constituents, from 1 to $n$;

$$\operatorname*{Limit}_{p=0}\Sigma\left[x_1(\bar{v}_1-v_{1p})\right]=\left[\Sigma x_1A_1-(\Sigma x_1A_1^{1/2})^2\right](1/RT) \tag{19}$$

$$\operatorname*{Limit}_{p=0}\Sigma\left[x_1(\partial/\partial T)_{px}(\bar{v}_1-v_{1p})\right]=-\left[\Sigma x_1A_1-(\Sigma x_1A_1^{1/2})^2\right](1/RT^2) \tag{20}$$

And for binary mixtures;

$$\operatorname*{Limit}_{p=0}\Sigma\left[x_1(\bar{v}_1-v_{1p})\right]=x_1x_2(A_1^{1/2}-A_2^{1/2})^2(1/RT) \tag{21}$$

$$\operatorname*{Limit}_{p=0}\Sigma\left[x_1(\partial/\partial T)_{px}(\bar{v}_1-v_{1p})\right]=-x_1x_2(A_1^{1/2}-A_2^{1/2})^2(1/RT^2) \tag{22}$$

### 4. Limiting Values of Some Important Functions at Zero Pressure

The values of $(\overline{U}_1-U_{1p})$ and $(\overline{H}_1-H_{1p})$ for real gases at zero pressure may be safely taken as zero as in the theory of ideal gases. The quantities $S$, $\mu$, and $W$ become infinite at zero pressure and a further hypothesis is necessary to show that differences of the type $(\overline{S}_1-S_{1p})$ become at zero pressure equal to the ideal gas values. If this is true of one of the differences it can be shown true of the others by the use of equations (8) and (13). The necessary

* This has very recently been discussed by W. E. Deming and L. E. Shupe, Jour. Franklin Inst., **208**, 389 (1929).

hypothesis was made however in the deduction of equation (2) of part 1, when a certain form of Dalton's law was assumed applicable to real gases at zero pressure. This equation reads, if we transform fugacities into chemical potentials:

$$\mu_1-\mu_{1p}=RT\ln x_1+\int_0^p(\bar{v}_1-v_{1p})dp. \tag{23}$$

We obtain directly

$$\underset{p=0}{\text{Limit}}\ (\mu_1-\mu_{1p})=RT\ln x_1 \tag{24}$$

From equation (8) we obtain

$$\underset{p=0}{\text{Limit}}\ (\bar{S}_1-S_{1p})=-R\ln x_1 \tag{25}$$

which is a positive quantity, and from equation (13) we finally obtain

$$\underset{p=0}{\text{Limit}}\ (\overline{W}_1-W_{1p})=RT\ln x_1. \tag{26}$$

For completeness let us repeat that the limiting value of $(f_1/f_p x_1)$ at zero pressure is unity.

### 5. Approximate Equations for the Functions at Low Pressures

We may obtain an approximate equation, which should be useful at reasonably low pressures, for the value of any of the above functions in terms of the pressure, temperature, composition, and the cohesive pressure ($A$) constants. This may be done by an integration in which the tangent is assumed constant and equal to the limiting value given in section 2A and for which the integration constant is the limiting value of the function at zero pressure. The latter value is given in section 4.

The equations for binary mixtures only are given below. In the first equation (27) a further approximation is made: that the ratio $(f_1/f_p x_1)$ remains unity over the pressure range. This is not assumed for the second equation (28).

Fugacity
$$f_1/f_p x_1=1+x_2^2\frac{(A_1^{1/2}-A_2^{1/2})^2}{(RT)^2}p \tag{27}$$

Fugacity
$$\ln(f_1/f_p x_1)=x_2^2\frac{(A_1^{1/2}-A_2^{1/2})^2}{(RT)^2}p \tag{28}$$

Chemical potential or partial moral free energy
$$\bar{\phi}_1-\phi_{1p}=\mu_1-\mu_{1p}=RT\ln x_1+x_2^2\frac{(A_1^{1/2}-A_2^{1/2})^2}{RT}p \tag{29}$$

Entropy
$$\bar{S}_1-S_{1p}=-R\ln x_1+x_2^2\frac{(A_1^{1/2}-A_2^{1/2})^2}{RT^2}p \tag{30}$$

Energy
$$\bar{U}_1-U_{1p}=x_2^2\frac{(A_1^{1/2}-A_2^{1/2})^2}{RT}p \tag{31}$$

Heat content $$\overline{H}_1 - H_{1p} = 2x_2^2 \frac{(A_1^{1/2} - A_2^{1/2})^2}{RT} p \tag{32}$$

Helmholtz free energy $$\overline{W}_1 - W_{1p} = RT \ln x_1 . \tag{33}$$

## 6. Approximate Equations for Some Functions whose Tangents Depend upon $(\bar{v}_1 - RT/p)$.

From the value of $(\bar{v}_1 - RT/p)$, tangents can be found for functions of the form $(\mu_1 - \mu_i)$ in which $\mu_i$ occurs instead of $\mu_{1p}$ and represents the value of $\mu$ for an ideal gas at the pressure $p$ of the mixture, i.e., the value that would be calculated for the pure gas 1 at the pressure $p$ by assuming $pV = RT$ for the integrations.

For this purpose equation (3) of part 1 is available: which is in terms of chemical potentials;

$$\mu_1 - \mu_i = \int_0^p (\bar{v}_1 - RT/p) dp .$$

The nature of the operations is such that in any of the equations of section 2 the subscripts $_{1p}$ may be replaced with the subscript $_i$ if $v_1$ is replaced with $RT/p$.

If approximate equations are derived from such tangents by integrating at constant ordinate the effect of the inaccuracy is presumably greater than in the previous case, because an approximation is made in the $v_1 dp$ integrals for the pure gases, and these integrals appear to have more importance in the final result than integrals $(\bar{v}_1 - v_1) dp$.

Such equations could be evaluated by means of the relations

$$\text{Limit}_{p=0} (\bar{v}_1 - RT/p) = B_1 - A_1/RT - c_1/T^3 + (A_1^{1/2} - \Sigma x_1 A_1^{1/2})^2/RT \tag{34}$$

wherein $A_1^{1/2} - \Sigma x_1 A^{1/2} = x_2 (A_1^{1/2} - A_2^{1/2})$ for binary mixtures.

There are given below only those approximate equations of this degree of accuracy (or of less) which appear at present to have particular usefulness or convenience.

Equation (3) of part 1 leads to the approximate relation

$$\ln (f_1/px_1) = \frac{\text{Limit} (\bar{v}_1 - RT/p)}{(RT)} p \tag{35}$$

and the less exact relation

$$f_1/px_1 = 1 + \frac{\text{Limit} (\bar{v}_1 - RT/p)}{RT} p \tag{36}$$

Now the function $f_1/px_1$ is intermediate between the function $f_1/f_p x_1$ and the function $p_1/px_1$ in which $p_1$ represents the equilibrium pressure of the gas 1 in the mixture. From equation (30) of Beattie[10] we can derive by approximate integration the following relation

[10] Beattie, Phys. Rev. **32**, 699 (1928).

$$\ln (p_1/px_1)=(B_1-A_1/RT-c_1/T^3)(p-p_1)/RT+(A_1^{1/2}-\Sigma x_1A_1^{1/2})^2p_1/R^2T^2. \quad (37)$$

This can readily be used to calculate the equilibrium pressure $p_1$ (which would in certain applications be the vapor pressure of a liquid under the total pressure of a gas mixture and subject to the lowering of vapor pressure due to dissolved gases). The equation is implicit in $p_1$ but in numerical calculations $p_1$ in the right hand side may be put equal to $px_1$ for the first approximation, and the improved value obtained from the logarithm may then be used for the second approximation, which will probably be the final value, as the convergence is rapid.

A more severe approximation, but one which may be useful when the equation of state constants are known for only gas 1, is obtained by assuming $(\bar{v}_1-v_1)$ constant and also zero. This gives

$$\ln (p_1/px_1)=(B_1-A_1/RT-c_1/T^3)(p-p_1)/RT. \quad (38)$$

A mass action equation derived by approximate integration in this way, and similarly limited by the assumption that $(\bar{v}_1-v_1)$ is zero at all pressures, has served to represent the pressure variation of the Haber equilibrium up to 100 atmospheres.[11]

It was given as

$$\log K_p=\log K_f+\frac{\Sigma(\nu_1A_1)}{2.3R^2T^2}p-\frac{\Sigma(\nu_1\beta_1)}{2.3RT}p$$

for evaluation by means of the Keyes equation of state. A form for either the Keyes or the Beattie-Bridgeman equation is

$$\log K_p=\log K_f-[\Sigma\nu_1(B_1-A_1/RT-c_1/T^3)]p/2.3RT. \quad (39)$$

The constants $A$ and $B$ are given as $A_0$ and $B_0$ by Beattie and Bridgeman, and correspond to the $A$ and $\beta$ of Keyes. For the Keyes equation $c$ may be put equal to zero. $K_f$ is the mass action function of the fugacities, and is a function of the temperature. The $\nu$ is the coefficient in the equation for the chemical reaction when this is written, $\Sigma(\nu_1M_1)=0$, $M$ being the symbol for the element or molecule.

The following mass action equation should be more accurate, since $(\bar{v}_1-v_1)$ is not assumed zero, but merely constant and equal to its limiting value at zero pressure.

$$\log K_p=\log K_f-[\Sigma\nu_1(B_1-A_1/RT-c_1/T^3)+\Sigma\nu_1(A_1^{1/2}-\Sigma x_1A_1^{1/2})^2/RT]p/2.3RT.$$

It is noteworthy that this equation (40) may be written for any definite chemical reaction among gases as follows:

$$\log K_p=F(T,p)-[\Sigma\nu_1(A_1^{1/2}-\Sigma x_1A_1^{1/2})^2]p/2.3R^2T^2. \quad (41)$$

No experiments seem to have been performed at high enough pressures to reveal any variation of $K_p$ with composition at constant $T$ and $p$. In his calculations on the pressure effect in the Haber equilibrium Keyes[12] observed,

[11] Gillespie, Jour. Amer. Chem. Soc. **48**, 28 (1926).

[12] Keyes, Jour. Amer. Chem. Soc. **49**, 1393 (1927).

without reporting the fact, that the composition terms in his mass action equation were small below 100 atmospheres, becoming appreciable in comparison with the other terms at the higher pressures. Considering therefore the state of our experimental knowledge and the evident smallness of the composition effects, equation (41) or (40) should be a valuable mass action equation in the usual sense giving the variation of the equilibrium function $K_p$ with the composition. This variation involves as parameters only the cohesive pressure $A$ constants, and will perhaps be important only when several molecules of some species enter into the reaction, for which species the $A$ constant differs considerably from the mean $A$ constant of the equilibrium mixtures.

Equation (40) can be reduced to an equation given by Keyes[12] (equation (19) ) by putting $c=0$ and rearranging into a form more suitable for numerical computation. It can also be shown consistent with an equation given by Beattie[13] in terms of the volume of the mixture, by expanding the term $\log (pV_m/RT)$ of his equation (22), rejecting higher terms of the expansion and rearranging, and finally putting $p/RT$ for $1/V_m$ as the factor which multiplies the whole pressure coefficient.

TABLE I.

| Gas | $A$ | $B$ | $c$ |
|---|---|---|---|
| Helium | 0.0216 | 0.01400 | $0.004 \cdot 10^4$ |
| Neon | 0.2125 | 0.02060 | $0.101 \cdot 10^4$ |
| Argon | 1.2907 | 0.03931 | $5.99 \cdot 10^4$ |
| Hydrogen | 0.1975 | 0.02096 | $0.0504 \cdot 10^4$ |
| Nitrogen and carbon monoxide | 1.3445 | 0.05046 | $4.20 \cdot 10^4$ |
| Oxygen | 1.4911 | 0.04624 | $4.80 \cdot 10^4$ |
| Air[15] | 1.3012 | 0.04611 | $4.34 \cdot 10^4$ |
| Carbon dioxide and nitrous oxide | 5.0065 | 0.10476 | $66.00 \cdot 10^4$ |
| Methane | 2.2769 | 0.05587 | $12.83 \cdot 10^4$ |
| Ethyl ether | 31.278 | 0.45446 | $33.33 \cdot 10^4$ |
| Ammonia | 2.3930 | 0.03415 | $476.87 \cdot 10^4$ |
| Ethylene | 6.1520 | 0.12156 | $22.68 \cdot 10^4$ |

For convenience suitable constants for $A$, $B$, and $c$ are given in Table I from the papers of Beattie and Bridgeman.[14] The units are atmospheres, liters per mole, and degrees Centigrade absolute ($=273.13+t$). The value of $R$ is 0.08206. Two other constants occur in their equation. These are needed for the calculation of pressures, but occur only as terms of higher order that have been neglected in the approximate equations given above.

[13] Beattie, Phys. Rev. **32,** 691 (1928). Equation (22). It is exactly integrated in terms of the volume.

[14] J. A. Beattie and O. C. Bridgeman, Jour. Amer. Chem. Soc. **50,** 3133 (1928); and **50,** 3151 (1928). In their second paper it was shown that the constants of $N_2$ and $CO_2$ could be used for their isosteres, CO and $N_2O$, respectively, in the calculation of the weight of a normal liter and therefore for other calculations at moderate pressures. The values for ethylene are by L. J. Gillespie, Jour. Physical Chem. **64,** 354 (1929).

[15] The algebra of the combination of constants is such that mixtures of air and one other gas may be treated as binary mixtures in the use of the formulas given in this paper.

# THE HEAT CAPACITIES OF REAL GASES AND MIXTURES OF REAL GASES

By James A. Beattie

(Received November 12, 1929)

Abstract

Simple approximate equations expressing $C_V$ and $C_p$ of gases as functions of $p$ and $T$ are given. They are derived by neglecting all powers of $1/V$ higher than the first and replacing $1/V$ by $p/RT$ in the complete equations for $C_V$ and $C_p$ which are obtained by use of the Beattie-Bridgeman equation of state and which express these quantities as functions of $V$ and $T$. The resulting relation for $C_p$ (Eq. (8)) reproduces the thermal data on air well, and those on ammonia fairly well.

The complete and approximate equations for $C_V$ and $C_p$ of gas mixtures expressing these quantities as functions of $V$ and $T$, and of $p$ and $T$, are given. They are derived by use of the generalized Beattie-Bridgeman equation of state for gas mixtures on the basis of one assumption; that of the additivity of energy of real gases at infinitely low pressures.

## 1. Heat Capacity of Pure Gases

THE molal heat capacities at constant volume $C_V$ and at constant pressure $C_p$ of a gas can be evaluated if either $C_V$ or $C_p$ is given as a function of the temperature for some one density or pressure and if an equation of state for the gas is known. When experimental measurements of the heat capacity of a gas over a range of pressures are available, this method of calculating the thermal properties gives a valuable check on the accuracy with which the equation of state represents the trends of the compressibility data, especially the variation of the curvature of the isometrics with both temperature and density; when thermal data are given only for low pressures, values for higher pressures can be computed.

Keyes[1] has applied his equation of state to the calculation of $C_V$ for air, carbon dioxide and nitrogen with good success.

Bridgeman[2] and the author[3] have used expressions derived from the Beattie-Bridgeman equation of state[4] to evaluate $C_p$ for air[2] and ammonia.[3] The computed values agree well with the experimental results of Roebuck[5] on air which cover the range from 0° to 280°C and 1 to 220 atmospheres; and fairly well with the measurements of Osborne, Stimson, Sligh and Cragoe[6] on ammonia extending from −30 to 150°C and to 20 atmospheres, the agree-

* Contribution from the Research Laboratory of Physical Chemistry, Massachusetts Institute of Technology, No. 229.

[1] Keyes, Jour. Amer. Chem. Soc. **43**, 1452 (1921); ibid. **46**, 1584 (1924); ibid. **49**, 896 (1927).

[2] Bridgeman, Phys. Rev. **34**, 527 (1929).

[3] Beattie, Jour. of Math. and Physics, M.I.T., (In press).

[4] Beattie and Bridgeman, Proc. Amer. Acad. Arts and Sci. **63**, 229 (1928).

[5] Roebuck, Proc. Amer. Acad. Arts and Sci. **60**, 537 (1925).

[6] Osborne, Stimson, Sligh and Cragoe, Scientific Papers of the Bureau of Standards **20**, 65 (1924).

ment being good above 100°C but increasingly bad as the temperature is decreased below 100°.

The equations for $C_V$ and $C_p$ can be obtained from the usual thermodynamic relations:

$$\left(\frac{\partial C_V}{\partial V}\right)_T = T\left(\frac{\partial^2 p}{\partial T^2}\right)_V \tag{1}$$

$$C_p = C_V + T\left(\frac{\partial p}{\partial T}\right)_V \left(\frac{\partial V}{\partial T}\right)_p. \tag{2}$$

By calculating the partial derivatives of (1) from the Beattie-Bridgeman equation of state and integrating between the limits $V=\infty$ and the variable volume $V$, we obtain:

$$C_V = C_V^* + \frac{Rc}{T^3 V}\left(6 + \frac{3B_0}{V} - \frac{2B_0 b}{V^2}\right). \tag{3}$$

When the partial derivatives of (2) are similarly evaluated and $C_V$ eliminated by use of (3) and the relation

$$C_V^* = C_p^* - R \tag{4}$$

there results:

$$C_p = C_p^* - R + \frac{Rc}{T^3 V}\left[6 + \frac{3B_0}{V} - \frac{2B_0 b}{V^2}\right] + \frac{R[1+(B_0+2c/T^3)/V+(-B_0 b+2B_0 c/T^3)/V^2-2B_0 bc/T^3V^3]^2}{1+2(B_0-A_0/RT-c/T^3)/V+3(-B_0 b+A_0 a/RT-B_0 c/T^3)/V^2+4B_0 bc/T^3V^3} \tag{5}$$

In these expressions $C_V^*$ and $C_p^*$ are the molal heat capacities of the gas at zero pressure; for a given gas they are temperature functions which can be obtained from thermal data on $C_V$ or $C_p$ measured at finite values of $V$ or $p$ and reduced to zero pressure by use of the relations (3) or (5). The quantities $R$, $A_0$, $a$, $B_0$, $b$ and $c$ are parameters occurring in the equation of state, which may be written in the virial form

$$\begin{aligned} pV &= RT + \beta/V + \gamma/V^2 + \delta/V^3 \\ \beta &= RTB_0 - A_0 - Rc/T^2 \\ \gamma &= -RTB_0 b + A_0 a - RB_0 c/T^2 \\ \delta &= RB_0 bc/T^2. \end{aligned} \tag{6}$$

Equations (3) and (5) express $C_V$ and $C_p$ as functions of $V$ and $T$. Simple approximate relations expressing these thermal quantities as functions of $p$ and $T$ can be derived from (3) and (5) by dropping all terms in $1/V$ of higher order than the first and replacing $1/V$ by $p/RT$. There then result:

$$C_V = C_V^* + \frac{6cp}{T^4} \tag{7}$$

$$C_p = C_p^* + \left(\frac{2A_0}{RT^2} + \frac{12c}{T^4}\right)p \tag{8}$$

These relations represent the experimental data surprisingly well; so well, in fact, that some compensation must have taken place between the various approximations made.

In Tables I and II are given the comparison of the values of $C_p$ calculated from (8) with the observed values for air and ammonia. The heat capacities at zero pressure of air were obtained by reducing the one atmosphere values used by Roebuck[5] to zero pressure by use of the relation (8); the zero values for ammonia are those given by Osborne, Stimson, Sligh and Cragoe.[6] The equation of state constants of air listed in Table I are those used by Bridgeman[2] and were derived from the compressibility measurements made by Holborn and Schultze;[7] the constants of ammonia are those used by the author[3] and determined from the compressibility data of Beattie and Lawrence.[8]

TABLE I. *Comparison of the calculated with the observed values of the heat capacity at constant pressure of air. Calculations made with equation (8). In units of atmospheres, liters per mole, degrees Kelvin the values of the constants are* $R=0.08206$, $A_0=1.0763$, $c=12\times10^4$. *Molecular weight* $=28.960$.

| Pressure, atm. = | | 0 | 20 | 60 | 100 | 140 | 180 | 220 |
|---|---|---|---|---|---|---|---|---|
| Temp. | | Specific heat, 15° calories per degree C per gram. | | | | | | |
| 0°C | obs. | 0.2400 | 0.249 | 0.266 | 0.280 | | | |
| | obs.-calc. | | −0.001 | −0.005 | −0.011 | | | |
| 25 | obs. | 0.2406 | 0.249 | 0.263 | 0.276 | 0.287 | 0.296 | 0.302 |
| | obs.-calc. | | 0.000 | −0.002 | −0.005 | −0.010 | −0.016 | −0.026 |
| 50 | obs. | 0.2412 | 0.248 | 0.260 | 0.272 | 0.282 | 0.290 | 0.296 |
| | obs.-calc. | | 0.000 | 0.000 | −0.001 | −0.004 | −0.009 | −0.016 |
| 75 | obs. | 0.2416 | 0.248 | 0.258 | 0.268 | 0.277 | 0.284 | 0.289 |
| | obs.-calc. | | 0.001 | 0.001 | 0.000 | −0.001 | −0.005 | −0.010 |
| 100 | obs. | 0.2422 | 0.247 | 0.256 | 0.265 | 0.273 | 0.279 | 0.284 |
| | obs.-calc. | | 0.000 | 0.001 | 0.001 | 0.000 | −0.003 | −0.007 |
| 150 | obs. | 0.2432 | 0.247 | 0.253 | 0.260 | 0.266 | 0.271 | 0.275 |
| | obs.-calc. | | 0.001 | 0.000 | 0.001 | 0.000 | −0.001 | −0.003 |
| 200 | obs. | 0.2442 | 0.246 | 0.251 | 0.257 | 0.261 | 0.264 | 0.268 |
| | obs.-calc. | | −0.001 | −0.001 | 0.001 | 0.000 | −0.002 | −0.003 |
| 250 | obs. | 0.2452 | 0.247 | 0.250 | 0.254 | 0.257 | 0.260 | 0.262 |
| | obs.-calc. | | 0.000 | −0.001 | −0.001 | −0.002 | −0.003 | −0.004 |
| 280 | obs. | 0.2457 | 0.247 | 0.249 | 0.252 | 0.254 | 0.257 | 0.259 |
| | obs.-calc. | | 0.000 | −0.002 | −0.002 | −0.004 | −0.004 | −0.005 |
| | Average deviation | | 0.0035 cal. | | | | | |
| | Average % deviation | | 1.25% | | | | | |

For the computation of Tables I and II, the last term of equation (8) was first evaluated in units of atmospheres, liters per mole and degrees Kelvin. The conversion factors by which this term must be multiplied are $24.212/M$ to reduce to 15° calories per gram per degree Centigrade and $24.235/M$ to

[7] Holborn and Schultze, Ann. d. Physik **47**, 1089 (1915); see also Holborn and Otto, Zeits. f. Physik **33**, 1 (1925).

[8] Beattie and Lawrence, Jour. Amer. Chem. Soc. **52**, January (1930).

reduce to 20° calories per gram per degree Centigrade, where $M$ is the molecular weight of the gas.

TABLE II. *Comparison of the calculated with the observed values of the heat capacity at constant pressure of ammonia. Calculations made with equation (8). In units of atmospheres, liters per mole, degrees Kelvin the values of the constants are* $R=0.08206$, $A_0=2.3930$, $c=476.87\times10^4$. *Molecular weight* $=17.0311$.

| Pressure, atm. = | | 0 | 2 | 4 | 6 | 8 | 10 | 12 | 14 | 16 | 18 | 20 |
|---|---|---|---|---|---|---|---|---|---|---|---|---|
| Temp. | | Specific heat, 20° calories per degree C per gram. | | | | | | | | | | |
| 0°C | obs. | 0.4917 | 0.553 | 0.639 | | | | | | | | |
| | obs.-calc. | | 0.030 | 0.084 | | | | | | | | |
| 50 | obs. | 0.5097 | 0.531 | 0.556 | 0.584 | 0.616 | 0.651 | 0.690 | 0.735 | 0.785 | 0.845 | 0.917 |
| | obs.-calc. | | 0.005 | 0.013 | 0.025 | 0.040 | 0.059 | 0.081 | 0.110 | 0.143 | 0.186 | 0.242 |
| 100 | obs. | 0.5306 | 0.541 | 0.553 | 0.565 | 0.577 | 0.591 | 0.604 | 0.619 | 0.634 | 0.650 | 0.667 |
| | obs.-calc. | | 0.001 | 0.003 | 0.006 | 0.008 | 0.012 | 0.016 | 0.021 | 0.027 | 0.033 | 0.040 |
| 150 | obs. | 0.5532 | 0.560 | 0.566 | 0.573 | 0.579 | 0.586 | 0.593 | 0.600 | 0.607 | 0.615 | 0.622 |
| | obs.-calc. | | 0.001 | 0.001 | 0.002 | 0.002 | 0.003 | 0.004 | 0.005 | 0.006 | 0.008 | 0.009 |

The agreement between the observed and calculated values of $C_p$ for air (Table I) is good, in fact there is practically no difference in the deviations whether the complete or approximate relation for $C_p$, that is equation (5) or (8), is used, the average deviations being 1.1% and 1.25% respectively.

For ammonia (Table II) the approximate equation (8) gives values whose deviations are of the same order of magnitude, but larger, than the complete equation (5). Below 100°C neither relation leads to satisfactory values. It has been pointed out[8] that ammonia is one of the most unfavorable cases for the calculation of the pressure variation of thermal quantities because the isometrics exhibit such great curvature. Part of the deviation in the region below 100°C may be due to failure of the equation of state to reproduce all of the trends of the compressibility data and part to an inconsistency between the compressibility and thermal data. Above 100°C the complete relation (5) gives a better representation of the experimental results than the approximate relation (8); but the approximate expression fits the data fairly well, the average deviations being 2.7% at 100°C and 0.7% at 150°.

In general it seems safe to state that values of $C_V$ or $C_p$ calculated from relations (7) or (8) will be accurate to several percent when the temperature is not too near the critical. At temperatures below the critical, the deviations may amount to 5% or more depending on the pressure. The representation by both the approximate and the exact equations may be unsatisfactory near the saturation line for gases whose $c$ constant of the equation of state is large.

## 2. HEAT CAPACITY OF GAS MIXTURES

For the determination of $C_V$ or $C_p$ of a gas mixture from known properties of the pure component gases it is necessary to make one assumption, namely: At infinitely low pressures the energy of a mixture of gases is equal to the sum of the energies of the pure component gases when each is at the temperature and occupies the total volume of the mixture. This assumption has been discussed by the author[9] and by Gillespie.[10]

[9] Beattie, Phys. Rev. **31**, 680 (1928); **32**, 691 (1928).
[10] Gillespie, Phys. Rev. **34**, 1605 (1929).

By use of this assumption, the heat capacity of any gas mixture can be evaluated when:

(1) $C_V$ or $C_p$ for all of the component gases are known as functions of the temperature for some one density or pressure, and

(2) a generalized equation of gas mixtures of the form

$$F(p,V,T,n_1,n_2,\cdots)=0$$

is available and the equation of state parameters of the pure gases known.

The thermodynamic relations (1) and (2) may be applied to a mixture of gases in which no change in composition occurs. If equation (1) is integrated at constant temperature and composition between the limits $V=\infty$ and the variable volume $V$, there results:

$$C_V=C_V^*+\int_\infty^V T\left(\frac{\partial^2 p}{\partial T^2}\right)_{V,n}dV \tag{9}$$

where $p$, $V$, $T$, and $C_V^*$ refer to the mixture and the subscript $n$ denotes differentiation at constant composition. Now

$$C_V^*=(\partial U^*/\partial T)_{V,n} \tag{10}$$

and if the assumption stated above holds:

$$U^*=\sum x_1U_1^* \tag{11}$$

where $x_1$ is the mole fraction of Gas 1 in the mixture, $U_1^*$ its molal energy at zero pressure (referred to some arbitrary state) and $U^*$ the molal energy of the mixture at zero pressure. The summation extends over all of the gases in the mixture. By differentiation of (11) with respect to temperature at constant composition and volume, we obtain

$$C_V^*=\sum x_1C_{V1}^*. \tag{12}$$

Equation (9) then becomes

$$C_V=\sum x_1C_{V1}^*+\int_\infty^V T\left(\frac{\partial^2 p}{\partial T^2}\right)_{V,n}dV. \tag{13}$$

To derive the relation for $C_p$ of a gas mixture, we substitute (13) and (4) into the relation (2). There results:

$$C_p=\sum x_1C_{p1}-R+\int_\infty^V T\left(\frac{\partial^2 p}{\partial T^2}\right)_{V,n}dV+T\left(\frac{\partial p}{\partial T}\right)_{V,n}\left(\frac{\partial V}{\partial T}\right)_{p,n}. \tag{14}$$

The partial derivative of (13) and (14) must be evaluated from an equation of state for mixtures. The Beattie-Bridgeman equation of state (6) has been generalized[11] to apply to gas mixtures, by use of essentially the same method of determining the parameters of the mixture from the composition and the parameters of the pure gases as that suggested by van der Waals and Galitzine[12] and by Keyes,[13] namely:

[11] Beattie, Jour. Amer. Chem. Soc. **51**, 19 (1929).

[12] van der Waals, "Die Continuität des Gasförmigen und Flüssigen Zustandes," Part II, Barth, Leipzig, 1900; Galitzine, Wied. Ann. **41**, 770 (1890).

[13] Keyes and Burks. Jour. Amer. Chem. Soc. **50**, 1100 (1928).

$$R_m = \sum x_1 R = R \qquad A_{0m} = (\sum x_1 A_{01}^{1/2})^2 \qquad a_m = \sum x_1 a_1$$
$$B_{0m} = \sum x_1 B_{01} \qquad b_m = \sum x_1 b_1 \qquad c_m = \sum x_1 c_1. \tag{15}$$

The subscript $m$ refers to the values of the parameters for a mixture whose composition is expressed in terms of the mole fractions $x_1, x_2, \cdots$; the subscript 1 to the values for the pure Gas 1. The complete equation of state of a mixture is obtained by substituting the value of the parameters of the mixture into equation (6), $V$ becoming the volume of an average mole of mixture if the composition is expressed in mole fractions.

Evaluating the partial derivatives of (13) and (14) from the generalized equation of state of mixtures and carrying out the indicated integration, we obtain:

$$C_V = \sum x_1 C_{V_1}{}^* + \frac{R \sum x_1 c_1}{T^3 V}\left(6 + \frac{3 \sum x_1 B_{01}}{V} - \frac{2 \sum x_1 B_{01} \sum x_1 b_1}{V^2}\right) \tag{16}$$

$$C_p = \sum x_1 C_{p_1}{}^* - R + \frac{R \sum x_1 c_1}{T^3 V}\left(6 + \frac{3 \sum x_1 B_{01}}{V} - \frac{2 \sum x_1 B_{01} \sum x_1 b_1}{V^2}\right) \tag{17}$$

$$+ \frac{R[1 + (\sum x_1 B_{01} + 2 \sum x_1 c_1/T^3)/V + (-\sum x_1 B_{01} \sum x_1 b_1 + 2 \sum x_1 B_{01} \sum x_1 c_1/T^3)/}{1 + 2[\sum x_1 B_{01} - (\sum x_1 A_0{}^{1/2})^2/RT - \sum x_1 c_1/T^3]/V + 3[-\sum x_1 B_{01} \sum x_1 b_1 +}$$
$$\frac{V^2 - 2 \sum x_1 B_{01} \sum x_1 b_1 \sum x_1 c_1/T^3 V^3]^2}{(\sum x_1 A_{01}{}^{1/2})^2 \sum x_1 a_1/RT - \sum x_1 B_{01} \sum x_1 c_1/T^3]/V^2 + 4 \sum x_1 B_{01} \sum x_1 b_1 \sum x_1 c_1/T^3 V^3}$$

The approximate equations corresponding to (7) and (8) are

$$C_V = \sum x_1 C_{V_1}{}^* + \frac{6 \sum x_1 c_1}{T^4} p \tag{18}$$

$$C_p = \sum x_1 C_{p_1}{}^* + \left(\frac{2(\sum x_1 A_{01}{}^{1/2})^2}{RT^2} + \frac{12 \sum x_1 c_1}{T^4}\right) p. \tag{19}$$

The Beattie-Bridgeman equation of state for gas mixtures has been shown to represent the experimental data satisfactorily[11, 14] and the assumption of the additivity of energy of real gases at low pressures should be quite accurate. Hence the complete expressions (16) and (17) as well as the "approximate equations" (18) and (19) for the molal heat capacities $C_V$ and $C_p$ of gas mixtures should give a satisfactory representation of these thermal properties. If any of the gases in the mixture have large $c$ constants the representation may be unsatisfactory near the condensation line.

For the use of these relations the quantities $(\sum x_1 A_{01}{}^{1/2})^2$, $\sum x_1 a_1$, $\sum x_1 B_{01}$, $\sum x_1 b_1$ and $\sum x_1 c_1$, which are constant for any one mixture, are first computed. These are then combined with the temperature in such a manner that the various coefficients of $1/V$ or of $p$ are obtained for each isotherm. A systematic manner of making the computations has already been suggested.[3]

[14] Gillespie, Phys. Rev. **34**, 352 (1929).

# A THEORY OF THE PERMANENT MAGNETIC FIELDS OF THE SUN AND EARTH: A CORRECTION

By Ross Gunn
Naval Research Laboratory, Washington, D. C.

(Received November 6, 1929)

Abstract

Calculations by Page applied to the problem of the origin of the magnetic fields of the sun and earth show that earth currents arising from internal electric or gravitational fields crossed with a self-generated magnetic field tend to magnetize the earth rather than demagnetize it as was originally assumed. By attributing the observed field to electric and magnetic effects alone, ion free paths of only $10^{-7}$ cm are required whereas the original current systems which were attributed to an inhomogeneous magnetic field indicated that free path lengths of $3\times10^{-6}$ cm were necessary. The qualitative features of the original theory are unchanged.

In a letter to the writer, Professor Leigh Page kindly pointed out an error that entered the calculations made in the author's recent paper on "A Theory of the Permanent Magnetic Field of the Sun and Earth."[1]

A re-examination of the calculations in the light of his criticism showed that in the transition from Eq. (8) of the original paper to Eq. (9), a constant term that should have been included in the expression for the ion drift was neglected. Actually, in electric or gravitational fields crossed with a magnetic field, a constant drift is imposed on the ions which is independent of the angular distribution of the ion paths in a plane perpendicular to the impressed magnetic field. This constant drift is of opposite sign and larger than the drift originally computed. The corrected expressions lead to a more satisfactory form of the theory than the original one.

Professor Page in a recent paper[2] has carefully considered the problem of drift currents produced by crossed electric and magnetic fields and has calculated the mean ion displacement between collisions for all possible values of the free path. The second term of Professor Page's Eq. (8), for the case of short free paths, corresponds (after division by the mean free time) to the third term of the writer's Eq. (9). The second term of Page's Eq. (8) for the case of short free path reduces to

$$\bar{x}=\frac{e^2HEs^3}{cm^2V^3}\left[\frac{1}{6}+\sin^2\theta\left\{\frac{-1}{2\gamma}\sin\phi\cos\phi+\frac{1}{6}\cos^2\phi-\frac{1}{2}\sin^2\phi\right\}\right] \qquad (1)$$

where $\gamma=eHs/cmV$. In the two dimensional case considered by the writer the mean value of the above expression is zero but if it is averaged over all three dimensions the mean drift velocity is given by

$$V_x=\frac{e^2HEs^2}{18cm^2V^2} \qquad (2)$$

[1] Gunn, Phys. Rev. **34**, 335 (1929).
[2] Page, Phys. Rev. **34**, 763 (1929).

and the current density expressed in the units employed by the writer is

$$i_x = \frac{Ne^3\lambda^2 H_z E_y}{54mkT} . \tag{3}$$

The sign of this quantity is opposite to that originally obtained and indicates that inside the sun and earth circular ion currents are set up due to crossed electric and magnetic fields which tend to magnetize the body rather than demagnetize it as was originally supposed.

It therefore becomes necessary to consider a slight revision of the original theory and the emphasis must now be placed on magnetizing currents which arise from crossed electric and magnetic fields rather than magnetizing currents arising from an inhomogeneous magnetic field even though this current sheet is in the correct direction to produce the observed field. The original calculations showed the earth possessed an internal electric field of 0.3 e.m.u./cm which was always radially outward and which arose from the gravitational separation of the ions within the earth. The mean westward current density necessary to account for the earth's magnetic field is $4\times10^{-11}$ abamps/cm$^2$ and the mean free path of the ions necessary to give this observed current density can be calculated by aid of Eq. (3). Taking the mean internal value of $H=0.5$ gauss, $N=10^{23}$ ions/cm$^3$ and the mean internal temperature as 5000°C, the necessary free path turns out to be $2\times10^{-7}$ cm. This is far more satisfactory than the requirement of the original theory that the free path approximate $3\times10^{-6}$ cm. Such a value was very difficult to account for and constituted perhaps the major objection to the original theory. A calculation shows that ion currents due to the inhomogeneity of the earth's magnetic field or to crossed gravitational and magnetic fields are negligible for free paths of the magnitude required by the present considerations. A mean free path for the ions of $10^{-7}$ cm seems to be readily allowable inside the earth and this value lends support to the modified position that the primary current system of the earth results from the ion motions imposed by the internal gravitational-electric field crossed with a self produced magnetic field in the regenerative manner described previously. This view is complicated by the fact that the resulting current density is a linear function of the resulting field and it is not yet clear just what limits the field to its observed steady value. Many things have been left out of the theory which might account for the field building up to a steady state and some of these factors are now being studied. While the present view is able to account quantitatively for the observed field in a very simple manner it is perhaps well to point out that many features of ordinary electrical conduction theory do not agree with experiment and we have no assurance that the ions in the hot interior of the earth behave in any simple manner. Until many of the present difficulties of simple conduction theory are cleared away, the original form of the theory should, perhaps not be completely discarded.

# LETTERS TO THE EDITOR

*Prompt publication of brief reports of important discoveries in physics may be secured by addressing them to this department. Closing dates for this department are, for the first issue of the month, the twenty-eighth of the preceding month; for the second issue, the thirteenth of the month. The Board of Editors does not hold itself responsible for the opinions expressed by the correspondents.*

## An Unusual Spectral Series

The recent measurement by Selwyn (Proc. Phys. Soc. London **41**, 361, (1929)) of certain copper arc lines in the Schumann region have led to the identification of the following terms (mostly known as levels previously) of the ordinary $d^{10}np\ ^2P$ series of Cu I.

| *Designation* | *Level* | *Interval* | *Ryd. denominator* |
|---|---|---|---|
| $4p^2P$ | 31772.8 | | 1.858 |
| | | 248.4 | |
| | 31524.4 | | 1.865 |
| $5p$ | 21925.0 | −0.3 | 2.913 |
| | 7523.9 | | 3.818 |
| $6p$ | | −243.6 | |
| | 7280.3 | | 3.881 |
| | 4889.4 | | 4.737 |
| $7p$ | | +530.6 | |
| | 4358.8 | | 5.016 |
| | 3031.9 | | 6.015 |
| $8p$ | | − 47.0 | |
| | 2984.9 | | 6.063 |

It is not surprising that such an array was not previously considered to form a series, but the evidence is now quite conclusive. The appearance of intervals of both signs from a configuration in which only one electron is not in a closed group is at variance with our ordinary ideas of the production of spectral terms. The explanation will probably be found when the wave mechanics is able to account for the occurrence of inverted $^2D$ and $^2F$ terms in the simple doublet spectra of the alkali metals. Such an explanation has not as yet been given.

A. G. SHENSTONE

Palmer Physical Laboratory,
Princeton University,
December 3, 1929.

## On the Possibilities of a Gravitational Drag of Light

I suggested in a recent paper[1] that the well known velocity distance relation for extragalactic nebulae might possibly be accounted for by a gravitational drag of light. In this paper I discussed the momentum which a particle $m$ moving in a straight line with the velocity $v$ transfers to a mass $M$ initially at rest. The velocity $c$ was assumed for the gravitational waves. For the change of momentum of $m$ along its path an expression of the following type was obtained:

$$\Delta G=(fmM/v)\left[g_0+g_1v/c+g_2(v/c)^2+\cdots\right] \quad (1)$$

where $g_0$ is due to the static gravitational potential and the rest of the terms represent the retardation, $g_1$ not being equal to zero. Now Professor Eddington kindly informs me in a letter that $g_1$ should be zero on account of the following consideration. The retarded potential can be represented as this series[2]

$$\Phi(r,t)=\frac{\text{const.}}{r(1-v_r/c)}\Bigg|_{t'=t-r/c}=\frac{\text{const.}}{r}\Bigg|_{t'=t}+(2)$$

terms of second and higher order in $v/c$. As the forces are derived from $\Phi$ they do not contain any terms in $v/c$ and $\Delta G$ should therefore not contain any such terms either. This is actually so provided that the particle $m$ is moving along the straight line without being started or stopped. But if it is started from rest at $P_1$ and stopped at $P_2$ a term in $v/c$ appears as given in my paper. This is due to the fact that at the time $t_0$ at which the signal from the start at $P_1$ has reached $M$, the mutual distance of the two particles

[1] F. Zwicky, Proc. of the Nat. Acad., Oct. 1929.

[2] A. S. Eddington, Phil. Mag. **46** 1112 (1923).

differs from $P_1M$ in terms $v/c$. It may very well be that the way in which I have introduced the time limits for the interaction between $M$ and $m$ is not justified. The problem is indeed quite complex because of the fact that the expulsion of a particle (light quantum) is accompanied by a direct recoil (atom) which would have to be considered.

It seems to me however that the question whether $g_1$ is zero or not has no direct bearing on the question of the existence of a gravitational drag of light. Indeed for $v=c$ all the terms in (1) become of equal importance. The above consideration for a moving particle of matter was given in my paper for the sole purpose of illustrating the effect of the retardation on the transfer of momentum. Any relation of the type (1) holds of course only for $v<c$. Only dimensional extrapolations can be made for $v=c$. It was therefore always my opinion that the existence of a gravitational drag of light must be derived or disproved from the general theory of relativity.

An approximate relativistic solution of the problem might possibly be obtained in this way. Suppose that a quantum $h\nu$ is passing by a mass $M$ (star, etc.). If we hold $M$ fixed, then the path of the quantum is given by Einstein's solution. Let now $M$ recoil, but retain as a first approximation Einstein's path for the light. Then four unknowns have to be determined; namely, the three velocity components of $M$ and the resulting shift in frequency from $\nu$ to $\nu'$. The four generalized equations for the conservation of "momentum" and "energy" should yield the necessary relations for the unknowns.

Finally I wish to mention some observational tests related to the velocity of recession of nebulae which might decide between a "geometrical" theory (de Sitter) and a physical explanation. In the latter case, the red-shift should essentially depend on the distribution of matter in space, which might result in some of the following phenomena.

(a) A dependency of the red-shift on direction should be expected, especially within our own galactic system.

(b) For very dense clusters of extragalactic nebulae (like the Coma cluster for instance) its different nebulae might show differences in apparent radial velocities larger than those due to peculiar motions.

(c) If a nebula appears inclined to the line of sight, the light from the far edge might show a larger red-shift then the light from the near edge. The possibility of such an effect has also been mentioned by Dr. I. S. Bowen in conversation. Some observations of this type have been made by F. G. Pease[3] on the Andromeda nebula. His data indicate a slight difference in red-shift (20 km/sec) from the near edge to the far edge which is of the order of magnitude one should expect from the theory. The observational uncertainties involved are, however, too large to justify any definite conclusions.

F. ZWICKY

California Institute of Technology,
December 4, 1929.

[3] F. G. Pease, Proc. of the Nat. Acad. **4**, 21 (1918).

## The Early Stages of Electric Spark Discharges

The broadening of spectrum lines in condensed spark discharges has been attributed to the Stark effect of inter-ionic fields. It occurred to us that probably the current density, and therefore the ionic density, in a spark is much greater immediately after breakdown than later and therefore that spectra at the beginning of spark discharges should be relatively more diffuse. By a slight modification, we have adapted the electro-optical shutter of Abraham-Lemoine and Beams to the observation of the width of spectrum lines at successive intervals of time after the beginning of sparks, and the results have led to interesting information on the density of the ions. We find, for example, that the spark doublets of Mg, Cd, and Zn are diffuse bands over 40A wide during 2 ($10^{-7}$) sec after breakdown. Assuming that the broadening of the lines is a second order Stark effect due to the ions in the discharge and with the aid of experimental data on the Stark effect of Mg we have calculated from our observations that *about 31 percent of the atoms and molecules in the path of the discharge are ionized.*

The electro-optical shutter has enabled us as well to measure the velocity of migration of the luminosity of the metallic spark lines from the anode. In the case of Zn the lumi-

nosity of the vapor travels away from the anode at the rate of 1.7 ($10^8$) cm per second during the first 2 ($10^{-7}$) sec after breakdown. We also have obtained actual photographs of the initial stages of single sparks *with exposure times as short as* 4 ($10^{-8}$) sec. These snapshots of the beginnings of single sparks show that a current of 1600 amperes is carried by a filament of cross-section 5 ($10^{-4}$) sq. cm at the anode which gradually widens out to a cross-section of 2 ($10^{-3}$) cm at the cathode. *Thus the current density in the discharge attains the enormous magnitude of* 3 ($10^6$) *amps per sq. cm.* This great current density produced the great brilliance of the spark as a light source which made possible the photography of the spark with the short exposures mentioned above.

It seems probable that the above recorded velocity of spreading of the spark luminosity from the anode really measures the velocity of the positive ions. Assuming this to be the case and that the positive ions carry one half the discharge current, *it is calculated from the cross-section of the discharge that about 30 percent of the molecules and atoms in the discharge are ionized.* This result is in striking agreement with the above estimate of the ionic density evaluated from the broadening of the spectrum lines. These calculations have not taken into account certain factors and therefore are approximate but certainly right in order of magnitude. Perhaps it does not seem valid to assume that the positive ions carry as much of the discharge current as the electrons because of the greater speeds of the latter carriers. This objection appears less serious when it is pointed out that the magnetic field produced by the discharge itself reaches the magnitude of 40,000 Gauss and therefore that the electrons are confined to spiral paths of very small radii in such a manner that their velocity of migration to the anode is diminished considerably.

Finally, we should like to mention that two of our photographs of early stages of sparks show off-shoots from the main filament of the discharge which remind one of Wilson cloud photographs of alpha-particle tracks. Because the off-shoots in both cases are bent towards the cathode the possibility is suggested that they are due to regions of ionization initiated by high velocity positive ions ejected from the main filament of the discharge.

ERNEST O. LAWRENCE
FRANK G. DUNNINGTON
University of California,
December 11, 1929.

## The Effect of Second Order Zeeman Terms on Magnetic Susceptibilities: Errata.

Due to a previous arithmetical error, the theoretical Bohr magneton numbers given in Table I of our note in the preceding (December 1) issue should read 3.68, 2.83, 1.66 and 3.53 for $Nd^{+++}$, $Ill^{+++}$, $Sm^{+++}$, and $Eu^{+++}$ respectively instead of 3.69, 2.87, 1.83 and 3.56. There is no change in the balance of this Table or in Table II. This revision is seen to be appreciable only for $Sm^{+++}$, and here improves the agreement with experimental values (1.54, Cabrera, or 1.32, St. Meyer) so that the situation for the whole rare earth group is now quite satisfactory. The first sentence of the last paragraph in our previous note obviously relates to the iron rather than rare earth group.

J. H. VAN VLECK
A. FRANK
University of Wisconsin,
December 13, 1929.

## Electron Emission by Metastable Atoms

It has been shown recently by Oliphant [Proc. Roy. Soc. **A124,** 793 (1919)] that helium metastable atoms cause a secondary electron emission when they strike a negatively charged target. Uyterhoeven [Proc. Nat. Acad. Sci. **15,** 32–37, (1929)] has observed that the currents to a negative probe in neon are greater than those calculated from the observed sheath thickness. This could be accounted for by the assumption that a portion of the current measured was due to secondary emission by metastable neon atoms. The writer (Science **68,** 598, 1928) has also reported observations with a negative probe in neon which can be accounted for by a secondary electron emission from the probe. More recent experiments in this laboratory (which will be reported shortly by Found and Lowe) indicate this secondary emission is due to metastable atoms.

There is considerable difficulty in separating the currents due to positive ions from that

due to secondary electrons. In the course of some experiments on sputtering by positive ions of neon, it was observed that the energy delivered to a sputtered wire target was much less than that calculated from the current and the voltage drop at the electrode.

This was ascribed to the fact that part of the measured current was due to secondary emission by metastable atoms. As Oliphant's results show that the difference in energy between the metastable state and the work function of the metal is taken up by the emitted electron, we may assume that the total energy to the target is carried by positive ions. Thus the positive ion current may be calculated from measurement of energy delivered to the target and the relation between secondary electron current and positive ion current determined.

A second method of calculating the contribution of secondary electrons to collector currents is the space charge equation developed by Langmuir and Mott Smith (G. E. Rev. 1924). If the secondary emission is due to metastable atoms, it will be proportional to the collector area, whereas the positive ion current is proportional to the sheath area. It has been proved by Langmuir that the secondary electron emission from a negatively charged collector does not vary by more than 0.1 percent per volt. A change of this magnitude can be neglected when dealing with a cylindrical collector of small diameter. If, with such a collector, we choose conditions such that the sheath area is large (i.e., low discharge currents and high voltages) we may assume as a first approximation that the current is due entirely to positive ions. On this basis an approximate value of sheath thickness can be calculated. By comparing the rate of change of collector current to the rate of change of sheath area, the random positive ion current density can be determined by a series of approximations. From this value, the contributions of secondary electrons to collector current is readily computed. Calculation by this method shows that in the positive column of a neon tube of 5 cm diameter at 300 baryes pressure and operating at 0.4 amperes discharge current, the secondary electron emission from a tungsten wire is 7.5 m.a./cm$^2$ compared to a random positive ion current density in the discharge of 0.82 m.a./cm$^2$. This means that a wire collector of 0.005 cm diameter and 3.5 cm long, 100 volts negative to the discharge, receives a positive ion current of 0.91 m.a. and emits a secondary electron current of 0.42 m.a. Results giving the secondary electron current as a function of discharge current and pressure will be given in a future publication.

CLIFTON G. FOUND

Research Laboratory,
General Electric Company,
Schenectady, New York,
December 12, 1929.

## Frequency Distribution in Raman Spectra

If we grant that most of the lines in the Raman spectra of organic compounds correspond to fundamental frequencies in the molecule, it is possible to explain the distribution of the frequencies in the spectra by assuming that the non-polar chemical bond always has about the same elastic constants independent of the atoms which it joins or their position in the molecule. In other words variations in frequency appear to be due in most part to the variations in the masses of the particles vibrating rather than to variations in bond strength when the bonds involved are non-polar single bonds.

We have taken the following values as representing the average state of the non-polar single bond: $k_1 = 4 \times 10^5$ dynes per cm for streching the bond; $k_1 = 0.66$ dynes per cm for bending the bond. In other words $k_1$ is the restoring force on an atom when it is moved unit distance along the line in which we think the bond to act, and $k_2$ is the restoring force when the atom is moved perpendicular to this line, the rest of the molecule being held still. This implies; (1) that the bond is a definite localized force closely analogous to a spring, at least for the small displacements involved in thermal vibration which are of the order of 0.2A; (2) that all bonds have a common mechanism as was first suggested by G. N. Lewis when he proposed the electron pair theory.

These assumptions lead us to expect the following groups of frequencies in the Raman spectra of typical organic molecules. (Values are in cm$^{-1}$.)

I. Hydrogen attached to C, O, or N vibrating
  a) along bond: calc. 2730; obs. 2830–3050
  b) perpendicular to bond: calc. 1500–1200; obs. 1500–1200.

II. Vibration of groups of C, O, and N atoms
  a) along bonds:
    1. Simple pairs 1068–1000
       Example: C–O; calc. 1000; obs. 1031 (in $CH_3OH$)
    2. Several bonds restricting one atom. 1300–1000.
    3. Motions involving several atoms such as in long chains: 1000–400 or lower depending on length of chain.
    4. Single groups attached to heavy radical. 150–250.
       Example: $CH_3$–$C_6H_4$ obs. 215.
  b) Perpendicular to bonds:
    1. In straight chains: 450–150 or lower depending on length of chain.
       Example: $CH_3CH_2OH$ calc. 415; obs. 450.
    2. In ring structure: 600–300.
       Example: Benzene calc. 612, 306; obs. 605, 360.

III. Heavy atoms such as Cl, Br, and I or groups such as $NO_2$, COOH.
  a) Vibration along bond.
     Example: Cl–$C_6H_5$ calc. 540; obs. obs. 607.
  b) Vibration perpendicular to bond.
     Example: Cl–$C_6H_5$ calc. 215; obs. 195.

The observed spectra are almost without exception in accord with the above scheme. Slight deviations may be due to the fact that actually the strength of a bond may vary by twenty percent from the average value and that exact analysis of the motion involved in many types of vibration is impossible. Further confirmation is given by the fact that with the help of the above the heat capacity can be calculated as a sum of Einstein and Debye functions, and the optically observed frequencies can be assigned in quite a definite and unequivocal manner to the different degrees of freedom. The values so calculated agree well with the experimentally observed values in the dozen cases for which data are available.

DONALD H. ANDREWS
Department of Chemistry,
Johns Hopkins University,
December 10, 1929.

*To the Editor of the Physical Review*

Dear Sir:

It has been called to my attention that the experiment described in the last paragraph of my "Letter" of November 15, [Phys. Rev. **34**, 1392 (1929)] really proves nothing at all. For it appears that the copper gauze used as an electrostatic shield also effectively decreases the electromagnetic field inside the tube. As a matter of fact, the electrostatic shield originally suggested to me by Dr. Breit consisted of a system of wires running parallel to the tube. I used, instead, the more convenient copper gauze, for at the time it did not occur to me that the electromagnetic forces inside the tube would be decreased because of the eddy currents set up in the gauze.

Accordingly, I have recently repeated that experiment using an electrostatic shield similar to the one originally suggested by Dr. Breit. It consisted of a set of parallel wires about 1 cm apart, joined at each end by a ring with a small gap in it. The eddy currents induced in such a shield would be negligible. Consequently it would function purely as an electrostatic shield. It was found that as soon as the tube was surrounded by this shield, the discharge ceased. Hence, we must conclude, as before, that the electrodeless discharge is principally an electrostatic phenomenon.

There seems to be one exception to this conclusion. In a recent paper, K. A. MacKinnon [Phil. Mag. **8**, 605, (1929)], has shown that the luminous annular ring which appears in electrodeless discharge under certain conditions of excitation is undoubtedly produced by electromagnetic forces. It seems that only spark excitation (i.e. damped waves) will produce this "ring." I have always used c.w. excitation and consequently, have never observed it.

Very truly yours,
CHARLES J. BRASEFIELD

University of Michigan,
December 11, 1929.

# BOOK REVIEWS

**Wein-Harms Handbuch der Experimental Physik. Vol. XVIII.** K. F. BOTTLINGER, R. LADENBURG, M. v. LAUE, HANS SCHULZ, AND E. WARBURG. Pp. 670+xiv, figs. 140. Akademische Verlagsgesellschaft m.b.H., Leipzig 1928. Price, bound, RM63.50.

This volume opens with a critical review by Ladenburg on the various measurements of the velocity of light in media at rest. This is an excellent up-to-date summary of the subject. The following section on optics of moving media, by v. Laue, is a discussion of optical phenomena due to relative motion, such as aberration, Doppler effect, and Fresnel coefficient, and the rotation experiments of Sagnac, Michelson, and Harress, together with the attempts to detect absolute motion of the earth through space. The experiments and their theoretical foundation are discussed in a masterly fashion, but the actual derivations of the various formulae are for the most part omitted. A brief section by Bottlinger deals with the measurements of the shift of spectral lines to the red and the deflection of light rays in a gravitational field as predicted by the theory of relativity. The fourth section, by v. Laue, is on the reflection and refraction of light at the boundary of two isotropic media. Especially noteworthy is the comparison of the various results with experiment. The effects of surface films are summarized. The treatment of metallic reflection, which includes the magneto-optic Kerr effect, is very good. It should be noted that dispersion phenomena are not included in this volume. The section on interference and diffraction of electromagnetic waves (with the exception of x-rays) is also by v. Laue. The first two chapters give a complete and interesting resumé of the many interference phenomena and their applications. The treatment of diffraction phenomena is excellent. Many photographic illustrations and intensity graphs add to the interest of the mathematical derivations. The subject of polarized light is written up by Schulz. The treatment is highly satisfactory from a descriptive standpoint, but one regrets that the development of most of the mathematical theory is omitted. The instruments used in the study of polarization phenomena are particularly well discussed. The volume ends with a brief treatment of photochemistry by Warburg. As this section was completed early in 1926, it is somewhat out-of-date.

The typography and binding are very good.

J. VALASEK

**Proceedings of the Seventh International Congress of Photography. London, July 9–14, 1928.** Editors: W. CLARK, T. SLATER PRICE, B. V. STORR. Pp. 571+xiv, figs. 199. W. Heffer and Sons Ltd. Cambridge 1929. Price 25/ net.

It is very difficult to write an adequate review of a book of this kind with its large number of short articles on different subjects ranging from artistic photography to the commercial, scientific, and theoretical aspects of the subject. The greatest space is devoted to the properties of photographic materials. The difficulties encountered in establishing standards for testing of photo-materials are well illustrated in the proposals made, the subsequent discussion, and the final postponement of action. The following section is a brief one dealing with apparatus and it includes a paper on super-speed lenses and shutters. In the next section on scientific applications one finds articles on such subjects as spectrography with the quartz spectrograph and the vacuum grating spectrograph, the photography of stress, and the photography of sound waves. The following section deals with photo-engraving, color photography, and kinematography with an article on sound films. The final group of papers is on record photography, history, and bibliography.

Because of the many applications of photography, there is something in this volume that will be of interest to everybody. The typography is good, but the binding is of paper.

J. VALASEK

# AUTHOR INDEX TO VOLUME 34

References with (A) are to abstracts of papers presented at meetings of the Physical Society and references with (L) are to Letters to the Editor.


**Adams, Arthur S.** Adsorption of air on glass as a function of temperature—1438

**Adams, Elliot G.** Capture of electrons by α-particles—537(L)

**Ader, O. B.** Extension and period of a conically wound spring—656

**Allison, Samuel K.** Experimental evidence for filling of electron levels from relative intensity of x-ray spectrum lines—7

——— Resolution of line $L\beta_2$ into its diagram components and relative widths of some x-ray spectrum lines—176

**Almy, G. M.** and **F. H. Crawford.** Zeeman effect in MgH bands—1517

**Anderson, Carl D.** Spatial distribution of photoelectrons ejected from a gas by x-rays —547(A)

**Andrews, Donald H.** Frequency distribution in Raman spectra—1626(L)

**Armstrong, Alice H.** X-ray diffracting power of copper and iron for molybdenum and copper radiation—931

——— Intensity of reflection of x-rays from diamond—1115

**Astin, Allen.** A new method for measuring the dielectric constants of conducting liquids—300

**Babcock, Harold D.** Relative abundance of the isotopes of oxygen—540(A)

**Bacher, R. F.** (see Goudsmit, S)—1501, 1499(L)

**Bainbridge, K. T.** A search for element 87 by analysis of positive rays—752

**Barnes, A. H.** (see Davis, Bergen)—152

——— Capture of electrons by alpha-particles—1229(L)

**Barnes, B. T.** Total radiation from polished and from soot-covered nickel—1026

**Bartlett, James H., Jr.** Relative intensities of nebular lines—1247

**Barton, Henry A.** A new regularity in the list of existing nuclei—1228(L)

**Bates, John R.** (see Urey, H. C.)—1541

**Bauer, H.** (see Jauncey, G. E. M.)—387

**Beattie, James A.** Heat capacities of real gases and mixtures of real gases—1615

**Becker, J. A.** Book reviews—820, 1291

——— Phenomena in oxide-coated filaments —1323

**Berger, C. E.** Effect of light on electron emission from cerium dioxide—1566

**Birge, Raymond T.** Further evidence of the carbon isotope, mass 13—379(L)

——— Heat of dissociation of oxygen and of nitrogen—1062(L)

——— (see King, Arthur S.)—376(L)

**Black, J. G., W. G. Nash** and **C. A. Poole.** Influence of argon and of hydrogen on spectra of zinc vapor—1138

——— (see Duffendack, O. S.)—35

**Black, N. Henry.** Book review—1291

**Bleakney, Walker.** A new method of positive ray analysis and its application to the measurement of ionization potentials in mercury vapor—157

**Bourgin, D. G.** Sound propagation in gas mixtures—521

**Bowen, I. S.** Additional series lines in spectra of C II and N II—534

——— Low energy states in C II and N II —540(A)

**Bozorth, Richard M.** Barkhausen effect in iron, nickel and permalloy. I. Measurement of discontinuous change in magnetization—772

**Bramley, A.** Scattering of light by Kerr cell—1061(L)

**Brasefield, Charles J.** Densities of hydrogen spectral lines as a function of electronic velocity of excitation—431

——— Nature of electrodeless ring discharge —1392(L), 1627(L)

**Brattain, Walter H.** Efficiency of excitation by electron impact and anomalous scattering in mercury vapor—474

**Breit, G.** Effect of retardation on interaction of two electrons—375(L), 553

——— On the possibility of nuclear disintegration by artificial sources—817(L)

**Breit, G.** A Correction to "The Propagation of Schroedinger Waves in a Uniform Field of Force"—1491

**Brice, Brooks A.** Double vibrational isotope effect in silver chloride band spectrum —1227(L)

**Bridgeman, Oscar C.** Joule-Thomson effect and heat capacity at constant pressure for air—527

**Bridgman, P. W.** Book reviews—383, 819, 998, 1230

——— General consideration on emission of electrons from conductors under intense fields—1411

**Brode, Robert B.** Absorption coefficient for s'ow electrons in alkali metal vapors—673

**Bryan, A. B.** Dielectric constants of argon and neon—615

**Buchta, J. W.** Book reviews—1395, 1396

**Burns, Laurence.** (see Stockbarger, Donald C.)—1263

**Burroughs, R. E.** A phenomenon observed in a rotary spark gap—161(L)

**Busang, P. F.** (see Smith, W. O.)—1271

**Byck, Harold T.** On a resonance-fluorescence phenomenon in cyanogen spectrum—453

**Cabannes, Jean.** Change in wave-length by molecular scattering—1497(L)

**Campbell, James R., Jr.** (see Race, Hubert H.)—1031

**Carman, A. P.** and **K. O. Smith.** Dielectric constants of three electrolytes by a static balance electrometer method—1042

——— **O. B. Young** and **K. O. Smith.** A static balance electrometer method of measuring dielectric constants of electrolytes—1040

**Cassen, Benedict.** Symmetry of nuclear wave functions—1061(L)

**Caswell, A. E.** New graphical arrangement of periodic table—543(A)

**Chandrasekhar, S.** Generalized form of new statistics—1204

**Chase, Carl T.** A test for polarization in a beam of electrons by scattering—1069

**Christensen, Carl J.** and **G. K. Rollefson.** A high intensity non-reversed sodium arc —1154

——— Influence of method of excitation on transition probabilities in sodium vapor —1157

**Christy, Andrew.** A new titanium band system—539(A)

**Colby, W. F.** Analysis of the HCl bands—53

**Condon, E. U.** Book reviews—1065, 1230

**Constant, F. W.** Magnetic properties of isolated ferromagnetic atoms—548(A), 1217

**Cook, F. W.** Photoelectric cell for use in erythema—1287(L)

**Cook, S. G.** Surface tension of mercury in presence of gas under varying pressures —513

**Cook, S. R.** Preliminary note on coefficients of relativity—549(A)

**Cox, Irwin W.** Scattering of positive lithium ions in mercury vapor—1426

**Cox, R. T.** (see Myers, Frank E.)—1067

**Crawford, F. H.** (see Almy, G. M.)—1517

**Curtiss, L. F.** Nature of cosmic radiation —1391(L)

**Daily, C. R.** Electric moments of $CH_3$ and Br radicals in certain organic molecules —548(A)

**Daugherty, J. Fenton.** Infra-red absorption spectra of benzene and its halogen derivatives—1549

**Davis, Bergen** and **A. H. Barnes.** Capture of electrons by swiftly moving alpha-particles —152

——— and **Harris Purks.** Fine structure in Compton effect—1

——— Unusual reflecting power of a pair of calcite crystals—181

**Dawson, L. H., L. P. Granath** and **E. O. Hulburt.** Attenuation of ultra-violet light by lower atmosphere—136

——— and **Joseph Kaplan.** Comet-tail bands—379(L)

**Delsasso, L. P.** An electro-mechanical frequency analyzer—550(A)

**Dempster, A. J.** Reflection of protons from crystals—1493(L)

**Dershem, Elmer.** Reflection of $K\alpha$ line of carbon from glass—1015

**Dewar, Margaret.** (see Kirkpatrick, Paul) —549(A)

**Dennison, D. M.** Book review—1395

**Dickinson, R. G., R. T. Dillon,** and **F. Rasetti.** Raman spectra of polyatomic gases —582

**Dillon, R. T.** (see Dickinson, R. G.)—582

**Dodd, L. E.** Field of view of secondary image, with point-object stationary, for two independently variable plane mirrors having limited widths—543(A)

——— A heavy electromagnetic pendulum for use as a self-regulating motor—545(A)

**Duffendack, O. S.** and **J. G. Black.** Studies on spectra of Cu I, Cu II, and Mn II by means of vacuum tungsten furnace—35

**Duffendack, O. S.** and **H. L. Smith.** Simultaneous ionization and excitation of diatomic molecules by impacts with positive ions and excited atoms—68

——— and **R. A. Wolfe.** Excitation of arc spectrum of nitrogen—409

———, **Clement L. Henshaw,** and **Marie Goyer.** The excitation of the Mg II spectrum by impacts of second kind with metastable atoms and ions of rare gases —1132

**Duncan, James F.** Experimental study of certain electronic bands of $CO_2$—1148

**Dunham, J. L.** Intensities in harmonic band of hydrogen chloride—438

**Dunnington, Frank G.**—(see Lawrence, E. O.) 1624(L)

**Easley, M. A.** (see Spence, B. J.)—730

**Eckart, Carl.** Continuous x-ray spectrum —167

**Edlefsen, N. E.** (see Lawrence, Ernest O.) —233, 1056

**Ellett, A., H. F. Olson,** and **H. A. Zahl.** Reflection of atoms from crystals—493

**Ellis, Joseph W.** Vibration spectrum of ammonia molecule—539(A)

**Engwicht, Harry.** Relative intensities of lines in a generalized multiplet of Ti II —541(A)

**Erikson, Henry A.** Factors affecting nature of ions in air—635

**Evjen, H. M.** Energy changes by a variation from crystallographic group—1385

**Farnsworth, H. E.** Electron emission and diffraction by a copper crystal—679

**Feather, N.** Status of $\gamma$-ray change—1558

**Focke, A. B.** (see Goetz, A.)—546(A)

**Foote, Paul D.** (see Smith, W. O.)—1271

**Found, Clifton G.** Electron emission by metastable atoms—1625(L)

**Frank, A.** (see Van Vleck, J. H.)—1494, 1625(L)

**Frayne, John G.** Influence of foreign gases on intensities of magnesium resonance lines 5471 and 2852—546(A), 590

**Frazer, J. H.** Adsorption of air and water vapor on rock-salt surfaces—644

**Fredrickson, W. R.** Rotational structure of red bands of sodium—207

**Freed, Simon** and **Frank H. Spedding.** Line absorption spectra of solids at low temperatures in visible and ultra-violet regions of spectrum—945

**Frerichs, Rudolf.** New terms in oxygen arc spectrum—1239

**Gartlein, C. W.** (see Gibbs, R. C.)—406

**Gaviola, E.** Remarks on efficiency of quenching collisions and radius of excited mercury atom—1049

——— On life and concentration of metastable atoms and quenching of mercury resonance radiation—1373

**Gibbs, R. C.** and **Alice M. Vieweg.** Extension of Cd I-like iso-electronic sequences to Sb IV and Te V—400

——— **Alice M. Vieweg,** and **C. W Gartlein.** Use of series inductance in vacuum spark spectra—406

**Gillespie, Louis J.** Expansion of gases on mixing, especially at very low pressures. I. Its relation to empirical calculation of fugacities in gaseous mixtures—352

—— Empirical calculation of fugacities in gaseous mixtures. II. Its relation to tangents on certain thermodynamic diagrams. Approximate equations for some important thermodynamic properties of gas mixture—1605

**Goetz, A., R. C. Hergenrother** and **A. B. Focke.** Effect of strong magnetic fields on formation of bismuth single-crystals—546(A)

——— and **M. Hassler.** Electric volume-effects in bismuth single-crystals grown in strong magnetic fields—549(A)

**Goudsmit, S.** (see Uhlenbeck, G. E.)—145

——— and **R. F. Bacher.** Separations in hyperfine structure—1501

——— and **R. F. Bacher.** Paschen-Back effect of hyperfine structure—1499(L)

**Goyer, Marie.** (see Duffendack, O. S.)—1132

**Granath, L. P.** (see Dawson, L. H.)—136

——— and **E. O. Hulburt.** Absorption of light by fog—140

——— Absorption of ultra-violet light by oxygen, water vapor and quartz—1045

**Guillemin, Victor Jr.** (see Zener, Clarence) —999

**Gunn, Ross.** Theory of permanent magnetic fields of sun and earth—335; A correction —1621

**Hanawalt, J. D.** (see Ingersoll, L. R.)—972

**Harnwell, Gaylord P.** Electron scattering in hydrogen—162(L)

——— Electron scattering in atomic and molecular hydrogen—661

**Harrison, George R.** Intensities in supermultiplets of titanium—540(A)

——— An electric vacuum furnace for quantitative line intensity determinations —545(A)

——— (see Hesthal, Cedric E.)—543(A)
**Harvey, A.** and **F. A. Jenkins.** Alternating intensities in absorption bands of $Li_2$—1286(L)
**Hassler, M.** (see Goetz, A.)—549(A)
**Heaps, C. W.** and **Josiah Taylor.** Discontinuities of magnetization in iron and nickel—937
**Hendricks, Sterling B.** Electron diffraction by a copper crystal—1287(L)
——— (see Langer, R. M.)—544(A)
**Henshaw, Clement L.** (see Duffendack, O. S.)—1132
**Hergenrother, R. C.** (see Goetz, A.)—546(A)
**Herzfeld, K. F.** Influence of surface conditions and space charges on conductivity of poor conductors—791
**Hesthal, Cedric E.** and **George R. Harrison.** A projection lantern microphotometer—543(A)
**Hidnert, Peter.** Thermal expansion of tantalum—544(A)
**Hildebrand, Joel H.** Intermolecular attractions in liquids—542(A)
——— Compressibilities and thermal pressure coefficients of certain liquids—649
——— Intermolecular forces in liquids—984
**Hill, E. L.** On Zeeman effect in doublet band spectra—1507
**Hollaender, Alexander** and **John Warren Williams.** Molecular scattering of light from solids: Plate glass—380(L)
——— and **John Warren Williams.** Molecular scattering of light from solids: crystalline sulfates and their water solutions—994
**Houston, William V.** Temperature dependence of electrical conductivity—279
——— Temperature dependence of electrical resistance—547(A)
**Howey, J. H.** Magnetic behavior of nickel and iron films condensed in vacuum upon various metal backings—1440
**Hughes, A. Ll.** and **V. Rojansky.** On analysis of electronic velocities by electrostatic means—284
——— and **J. H. McMillen.** Re-focussing of electron paths in a radial electrostatic field—291
**Hulburt, E. O.** (see Dawson, L. H.)—136
——— (see Granath, L. P.)—140
——— Wind mixing and diffusion in upper atmosphere—161(L)
——— On ultra-violet light theory of aurorae and magnetic storms—344
——— Temperature of planets—1063(L)
——— Ions and electrical currents in upper atmosphere of earth—1167
**Hyatt, J. M.** Distribution of electrons between plate and grid of a three electrode tube as determined by positive caesium ions—486

**Ingersoll, L. R.** and **J. D. Hanawalt.** Gas content, crystal structure and hydrogen absorption of sputtered nickel films—972
**Ingram, S. B.** Classification of arc spectra of nitrogen and carbon—421
**Ives, Herbert E.** and **A. R. Olpin.** Maximum excursion of photoelectric long wave limit of alkali metals—117

**Jauncey, G. E. M.** and **H. Bauer.** Temperature and Compton effect—387
**Jenkins, F. A.** (see Harvey, A.)—1286(L)
**Jenness, J. R.** Effect of temperature upon fluorescence of some organic solutions—1275
**Johnson, Arthur J. M.** *M*-series absorption spectra of metallic platinum and gold—1106
**Johnstone, J. H. L.** and **John Warren Williams.** Variation of dielectric constant with frequency—1483
**Jones, Roderick Bissell.** Photoelectric threshold of a doubly evaporated film—227

**Kaplan, Joseph.** (see Dawson, L. H.)—379(L)
——— Excitation of $\beta$ bands of nitric oxide—165(L)
——— Electron scattering in hydrogen—1227(L)
——— Raman lines in spectrum of electric discharge—1393(L)
——— (see Kinsey, E. L.)—545(A), 546(A)
**Kassel, Louis S.** Heat of dissociation of oxygen—817(L)
**King, Arthur S.** and **Raymond T. Birge.** An isotope of carbon, mass 13—376(L)
——— Characteristics of electric furnace spectra of europium, gadolinium, terbium dysprosium and holmium, λ3900–λ4700—540(A)
——— Features of furnace, arc and spark spectra of hafnium—544(A)
**Kingdon, K. H.** (see Langmuir, Irving)—129
**Kinsey, E. L.** Raman effect in water—541(A)

**Kinsey, E. L.** and **Joseph Kaplan.** Recombination of atoms—545(A)
——— and **Joseph Kaplan.** Transition probabilities—546(A)
**Kirkpatrick, Paul** and **Margaret Dewar.** Classical scattering in x-ray reflection 549(A)
**Knudsen, V. O.** Speech-power of speakers in auditoriums—549(A)
**Korff, S. A.** Dispersion and absorption line width in alkali vapors—457
**Kovarik, Alois F.** Book review—166
**Kruger, Gerald.** Extension of spark spectrum of copper—1122
**Kurt, O. E.** and **T. E. Phipps.** Magnetic moment of oxygen atom—1357

**Laird, Harold R.** Effect of hydrogen on thermionic emission from potassium—463
**Lang, R. J.** Spark spectra of germanium—697
——— (see Sawyer, R. A.)—712
**Langer, R. M.** Quantum mechanics of chemical reaction—92
——— and **S. B. Hendricks.** Multiple processes in x-ray region—544(A)
**Langmuir, Irving** and **K. H. Kingdon.** Contact potential measurements with adsorbed films—129
——— (see Tonks, Lewi)—876
**Lansing, William D.** New terms in spectra of Al I, Ga I, and In I—597
**Laporte, O.** and **L. A. Young.** Regularities in ionization potentials of light elements —1225(L)
**Lawrence, Ernest O.** and **N. E. Edlefsen.** Photo-ionization of vapors of caesium and rubidium—233
——— and **Frank G. Dunnington.** Early stages of electric spark discharges—1624(L)
——— and **N. E. Edlefsen.** Photo-ionization of potassium vapor—1056
——— and **Leon B. Linford.** Effect of intense electric fields on photoelectric behavior of alkali films on tungsten—1492(L)
**Levin, Aaron.** (see Meyer, Charles F.)—44
**Lewis, Evan Jarrett.** Some thermal and electrical properties of beryllium—1575
**Lindsay, R. B.** Note on theory of acoustic wave filters—652
——— Connectors in acoustical conduits—808
——— Book review—383
**Linford, Leon B.** (see Lawrence, Ernest O.) —1492(L)
**Livingood, J. J.** Arc spectrum of platinum —185
**Loeb, Leonard B.** and **Lauriston C. Marshall.** Theory of recombination of gaseous ions —542(A)
——— Note concerning emission of beta-rays in radioactive change—1212

**Mack, J. E.** Vector coupling in nickel-, palladium- and platinum-like spectra—17
**Mackeown, S. S.** Cathode drop in electric arc—611
**Marshall, Lauriston C.** Recombination of ions and of ions and electrons in gases—541(A), 618
——— (see Loeb, Leonard B.)—542(A)
**Matuyama, E.** (see Okubo, J.)—1474
**Maxwell, Louis R.** Mean life for mercury spark spectrum—199
**McAlister, E. D.** and **H. J. Yearian.** New method of measuring thermal conductivities of gases—542(A)
——— Spectrum of neutral mercury atom in wave-length range from 1 to 2$\mu$—1142
**McKeehan, L. W.** Book Reviews—384, 660
**McMillen, J. H.** (see Hughes, A. Ll.)—291
**McRae, Daniel B.** (see Tolman, Richard C.) —1075
**Mendenhall, C. E.** Determination of Stefan-Boltzmann constant of radiation—502
**Merritt, Ernest.** Book Review—384
**Messenger, Helen A.** (see Webb, Harold W.) —1463
**Meyer, Charles F.** and **Aaron A. Levin.** On absorption spectrum of hydrogen chloride —44
**Miles, John B., Jr.** Dielectric constant and electric moment of some alcohol vapors —964
**Miley, H. A.** (see Pietenpol, W. B.)—1588
**Monk, George S.** (see Mulliken, Robert S.) —1530
**Morse, Philip M.** Diatomic molecules according to wave mechanics. II. Vibrational levels—57
**Mouzon, J. C.** (see Sutton, Richard M.) —547(A)
**Mulliken, Robert S.** and **George S. Monk.** Fine structure and Zeeman effects in helium band lines—1530
**Myers, Frank E.** and **R. T. Cox.** Transmission of $\beta$-rays through magnetized iron foil: attempt to polarize a beam of electrons —1067

**Nash, W. G.** (see Black, J. G.)—1138

**Naudé, S. M.** An isotope of nitrogen, mass 15—1498(L)
**Neuman, L. J.** Mechanism of spark discharge —550(A)
**Newbury, Kirsten.** Effect of light on electron emission from oxide-coated filaments—1418
**Niessen, K. F.** On saturation of electric and magnetic polarization of gases in quantum mechanics—253
**Okubo, J.** and **E. Matuyama.** On wave form of a sound produced by a spark—1474
**Olpin, A. R.** (see Ives, Herbert E.)—117
——— Apparent modulation of light by films of dielectrics on cathodes of alkali metal photoelectric cells—544(A)
**Olson, H. F.** (see Ellett, A.)—493
**Ornstein, L. S.** and **J. Rekveld.** Intensity measurements in Raman effect and distribution law of Maxwell-Boltzmann—720
**Osgood, Thomas H.** Ranges of ionizing electrons in helium—1234
**Ostensen, Floyd C.** A new method for study of voltage-intensity relations and its application to mercury 2537A line—1352
**Owen, G. E.** Dielectric losses at high frequencies—1035
**Page, Leigh.** Conductivity of ions in crossed electric and magnetic fields—763
**Parlin, W. A.** Effect of temperature on absorption bands of fused quartz in infra-red—81
**Pauling, Linus.** Photo-ionization in liquids and crystals and dependence of frequency of x-ray absorption edges on chemical constitution—954
——— (see Podolsky, Boris)—109
**Pearson, Gerald L.** Relative probabilities of ionization of $K$ and $L$-series electrons of equal ionization energy—542(A)
**Phipps, T. E.** (see Kurt, O. E.)—1357
**Pielemeier, W. H.** Pierce acoustic interferometer as an instrument for determination of velocity and absorption—1184
**Pietenpol, W. B.** and **H. A. Miley.** Electrical resistivities and temperature coefficients of lead, tin, zinc and bismuth in solid and liquid states—1588
**Plyler, E. K.** and **P. J. Steele.** Infra-red absorption spectra of organic nitrates—599
**Podolsky, Boris** and **Linus Pauling.** Momentum distribution in hydrogen-like atoms —109
——— and **Vladimir Rojansky.** On theory of Smekal-Raman effect in hydrogen-like atoms—1367
**Poole, C. A.** (see Black, J. G.)—1138
**Purks, Harris.** (see Davis, Bergen)—1, 181

**Race, Hubert H.** and **James R. Campbell, Jr.** Dielectric polarization potential and law of superposition for hard rubber—1031
**Rasetti, F.** Incoherent scattered radiation in diatomic molecules—367
——— Incoherent scattering and structure of diatomic molecules—548(A)
——— (see Dickinson, R. G.)—582
**Redeker, H. E.** (see Stowell, E. Z.)—978
**Reich, Herbert J.** New type of glow discharge tube—997(L)
**Rekveld, J.** (see Ornstein, L. S.)—720
**Rice, Oscar Knefler.** Temperature coefficient of radioactive disintegration—550(A)
——— On quantum mechanics of chemical reactions: predissociation and unimolecular decompositions—1451
**Richtmyer, F. K.** and **R. D. Richtmyer.** Satellites of x-ray lines $L\alpha$, $L\beta_1$, and $L\beta_2$ —574
**Richtmyer, R. D.** (see Richtmyer, F. K.) —574
**Robertson, H. P.** Uncertainty principle —163(L)
**Rojansky, V.** (see Hughes, A. Ll.)—284
——— (see Podolsky, Boris)—1367
**Rollefson, A. H.** Infra-red absorption spectrum of hydrogen sulphide—604
**Rollefson, G. K.** (see Christensen, Carl J.) —1154, 1157
**Russell, Henry Norris.** Book review—385
——— Arc spectrum of nickel—821
——— Letter to Editor—1394(L)

**Samson, E. W.** (see Turner, Louis A.) —743, 747
**Sawyer, R. A.** and **R. J. Lang.** Spectrum of gallium II and ($4s4p^2$) configuration in gallium I and indium I—712
**Sawyer, R. B.** Reflection of lithium ions from metal surfaces—1288(L)
**Schulwas-Sorokina, R. D.** Is it possible to determine piezoelectric constant at high temperatures by statical method?—1448
**Sears, R. W.** (see Smith, Alpheus W.)—1466
**Shenstone, A. G.** Secondary diffraction maxima of spectral lines—726
——— An unusual spectral series—1623(L)
**Slater, J. C.** Theory of complex spectra—1293
**Smith, Alpheus W.** and **R. W. Sears.** Hall effect in permalloy—1466
**Smith, H. L.** (see Duffendack, O. S.)—68

**Smith, K. O.** (see Carman, A. P.)—1040, 1042
**Smith, L. P.** Positive ion emission from tungsten and molybdenum—1496(L)
**Smith, Stanley.** Second spark spectrum of lead, Pb III—393
**Smith, W. O., Paul D. Foote** and **P. F. Busang.** Packing of homogeneous spheres—1271
**Smyth, Charles P.** Book review—166
**Spedding, Frank H.** (see Freed, Simon)—945
**Spence, B. J.** and **M. A. Easley.** Near infrared absorption spectra of some halogen derivatives of ethane—730
**Stauss, H. E.** Reflections of x-rays from platinum films sputtered on glass—1021
——— Errors in use of gratings with x-rays due to divergence of radiation—1601
**Steele, P. J.** (see Plyler, E. K.)—599
**Stewart, John Q.** Definition of frequency —1052
——— Indetermination principles involving $k$ and $e$—1289(L)
**Stockbarger, Donald C.** and **Laurence Burns.** On methods of filter radiometry—1263
**Stone, S. Bradford.** Kinetic correction in fluid flow—1391(L)
**Stowell, E. Z.** and **H. E. Redeker.** Role of hydrogen in oscillating arc—978
**Stueckelberg, E. G. C.** Simultaneous ionization and dissociation of oxygen and intensities of ultra-violet $O_2^+$ bands—65
**Sugiura, Y.** On transition probability between two states with positive energy in a central field—858
**Sutton, Richard M.** and **J. C. Mouzon.** Ionization of nitrogen and air by positive ion bombardment—547(A)

**Tate, John T.** Book reviews—382, 660, 998, 1065.
**Taylor, Josiah.** (see Heaps, C. W.)—937
**Tolman, Richard C.** and **Daniel B. McRae.** Experimental demonstration of equivalence of a mechanically oscillated electrostatic charge to an alternating current—1075
**Tonks, Lewi** and **Irving Langmuir.** General theory of plasma of an arc—876
**Turner, Louis A.** and **E. W. Samson.** Dissociation of nitrogen by electron impact —743
——— and **E. W. Samson.** Excitation potential of negative bands of nitrogen—747
**Uhlenbeck, G. E.** and **S. Goudsmit.** A problem in Brownian motion—145
**Urey, H. C.** and **John R. Bates.** Continuous spectra of flames containing halogens—1541
**Utterback, C. L.** Total radiation from nickel and cobalt—785

**Valasek, J.** Book review—1065, 1628
——— Precision measurements in $K$-series of elements 48 Cd and 49 In—1231
**Van den Akker, J. A.** (see Watson, E. C.) —547(A)
**Van Vleck, J. H.** Book review—1230
——— and **A. Frank.** Effect of second order Zeeman terms on magnetic susceptibilities in rare earth and iron groups—1494(L); correction—1625(L)
**Vieweg, Alice M.** (see Gibbs, R. C.)—400, 406
**Villars, Donald Statler.** Chemical heats of activation—1063(L)

**Wahlin, H. B.** Emission of positive ions from metals—164(L)
**Wang, S. C.** On the asymmetrical top in quantum mechanics—243
**Watson, E. C.** and **J. A. Van den Akker.** Differences in directions of ejection of x-ray photoelectrons from various atomic levels—547(A)
**Watson, William W.** Heat of dissociation at diatomic hydride molecules—372
——— Rotational instability and uncoupling of electronic orbital angular momentum from axis in diatomic molecules—1010
**Webb, Harold W.** and **Helen A. Messenger.** Short duration phosphorescence in fused quartz—1463
**Welo, L. A.** On absence of change in magnetic susceptibility with crystallization in strong magnetic fields—296
**White, H. E.** Interpretation of hyperfine structure in spectral lines—1288(L), 1404
——— Hyperfine structure in single ionized praseodymium—1397
**Whitelaw, Neill G.** Raman effect of ketones —376(L)
**Whitney, John D.** Inelastic collisions in mercury vapor—923
**Williams, John Warren.** (see Hollaender, Alexander)—380(L), 994.
——— (see Johnstone, J. H. L.)—1483
**Williamson, R. C.** Book review—1291
**Wilson, H. A.** Book review—382
——— On value of electronic charge— 1493(L)
**Winger, Ralph.** Valence of sulfur in dithionates —548(A)
——— Relation between lattice energy and shift in x-ray absorption edges—549(A)

**Wolfe, R. A.** (see Duffendack, O. S.)—409

**Yearian, H. J.** (see McAlister, E. D.)—542(A)
**Young, L. A.** (see Laporte, O.)—1225(L)
——— Binding energy of light atoms—1226(L)
**Young, O. B.** (see Carman, A. P.)—1040

**Zahl, H. A.** (see Ellett, A.)—493
**Zemansky, M. W.** Radii and collision probabilities of metastable neon and mercury atoms—213
**Zeleny, John.** Distribution of mobilities of ions in moist air—310
**Zener, Clarence** and **Victor Guillemin, Jr.** *B*-state of hydrogen molecule—999
**Zwicky, F.** On the possibility of a gravitational drag of light—1623(L)

# ANALYTIC SUBJECT INDEX TO VOLUME 34

References with (A) are to abstracts of papers presented at meetings of Physical Society. References with (L) are to Letters to Editor.


**Absorption of light (see also Spectra)**

Alkali vapors, dispersion and line width, S. A. Korff—457
Benzene and halogen derivatives, infra-red, J. Daugherty—1549
Crystals at low temperatures, line absorption, S. Freed, F. H. Spedding—945
Fused quartz, infra-red bands, effect of temperature, W. A. Parlin—81
Fog, L. P. Granath, E. O. Hulburt—140
Lower atmosphere, ultra-violet, L. H. Dawson, L. P. Granath, E. O. Hulburt—136
Organic nitrates, infra-red, E. K. Plyler, P. J. Steele—599
Oxygen, water vapor and quartz in ultra-violet, L. P. Granth—1045

**Acoustics**

Connectors in acoustical conduits, R. B. Lindsay—808
Pierce interferometer for measuring velocity and absorption of sound, W. H. Pielemeier—1184
Propagation in gas mixtures, theory, D. G. Bourgin—521
Speech power of speakers in auditoriums, V. O. Knudsen—549(A)
Wave-filters, theory, R. B. Lindsay—652
Wave form of sound produced by spark, J. Okubo, E. Matuyama—1474

**Activation**

Chemical heats, D. S. Villars—1063(L)

**Adsorption**

Air and water vapor on rock salt, J. H. Frazer—644
Air on glass, temperature variation, A. S. Adams—1438
Gas on sputtered Ni films, L. R. Ingersoll, J. D. Hanawalt—972

**Alpha-particles**

Recombination with electrons, probability, B. Davis, A. H. Barnes—152; theory, E. Q. Adams—537(L); discussion, A. H. Barnes—1229(L)

**Arc (see also Discharge of electricity in gases, Electrons in gases)**

Cathode drop, theory, S. S. Mackeown—611
Oscillating arc, role of hydrogen, E. Z. Stowell, H. E. Redeker—978
Sodium arc, high intensity, Carl J. Christensen, G. K. Rollefson—1154
Theory of plasma, L. Tonks, I. Langmuir—876

**Astrophysics**

Gravitational drag of light, F. Zwicky—1623(L)
Partial pressure of oxygen in sun, A. Christy—539(A)
Temperature of planets, E. O. Hulburt—1063(L)

**Atomic beams**

Of protons, reflection from crystals, A. J. Dempster—1493(L)
Reflection from crystals, A. Ellett, H. F. Olson, H. A. Zahl—493

**Atomic structure (see also Mechanics, quantum, Spectra, X-rays)**

Occupation of electron levels, from x-ray spectra, S. K. Allison—7
Momentum distribution in hydrogenic atoms, B. Podolsky, L. Pauling—109
Radii and collision probabilities of metastable Ne and Hg, M. W. Zemansky—213

**Atmospheric electricity (see also Geophysics)**

Ions and electric currents in upper atmosphere, E. O. Hulburt—1167

**Aurora**

Ultra-violet light theory of origin, E. O. Hulburt—344

**Barkhausen effect (see also Magnetic properties)**

Fe and Ni, C. W. Heaps, J. Taylor—937
Iron, nickel and permalloy, R. M. Bozorth—772

**Beta-rays**

Emission energies, discussion, L. B. Loeb—1212
Transmission through magnetized Fe foil, F. E. Myers, R. T. Cox—1067

**Book reviews**

Audubert, R., Ch. de Massacre, A. Buffat, L.

Durand, and G. Foex, Donneés Numériques d'Electricité Magnetisme et Electrochimie—382
Barus, Carl, Acoustic Experiments with the Pin-Hole Probe and the Interferometer U-Gauge—383
Birtwistle, George, The Principles of Thermodynamics—1230
Bragg, Sir William H., An Introduction to Crystal Analysis—384
Campbell, J. W., Numerical Tables of Hyperbolic and Other Functions—1065
Clark, W., T. Slater Price, B. V. Storr, Proceedings of the Seventh International Congress of Photography—1628
Debye, P., Polar Molecules—1230
Eberhard, G., A. Kohlschutter, and H. Ludendorff, Handbuch der Astrophysik. Bd. IV—385
Errera, J., Polarisation Dielectrique—166
Eucken, A., Energie und Wärmeinhalt—998
Fitch, A. L., Fundamentals of Physics—1291
Fletcher, Harvey, Speech and Hearing—1396
Frenkel, J., Einführung in die Wellenmechanik—1065
Gmelin's Handbuch der Anorganischen Chemie, System-Nummer 21: Natrium, System-Nummer 31: Radium und Isotope, System-Nummer 59: Eisen—660
Guertler, W. and W. Leitgebel, Vom Erz zum Metallischen Werkstoff—383
Günther-Schulze, A., Elektrische Gleichrichter und Ventile—820
Kilby, C. M., Introduction to College Physics—1291
Manfred von Ardenne, Verstärkermesstechnik—1291
McDonald, Philip B., English and Science—660
Milne-Thomson, L. M., Standard Table of Square Roots—998
Pacotte, Julien, Les Methodes Nouvelles en Analyse Quantique—1230
Pettersson, Hans, Künstliche Verwandlung der Elemente—166
Rawlins, F. I. G. and A. M. Taylor, Infra-Red Analysis of Molecular Structure—1395
Rinne, Friedrich, Zur Nomenklatur der 32 Kristallklassen. Über eine neue Herleitung und Nomenklatur der 230 Kristallographischen Raumgruppen. Ernst Schiebold—384
Schottky, W., H. Ulich and C. Wagner, Thermodynamik. Die Lehre von den Kreisprozessen, den physikalischen und chemischen Veränderungen und Gleichgewichten. Eine Einführung zu den thermodynamischen Problemen unserer Kraft- und Stoffwirtschaft—819
Sheldon, H. Horton and E. N. Grisewood, Television—1396
Wagner, Albert F., Experimental Optics—1065
Wien und Harms, Handbuch der Experimentalphysik. Bd. 13, Teil I. Die Ionenleitung in Gasen, Shweidler. Teil II. Die Elektrischen Eigenschaften der Flamme, Becher—382
Wien und Harms, Handbuch der Experimentalphysik. Bd. 18. K. F. Bottlinger, R. Ladenburg, M. v. Laue, Hans Schulz, and E. Warburg—1628
Wien und Harms, Handbook der Experimentalphysik. Bd. 23, Phosphoreszenz. P. Lenard, F. Schmidt and R. Tomaschek—384

**Brownian motion**
Rotatorial, of small mirror, theory, G. E. Uhlenbeck, S. Goudsmit—145

**Chemical reaction**
Quantum mechanics of, R. M. Langer—92; O. K. Rice—1451

**Compressibility**
Liquids, J. H. Hildebrand—649

**Compton effect**
Fine structure, B. Davis, H. Purks—1
Relation to temperature, G. E. M. Jauncey, H. Bauer—387

**Conductivity, electrical (see Electrical conductivity)**
**Conductivity, thermal (see Thermal conductivity)**

**Contact potential**
Measurements with absorbed films on tungsten, I. Langmuir, K. H. Kingdon—129

**Cosmic radiation**
Nature, L. F. Curtiss—1391(L)

**Crystals and crystal structure**
Bi, effect of magnetic force on formation, A. Goetz, R. C. Hergenrother, A. B. Focke—546(A)
Bi, grown in magnetic fields, electric volume effects, A. Goetz, M. Hassler—549(A)
Energy changes by variation from crystallographic group, H. M. Evjen—1385
Lattice energy and shift in x-ray absorption energies, R. Winger—549(A)
Sputtered Ni films, L. R. Ingersoll, J. D. Hanawalt—972

**Dielectric properties**
Alcohol vapors, J. B. Miles, Jr.—964
Argon, neon, constants, A. B. Bryan—615
$CH_3$ and Br radicals, electric moments, C. R. Daily—548(A)
Conducting liquids, method of measuring, A. Astin—300
Electrolytes, dielectric constants, measurements, A. P. Carman, K. O. Smith—1042

Electrolytes, dielectric constants, method, A. P. Carman, O. B. Young, K. O. Smith—1040
Hard rubber, polarization potential and law of superposition, H. Race, J. R. Campbell, Jr.—1031
Power losses at high frequencies, G. E. Owen—1035
Saturation of electric polarization in gases, K. F. Niessen—253
Variation with frequency, J. H. L. Johnstone, J. W. Williams—1483

**Diffraction of light (see also X-rays)**
In spectra, secondary maxima, A. G. Shenstone—726

**Diffraction of matter (see also Electron diffraction)**
Atomic beams, reflection from crystal, A. Ellett, H. F. Olson, H. A. Zahl—493
Proton beams, reflection from crystal, A. J. Dempster—1493(L)

**Discharge of electricity in gases (see also Arcs, Electrons in gases, Spark discharge)**
Electrodeless ring discharge, nature, C. J. Brasefield—1393(L), 1627(L)
New type of glow discharge tube, H. J. Reich—997(L)

**Discharge of electricity in high vacua**
Electron emission in high fields, theory, P. W. Bridgman—1411

**Disintegration of nucleus**
By artificial means, possibility, G. Breit—817(L)

**Dispersion of light**
In alkali vapors, absorption line width, S. A. Korff—457

**Electric moment**
Alcohol vapors, J. B. Miles, Jr.—964
$CH_3$ and Br radicals, C. R. Daily—548(A)

**Dissociation**
Nitrogen by electron impact, L. A. Turner, E. W. Samson—743
$O_2$, by electron impact, theory, E. C. G. Stueckelberg—65

**Dissociation, heat of**
$O_2$ and $N_2$, from spectra, R. T. Birge—1062(L)
$O_2$, calculation, L. S. Kassel—817(L)
Of diatomic hydride molecules, from spectra, W. W. Watson—372

**Elasticity**
Conically wound spring, extension and period, O. B. Ader—656

**Electrical conductivity**
Bi crystals grown in magnetic field, A. Goetz, M. Hassler—549(A)
Metals, temperature dependence, theory, W. V. Houston—279, 547(A)
Ions in crossed electric and magnetic fields, L. Page—763
Pb, Sn, Zn, Bi, solid and liquid, temperature coefficients, W. B. Pietenpol, H. A. Miley—1588
Poor conductors, influence of surface conditions and space charges, K. F. Herzfeld—791
Thin K layer, effect of hydrogen, H. R. Laird—463

**Electrical properties**
Be, E. J. Lewis—1575

**Electromagnetic theory**
Effect of retardation on interaction of two electrons, G. Breit—553
Equivalence of an oscillating charge to an alternating current, R. C. Tolman, D. B. McRae—1075

**Electron, charge**
Value of $e$, discussion, H. A. Wilson—1493 (L)

**Electron, diffraction**
By Cu crystal, H. E. Farnsworth—679; discussion, S. B. Hendricks—1287(L)

**Electrons (see also Thermionic emission)**
Attempt to polarize beam by transmission through magnetized Fe foil, F. E. Myers, R. T. Cox—1067
Emission by metastable atoms, C. G. Found—1625(L)
Interaction of two electrons, theory, G. Breit—375(L)
Motion in electrostatic fields, analysis of velocity, A. Ll. Hughes, V. Rojansky—284; refocussing of electron paths, A. Ll. Hughes, J. H. McMillen—291
Polarization of beam, test for, C. T. Chase—1069

**Electrons in gases**
Alkali metal vapors, absorption, R. B. Brode—673
Atomic and molecular hydrogen, G. P. Harnwell—661
Dissociation of nitrogen, L. A. Turner, E. W. Samson—743
Hg, efficiency of excitation of λ2537, F. C. Ostensen—1352
Hg vapor, inelastic collisions, probabilities, W. H. Brattain—474; John D. Whitney—923
In He, ranges, T. H. Osgood—1234
Theory of arc plasma, L. Tonks, I. Langmuir—876

**Electrons in metals (see also Electrical conductivity)**
Emission under high fields, theory, P. W. Bridgman—1411

**Electron scattering**
In hydrogen, angular distribution, G. P. Harnwell—162(L); discussion, J. Kaplan—1227(L)
Hg vapor, anomalous, W. H. Brattain—474
Test for polarization, C. T. Chase—1069

**Electrons, secondary**
From Cu crystal, H. E. Farnsworth—679

From grid under $Cs^+$ ion bombardment, J. M. Hyatt—486

**Energy states (see also Spectra)**

Of light atoms, binding energy, L. A. Young—1226(L)

**Errata**

To propagation of Schroedinger waves in uniform field, G. Breit—1491

To perterbations in molecules and theory of predissociation and diffuse spectra, O. K. Rice—1462

To effect of second order terms on magnetic susceptibilities, J. H. Van Vleck, A. Frank—1625(L)

**Excitation of atoms and molecules**

Diatomic molecules by positive ions and excited atoms, O. S. Duffendack, H. L. Smith—68

Excitation of Mg II spectrum by impacts of second kind, O. S. Duffendack, Clement L. Henshaw, Marie Goyer—1132

Hg, radius, E. Gaviola—1049

**Field currents**

Theory, P. W. Bridgman—1411

**Flames**

Containing halogens, continuous spectra, H. C. Urey, J. R. Bates—1541

**Fluorescence**

Na vapor, transition probabilities, C. J. Christensen, G. K. Rollefson—1157

Organic solutions, effect of temperature, J. R. Jenness—1275

Quenching collisions in Hg vapor, efficiency, E. Gaviola—1049

Resonance-fluorescence in CN spectrum, H. T. Byck—453

**Frequency**

Definition of, J. Q. Stewart—1052

**Frequency analyzer**

Electro-mechanical, L. P. Delsasso—550(A)

**Fugacities**

In gaseous mixtures, calculation, L. J. Gillespie—1605

**Furnace spectra (see Spectra)**

**Galvanomagnetic effects**

Hall effect in permalloy, A. W. Smith, R. W. Sears—1466

**Gamma rays**

Status of gamma-ray change, N. Feather—1558

**Geissler discharge (see Discharge of electricity through gases)**

**Geophysics**

Ions and electric currents in upper atmosphere, E. O. Hulburt—1167

Magnetic field of sun and earth, theory, R. Gunn—335; correction—1621

Ultra-violet light theory of aurorae magnetic and storms, E. O. Hulburt—344

**Hall effect**

In permalloy, A. W. Smith, R. W. Sears—1466

**Heat conductivity (see Thermal conductivity)**

**Hydrodynamics**

Fluid flow, kinetic correction. S. B. Stone—1392(L)

**Indetermination principles**

Involving $k$ and $e$, J. Q. Stewart—1289(L)

**Intensities in spectra**

Forbidden nebular lines, theory, J. H. Bartlett, Jr.—1247

HCl, harmonic band, J. L. Dunham—438

Hg, λ2537, voltage-intensity, F. C. Ostensen—1352

Hydrogen, as function of electron velocity, C. J. Brasefield—431

$Li_2$ absorption bands, alternating intensities, A. Harvey, F. A. Jenkins—1286(L)

Mg 4571 and 2852, effect of foreign gases, J. G. Frayne—546(A), 590

Ti I, intensities in super-multiplets, G. R. Harrison—540(A)

Ti II, in generalized multiplet, H. Engwicht—541(A)

Vacuum furnace for measurement, G. R. Harrison—545(A)

**Ionization**

Diatomic molecules by positive ions and excited atoms, O. S. Duffendack, H. L. Smith—68

Hg vapor, ionization potentials for $Hg^+$, $Hg^{2+}$, $Hg^{3+}$, $Hg^{4+}$, Walker Bleakney—157

$K$ and $L$-series electrons, relative probabilities, G. L. Pearson—542(A)

$N_2$ and air by positive ions, R. M. Sutton, J. C. Mouzon—547(A)

$O_2$, by electron impact, theory, E. C. G. Stueckelberg—65

**Ionization by radiation (see Photo-ionization)**

**Ions**

Emission from metals, H. B. Wahlin—164(L)

Emission from W and Mo, L. P. Smith—1496(L)

$Li^+$, reflection from metals, R. B. Sawyer—1288(L)

Motion in crossed electric and magnetic fields, L. Page—763

Recombination in gases, L. C. Marshall—541(A), 618; theory, L. B. Loeb, L. C. Marshall—542(A)

Reflection of $H^+$ from crystals, A. J. Dempster—1493(L)

Scattering of $Li^+$ in Hg vapor, I. W. Cox—1426

**Ions, mobility**
In moist air, J. Zeleny—310
Nature of ions in air, H. A. Erikson—635
**Isotopes**
Ag and Cl, from AgCl spectrum, B. A. Brice—1227(L)
Carbon, from band spectra, A. S. King, R. T. Birge—376(L); further evidence—379(L)
Nitrogen, S. M. Naudé—1498(L)
Oxygen, relative abundance, from spectra, H. D. Babcock—540(A)
**Joule-Thomson effect**
For air, O. C. Bridgeman—527
**Liquids**
Intermolecular forces, J. H. Hildebrand—984
**Magnetic fields**
Of sun and earth, theory, R. Gunn—335; correction—1621
**Magnetic properties**
Bi, effect on single crystal formation, A. Goetz, R. C. Hergenrother, A. B. Focke—546(A)
Fe and Ni, Barkhausen effect, C. W. Heaps, J. Taylor—937
Iron, nickel and permalloy, Barkhausen effect, R. M. Bozorth—772
Isolated ferromagnetic atoms, F. W. Constant—548(A), 1217
Ni and Fe films, J. H. Howey—1440
Oxygen, magnetic moment, O. E. Kurt, T. E. Phipps—1357
Permalloy, Hall effect, A. W. Smith, R. W. Sears—1466
Saturation of magnetic polarization of gases, quantum theory, K. F. Niessen—253
Susceptibilities of crystals, absence of change with crystallization in strong fields, L. A. Welo—296
Susceptibilites of rare earth and iron group, effect of second order Zeeman terms, J. H. Van Vleck, A. Frank—1494(L); errata—1625(L)
**Magnetic storms**
Ultra-violet light theory of origin, E. O. Hulburt 344
**Mechanics, quantum**
Asymmetrical top, S. C. Wang—243
*B* state of $H_2$, C. Zener, V. Guillemin, Jr.—999
Chemical reaction, R. M. Langer—92
Chemical reaction, O. K. Rice—1451
Complex spectra, J. C. Slater—1293
Continuous x-rays, C. Eckart—167
Diatomic molecules, vibrational levels, P. M. Morse—57
Hyperfine structure, H. E. White—1404; 1288(L)
Intensities of forbidden nebular lines, J. H. Bartlett, Jr.—1247
Interaction of two electrons, G. Breit—553(L)
Magnetic susceptibility, effect of second order Zeeman terms, J. H. Van Vleck, A. Frank—1494(L); errata—1625(L)
Metallic conductivity at low temperatures, W. V. Houston—279
Momentum distribution in hydrogenic atoms, B. Podolsky, L. Pauling—109.
Perturbation in molecules and theory of predissociation and diffuse spectra, a correction, O. K. Rice—1462
Propagation of Schroedinger waves in uniform field, a correction, G. Breit—1491
Saturation of electric and magnetic polarization of gases, K. F. Niessen—253
Smekal-Raman effect in hydrogenic atoms, B. Podolsky, V. Rojansky—1367
Transition probabilities, E. L. Kinsey, J. Kaplan—546(A); Y. Sugiura—858
Uncertainty principle, H. P. Robertson—163(L)
**Mechanics, statistical**
Generalized form of new statistics, S. Chandrasekhar—1204
**Metastable atoms**
Electron emission by, C.G. Found—1625(L)
Life and concentration, E. Gaviola—1373
Ne and Hg, radii and collision probabilities, M. W. Zemansky—213
Of rare gases, excitation of Mg II spectrum by collision, O. S. Duffendack, C. L. Henshaw, M. Goyer—1132
**Meteorology**
Wind mixing and diffusion in upper atmosphere, E. O. Hulburt—161(L)
**Methods and instruments**
Electro-mechanical frequency analyzer, L. P. Delsasso—550(A)
Electrostatic analyzer of electron velocities, A. Ll. Hughes, V. Rojansky—284, 291
For determining hysteresis loops in small specimens, C. W. Heaps, J. Taylor—937
For filter radiometry, D. C. Stockbarger, L. Burns—1263
For measuring dielectric constants of conducting liquids, A. Astin—300
For measuring dielectric constants of electrolytes, A. P. Carman, O. B. Young, K. O. Smith—1040
For measuring power losses in dielectrics at high frequencies, G. E. Owen—1035
For measuring thermal conductivities of gases, E. D. McAlister, H. J. Yearian—542(A)
For positive ray analysis, W. Bleakney—157

Glow discharge tube, new type, H. J. Reich—997(L)
Photoelectric cell for erythema, F. W. Cook—1287(L)
Projection lantern microphotometer, C. E. Hesthal, G. R. Harrison—543(A)
Sodium arc of high intensity, C. J. Christensen, G. K. Rollefson—1154
Use of series inductance in vacuum spark spectra, R. C. Gibbs, A. M. Vieweg, C. W. Gartlein—406
Vacuum furnace for spectra, O. S. Duffendack, J. G. Black—35
Vacuum furnace for spectral intensity measurements, G. R. Harrison—545(A)
Vacuum tube calibration, J. M. Hyatt—486

**Microphotometer**
For projection lantern, C. E. Hesthal, G. R. Harrison—543(A)

**Mobility of ions (see Ions, mobility)**

**Modulation of light**
By dielectric films on alkali metals, A. R. Olpin—544(A)
By Kerr cell, A. Bramley—1061(L); comments, J. Cabannes—1497(L)

**Molecular structure (see also Spectra, molecular)**
Constants for $Na_2$, from spectrum, W. R. Fredrickson—207
Rotational instability and uncoupling of electronic orbital angular momentum from axis in diatomic molecules, W. W. Watson—1010

**Motor, electric**
Self-regulating, L. E. Dodd—545(A)

**Nucleus**
Disintegration by artificial means, possibility, G. Breit—817(L)
Regularities in existing types, H. A. Barton—1228(L)
Symmetry of nuclear wave functions, B. Cassen—1061(L)

**Optics, geometrical**
Field of view for two variable plane mirrors, L. E. Dodd—543(A)

**Packing**
Of homogeneous spheres, W. O. Smith, P. D. Foote, P. F. Busang—1271

**Paschen-Back effect**
In hyperfine structure, S. Goudsmit, R. F. Bacher—1499(L)

**Periodic system**
New graphical arrangement, A. E. Caswell—543(A)

**Phosphorescence**
Fused quartz, duration, H. W. Webb, H. A. Messenger—1463

**Photoelectric cell**
For use in erythema, F. W. Cook—1287(L)

**Photoelectric effect**
Alkali metal films, effect of intense electric fields, E. O. Lawrence, L. B. Linford—1492
Alkali metals, maximum long wave limit, H. E. Ives, A. R. Olpin—117
Cerium dioxide, effect on thermionic emission, C. E. Berger—1566
Gases, by x-rays, direction of ejection, C. D. Anderson—547(A); E. C. Watson, J. A. Van den Akker 547(A)
Modulation of light by dielectric films on alkali metals, A. R. Olpin—544(A)
Oxide-coated filaments, influence on thermionic emission, K. Newbury—1418
Threshold for doubly evaporated films, R. B. Jones—227

**Photo-ionization**
Cs and Rb vapor, E. O. Lawrence, N. E. Edlefsen—233
Liquids and crystals, theory, L. Pauling—954
K vapor, E. O. Lawrence, N. E. Edlefsen—1056

**Piezo-electric effect**
Determination of constant, R. D. Schulwas-Sorokina—1448

**Planets**
Temperature, E. O. Hulburt—1063(L)

**Positive ions (see Ions)**

**Positive ray analysis**
Of ions produced in Hg vapor, W. Bleakney—157
Search for element 87, K. T. Bainbridge—752

**Potentials, critical**
For excitation of negative bands in nitrogen, L. A. Turner, E. W. Samson—747
Hg, efficiency of excitation of 6.7, W. H. Brattain 474
Ionization potentials of $Hg^+$, $Hg^{2+}$, $Hg^{3+}$, $Hg^{4+}$, W. Bleakney—157
Ionization of Cu II, G. Kruger—1122
Ionization of Ga II, spectroscopic, R. A. Sawyer, R. J. Lang—712
Ionization of Ni I, H. N. Russell—821
Ionization potentials of light elements, regularities, O. Laporte, L. A. Young—1225(L)

**Proceedings**
American Physical Society, Berkeley meeting, June 21 and 22, 1929—538

**Protons**
Reflection from crystals, A. J. Dempster—1493(L)

**Quantum theory (see Mechanics, quantum)**

**Raman effect**
Crystalline sulfates and water solutions, A. Hollaender, J. W. Williams—994
Diatomic molecules, F. Rasetti—367, 548(A)

Frequency distribution, D. H. Andrews—1626(L)
Ketones, N. G. Whitelaw—376(L)
Plate glass, A. Hollaender, J. W. Williams—380(L)
Polyatomic gases, R. G. Dickinson, R. T. Dillon, F. Rasetti—582
Quantum mechanical theory, B. Podolsky, V. Rojansky—1367
Relation of intensity of lines to Maxwell-Boltzmann law, L. S. Ornstein, J. Rekveld—720
Spectra of electric discharges, J. Kaplan—1393(L)
Water, E. L. Kinsey—541(A)

**Radiation, black body**
Stefan-Boltzmann constant, determination, C. E. Mendenhall—502

**Radiation, thermal**
From Ni and Co, C. L. Utterback—785
From polished and soot-covered nickel, B. T. Barnes—1026

**Radioactivity**
Beta-ray emission, energies, discussion, L. B. Loeb—1212
Status of gamma-ray charge, N. Feather—1558
Temperature coefficient, O. K. Rice—550(A)

**Radiometry**
Methods of filter radiometry, D. C. Stockbarger, L. Burns—1263

**Recombination**
Alpha-particles and electrons, probability as function of relative velocity. B. Davis, A. H. Barnes—152; theory, E. Q. Adams—537(L); discussion, A. H. Barnes—1229(L)
Atoms, theory, E. L. Kinsey, J. Kaplan—545(A)
Ions and electrons in gases, L. C. Marshall—541(A), 618; theory, L. B. Loeb, L. C. Marshall—542(A)

**Reflecting power**
Calcite crystals for x-rays, B. Davis, H. Purks—181

**Relativity**
Coefficients of, S. R. Cook—549(A)

**Resonance radiation**
Excitation of spectra, O. S. Duffendack, J. G. Black—35
Quenching in Hg, E. Gaviola—1373

**Scattering of electrons (see Electrons in gases)**

**Scattering of ions (see Ions)**

**Scattering of light (see also Raman effect)**
By Kerr cell, A. Bramley —1061(L), discussion, J. Cabannes—1497 (L)

**Scattering of radiation (see Raman effect, X-rays)**

**Sound (see Acoustics)**

**Spark discharge**
Early stages, E. O. Lawrence, F. G. Dunnington—1624(L)
Mechanism,L. J. Neuman—550(A)
Phenomenon in rotary spark gap, R. E. Burroughs—161(L)

**Specific heat**
Air, constant pressure, O. C. Bridgeman—527
Be, E. J. Lewis—1575
Gases and mixtures of gases, theory, J. A. Beattie 1615—

**Spectra, atomic**
Al I, Ga I, In I, new terms, W. D. Lansing—597
C II, N II, additional series lines, I. S. Bowen—534
C II, N II, low energy states, I. S. Bowen—540
Cu I, Cu II, Mn II, in vacuum furnace, O. S. Duffendack, J. G. Black—35
Cu II, extension of analysis, G. Kruger—1122
Eu, Gd, Tb, Ds, Ho, furnace spectra, A. S. King—540(A)
Ga II, Ga I, In I, classification, R. A. Sawyer, R. J. Lang—712
Gd, by absorption of $GdCl_3$ crystal, S. Freed, F. H. Spedding—945
Ge II, Ge III, Ge IV, new terms and combinations, R. J. Lang—697
Hf, furnace, arc and spark, A. S. King—544(A)
Hg I, from 1 to 2$\mu$, wave-lengths and classification, E. D. McAlister—1142
Hg II, III, IV, mean life, L. R. Maxwell—199
H, intensities as function of electron velocity, C. J. Brasefield—431
Hyperfine structure, interpretation, H. E. White 1404
Hyperfine structure, Paschen-Back effect, S. Goudsmit, R. F. Bacher—1499(L), 1501
Hyperfine structure, theory, H. E. White—1288(L)
Intensities of lines, vacuum furnace for measurements, G. R. Harrison—545(A)
Mg II, by impacts of second kind with ions and metastable atoms, O. S. Duffendack, C. L. Henshaw, M. Goyer—1132
Mg 4571 and 2852, effect of gases on intensity, J. G. Frayne—590
Mg 4571, effect of gases on intensity, J. G. Frayne—546(A)
Nebular forbidden lines, theory of intensity, J. H. Bartlett, Jr.—1247
N I, C I, classification, S. B. Ingram—421
N I, excitation, wave-lengths and classification, O. S. Duffendack, R. A. Wolfe—409
Ni I, analysis, H. N. Russell—821; note—1394(L)
O I, new terms, R. Frerichs—1239
Pb III, Tl II, analysis, S. Smith—393
Pb V, classification, J. E. Mack—17.
$Pr^+$, hyperfine structure, H. E. White—1397

Pt I, analysis, J. J. Livingood—185
Sb IV, Te V, extension of Cd I-like isoelectronic sequence, R. C. Gibbs, A. M. Vieweg—400
Theory of complex spectra, J. C. Slater—1293
Ti I, intensities in supermultiplets, G. R. Harrison—540(A)
Ti II, intensities in generalized multiplet, H. Engwicht—541(A)
Tl IV, classification, J. E. Mack—17.
Unusual spectral series, A. G. Shenstone—1623(L)
Vector coupling in Ni, Pd, Pt-like spectra, J. E. Mack—17
Zn, influence of A and $H_2$, J. G. Black, W. G. Nash, C. A. Poole—1138

**Spectra, continuous**
Of flames containing halogens, H. C. Urey, John R. Bates—1541

**Spectra, molecular**
AgCl, isotope effect, B. A. Price—1227(L)
Benzene and halogen derivatives, infra-red absorption, J. F. Daugherty—1549
CN, resonance-fluorescence phenomenon, H. T. Byck—453
CO and $N_2$, excited by positive ions and excited atoms, O. S. Duffendack, H. L. Smith—68
CO, comet-tail bands, L. H. Dawson, J. Kaplan—379(L)
$CO_2$, electronic bands, J. F. Duncan—1148
Diatomic molecules, rotational instability and uncoupling of electronic orbital angular momentum, W. W. Watson—1010
Diatomic molecules, wave mechanics, P. M. Morse—57
Diffuse, perturbation and predissociation, theory, a correction, O. K. Rice—1462
Doublet band, Zeeman effect, E. L. Hill—1507
Flames containing halogens, H. C. Urey, J. R. Bates—1541
Halogen derivatives of ethane, near infra-red, B. J. Spence, M. A. Easley—730
HCl, absorption, C. F. Meyer, A. A. Levin—44
HCl, analysis of bands, W. F. Colby—53
HCl, intensities in harmonic band, J. L. Dunham—438
He band lines, fine structure and Zeeman effects, R. S. Mulliken, G. S. Monk—1530
$H_2$, intensities as function of electron velocity, C. J. Brasefield—431
$H_2S$, infra-red absorption, A. H. Rollefson—604
$H_2$, theory of *B* state, C. Zener, V. Guillemin, Jr.—999
$Li_2$, alternating intensities, A. Harvey, F. A. Jenkins—1286(L)
MgH, Zeeman effect, G. M. Almy, F. H. Crawford—1517
$Na_2$, rotational structure, W. R. Fredrickson—207
$N_2$, excitation potential for negative bands, L. A. Turner, E. W. Samson—747
$NH_3$, vibration spectrum, J. W. Ellis—539(A)
NO, beta bands, J. Kaplan—165(L)
$O_2$, intensities in ultra-violet, theory, E. C. G. Stueckelberg—65
Organic nitrates, absorption in infra-red, E. K. Plyler, P. J. Steele—599
Ti O, new band system, analysis, A. Christy—539(A)

**Spectra, Raman (see Raman Effect)**
**Spectra, X-ray (see X-ray, spectra)**

**Spectroscopy, technique**
Secondary diffraction maxima of spectral lines, A. G. Shenstone—726
Use of series inductance in vacuum spark spectra, R. C. Gibbs, A. M. Vieweg, C. W. Gartlein—406

**Sputtered films**
Ni, properties, L. R. Ingersoll, J. D. Hanawalt—972

**Statistical mechanics (see Mechanics, statistical)**

**Stefan-Boltzmann constant**
Determination, C. E. Mendenhall—502

**Surface tension**
Hg, in gases, S. G. Cook—513

**Thermal conductivity**
Gases, new method, E. D. McAlister, H. J. Yearian—542(A)

**Thermal expansion**
Ta, P. Hidnert—544(A)

**Thermal properties**
Be, E. J. Lewis—1575

**Thermionic emission of electrons**
By cerium dioxide, effect of light, C. E. Berger—1566
From K, effect of hydrogen, H. R. Laird—463
From oxide-coated filaments, characteristics, J. A. Becker—1323
From oxide-coated filaments, influence of light, K. Newbury—1418

**Thermodynamics**
Compressibilities and thermal pressure coefficients of liquids, J. H. Hildebrand—649
Fugacities in gaseous mixtures, calculation, L. J. Gillespie—1605
Heat capacities of gases and gaseous mixtures, J. A. Beattie—1615
Intermolecular attractions in liquids, J. H. Hildebrand—542(A)
Joule-Thomson effect and $C_p$ for air, O. C. Bridgeman—527
Of gases and mixtures, fugacities, L. J. Gillespie—352

Of liquids, intermolecular forces, J. H. Hildebrand—984

**Thermoelectric effect**
Bi, crystal grown in magnetic field, A. Goetz, M. Hassler—549(A)

**Transition probabilities**
In Na vapor, influence of method of excitation, C. J. Christensen, G. K. Rollefson—1157

**Vacuum tube**
Distribution of electrons between plate and grid, J. M. Hyatt—486

**Valence**
Of S, from x-ray absorption, R. Winger—548(A)

**Vapor pressure**
Of K, Rb, Co, K. T. Bainbridge—752

**Wave-filters**
Acoustical, theory, R. B. Lindsay—652

**Wave mechanics (see Mechanics, quantum)**

**Work function (see also Thermionic emission)**
Relation to contact potentials, for absorbed films on tungsten, I. Langmuir, K. H. Kingdon —129

**X-rays, absorption**
Dependence of frequency on chemical constitution, theory, L. Pauling—954
In crystals, effect of lattice energy, R. Winger —549(A)
Of S, relation to valence, R. Winger—548(A)
Pt and Au, *M*-series, A. J. M. Johnson—1106

**X-rays, continuous**
Intensity, quantum mechanical theory, C. Eckart —167; Y. Sugiura—858

**X-rays, diffraction**
By gratings, errors due to divergence, H. E. Stauss—1601
Of Cu and Fe for Mo and Cu radiation, A. H. Armstrong—931

**X-rays, photoelectric effect**
Direction of ejection, E. C. Watson, J. A. Van den Akker—547(A)
In gases, direction of ejection, C. D. Anderson —547(A)

**X-rays, reflection**
By calcite, B. Davis, H. Purks—181
Classical scattering, P. Kirkpatrick, M. Dewar —549(A)
From diamond, intensity, A. H. Armstrong—1115
From Pt films sputtered on glass, H. E. Stauss —1021
Of C $K\alpha$ from glass, E. Dershem—1015

**X-rays, scattering**
Fine structure in Compton effect, B. Davis, H. Purks—1
From Al and Cu, effect of temperature on Compton shift, G. E. M. Jauncey, H. Bauer—387

**X-rays, spectra**
Cd and In *K*-series, precision measurements, J. Valasek—1231
Components of $L\beta_2$ and relative widths of lines, S. K. Allison—176
Fine structure in Compton effect, B. Davis, H. Purks—1
Multiple excitation, R. M. Langer, S. B. Hendricks—544(A)
Pt and Au, *M*-series absorption, A. J. M. Johnson —1106
Relative intensities, S. K. Allison—7
Satellites of $L\alpha$, $L\beta_1$, $L\beta_2$, F. K. Richtmyer, R. D. Richtmyer—574

**Zeeman effect**
Effect of second order terms on susceptibilities of rare earth and iron group, J. H. VanVleck A. Frank—1494 (L); errata—1625(L)
In doublet band spectra, E. L. Hill—1507
In MgH bands, G. M. Almy, F. H. Crawford —1517
In He band lines, R. S. Mulliken, G. S. Monk —1530
In Pt I spectrum, J. J. Livingood—185

# The Physical Review Supplement

## ARTICLES IN PREPARATION

The following reviews are being prepared and will appear in forthcoming issues of the Supplement.

***Thermionic Emission*** - - - - - - - - - - - - SAUL DUSHMAN

Theory, technique of measurements, data for pure metals and coated surfaces, behavior of thoriated, caesiated and oxide coated filaments. Schottky and cold-cathode effects, effect of gases, effect of space charge and magnetic fields.

***Electrodynamics and Relativity*** - - - - - - - - W. F. G. SWANN

A review of the historical origin of electrodynamics and restricted relativity; their present logical significance and basis; their place in the new quantum mechanics. An outline of the significant facts and features pertaining to the general theory of relativity and its relation to the restricted theory.

***Review of Line Spectroscopy*** - - - - - - - - - - R. C. GIBBS

Illustrative description and theory of various kinds of line spectra, Landé's interval rule, Hund's rule for relative position of terms, iso-electronic sequences, regular and irregular doublet laws, series limits, ionization potentials, displacement law, intensity rules, criteria used in identification work, Zeeman effect, hyperfine structure.

***Quantum Mechanics of Collision Processes*** - - - - - E. U. CONDON

The principles underlying and the results of the theoretical treatment of simpler problems in which particles are scattered by fields of force and by atoms.

***Application of Group Theory to the Quantum Mechanics of Monatomic Systems*** - - - - - - - - - - - - - - - CARL ECKART

A review of the quantum dynamics of complex atomic spectra. The rigorous selection principles and sum rules are derived from the symmetry of the wave equation, and the theory of the periodic table of elements is treated by perturbation methods. Practicable methods for solving the secular equations are discussed.

***Magnetism in Discontinuous Media*** - - - - - - L. W. MCKEEHAN

A discussion, in terms of modern ideas concerning atoms and their interactions, of experimental results, both old and new, which theories of magnetism have ignored or endeavored to explain.

***Electrical Conductivity of Flames*** - - - - - - - - H. A. WILSON

(1) Relation between current, potential and distance between electrodes in a Bunsen flame.
(2) Conductivity of alkali metal vapors in flames.
(3) Conductivity of flames for alternating currents.
(4) Mobility of the ions in flames.
(5) Effects of a magnetic field on the conductivity of flames.

***Polyatomic Molecules and Their Infra-Red Spectra*** - - - - - - - - - - - - - - - - - - - - - - - - - - - - DAVID M. DENNISON

In treating the problem of polyatomic molecules a review is made of the theory of their vibrations and rotations. A survey is given of the principle experimental data and these are critically discussed in the light of the theory to show in what cases the essential features of the bands may be explained.

# The Physical Review Supplement

## SUBSCRIPTION PRICE

To members of the American Physical Society or of the American Chemical Society ..... per year $3.00

To all others ..... per year 4.00

Single copies ..... 1.25

Address all correspondence to THE PHYSICAL REVIEW SUPPLEMENT, 450 Ahnaip St., Menasha, Wis., or University of Minnesota, Minneapolis, Minnesota.

# The Physical Review Supplement

## CONTENTS OF JANUARY ISSUE

*Electrical Discharges in Gases: Part I. Survey of Fundamental Processes* - - - - - - KARL T. COMPTON and I. LANGMUIR

An analysis and discussion of the physical processes fundamental in electric arcs, glow discharges, sparks, coronas, electrodeless ring discharges and hot cathode discharges.

*General Principles of Quantum Mechanics, Part II* - - - - - - - - - - - - - - - - - - - - E. C. KEMBLE and E. L. HILL

Review of the essential features of the Schroedinger wave mechanics, the Heisenberg matrix theory and the Dirac-Jordan transformation theory, with typical applications.

*Fundamentals of Band Spectrum Analysis* - - - - R. S. MULLIKEN

A survey of the theory of band spectra and of the related theories of molecular structure with a review of the problem of interpreting band spectrum data so as to obtain knowledge of electron levels of molecules, their properties and their relationship to atomic levels.

*X-Ray Diffraction in Liquids* - - - - - - - - - G. W. STEWART

A general description of the results of experimental study of x-ray diffraction halos, their interpretation on the theory of temporary molecular groupings, and their general significance in theories of molecular structure and constitution of liquids.